The Genetic and Functional Role of ABCA12 in Harlequin Ichthyosis

Philip James Bland

Supervisor: Professor David Kelsell

Second Supervisor: Professor Edel O'Toole

A thesis submitted for the degree of PhD

Centre for Cutaneous Research, Blizard Institute, Barts and the London School of Medicine and Dentistry, Queen Mary University of London

I, Philip James Bland, confirm that the research included within this thesis is my own work or that where it has been carried out in collaboration with, or supported by others, that this is duly acknowledged below and my contribution indicated. Previously published material is also acknowledged below.

I attest that I have exercised reasonable care to ensure that the work is original, and does not to the best of my knowledge break any UK law, infringe any third party's copyright or other Intellectual Property Right, or contain any confidential material. I accept that the College has the right to use plagiarism detection software to check the electronic version of the thesis. I confirm that this thesis has not been previously submitted for the award of a degree by this or any other university.

Signature: Philip James Bland

Date: 04/09/2015

Abstract

Harlequin Ichthyosis (HI) is the most severe disorder in the family of autosomal recessive congenital ichthyosis (ARCI). Recessive mutations in the ABC transporter *ABCA12* were found to be causative in HI. Loss of *ABCA12* leads to defective transport of ceramides, impaired transportation of proteases, premature terminal differentiation, transepidermal water loss (TEWL) and the retention of squames, which leads to the characteristic clinical phenotype of thickened hyperkeratotic plates overlying the skin. This thesis focuses on the genetic and functional role of *ABCA12* in the skin and how loss of *ABCA12* leads to the HI epidermis.

Several molecular genetic techniques were utilised to ascertain and evaluate possible causative mutations for HI in the gene *ABCA12*. The identification of novel and known, point and complex mutations give molecular diagnostics a greater reservoir to help identify possible causative mutations in future cases. The spectrum of *ABCA12* mutations, which have been attributed to different diseases within ARCI, was discussed.

A HI immortalised cell line was derived from a patient with a compound heterozygote mutation in *ABCA12*, with a nonsense p.Glu2264X and c.5382-2a/g, a complex splice site mutation of the putative acceptor site (AG) preceding exon 35. Further investigations assessed the use of low affinity acceptor sites by the spliceosome. Immunohistochemistry of the patient biopsy showed an absence of ABCA12 and a reduction of ABCA1 proteins. Knockdown of *ABCA12* in control K17 immortalised keratinocytes decreased expression levels of ABCA1 and LXRβ proteins. Functional studies of the HI patient derived cell line validated a HI cellular phenotype in monolayer.

The expression levels of involucrin, TGM1 and K10 proteins showed how the patient derived HI cell line under calcium shift initiated premature terminal differentiation *in vitro,* compared to controls. The activation of nuclear hormone receptors PPARβ/δ and LXRβ by the application of their agonists on the HI cell line increased the transcript and protein levels of the reduced ABCA1. The same agonists reduced specific markers of differentiation, which were activated prematurely in the HI cell line under calcium shift, suggesting a potential therapeutic strategy to explore.

Table of Contents

List of Figures and Tables

Abbreviations

A_T	Annealing temperature
ABC	Adenosine triphosphate (ATP) binding cassette
ApoA1	Apolipoprotein A1
AP-1	Activator protein-1
bp	Base pair
BMZ	Basement membrane zone
BSA	Bovine serum albumin
$CaCl_2$	Calcium chloride
CDC	Cell division cycle
CDK	Cyclin-dependent kinase
cDNA	Complementary DNA
CIE	Congenital ichthyosiform erythroderma
CNV	Copy number variation
CTSD	Cathepsin D
CTSC	Cathepsin C
DAPI	4',6-diamidino-2-phenylindole
DNA	Deoxyribose nucleic acid
ddH_20	Double distilled water
DEB	Dystrophic epidermolysis bullosa
DDEB	Dominant dystrophic epidermolysis bullosa
DMEM	Dulbecco's modified Eagle's medium
DMSO	Dimethyl sulfoxide
DNA	Deoxyribonucliec acid
dNTP	Deoxyribonucleotide triphosphate
DSB	Double strand breaks
DTT	Dithiothreitol
EB	Epidermolysis bullosa
ECM	Extracellular matrix
EDTA	Ethylenediaminetetraacetic acid
EGF	Epidermal growth factor
EGFR	Epidermal growth factor receptor
EST	Expressed sequence tag
EtOH	Ethanol
FACS	Fluorescence activated cell sorting
FBS	Fetal bovine serum
FCS	Fetal calf serum

FGF	Fibroblast growth factor
GAPDH	Glyceraldehyde 3-phosphate dehydrogenase
GFP	Green fluorescent protein
HCl	Hydrochloric acid
HKGS	Human keratinocyte growth supplement
HI	Harlequin ichthyosis
HR	Homologous recombination
IBS	Ichthyosis bullosa of Siemans
ICC	Immunocytochemistry
IHC	Immunohistochemistry
IF	Immunofluorescence
IFE	Interfollicular epidermis
IV	Ichthyosis vulgaris
K	Keratin
K1	Keratin 1
K5	Keratin 5
K10	Keratin 10
K14	Keratin 14
Kb	Kilobase
kDa	Kilodalton
KIFs	Keratin intermediate filaments
KLK5	Kalikrein 5
KLK7	Kalikrein 7
LEKTI	Lympho-epithelial Kazal-type-related inhibitor
LG	Lamellar granule
LXR	Liver X receptor
M	Molar
mA	Milli amp
mM	Millimolar
miRNA	MicroRNA
$MgCl_2$	Magnesium chloride
Mock	Keratinocytes treated with transfection reagent only
mRNA	Messenger RNA
NaCl	Sodium chloride
NaOH	Sodium hydroxide
NBCIE	Non-bullous congenital ichthyosiform erythroderma
NBD	Nuclear binding domain
ncRNA	Non-coding RNA
NEM	N-ethylmalemide

NGS	Next generation sequencing
nt	Nucleotide
NTP	Nucleoside triphosphate
OTCC	Organotypic co-culture
PAGE	Polyacrylamide gel electrophoresis
PBS	Phosphate buffered saline
PBST	Phosphate buffered saline supplemented with 0.1% Triton X-100
PCR	Polymerase chain reaction
PFA	Paraformaldehyde
Pri-RNA	Primary RNA
PPAR	Peroxisome proliferator-activated receptors
P/S	Penicillin/streptomycin
qPCR	Quantitative polymerase chain reaction
RISC	RNA-induced silencing complex
RDEB	Recessive dystrophic epidermolysis bullosa
ROS	Reactive oxygen species
RNA	Ribonucleic acid
RNAi	RNA interference
RNase	Ribonuclease
RT	Room temperature
RT-PCR	Reverse transcription PCR
RXR	Retinoid X receptor
SAGE	Serial analysis of gene expression
SDS	Sodium dodecyl sulfate
shRNA	Small hairpin RNA
siRNA	Small interfering RNA
SMOC	Secreted modular calcium binding protein
SNP	Single nucleotide polymorphism
SPR	Small proline-rich protein
SPRR	Small proline rich region
STS	Steroid sulfatase
TBS	Tris-buffered saline
TGF	Transforming growth factor
TGM	Transglutaminase-1
TGN	Trans-Golgi network
TMD	Transmembrane domain
TINCR	Terminal differentiation-induced ncRNA
UTR	Untranslated region
UVR	Ultra violet radiation
WB	Western blot

v/v	Volume per volume
v/w	Volume per weight
XLRI	X-linked recessive ichthyosis

Publications, presentations, and awards arising from this work

Publications

Manuscripts

Bland, P. J., Chronnell, C., Plagnol, V., Kayserili, H., & Kelsell, D. P. (2014). A severe collodion phenotype in newborn period associated with a homozygous missense mutation in ALOX12B. *British Journal of Dermatology*, *173*(1), 285–287. doi:10.1111/bjd.13627

Aggarwal, S., Kar, A., **Bland, P.**, Kelsell, D., & Dalal, A. (2014). Novel ABCA12 mutations in harlequin ichthyosis: A journey from photo diagnosis to prenatal diagnosis. *Gene*, *556*(2), 254–256. doi:10.1016/j.gene.2014.12.002

Scott, C. a, Plagnol, V., Nitoiu, D., **Bland, P. J.**, Blaydon, D. C., Chronnell, C. M., … Kelsell, D. P. (2013). Targeted sequence capture and high-throughput sequencing in the molecular diagnosis of ichthyosis and other skin diseases. *The Journal of Investigative Dermatology*, 133(2), 573–6. doi:10.1038/jid.2012.332

Blaydon, D. C., Nitoiu, D., Eckl, K.-M., Cabral, R. M., **Bland, P.**, Hausser, I., … Kelsell, D. P. (2011). Mutations in CSTA, encoding Cystatin A, underlie exfoliative ichthyosis and reveal a role for this protease inhibitor in cell-cell adhesion. *American Journal of Human Genetics*, *89*(4), 564–71. doi:10.1016/j.ajhg.2011.09.001

Abstracts

P Bland, B Fell and D P Kelsell. *"The up-regulation of ABCA1 by the activation of LXRβ and PPARδ/γ to renew archetypical differentiation in Harlequin Ichthyosis"*, European Society for Dermatological Research (ESDR) Meeting Copenhagen, Denmark, 10-13 September 2014.

P Bland and D P Kelsell. *The functional mechanisms underlying Harlequin Ichthyosis*. William Harvey Symposium, Barts and the London, London, 16 October 2013.

Oral presentations

Talk at the 44th Annual European Society for Dermatological Research (ESDR) Meeting, *"The up-regulation of ABCA1 by the activation of LXRβ and PPARδ/γ to renew archetypical differentiation in Harlequin Ichthyosis"*, Copenhagen, Denmark, 10-13 September 2014.

Talk at the Blizard Institute Graduate Studies Day, *"The genetic and functional role of ABCA12 in Harlequin Ichthyosis"*, London, UK, 22 April 2014.

Awards

Awarded £5,000 for a successful grant application from the Ichthyosis Support Group, "Recovery from the Harlequin Ichthyosis cellular phenotype through the over expression of ABCA1 by the activation of LXR and PPARs", January 2012.

Acknowledgements

I would like to acknowledge and thank my supervisor, Professor David Kelsell, for the opportunity to undertake this PhD and for the constant guidance and supervision throughout. David has been ever present throughout this process and always willing to lend his expertise, which has been instrumental in the development of this work. I would also like to give thanks to my second supervisor Professor Edel O'Toole for continued support and advice through the entirety of this project. A large amount of thanks must also be given to the SHHiRT charity for funding this project, their first and hopefully not last studentship.

I would like to thank all the members of the Kelsell group, past and present for sharing their knowledge and technical know-how, particularly Dr Diana Blaydon, who introduced me to research, the lab and was a constant source of technical support. A special thanks to Dr Vera Martins, Dr Supatra Marsh, Dr Thiviyani Maruthappu and Benjamin Fell, for unique friendships that helped me through the difficult times. Thanks to the Centre for Cutaneous Research for creating a friendly and professional environment.

Finally a big thank you to my family and friends and to Sarah Griesler whose eunoia has been a constant source of inspiration and strength.

Chapter 1: Introduction

1.1. The Skin

The skin is a complex organ that envelops the vast majority of the human body, its functions are numerous and critical to survival. The most discernible of which is the physical barrier the skin produces that shields the body from the immediate external environment. The skin helps to maintain homeostasis, the immune system and the physical form. Succinctly, the skin consists of three layers; the hypodermis, dermis and (outermost) epidermis.

The subcutaneous layer or hypodermis contains; lymphatic vessels, blood vessels, adipose tissue and is connected through striated muscle to the body. The dermis is found directly above the hypodermis and forms from the embryonic development of the mesoderm. It also contains lymphatic and blood vessels, but differs from the hypodermis in composition greatly. It generates the skin's elasticity, thermoregulation, strength and supplies the epidermis with nutrition. The matrix of this layer is predominately formed from proteoglycans and collagen, the former helps retain water when processed in the epidermis and the latter, with elastin, gives rise to the flexibility and suppleness of the skin. The principle cell type of the dermis is the fibroblasts, which secrete the constitutional components of the matrix. They are joined in the dermis by ephemeral immune cells, adipocytes and macrophages (Chu 2008).

1.1.1. The Epidermis

The epidermis adheres to the dermis through the dermoepidermal junction, a key structure in anchoring the epidermis through anchoring filaments and fibres that increase the skin's tensile capability. Within the skin, the epidermis itself has several layers; the first or basal layer is where the keratinocytes proliferate before they undergo terminal differentiation in the subsequent suprabasal layers. The main role of the epidermis is to maintain the skin's physical barrier against the environment; this barrier is maintained through the constant production and shedding of squamous keratinocytes. The rest of the cellular composition of the epidermis contains; Merkel cells, dendritic Langerhans' cells and melanocytes that bequeath melanin to keratinocytes. The epidermis is also a key structure in the skin's water retention, UV protection, vitamin D synthesis and immune function (Freinkel & Woodley 2001).

The predominant cell type in the epidermis is the keratinocyte and it is the differentiation of this cell type that generates the stratified layers key to the structure and function of the epidermis. During the migration of these terminal differentiating cells, the four layers of the epidermis are created; the basal layer or stratum basal, spinous layer or stratum spinosum, granular layer or stratum granulosum and the stratum corneum, shown in **Figure.1.1.** (Chu 2008).

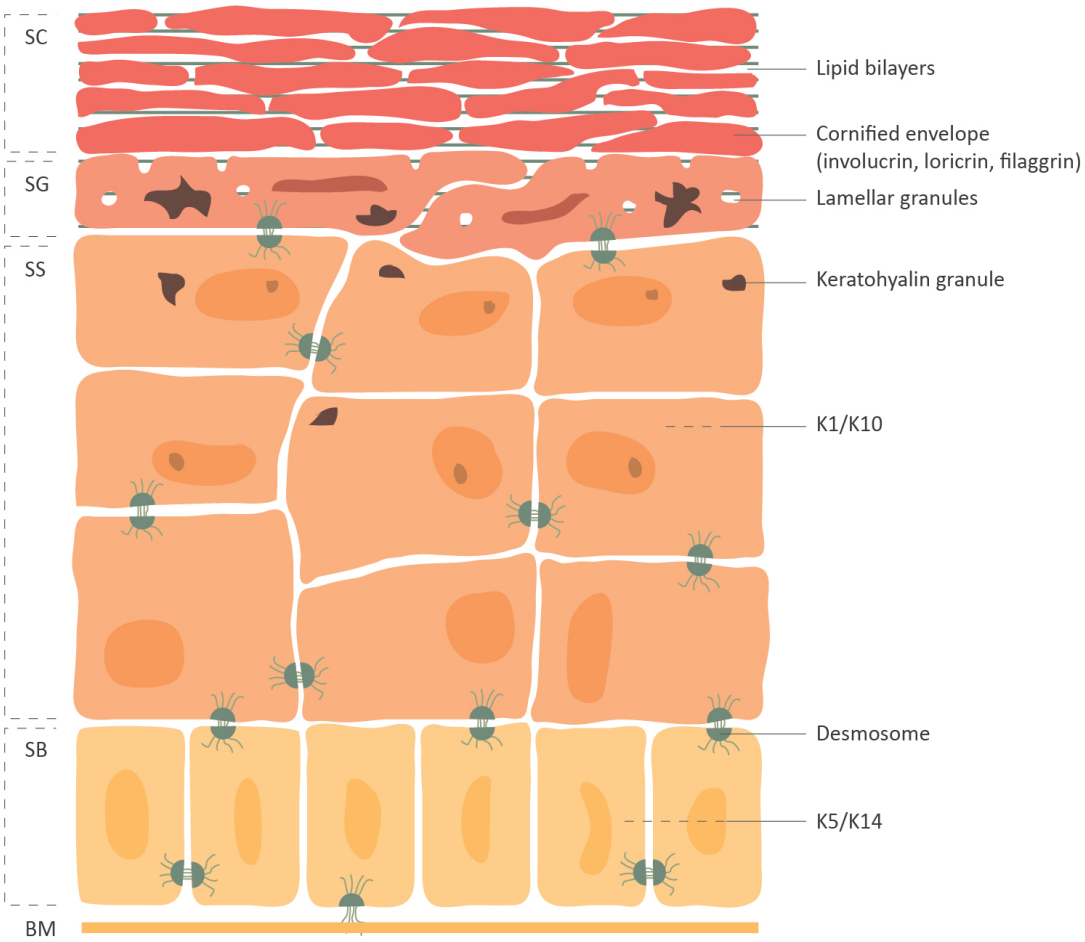

Figure 1.1. Schematic of the epidermis. The journey of a keratinocyte through the epidermis is unidirectional and designed by terminal differentiation. Keratinocytes become flattened and lose cellular content including the nucleus as they reach the upper layers. In the upper layers their morphology, protein content, organelle compliment and function changes, as they establish important skin barriers and undergo programmed cell death. BM, basement membrane; SB, stratum basale; SS, stratum spinosum; SG, stratum granulosum; SC, stratum corneum.

The stratum basale adheres to the basement membrane through hemidesmosomes, which sequester keratin and often integrate to the dermis through laminin-derived anchoring fibrils. The sequestered keratins of proliferating cells are different to that of differentiating cells; of note, keratin 5 and 14 (K5 and K14) are the main structural proteins expressed by the proliferating keratinocytes in the stratum basale, whereas keratin 1 and keratin10 (K1 and K10) are markers of a suprabasal differentiating keratinocyte. K5 and K14 form keratin intermediate filaments (KIF), which are heterodimers of one type I and one type II keratin, in the basal layer keratinocytes, the KIFs alongside microfilaments and microtubules are key structural components that travel to the nuclear lamina from desmosomes (Fuchs 1998).

The epidermis regenerates by the propagation and differentiation of slow cycling epidermal stem cells, which are located in the stratum basale. Specific compartments of stem cells give rise to the individual lineages, compartments such as; basal region of the sebaceous glands, interfollicular bulge and interfollicular epidermis (Jiang et al. 2010). The delamination of stem cells from the stratum basale or direct differentiation of keratinocytes from stratum basale to the stratum spinosum can start the process of terminal differentiation, though mitotic spindle orientation is a crucial differentiation initiator (Lechler & Fuchs 2005). Symmetrical mitosis encourages the keratinocytes to migrate laterally across the stratum basale increasing surface area, whereas asymmetric mitosis orientates keratinocytes for stratification through terminal differentiation. Spindle trajectory is thought to coordinate migration, as spindles in parallel with the basement membrane will favor symmetrical division and *vice versa.* Spindle orientation involved in asymmetric cell division is driven by the localization of nuclear mitotic apparatus protein (NuMA), but not by the transcription regulator of stratification P63 (Poulson & Lechler 2010).

The stratum spinosum comprises of keratinocytes with polyhedral morphology, highly spherical nuclei lying adjacent to the stratum basale, as recent products of asymmetrical mitoses. At this point of epidermal differentiation keratinocytes cease the normal cell cycle and start to initiate further cell attachments through an increase in desmosomes and gap junctions. Protein production of K5 and K14 is terminated, though the proteins are retained and K1 and K10 expression is actuated, which producers a larger and flatter keratinocyte bordering the stratum granulosum (Simpson et al. 2011). The K1/K10

heterodimer replaces the K5/K14 heterodimer in the KIFs, which is crucial for nuclear and desmosomal stability during keratinocyte differentiation (Wallace et al. 2012).

K10 and K1 are two of the most prevalent proteins in the suprabasal layers of the epidermis; synonymous with differentiation, K10 inhibits proliferation through cell cycle arrest when incorporated into the cytoskeleton via non-helical terminal domains. In turn this process can be inhibited in such hyperproliferative states as wound healing the expression and IF binding of keratin 16 (K16) reverses the K10-induced inhibition and renews proliferation (Paramio et al. 1999). The type I keratin K16 forms heterodimers with the type II keratin 6 (K6), together they aid keratinocyte migration and resistance from mechanical stress, though in an aged epidermis an increase in K16 alone creates a defect in cell migration (Trost et al. 2010). In keratinocytes found in the uppermost regions of the stratum spinosum lamellar granules (LGs) are synthesized for the first time, an organelle crucial for the correct barrier formation (Chu 2008). The highest concentration of lamellar granules and their extruded contents are localised to stratum granulosum, with the permeability barrier formation occurring at the periphery with the stratum corneum, which will be discussed in more detail (**1.3**) (Vielhaber et al. 2001).

The stratum granulosum is the layer of the epidermis where keratinocytes manufacture the vast majority of the components needed to assemble the cornfield cell envelope. Keratinocytes that occupy this stratified layer possess keratohyalin granules containing predominately profilaggrin and lesser proportions of loricrin and keratin (Elias & Feingold 2005). Profilaggrin is a large phosphoprotein containing multiple repeating subunits of filaggrin, during terminal differentiation profilaggrin is dephosphorylated and cleaved (Presland et al. 1997). Profilaggrin contains two different linker sequences, which are cleaved by specific enzymes; following this calcium-dependent proteolytic cleavage by profilaggrin endoproteinase I and calpain I, filaggrin is produced (Resing et al. 1989). In the stratum corneum filaggrin aggregates with keratin to form macrofilaments that are degraded to simpler molecules with hydrating and UV-protective properties.

The basal layer keratinocytes are susceptible to malignant transformation by UVB irradiation and are thus protected by the reflection and absorption of UVB in the upper

layers of the skin. The aromatic amino acid residues of proteins, DNA and melanin of the upper layers of the epidermis are all chromophores of UVB and help to protect the proliferating basal layer keratinocytes (Young 1997). Processed filaggrin in the epidermis interacts with intermediate filaments that form the intracellular matrix of keratinocytes, then its proteolytic degradation forms components of moisturizing surfactants, all contributing to the primary role of filaggrin in the formation of cornified layer and the physical barrier of the skin (Pendaries et al. 2014). Filaggrin also plays a role in UVB protection, as a reduction in processed filaggrin in the skin has been shown to increase sensitivity to UVB and reduce the amount of urocanic acid (UCA) in late differentiation (Mildner et al. 2010). UCA has been shown to accumulate in the stratum corneum and is the product of the enzymatic activity of histidase on histidine. Ablation of the histidase enzyme causes a UVB-photosensitive phenotype in mice that accumulates more DNA damage under UVB irradiation than wild type (Barresi et al. 2011).

In the upper granular layer transglutaminase 3 (TGM3) initiates the first cross-linking in the formation of the cornified envelope, TGM3 acts as the catalyst forming the isopeptide bonds between loricrin and involucrin. This cross-linking is increased in the stratum corneum as other calcium-dependent transglutaminases, 1 and 5 (TGM1) (TGM5) join TGM3 in the creation of the insoluble and resistant cornified envelope (Lorand & Graham 2003). The calcium gradient within the epidermis is referred to in greater detail later in **(1.2.1)**. Filaggrin aggregates with the KIFs forming tight bundles, which account for a great percentage of the mass of the epidermis and change the morphology of the keratinocytes, making them flatter with pronounced cellular projections. Keratinocytes of the stratum granulosum takes on a more differentiated morphology, they form tight junctions that help to promote a barrier against the external environment. By forming these knot type adhesions between neighboring cells the epidermis allows exclusively for the transition of ions and small molecules between keratinocytes. Desmosomes continue to play a role in differentiation, in the stratum granulosum/corneum boundary, they bind to the adjacent plasma membrane through loricrin, and involucrin via TGM1 activity, further defining the permeability barrier of the skin (Candi et al. 2005).

The stratum lucidum resides between the stratum granulosum and stratum corneum and is prevalent in palmar-plantar skin, the glabrous, non-hairy, skin of the soles of the feet and palms of the hands (Freinkel & Woodley 2001). This specialized additional layer was postulated through the characterization of palmar-plantar skin, in particular by the comparison of the keratin profiles of palmar-plantar and normal skin. It is rich in lipids and thiol groups secreted by the keratinocytes of the stratum granulosum that aid the structural integrity of the epidermis in these areas of high mechanical stress (Swensson et al. 1998). The type I intermediate filament keratin, keratin 9 (K9) is expressed uniquely in the suprabasal layers of the epidermis of palmar-plantar skin and is required for terminal differentiation and maintaining the mechanical integrity of the palmoplantar epidermis (Fu et al. 2014).

The stratum corneum is the uppermost layer of the epidermis and holds keratinocytes in their final stage of terminal differentiation. The keratinocytes here are labelled as corneocytes as they have undergone apoptosis and exocytosed or degraded much of their intracellular content forming a layer of flat cell remnants creating a physical barrier of the skin. This physical barrier is the cornified envelope, which has a general structure containing a multitude of proteins cross linked together through the enzymatic work of several transglutaminases, creating a continuous insoluble boundary replacing the plasma membranes in the layer of corneocytes (Kalinin et al. 2001). The ~15 nm thick cornified envelope consists of a scaffold of KIFs and filaggrin upon which other structural proteins are added, including loricrin, involucrin and the small proline-rich (SPR) family of proteins (Hohl 1990). Corneocytes are affixed to one another through corneodesmosomes, embedded in a lipid complex of cholesterol, phospholipids, ceramides and free fatty acids (Candi et al. 2005). This lipid complex forms lipid bilayers, crucial for the skin barrier and the only continuous structure bridging the upper layers of the epidermis and tight bundle formation of K1 and K10 with filaggrin within the cytoskeleton of corneocytes resulting in a dramatic flattening of the cells of the cornified envelope (Manabe et al. 1991).

The cornified envelope is a key structure in establishing the mechanical resilience and insolubility of the epidermis; these properties are shaped by its structure, which has many attributes. One of which is the addition of TGM cross linked structural proteins, involucrin, loricrin and the S100 family of proteins. They S100 family is classified by

containing the calcium binding EF-Hand domains and binding calcium to rely cell regulatory signals. Found in the cornified envelope their expression is initiated in the stratum basale and spinosum, as keratinocyte differentiation takes place the localization of S100A7 and A11 moves from the nucleus, to the cytoplasm and finally the plasma membrane (Broome et al. 2003). S100 proteins regulate target protein activity through calcium-dependent binding and are themselves cross linked in the cornified envelope by calcium-dependent TGM1 and TGM2 a mechanism deemed to regulate the activity of the S100 family (Ruse et al. 2001).

Loricrin is a central component of the cornified envelope and accounts for ~80% of the total protein mass of the cornified envelope (Steinert 1998). The expression of loricrin is initiated in keratinocytes of the stratum granulosum and once translated it is frequently cross linked by the addition of isopeptide bonds through the activity of TGM1, 3 and 5. Found cross linked to itself forming loricrin oligomers, attached to SPR proteins or both this heterogeneity promotes disorder in the cornified envelope that contributes to its elasticity (Yoneda & Steinert 1993). The loricrin protein is rich in glycine-serine-cysteine residue repeats, the number of which is not conserved, though the loops they form are flanked by either aromatic or aliphatic residue forming a common motif in the protein. The binding of which forms either inter or intramolecular disulfide and N-(γ-glutamyl)lysine isodipeptide bonds, which stabilise loricrin into a rosette like structure (Hohl et al. 1991). These glycine rich loops separated by hydrophobic interactions create flexible Ω-loop like structures that impart the elasticity characteristic on cornified envelope.

Involucrin localises to the cytosol of keratinocytes in the stratum granulosum, eventually it is cross linked to other structural proteins of the plasma membrane in the stratum corneum, where the formation of the cornified envelope takes place. The involucrin gene comprises of one central exon containing a 30 nucleotide sequence repeated 39 times, high in glycine and aspartic acid residues, with intermittent rearrangements occurring through recent evolution (Eckert & Green 1986). Comparable with loricrin, involucrin forms cross links with N-(γ-glutamyl)lysine isodipeptide bonds through the enzymatic activity of TGM1. The structure of involucrin is predominately α-helical culminating in a flexible rod 3D structure that translocates and strengthens with Gln495 and Gln496 available for cross linking to loricrin and SPR proteins

(Envelope et al. 1992). The involucrin protein provides the cornified envelope with the physical cross links needed to produce the mechanical resilience found in the epidermis, it may also be pivotal in the attachment of extracellular lipids a constituent of the skin's permeability barrier. A type of TGM1 can function located on the plasma membrane and forms ester bonds linking the available glutaminyl residues involucrin to ω-hydroxyceramides (Nemes et al. 1999).

The SPR family of proteins contains 13 proteins divided into three classes, SPR1-3, all of which are 6-18 kDa and rich in proline amine acid residues. Similar to the aforementioned loricrin protein, the size and structure of SPR make them ideal for cross linking to other constituents of the cornified enveloped. However, unlike loricrin, which is constitutively expressed in the stratum corneum of the epidermis, SPR proteins are facultatively expressed at varying levels depending on the physical requirements of the skin (Steinert et al. 1998). This natural variation to the ratio of loricrin to SPR proteins varies from less than 1:100 in skin with a relatively thin skin to around 1:10 in areas containing a thickened epidermis such as the palms and soles. Upon which it can be postulated that SPR proteins play a role in constructing or maintaining a thickened epidermis (Steinert 1998).

These elements of the cornified envelope sit entrenched within the lipid envelope, a complex structure of lamellae originating from a highly organised myriad of lipids, which helps to negate transepidermal water loss (TEWL) from the skin. The lipid envelope and the lamellar granules (LG) that supply them are disseminated in **1.3.** and **1.4.** respectively. The complementation of the cornified and lipid envelopes is fundamental in giving the epidermis its distinctive resilience and creating an environment for microbial defense. Antigen invasion through a physical disruption to the barrier causes an inflammatory response through the extension of dendrites from active Langerhans' cells, when the microbial defense is breached (Simpson et al. 2011). The layers of fully differentiated corneocytes forming the stratum corneum produce an ideal cuticle against the external environment, but are continuously attenuated by proteases. Proteases from the LGs degrade the remaining corneodesmosomes and lipid complexes, shredding the non-viable corneocytes (Freinkel & Woodley 2001).

1.1.2. The Dermis

The main bulk of the skin is made up of the dermis, which provides much of the elasticity, structural integrity and flexibility that are characteristic of this organ. The dermal layers adhere to the epidermis through the dermoepidermal junction, a section of the skin comprising of anchoring filaments, type VII collagen containing hemidesmosomes, which connect the dermis to the basement membrane. The dermis contains many different cell types such as mast cells, immune cells, macrophages and predominately fibroblasts. All of which are located in a blend of cellular, fibrous, filamentous and diffuse connective tissue elements that house vascular and nerve networks aiding water retention, thermoregulation and holding the sensory receptacles. During repair after wounding and embryonic development the dermis is continuously interacting with the dermoepidermal junction and the epidermis for nourishment and maintenance (Chu 2005).

1.2. Keratinocyte Differentiation

The differentiation of keratinocytes is a highly specialised function that enables the separation of organism from the environment by the formation of the stratified epidermis. Markers of early keratinocyte differentiation, such as the aforementioned TGM1 and involucrin portray the initiation of this process in the stratum spinosum and through a complex gene regulatory network, this process ends with cornification in the stratum corneum. Differentiation of the epidermis is promoted by many factors including an increase in the concentration of calcium, hydrocortisone, Vitamin D, cell to cell contacts and the reduction of vitamin A (Hennings et al. 1980; Cline & Rice 1983; Bikle 2010; Dotto 1999; De Luca 1977). The expression of markers of terminal differentiation, cornified envelope formation and general epidermal stratification is reduced by the action of retinoids on the epidermis (Eckert & Rorket 1989).

1.2.1. Calcium Gradient

Calcium is the main factor in promoting keratinocyte differentiation within the epidermis. The path of differentiation mirrors the change in the concentration of calcium in the skin, with the proliferating, undifferentiated keratinocytes of the stratum basale present at a relatively low calcium concentration that increases as the progression

is made through the subsequent layers of the epidermis to the stratum corneum. This calcium gradient coincides with increased cytosolic free calcium and calcium contained within organelles of keratinocytes of the upper epidermal layers (Pillai et al. 1993). As the keratinocytes start to differentiate they migrate through the stratified layers of the epidermis, their morphology changes driven by the increase in calcium, which affects the cell in many ways before terminating as anucleate squames. The constituents of the IF change, keratinocytes become flattened, start to express proteins of the cornified envelope and have a greater permeability to calcium and other ions (Eckert & Rorket 1989). Keratinocytes exit the cell cycle when migrating from the proliferating stratum basale. In monolayer culture when calcium shifted, keratinocytes show increased intercellular connections, including desmosomes within hours, minor stratification and termination of DNA synthesis by 2 days, and between 3-4 days transcription and translation are reduced by half, preceding the end of terminal differentiation (Hennings et al. 1980).

The maintenance of intracellular calcium levels in proliferating keratinocytes and those undergoing calcium switch into differentiation is managed by two elements of the store-operated calcium entry (SOCE) pathway. These are the endoplasmic reticulum (ER)-located calcium sensor STIM1 and the partial calcium channel Orai1, knockdown of either of these proteins suppresses SOCE through the phospholipase-C activated calcium response. This significantly reduces the ability of keratinocytes to initiate differentiated and express early epidermal differentiation markers (Numaga-Tomita & Putney 2013).

As the calcium gradient continues to rise in the stratum spinosum, stimulation of calcium-dependent keratinocyte differentiation is coupled with the phosphorylation of the group of ErbB receptors, which encompass the epidermal growth factor receptor (EGFR). Activating EGFR induces the expression of activator protein-1 (AP-1) in keratinocytes, which helps to drive differentiation. Proteins involved in late epidermal differentiation such as TGM1, filaggrin, involucrin and loricrin all hold AP-1 binding sites in their promoter regions (Hanley et al. 2000; Schmuth et al. 2004). In calcium shift experiments the ErbB receptor activated changes with the amount of time spent under high calcium conditions, which also correlates to the localisation of ErbB receptors to specific stratified layers of the epidermis. There is a complex network that

leads to the timely expression of differentiation-related proteins in the epidermis, which is controlled by the calcium gradient through the activation of ErbB receptos, AP-1 induction and further transcriptional promotion. As shown when either ErbB receptors or AP-1 proteins are aberrant terminal differentiation is inhibited (Saeki et al. 2012).

As calcium levels continue to rise throughout the stratification of the epidermis a group of proteins that were expressed due to the initial suprabasal influx of calcium, envoplakin, periplakin and involucrin localise to the plasma membrane. Here they are accompanied by TGM1, the expression of which is also triggered in keratinocytes undergoing differentiation, this enzyme is activated by the further rise of intracellular calcium during late differentiation. TGM1 cross links involucrin to the plakins through the formation of isopeptide bonds as well as joining these proteins to other membrane bound proteins. This growing network of bound structural proteins at the plasma membrane develops into the scaffold that will hold the cornified envelope (Kalinin et al. 2001).

1.2.2. Desquamation

Terminal differentiation in the epidermis concludes with keratinocytes undergoing cornification in the outermost layer, the stratum corneum. At this stage they have helped produce the intercellular structures of the interconnected cornified envelope and the complex lamellae of the lipid envelope. The squames accumulate at the periphery of the stratum corneum generating a thickness that varies for specific locations on the body. The growth of this tightly packed layer of retained squames is curtailed by the process of desquamation, through the action of proteases this process degrades structural proteins and allows a continuous shedding of the outermost squames (Egelrud et al. 2000). This epidermal homeostasis is needed for the continuous turn over of the epidermis, with keratinocytes moving from proliferation, migrating to differentiation and becoming part of the stratum corneum in ~3 weeks (Baker & Kligman 1967).

Proteases are crucial in the process of desquamation; they start to degrade the intercellular attachments to shed the outermost squames as differentiation finishes. In corneocytes the proteolytic degradation of corneodesmosomes is performed by the serine proteases kallikreins 5 and 7 (KLK5 and KLK7), which perform in tandem upon

the corneodesmosin, desmocollin-1 and desmoglein-1 structural proteins (de Veer et al. 2014). Other kallikreins may also play roles in desquamation and have been shown to be present in the epidermis, such as the desmoglein-1 cleaving KLK14 and KLK8 (Borgoño et al. 2007). The acidic environment of the stratum corneum is due to the lowering of the pH throughout epidermal differentiation. The low pH is an optimal working condition for the lysosomal aspartyl protease cathepsin D and the cysteine protease cathepsin V, both of which co-localise with corneodesmosomes (Igarashi et al. 2004; Zeeuwen et al. 2007).

The lympho epithelial kazal type related inhibitor (LEKTI) controls the degradation of corneodesmosomes by serine proteases in the stratum corneum. LEKTI is cleaved into its 15 functional protease inhibitor domains by the protease furin (Fortugno et al. 2011). The inhibition LEKTI exhibits on the kallikreins (KLK5, KLK7 and KLK14) of the epidermis ceases when the pH is at its lowest in the stratum corneum, this avoids any unspecific premature degradation in the lower levels of the epidermis (Deraison et al. 2007). Proteolytic activity is further regulated by another group of kazal type protease inhibitors known as SPINK6 and SPINK9 (Meyer-Hoffert et al. 2009). The other main group of protease inhibitors in the epidermis regulating desquamation is the cystatins. Cystatin A (CSTA) for example has been shown to be present in the stratum corneum where it inhibits both cathepsin L and V and the exogenous proteases secreted from dust mites (Cheng et al. 2006). CSTA also localised to the lower levels of the epidermis where it was found to be important in maintaining cell-cell adhesion and thus epidermal stability under mechanical stress (Blaydon et al. 2011). The probable activity of cystatin M/E however is involved in the regulation of protease modulated TGMs (Zeeuwen et al. 2010). The activation of the TGMs that cross link the pre-cursor proteins of the cornified envelope is regulated by a cascade of proteases including legumain and cathepsins L and D (CTSL and CTSD) (Egberts et al. 2004; Zeeuwen et al. 2010).

1.3. Lamellar Granules

The lamellar granule (LG) is a subcellular structure that can be detected by electron microscopy and can be roughly described as a storage vehicle or a secretary organelle. LGs are also known as lamellar bodies, Odland bodies or membrane coating granules; they are employed in several tissue types offering a host of cargos for different

extracellular roles. In the lungs LGs are synthesised in pneumocytes and transport phospholipid derivatives that are extruded as alveoli surfactants (Haller et al. 1998). They also help maintain the protective hydrophobic lining of the gastric mucosa and have a key role in synoviocytes and their role in the lubrication of joints (Dobbie et al. 1995; Stremmel et al. 2012). LGs in the epidermis measure 200 – 300 nm and are a secretory vesicle crucial for correct late epidermal formation, they extrude a specific group of lipids and proteases involved in desquamation into the extracellular space of the upper stratum granulosum and the stratum corneum. This specific group of lipids forms the lipid envelope and in doing so the permeability barrier of the epidermis, a structure known to stop TEWL. The main constituent of this group of lipids are ceramides, though additionally LGs also carry cholesterol and fatty acids (Schmitz & Müller 1991).

1.3.1. Ultrastructural organisation

The presupposition with regard to the formation and structure of the LG leaned towards an ovoid shaped discrete organelle, made from a bilayer of membrane lipids. Formed from the folding and budding of the trans-Golgi network and then moving towards and fusing with the plasma membrane the LG would then extrude its contents into the extracellular matrix (Bouwstra et al. 2003). This concept was challenged due to the contents of LGs, the topology of the vesicles and the thermodynamic cost of the budding to fuse, when a continuous lamellae structure could be present (Norlén 2001a). A continuous trans-Golgi like structure was hypothesized in the ‘membrane-folding model’ conceived by Norlén. Norlén postulated that LGs do not become separate organelles from the Golgi, rather, produced by branching of a continuous trans-Golgi network. These bind with the plasma membrane and then unfold into the extracellular matrix of the stratum corneum, preserving membrane continuity (Norlén 2001a). Further investigation into the nature of LGs using a range of electron microscopy shows a LG predominately fitting the folding membrane model with some discrete ovoid shaped LGs. From which, it appears that morphology is cargo-dependent (Ishida-Yamamoto et al. 2004; Fartasch 2004).

1.3.2. Molecular composition and cargo

The LG can transport a diverse set of cargos from the precursors of the lipid envelope; glucosylceramides, cholesterol, phospholipids and sphingomyelin to their respective enzymes; β-glucocerebrosidase, steroid sulfatase, phospholipase A_2 and sphingomyelinase (Hachem et al. 2006). Either as a continuous structure or a discrete organelle packing of the LG is crucial for lipid envelope formation. The delivery of lipids from either the Golgi or cytosol into the inchoate LGs allows for not only a high concentration of lipids to be transported, but also the coordinated packaging of enzymes. As without lipid transportation into the LGs there is no enzyme transportation into LGs and therefore they cannot act in envelope formation (Rassner et al. 1999). This briefly highlights the importance of the lipid transporter ABCA12. Mature ABCA12 was shown to be present in the Golgi and retained in the developing or budding LGs. The co-localization of ABCA12 to the Golgi markers TGM46 (glycoprotein) and GM130 was present throughout the epidermis, whereas ABCA12, glucosylceramides and developed LGs co-localise exclusively in the stratum granulosum layer (Sakai et al. 2007). This, and the action of ABCA12, are further discussed in **1.8.1.**

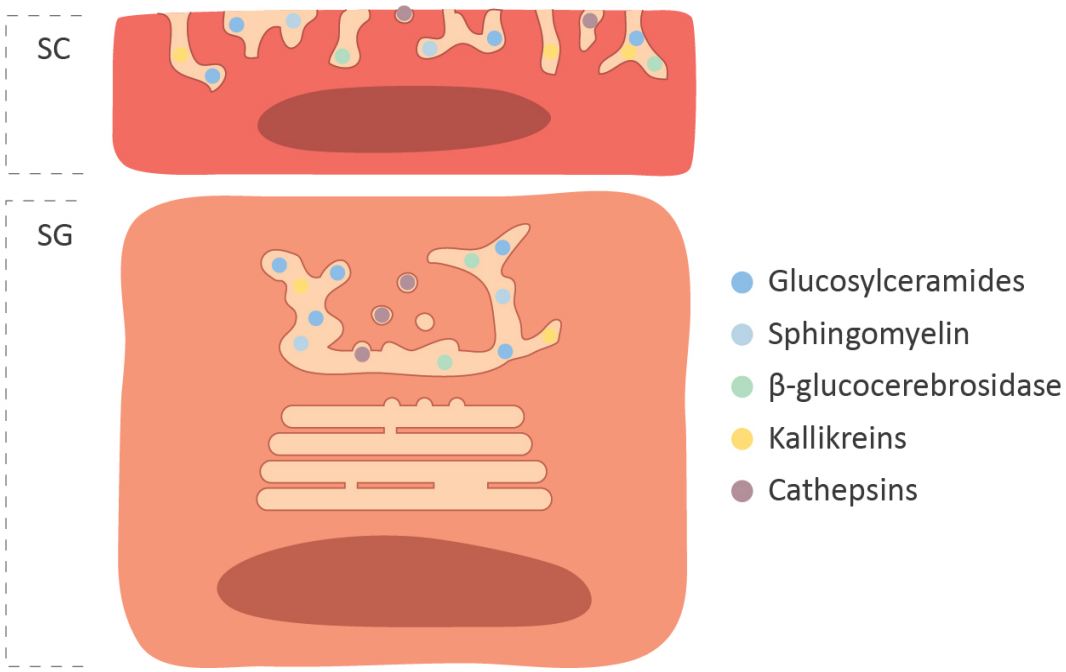

Figure 1.2. Lamellar granule transportation model. LGs in keratinocytes are heterogeneous in form and the cargo they transport. LGs are derived from the trans-Golgi network and further their projection towards the membrane by an addition of lipids creating a continuous tubular structure. Cargos are predominately transported in these continuous lamellar structures until they fuse with the degrading apical membrane in keratinocytes of upper stratum granulosum early stratum corneum. Cathepsins are the caveat here; LGs that transport these proteases are discreet ovoid vesicles that are budded from inchoate LGs and possibly fuse later with the continuous form. Both forms extrude their contents into the extracellular space of the stratum corneum creating the lipid and cornified envelopes.

As shown in **Figure 1.3.** the secretion from LGs into the extracellular space occurs near the conclusion of terminal differentiation at the superficial cells of the stratum granulosum. Not only do LGs extrude a range of lipids and their respective enzymes, they also transport structural proteins involved in cornification like corneodesmosin and proteases such as KLK7, KLK8 and CTSD, that are involved in desquamation (Ishida-Yamamoto et al. 2004). The deregulation of which can be seen when aberrant LGs do not transport their protease cargos, which leads to the retention and subsequent build up of squames in the stratum corneum. Disruption of the upper layers of the epidermis whether by means of tape stripping (mechanical stress) or detergents, results in a great and swift promotion of LG synthesis and secretion from the uppermost remaining keratinocytes. This is to repair barrier function and demonstrates the relationship between the concentration of lipids in the stratum corneum, barrier formation and LGs (Grubauer, et al. 1989).

This rapid response to skin barrier disruption is produced by two interlinked properties of the epidermis, TEWL and the calcium gradient that runs throughout the epidermis. Disruption of the lipid envelope causes a transepidermal water flux and with it, an increase in calcium concentration in the area of perturbation. This increase up-regulates differentiation and lipid synthesis in the remaining stratum granulosum and enables the redistribution of lipids in the stratum corneum normalising barrier function (Grubauer, et al. 1989).

1.4. Epidermal Lipids and the Permeability Barrier

The epidermis of mammals protects them from the possible physical damage and dehydration inflicted upon them by the environment. The previously described cornified envelope consisting of corneocytes embedded into insoluble proteins and the lipid envelope achieves these properties. The lipid envelope or extracellular hydrophobic lipid matrix is a product of the differentiation of keratinocytes, made from skin-specific lipids it provides the permeability barrier against the movement of water and electrolytes (Ponec 1994). Alongside their pivotal function in the permeability barrier epidermal lipids also provide a defence against the invasion and colonisation of microorganisms whether they are commensal or pathogenic. When both barriers are non-functioning as described in patients with burns or very premature births, mortality

becomes a factor highlighting the importance of a functioning epidermis. The permeability barrier is located in the stratum corneum and accounts for 10% of the stratum corneum's tissue mass and on average 50% of the lipid mass is ceramides, 25% cholesterol, and 15% free fatty acids with very few phospholipids (Gray et al. 1982; Feingold 2007).

Lipids in the epidermis are key in the formation of the lipid envelope and thus in the formation of skins permeability barrier. The prevention of water loss through the skin is crucial and to this affect the barrier has to be kept as tight as possible (Blank 1952). Hydration is closely regulated in the stratum corneum, as apart from the minute amount of water needed in corneocytes to hydrate keratins present in IF, the over hydration of corneocytes causes them to swell uniformly and stratum corneum to expand 3-4 fold (Warner et al. 2003). Lipids expelled from the top of stratum granulosum form the complex lamellar membranes that reside in extracellular domains of stratum corneum. The majority of ceramide processing in the stratum corneum occurs extracellular, by the lamellar granules, though significant levels of glucosylceramides and ceramides are found within the cells and throughout the layers of the epidermis (Vielhaber et al. 2001).

Through LG exocytosis lipids and their respective catalytic enzymes are secreted together aiding the quick assembly of the lipid envelope, but also providing the extracellular matrix with bi-products like glycerol, formed from the catalysis of phospholipids, that aids water retention. Furthermore, the pH of the permeability barrier (5-5.5) is maintained by the production of free fatty acids, which is the optimal pH for the secreted enzymes β-glucocerebrosidase and sphingomyelinase and later the pH is further lowered for the proteases of desquamation (Fluhr et al. 2001). β-glucocerebrosidase in turn reduces glucosylceramide into glucose and free ceramide, which itself can form sphingosine (Grubauer, et al. 1989).

The entire epidermis produces a myriad of different lipids throughout the differentiation process; those meant for the lipid envelope have precursors that can be traced back to basal levels, existing as sphinganine, cholesterol sulfate and inchoate fatty acids. There is a pronounced change in lipids, their composition and cellular localisation through keratinocyte terminal differentiation (Elias 1983). In the lower levels of the skin both

polar and neutral lipids reside, which is the composition throughout many mammalian tissues, this balance is replaced with a bias towards a predominant neutral mixture of lipids. The neutral lipid cholesterol is one of these lipids found in the upper layers of the stratum granulosum. It exists as the metabolite cholesterol sulphate in the proliferating keratinocytes of the basale layer, where at a high concentration it acts as a protease inhibitor. The expression of the cholesterol sulfate catabolic enzyme steroid sulfatase in keratinocytes of the stratum granulosum reduces the level of cholesterol sulfate. The intracellular concentration of its' enzymatic product cholesterol then subsequently increases to the amount found in the lipid envelope (Elias, et al. 1984). Later in differentiation the reduction of cholesterol sulfate reduces the inhibition of proteases involved in desquamation. In conditions with a dysfunctional cholesterol sulfatase enzyme the resulting cholesterol sulfate build up creates abnormalities in plasma membrane structure and extensive lamellar-phase separation in the lipid envelope (Zettersten et al. 1998).

The neutral lipids at the greatest concentration in the stratum corneum belong to the group of ceramides, synthesized through the salvage pathway and hydrolysis of sphingomyelin or the *de novo* product of the addition of serine to palmitate (Mao-Qiang et al. 1993). Ceramides are lipid molecules comprising of a fatty acid and a sphingosine molecule, they are a common subunit of cell membranes. Ceramides are a precursor to the main component of the lipid envelope glucosylceramide, which is the structural crux of extracellular lamellar sheaths. Glucosylceramide is produced via the enzyme glucosylceramide synthase which forms a glycosidic between a carbohydrate head and a ceramide chain and is present at a high concentration in the stratum granulosum (Galadari et al. 1998).

Though the importance of nonpolar ceramides cannot be overlooked in lipid envelope formation, the other lipids in the composition have pivotal roles too. As experiments have shown the removal of loosely bound nonpolar species alone histologically appears to cause only a modest level of barrier disruption, whereas the removal of sphingolipids and sterols leads to a more profound level of barrier perturbation (Grubauer, et al. 1989). Ceramides are also part of the molecular relay activated as a cellular response to extracellular stress or signaling, like terminal differentiation, the suppression of cell growth and division and initiation of apoptosis (Galadari et al. 1998).

The polar lipids glycoslyceramide and sphingomyelin are both products of ceramide processing in the lower stratum granulosum; they are then package into LGs through the lipid transporter ABCA12 (Sakai et al. 2007). They travel with catabolic enzymes and other lipids in LGs until they are extruded into the extracellular matrix where they are further processed into ceramides of different lengths establishing the extracellular lamellar membrane structures of the lipid envelope (Uchida & Holleran 2008).

Alongside the array of processed ceramides of different lengths, free fatty acids and cholesterol, the other main component of the lipid envelope are the acyl ceramides. Acyl ceramides are a subgroup of the most dominant type of lipid in the lamellae, the ceramides. They are a key component in barrier formation as they aid the folding of the lipid lamellae (Holleran et al. 2006). The formation of acyl ceramides in the epidermis is a multi-step metabolic process, of which hydroxylation involving a cytochrome p450 enzyme and elongation of the long chain fatty acid via ELOVL4 are crucial steps. In mouse models, mutant forms of either of these enzymes leads to high rates of neonatal mortality due to the inability to form a permeability barrier (Uchida & Holleran 2008).

In the stratum corneum, free fatty acids bind covalently to the extracellular side of the membrane of coneocytes, forming a safe hold for other lipids to bind and aiding in the complementation of the lipid and cornified envelopes (Swartzendruber et al. 1987). Upon elongation free fatty acids become very long fatty acids (VLFA) in the stratum corneum, these are needed to covalently link the two envelopes together a process made viable by the exposure of the hydroxyl group on the VLFA. Two enzymes unique to the epidermis, ALOXE3 and ALOX12B, perform this manipulation of VLFA. They simultaneously oxygenate the separate double bonds of the free fatty acids and if either are mutated they cause barrier defects that are phenotypically similar (Fischer 2009). First of all the enzyme 12R-LOX encoded by the gene ALOX12B acts upon the fatty acid producing a hydroperoxide, then the enzyme eLOX3 encoded by the gene ALOXE3 converts the substrate into epoxyalcohol. This functional group is generated on the VLFA to help interlink the proteins of the cornified envelope with the lipids of the lipid envelope (Zheng et al. 2011).

1.4.1. Composition and Structure

The lipid envelope, which is the crux of the epidermal barrier, can exist in different phases depending on its composition. When the components of the envelope are in their optimal arrangement the barrier can resist the ever-changing environmental conditions the skin is routinely subjected to, such as changes in humidity, temperature, pH, etc. To produce the most robust lipid envelope and thus stop phase transitions within that can cause lamellae separation and unwanted pore formation, a great homogeneity of physical arrangement is employed (Clerc & Thompson 1995). As interconnected lamellae are a mixture ceramides, sphingolipids and free sterols (Grubauer, et al. 1989).

Predicted in the single gel phase model the next reducible level is actually highly heterogeneous in respect to lipid components and their orientation. Within the lipid lamella, lipids are orientated with alkyl hydrocarbon chains perpendicular to one other, either in a hexagonal state on a rotational axis or an orthorhombic system where hydrophobic chains are fixed, producing a rotational disorder (Norlén 2001b). This combined with the range of ceramide alkyl hydrocarbon chain lengths and the addition of cholesterol promotes lamellar structures and a gel phase envelope with greater pliability and plasticity where a single repeated phospholipid would not (Takahashi et al. 1996). A reduction of cholesterol in the stratum granulosum leads to a dysfunctional permeability barrier with slight deformities in membrane structure and widespread lamellar-phase separation (Zettersten et al. 1998). The repetitive nature of this continuous lamellar gel phase produces a robust lipid envelope functional in all environmental conditions.

1.5. The Nuclear Hormone Receptors

The intracellular lipids that undergo packaging and secretion to eventually become the building blocks of the lipid envelope also have a regulatory effect on gene expression by means of nuclear hormone receptor interaction. When these fundamental lipids reach a concentration threshold in the stratum granulosum they or their respective metabolites serve as signaling molecules, acting as ligands they bind to nuclear hormone receptors (Schmuth, et al. 2004).

1.5.1. Nuclear Hormone Receptors and their Ligands

Lipids in the epidermis can be thought of as prompting their own packaging and in doing so the later stages stratum corneum formation. They do this through the activation of nuclear hormone receptors and the increased expression of the genes they regulate, genes coding the transport proteins that package lamellar granules. In keratinocytes the nuclear hormone receptors, liver X receptors (LXRs) are activated when bound to oxysterols, an oxidized form of cholesterol. LXRs have shown to be key protagonists in the initiation of keratinocyte differentiation and cholesterol transport (Schultz et al. 2000). In comparison, fatty acids are the ligands of the peroxisome proliferator-activated receptors (PPARs), which through an independent pathway also regulate terminal differentiation and lipid transport in keratinocytes. Together, LXR and PPAR stimulation facilitates the production of the lamellar membranes within the lipid envelope and epidermal development (Feingold & Jiang 2011).

LXR and PPAR are two of the 36 nonsteroidal nuclear hormone receptors; other examples include the (VDR) vitamin D3 receptor and the farnesoid X-activated receptor (FXR). Crucially these nuclear hormone receptors; LXR, PPAR, VDR and FXR once liganded must dimerise with the retinoid X receptor (RXR) forming a functional heterodimer before transcriptional activation is attained (Edwards, Kennedy, et al. 2002). To facilitate a precise change of epidermal formation activation of LXR or PPAR is preferred over the more ubiquitous RXR homodimer with it's' retinoid ligands. Retinoids have been known to suppress keratinocyte differentiation and epidermal stratification for some time; they act upon both keratin expression and the formation of the cornified envelope. RXR stimulation by retinoids activates a wide down stream regulatory pathway that ranges from the suppression of keratins involved in differentiation to the inhibition of cornified envelope formation. Though a 10 – 100 fold increase in retinoid concentration is needed to reduce keratin expression compared to a reduction in cornified envelope formation (Gilfix & Green 1984; Eckert & Rorket 1989).

Nuclear hormone receptors bind to DNA at specific cis elements called hormone response elements (HREs), which are located in close proximity to the upstream promoter and distal enhancers of the target genes. Structurally, ligand binding occurs close to the C-terminal of the protein, whilst DNA binding is orientated via conserved

twin zinc fingers located centrally in all nuclear hormone receptor proteins (Edwards, et al. 2002).

PPARβ/δ is expressed at the greatest concentration within the epidermis; the other two constitutively expressed PPAR isoforms are α and γ (Westergaard et al. 2003). Both LXR isoforms, α and β, are present in the epidermis and are activated by the same group of oxysterol, cholesterol derivatives (Chen et al. 2011). Generally in mammals LXRs play a crucial role in cholesterol homeostasis and form part of the reverse cholesterol response, regulating genes, such as ABCA1, which actively transports cholesterol. Once extracellular, cholesterol binds to the Apo-A1 protein producing a high-density lipoprotein (HDL), a transportation and storage molecule able to travel through the blood stream and reduce cholesterol concentration (Edwards et al. 2002).

1.5.2. Nuclear Hormone Receptors and Terminal Differentiation

The nuclear hormone receptors are important mediators of pathways involved in the terminal differentiation of keratinocytes. Upon topical treatment of mouse skin or cultured keratinocytes from mice, with agonists of PPARβ/δ, PPARγ and LXRs there is an increase in transcription and the subsequent translation of proteins involved in keratinocyte differentiation, TGM1, filaggrin, involucrin and loricrin (Mao-Qiang et al. 2004; Schmuth, et al. 2004). In addition, enzymes involved in the processing of lipids for the lipid envelope like beta-glucocerebrosidase, a processor of ceramides in the upper layers of epidermis, showed increased expression and activity in murine epidermis treated with LXR/PPAR agonists. The overall effect of the LXR/PPAR agonists showed an improvement to a dysfunctional permeability barrier after treatment in mice via nascent lamellae formation (Man et al. 2006). Agonists of LXR/PPAR nuclear hormone receptors are the derivatives of or the lipid metabolites produced in the lower layers of the epidermis. Examples of which are oxysterols and fatty acids produced in the basale layer, which up-regulate the epidermal lipid processing, LG secretion and the successive extracellular lipid production (Man et al. 2006).

Genes involved in epidermal differentiation such as TGM1, filaggrin, involucrin and loricrin all contain activator protein-1 (AP-1) binding sites within their promoter regions. When the recognition sequences of AP-1 are mutated up-regulation of these

genes through PPAR/LXR agonists is quiesced (Hanley et al. 2000). This suggest that AP-1 is a transcription enhancer through which the activation of LXR/PPAR nuclear hormone receptors increase the regulation of proteins involved in terminal differentiation in keratinocytes (Kömüves & Hanley 2000).

In LG synthesis the lipid transporter protein ABCA12 packages glucosylceramides into developing LGs (Sakai et al. 2007; Akiyama 2013). Abnormalities in the ABCA12 protein generate a reduction in LG formation or LGs with an irregular morphology and cargo (Expanded in section **1.8.1**). PPARβ/δ, PPARγ and with a reduced effect LXR agonists all increase ABCA12 expression in cultured human keratinocytes which in turn increase the rate of LG formation, (Jiang et al. 2008) described in **Figure 1.5.** Furthermore, in the modeling of barrier dysfunction in mouse skin, activation of PPARβ/δ and RXRα/β heterodimers increase LG synthesis and secretion, which counteracts the perturbation of the lipid envelope. Lipid envelope restoration is not mirrored with the activation of either PPARα or PPARγ nuclear hormone receptors (Calléja et al. 2006).

Topical application of retinoic acid to human skin, through the RXR nuclear hormone response, triggers the expression of many proteins that are crucial in the differentiation of keratinocytes, proteins like; TGMs, filaggrin, keratins 6 and 13, involucrin and loricrin (Gericke et al. 2013). Retinoid signaling in the skin does not specifically act in barrier formation and the proteins activated do not all work together in epidermal differentiation. However, retinoids have been trailed for use in combating Ichthyosis type skin disorders (Mihály et al. 2012).

Keratinocytes are required to transport cholesterol to supply the lipid envelope with this pivotal constituent. ABCA1 is the membrane transport protein responsible for cholesterol efflux in keratinocytes, thereby regulating cellular and extracellular concentrations. This process does not involve the LG, but is integral to obtain the correct lipid envelope composition and in doing so permeability barrier plasticity (Feingold & Jiang 2011). LXRs when activated, by the binding of oxysterols, increase the mRNA and protein levels of ABCA1, with a greater up-regulation obtained from LXRβ over LXRα, in cultured human keratinocytes and mouse model epidermis (Jiang et al. 2006). Keratinocytes amass large quantities of the desquamation-regulating

compound cholesterol sulfate. Cholesterol sulfate stimulates differentiation through the increased expression of involucrin via the AP-1 protein. All the molecules mentioned free fatty acids, ceramides, cholesterol and cholesterol sulfate, have roles in keratinocyte differentiation and lipid envelope formation (Feingold & Jiang 2011).

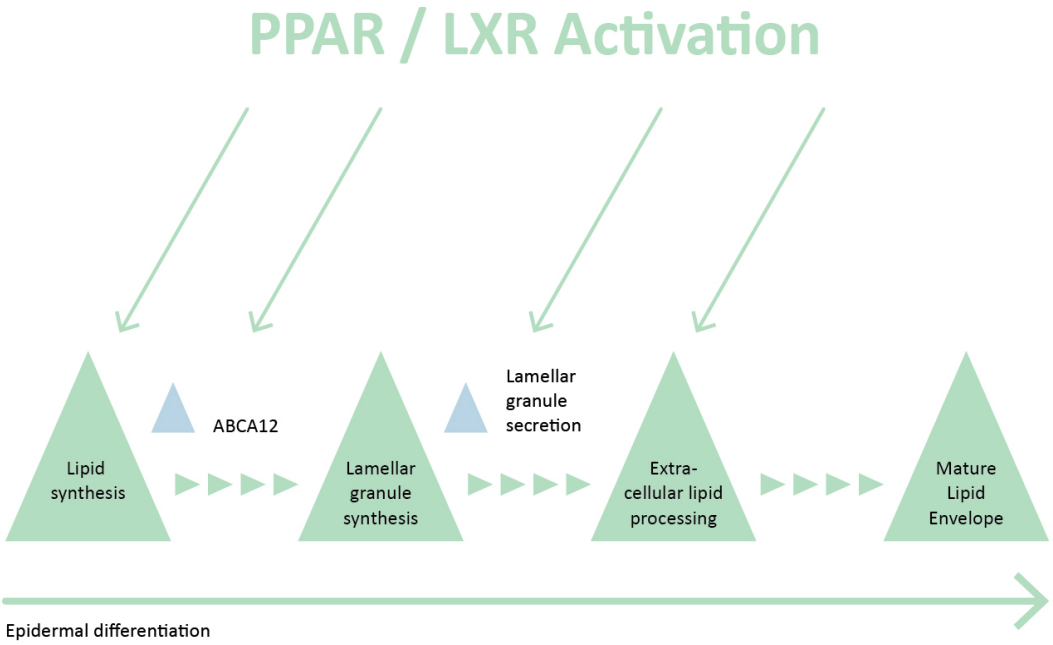

Figure 1.3. The activation of nuclear hormone receptors in the epidermis. The effect PPAR/LXR activation has on the development of the epidermis is multifaceted with regard to the formation of the lipid envelope. Ranging from lipid synthesis, to the up-regulation of proteins involved in transport and envelope structure, PPAR/LXR activation is a key pathway in a correct epidermal differentiation.

1.6. The Ichthyoses

Ichthyoses are a heterogeneous group of skin disorders, which through aberrant keratinocyte differentiation and desquamation, produces disorders of cornification characterized by tenacious scaling. In disorders with an inherited aetiology when causative genes have been segregated, their ensuing proteins are predominately involved in the synthesis, transport and formation of the lipid envelope or the desquamation of the upper cornified layer (Akiyama 2011).

With rough divisions ichthyoses can be separated into three groups; the congenital forms, the acquired ichthyosis that are a systemic disease and the ichthyosiform disorders. The rare congenital ichthyoses present at birth with collodion membranes or an ichthyosiform erythroderma, the relatively more common inherited types like X-linked recessive ichthyosis (XLRI) and ichthyosis vulgaris (IV) present immediately after birth (Oji & Traupe 2006). The acquired/systemic ichthyoses present with a variety of non-epidermal phenotypes, for instance acquired ichthyosis associated with systemic lupus erythematosus can trigger a range of hyperactive immune symptoms (Tlacuilo-Parra et al. 2004). The different mechanisms by which ichthyoses cause perturbations in the epidermis provide a unique insight into the function of a myriad of lipids, proteins and enzymes involved in the terminal differentiation of keratinocytes.

1.7. Harlequin Ichthyosis

1.7.1 Clinical Features

Harlequin Ichthyosis (HI; MIM242500) is the most severe disorder in the family of autosomal-recessive congenital ichthyosis (ARCI). The first recorded case was noted in 1750 in the accounts of Reverend Oliver Hart (Waring 1932). In the past premature babies often died in the neonatal stage, at the early stage diagnosis of HI can be easily made due to a characteristic phenotype. HI is a chronic disorder that is infrequently fatal, due to the possible use of oral retinoids and modern neonatal care the mortality rates have declined to around 56%, in a study of 45 cases (Rajpopat et al. 2011). Sufferers from HI present with a dramatically thickened dehydrated skin over the

majority of the body, with large diamond shaped hyperkeratotic plates separated by deep fissures (Francisco et al. 2004). The abnormal skin restricts movement, breathing and can constrict limbs causing *in utero* autoamputation. Furthermore, neonates show anatomical disfiguration of the lips causing eclabium, eyelids causing ectropion and vestigial ears (Kelsell et al. 2005). With an extremely compromised skin barrier, HI neonates have a high probability of dehydrating through TEWL and sepsis due to secondary infection. Neonatal treatment is commonly supplemented with the application of retinoid drugs that stimulate the shedding of the retained squames to reduce the dramatically thickened epidermis (Brecher & Orlow 2003). HI infants that survive the early stages of childhood and further, produce a skin phenotype akin to a severe non-bullous congenital ichthyosiform erythroderma (NBCIE), an erythrodermic form of lamellar ichthyosis (Haftek et al. 1996).

Figure 1.4. A typical presentation of HI at birth. The newborn exhibits the characteristic HI phenotype with hyperkeratotic plates, fissures, eclabium and flattened ears. HI past infancy presents as shown with hyperkeratosis, erythema and disrupted hair follicle growth similar to a severe NBCIE.

1.7.2. Ultrastructural Features of Harlequin Ichthyosis

The histological study of HI has found a collection of abnormalities present in the epidermis of the majority of cases. The most striking feature is the hyperkeratosis, this thickening of the stratum corneum of retained, compressed squames is present in all cases of HI (Dale et al. 1990). There is increased stratification of the epidermis, not as dramatic as the enlarged stratum corneum, though each layer does show elongation and contain more keratinocytes in the relative phase of differentiation. Nuclei of keratinocytes are flattened in the HI epidermis at an earlier stage of differentiation relative to normal skin; however in some cases of HI parakeratosis occurs and these nuclei are retained in the uppers layers and not degraded (Hsu et al. 1989).

Morphologically abnormal or absent LGs were detected with electron microscopy, though when present their location was confined to the lower levels and not in their normal transit between the stratum granulosum and corneum. This absence correlates to the lack of extracellular lipid lamellar and further disruption to the normal trafficking of lipids, structural proteins and proteases bound for the stratum corneum (Akiyama et al. 1996). Electron microscopy indicates other types of disruption alongside the characteristic HI histology, such as the multitudes of vacuoles, autophagic in nature, neighbouring an accumulation of cholesterol and its' derivatives in crystal form, both of which are retained in the cytoplasm of keratinocytes of the stratum corneum in the epidermis of HI patients (Buxman et al. 1979).

1.7.3. Genetics of Harlequin Ichthyosis

HI was shown to follow an autosomal recessive pattern of inheritance after a period of uncertainty due to cases of multiple family members affected and that the underlying cause could be through a dominant mutation. However, in 2005 Kelsell *et al* used a combination of single nucleotide polymorphism (SNP) chip array to map and microsatellite markers to confirm, a region of homozygosity, 2q35. Within this region causative mutations were found in the gene *ABCA12* in 11 of the 12 individuals with HI screened.(Kelsell et al. 2005) The aetiology of HI coincides with defects in the gene *ABCA12*; the transcribed protein is a constituent of the superfamily adenosine triphosphate (ATP)-binding cassette (ABC) active transporters. All the mutations in this study were predicted to result in a truncated protein, they included nonsense mutations,

frameshift deletions and whole exon deletions (Kelsell et al. 2005). Around the same point in 2005 Akiyama *et al* corroborated this finding by showing HI segregating with recessive mutations in the gene *ABCA12* (Akiyama et al 2005).

In 2011 a clinical review of 45 HI cases added further confirmation that mutations in *ABCA12* were causative and some of which were missense mutations. The review found that homozygous mutations produced a greater chance of early mortality than babies with compound heterozygous mutations, or the other prospective, compound heterozygotes have a survival advantage or benefit more from treatment. A possibility here is that another recessive disease may be lingering with no diagnosis. More plausible is the relationship of location of mutation in the protein and severity of disease phenotype (Rajpopat et al. 2011).

1.8. *ABCA12*

The gene *ABCA12* can be found on the reverse strand of chromosome 2 between the coordinates 214,931,542-215,138,428. It holds three main transcripts, with the longest protein coding transcript holding 53 exons at a transcript length 9100bp and a translated length of 2595 amino acid residues. The second transcript starts in the 8 exon of the primary transcript and runs until completion, whereas the third is the first 3 exons of primary transcript only (Lefévre et al. 2003). The translation of the ABCA12 protein starts from the 221st residue in exon 1 and apart from the aforementioned alternative transcripts has no other splice variants. Membrane spanning ABC transporters such as ABCA12 mediate allocrites across membranes by conformational changes in their trans-membrane domains (TMD) via an ATP dependent translocation. The ABCA12 protein holds two TMD, which house 6 membrane spanning α-helices and form the bridge that straddles the plasma membrane. Bound to the cytoplasmic end of each of these TMD are the ABC transporter domains (1 and 2) that hydrolyse ATP to ADP releasing the energy needed for transportation. ABC transporter domains contain the ATP binding domains or nucleotide binding domain (NBD), translated from 3 conserved sequence motifs: Walker A and B domains and the signature C motif situated between the two Walker domains (Walker et al. 1982; Hyde et al. 1990).

The 3 motifs synonymous with ABC transporters; Walker A, B and signature C are crucial in the binding and hydrolysis of ATP, obtaining the energy required to alter the structural configuration of the TMD to transport allocrites across membranes. In the case of ABCA12 transporting lipids into LG transport vesicles against the electro-chemical and concentration gradients (Vasiliou et al. 2009). The Walker A motif supplies a phosphate binding loop that holds the triphosphate in place for hydrolysis and remains bound to the ADP afterwards. While ATP is bound to the NBD the Walker B motif with its' many hydrophobic residues and terminal aspartate creates a local environment that coordinates the positioning of a magnesium ion. This charged molecule induces a dipole across a bound phosphate that initiates ATP hydrolysis (Walker et al. 1982).

The ABC transporter domains 1 and 2 of *ABCA12* only share 36% sequence homology compared to that of NBD1 and 2, with their conserved structural motifs, share 87.5% homology. The dissimilarities in the two ABC transporter domains may infer slightly different roles and cause different severity of protein dysfunction when mutated. This is further explored in **1.8.3.** The structure of the ABCA12 protein has not yet been resolved possibly as X-ray crystallography of such a large hydrophobic membrane spanning protein is extremely difficult to perform.

1.8.1. The Role of *ABCA12* in the Epidermis

The ABCA12 protein is a member of the ABCA subfamily of ABC transport proteins; it actively transports allocrites against a concentration gradient into transport vesicles. In the epidermis ABCA12 is constitutively expressed in the suprabasal layers, but markedly up-regulated in keratinocytes of the stratum granulosum and still present in some retained corneocytes of the stratum corneum (Akiyama 2005). The mature ABCA12 protein localises to the Golgi apparatus, TGN and both forms of LGs. The co-localization of ABCA12 to the cis-Golgi (GM130) and trans-Golgi (TGM-46) markers is continuous throughout suprabasal epidermis, though only in the upper stratum spinosum and stratum granulosum do LGs, ABCA12 and glucosylceramides co-localise (Sakai et al. 2007). At this point in epidermal differentiation ABCA12 packages lipids

from the cytoplasm and Golgi apparatus into the developing LGs (Sakai et al. 2007; Akiyama 2013).

The lipids glycoslyceramide and sphingomyelin are products of ceramide processing in keratinocytes of the upper stratum spinosum and lower stratum granulosum. They are then package into LGs through the lipid transporter protein ABCA12 (Sakai et al. 2007). When this trafficking is impaired through an aberrant *ABCA12* there is an accumulation of glycoslyceramide and sphingomyelin in keratinocytes of the lower stratum granulosum and a reduction of these lipids in LGs (Mitsutake et al. 2010). In functional LGs they are accompanied by other lipids, which when extruded are further processed into ceramides with a range of properties that help manufacture the extracellular lamellar membrane structures of the lipid envelope (Uchida & Holleran 2008). Suprabasal ceramides of the epidermis have been shown to up-regulate the transcription of the gene *ABCA12* through the PPARβ/δ pathway. Showing that ceramide precursors of ABCA12 allocrites induce the expression of the protein that will transport their lipid derivatives (Jiang et al. 2009).

Terminal differentiation of the epidermis concludes with the desquamation of keratinocytes from the stratum corneum. This shedding of the outermost layer of skin helps maintain the structural and functional integrity of the epidermis, which is prevented in HI. As extruded lamellar granule content, predominately complex lipids and enzymes, when released into the extracellular space is involved in the desquamation of the stratum corneum (Akiyama 2006). In HI hyperkeratosis and the retention of squames leads to a dramatically thickened stratum corneum and through histological study and *in vitro* modelling has been correlated to a reduction of proteases in the stratum corneum (Milner et al. 1992).

Proteases are expressed late in epidermal differentiation, where they act in the desquamation of squames. They are transported to the point of desquamation by the LG system. In an organotypic co-culture (OTCC) with an ablated *ABCA12* there was a reduction in protease activity in the stratum corneum due to a dysfunctional LG system. This OTCC mirrored HI epidermis and showed how the LG cargos and desquamation proteases CTSD and KLK5 are reduced in the upper layers of the epidermis (Thomas et al. 2009a). As previously described in **1.2.2.** these proteases alongside others act in

cascades to degrade the structural proteins of the cornified envelope like desmoglein-1 and corneodesmosin (Caubet et al. 2004; Descargues et al. 2006).

While the distribution of CTSD and KLK5 are abnormal and their expression is reduced in *ABCA12*-ablated epidermis, this is not a constant theme with all proteins involved in desquamation. For example, KLK7 and its' inhibitor LEKT1 are expressed normally in *ABCA12*-ablated OTCC (Thomas et al. 2009a). Taken into consideration that neither LEKT1 nor KLK7 co-localise with the ABCA12 protein, it can be postulated that there are parts of LG formation *in absentia* of ABCA12. This in turn corroborates with that to some extent LG formation is determined by cargo, as described in **1.3.1.** This highlights the point that although ABCA12 is not directly or indirectly involved in the transportation of all proteases, when aberrant and unable to transport its' lipid allocrites the fitness of these respective LGs is severely impaired.

Through the study of patient material, mouse models and *in vitro* models many of the ways in which HI effects normal epidermal differentiation have been brought to light. Not only does the typical HI epidermis hold a dysfunctional lipid envelope and a reduction in the activity of desquamation proteases, it also exhibits premature terminal differentiation (Yanagi et al. 2008a). Immunohistochemistry demonstrates the change in differentiation marker localisation, where K2e, involucrin, loricrin, and TGM1 would normally be found in the stratum granulosum and corneum exclusively, in HI epidermis these markers can be found throughout the suprabasal layers. Furthermore, levels of profilaggrin in skin from individuals with HI and a mouse model have found to be either elevated or normal, though levels of the processed, functional (27kDa) filaggrin monomer involved in cornified envelope formation and hydration are significantly deceased (Dale et al. 1990; Smyth et al. 2008). All of which suggests that either ABCA12 has a role in regulating keratinocyte differentiation or that the disruption caused in the upper layers of the epidermis by an aberrant ABCA12 has a negative effect on the biology of suprabasal keratinocytes.

Oral retinoids are the most frequently used treatment for HI, as they stimulate the shedding of the retained squamous cells through the previously described RXR pathway (Brecher & Orlow 2003). Though the multitude of genes up-regulated by RXR stimulation in the epidermis seems slightly unspecific, retinoid treatment does aid

desquamation with relatively limited side effects (Eckert & Rorket 1989). In a clinical study of 45 HI cases, on only one single occasion did treatment with a RXR agonist have a related adverse effect, with a child contracting cataracts. A link between retinoids and cataracts was previously reported, but it was thought to be an association solely with adults and not with children (Rajpopat et al. 2011).

1.8.2. The Role of *ABCA1* in the Epidermis

In HI there is an accumulation of glucosylceramides in the basal layers of the epidermis due to decreased transportation by LGs. Subsequently, there is a reduction in the concentration of ceramides, such as ω-hydroxyceramides in the stratum corneum (Zuo et al. 2008). Alongside these changes in ceramide transportation is the possible reduction in cholesterol regulation within the epidermis and the subsequent loss of cholesterol as a regulating molecule, as an aberrant *ABCA12* has been shown to diminish ABCA1 cholesterol efflux (Fu et al. 2013).

Keratinocytes are required to transport cholesterol to supply the lipid envelope with a pivotal constituent. ABCA1 is the membrane transport protein responsible for cholesterol efflux in keratinocytes, thereby regulating cellular and extracellular concentrations. This process does not involve the LG, but is integral to obtain the correct lipid envelope composition and in doing so permeability barrier plasticity (Feingold & Jiang 2011). When cholesterol combines with the range of ceramides in the lipid envelope they form gel phase lamellar structures that are predicted to have a greater pliability then those made from repeating phospholipids alone (Takahashi et al. 1996). When the amount of cholesterol in the stratum corneum is reduced the permeability barrier becomes susceptible to TEWL through deformities in membrane formation (Zettersten et al. 1998).

LXR and PPAR agonist have been implicated in the redistribution of terminal differentiation markers, which are premature in HI epidermis (Jiang et al. 2008). The activation of LXRs through the binding of oxysterols induces a significant increase in transcript and protein levels of ABCA1. The subtype LXRβ has a much greater affect then LXRα, as shown with studies utilizing mouse models and cultures human keratinocytes with LXR agonists (Jiang et al. 2006). With the ABCA1 protein known to

transport cholesterol and other phospholipids out of keratinocytes and its' possible down-regulation under *ABCA12* ablation there is an opportunity to re-establish this pathway through LXRβ (Schmitz & Langmann 2005; Fu et al. 2013).

The metabolite and precursor to cholesterol in keratinocytes of the stratum basale is cholesterol sulfate, which in large quantities aids the regulation of differentiation and desquamation. Without the transportation of cholesterol via the ABCA1 protein, the intracellular build-up could limit the forward reaction of steroid sulfatase, resulting in an accumulation of cholesterol sulfate (Elias, et al. 1984; Zettersten et al. 1998). Cholesterol sulfate stimulates involucrin expression through the differentiation activator protein AP-1 and inhibits serine proteases involved in desquamation (Feingold & Jiang 2011).

1.8.3 *ABCA12* and Disease

A dysfunctional *ABCA12* gene has been attributed to several autosomal recessive congenital ichthyosis (ARCIs); lamellar ichthyosis-2 (LI2) associated with missense mutations restricted to the first ATP binding domain (NBD1) and Nonbullous congenital ichthyosiform erythroderma (NBCIE) associated with missense mutations throughout the protein (Lefévre et al. 2003; Jobard et al. 2002). ABC transporter domains 1 and 2 have 36% homology and within these domains the NBD1 and 2 share 87.5% homology. However, highly deleterious mutations in ABCA12, such as nonsense substitutions and frameshifts predominately underlie HI (Thomas et al. 2006; Scott, Rajpopat, et al. 2013). Missense mutations isolated to specific domains of the ABCA12 protein also underlie some cases of HI, all of which infers there is a genotype to phenotype relationship for *ABCA12*, which is discussed further in **chapter 3**, (Thomas et al. 2006).

1.9. ABC Transporters

ABCA12 belongs to the ABC transporter superfamily, which is the largest transporter gene family. ABC transporters have lineages tracing from prokaryotic membrane transporters and have diverged into a diverse transporter family genetically present in

model organisms: Saccharomyces cerevisiae, Caenorhabditis elegans, Drosophila melanogaster and in all higher eukaryotes. They transport a large range of allocrites including lipids, sugars, proteins, peptides, metal ions and amino acids across both intra and extracellular membranes (Dean et al. 2001). The general organisation throughout the ABC family is a TMD and a NBD in half transporters or two of each TMD and NBD in full transporters. In full transporters the two halves share topological features and varying levels of homology depending on the transporter sub family. Within all the eukaryotic ABC transporters are the Walker A, B and signature C motifs, which are all highly conserved due to their participation in ATP binding and hydrolysis (Vasiliou et al. 2009).

1.9.1. The ABCA Subfamily

The ABCA subfamily consists of twelve full transporter proteins and a single non-transcribed pseudo gene, *ABCA11*. The twelve functional transporters can be split roughly into two groups with the first group comprising of *ABCA5*, *6* and *8-10* forming a gene cluster on chromosome 17q24. This group of *ABCA* genes are still relatively unknown in terms of associated diseases, tissue location and function (Dean et al. 2001). The second group are sparsely located on six different chromosomes and consist of the genes *ABCA1-4, 7, 12 and 13.* This group transport a range of lipids in different tissues at different points of differentiation.

The cholesterol transporter protein ABCA1 plays a major role in regulating the levels of the intracellular high-density lipoprotein and cholesterol. Mutations in the gene *ABCA1* can cause familial hypoalphalipoproteinaemia or the more severe Tangier disease, the presentation on which form is determined by the location and type of mutation within the gene (Slatter et al. 2008). *ABCA1* ablation causes a significant reduction in the amount of high-density lipoprotein in the blood and an accumulation of intracellular cholesterol in several tissues (Brooks-Wilson et al. 1999).

The ABCA3 protein transports lipids into lamellar bodies found in the lungs. These lipid packed lamellar bodies extrude a surfactant on the alveolar type II cells, which maintains a low alveolar surface tension during respiration and is essential for normal lung function (Haller et al. 1998; Yamano et al. 2001). Mutations in the gene *ABCA3*

cause a deficiently in this lung surfactant and an increase in alveolar surface tension in new born babies (Shulenin et al. 2004). The lipid transporter that is expressed in the brain is *ABCA13,* mutations in which have been associated with a susceptibility to develop bipolar disorder and schizophrenia (Knight et al. 2009).

In *ABCA12*, as with other ABC transporters there is a direct relationship between type and location of mutation with severity of disease. For example, *ABCA4* ablation causes four forms of degenerative retinal dystrophy: Stargardt disease, cone rod dystrophy and retinitis pigmentosa, here severity of retinal perturbation and age of onset are dependent on the type of causative mutation in the gene *ABCA4* (Heathfield et al. 2013; Kitiratschky et al. 2008).

1.10. ARCI

ARCI is a set of rare ichthyoses that can be genetically and clinically heterogeneous (Oji & Traupe 2006). With NBCIE the affected neonates present with a widespread collodion-like membrane, although the presentation and severity of the disease can be diverse (Sandler & Hashimoto 1998). At the most severe end of the spectrum is HI, which can be fatal. LI and NBCIE are less severe with better prognoses.

NBCIE is phenotypically characterised by widespread erythema and overlying fine white scales. Affected individuals may develop palmoplantar keratoderma and nail dystrophy (Williams & Elias 1985). Biallelic mutations in the genes *TGM1* (MIM 190195), *ALOXE3* (MIM607206) and *ALOX12B* (MIM 603741) have been found to be causative in patients with NBCIE (Huber et al. 1995; Krebsová et al. 2001; Jobard et al. 2002). ALOXE3 and ALOX12B are a distinct subclass of mammalian lipoxygenases primarily confined to the epidermis. A mouse model of ARCI with a mutated *ALOX12B* gene produced pups with severe scaling and a deregulated epidermal formation with a thickened stratum corneum. This model and a subsequent in vitro study, utilising human epithelial cells found a dramatic reduction in the epidermal enzymatic products of 12R-lipoxygenase (12RLOX), when *ALOX12B* contained nonsense or missense mutations (Eckl et al. 2005; Moran et al. 2007).

1.11. Hypothesis and Aims

To further the understanding of the role of ABCA12 in HI, molecular diagnosis of HI patients and the genetic and functional characterisation of the patient derived HI cell line will be undertaken. The hypothesis underlying this study is that the aberrant ABCA12 in the patient derived cell line will induce *in vitro* aspects of HI, which represent the malformed HI epidermis and under the application of nuclear hormone receptor agonists these aspects will be modulated.

- The identification of novel or known causative mutations in *ABCA12* by a range of methods to further the understanding of the genotype to phenotype relationship in HI.

- The development and utilisation of techniques to identify complex/regulatory mutations.

- The complete genetic analysis of ABCA12 in the patient derived HI immortalised cell line and identification of the subsequent effects on the *ABCA12* transcript and protein.

- The use of calcium shift culture and the HI cell line to analyse the premature expression of terminal differentiation markers and the modulation of *ABCA1*.

- Determine whether a recovery from the HI cellular phenotype can be achieved by renewed expression of ABCA1, through the application of LXR and PPAR agonists in monolayer and organic cultures.

Chapter 2: Materials and Methods

2.1.1. Nucleic Acid Methods

2.1.2. DNA and RNA extraction

DNA extraction from patient blood and keratinocytes was carried out with the QiaAmp DNA blood mini kit (Qiagen; Manchester, UK), using the blood sample and cultured cells protocols according to manufacturer's instructions. Cells were plated in a well plate and grown until confluent, when they were detached by use of trypsin, washed and resuspended in 200 µl PBS. 20 µl protease and 200 µl lysis buffer AL was added and this mixture vortexed and incubated at 56°C for 10 minutes. After which the samples were briefly centrifuged and 200 µl of 70% ethanol was added. Following another few seconds of centrifuge the samples were pipetted into a QiaAmp spin column and spun at 8,000 rpm for 1 minute. After the subsequent column washes with the AW1 and 2 buffers the column was transferred to a new microcentrifuge tube, spun again to remove and remaining ethanol. 200 µl of buffer AE was used to elute DNA from the column.

Isolation of total RNA was obtained from cells usually at high confluency at the termination of the experiment. RNA was also obtained from skin and hair using a handheld homogeniser to reduce the fibrous content. Obtained from hair by plucking of a few strands of hair with the hair follicle attached, the follicle was then detached and homogenised in 350 µl buffer RLT supplemented with 3 µl β-mercaptoethanol. The protocol was adapted from a Takeichi group publication (Takeichi et al. 2013). The cells were washed twice using PBS and then lysed directly in the well of the cell culture plate using 350 µl buffer RLT supplemented with 3 µl β-mercaptoethanol to inactivate the endogenous RNases. Cells were removed from the cell culture dish with a cell scraper (Fisher Scientific; Loughborough, UK), QIAshredder (Qiagen) was used to homogenise cell and tissue lysates and to degrade high molecular weight genomic DNA and cellular components. Following that the RNeasy mini kit (Qiagen) was used and the protocol followed to the manufacturer's specifications. The RNA was eluted and resuspended from the column using 34 µl of RNase-free water. This was the same kit used for the extraction of RNA from cultured cells. All RNA obtained was stored at -80 °C while not in use.

2.1.3. DNA and RNA quantification

Both patient and control DNA was quantified by use of a NanoDrop (Qiagen; UK), ND1000 spectrophotometer. To operate, 1 µl of DNA is pipetted onto the measurement pedestal of the NanoDrop machine. The machine records the optical density of the sample at an absorbance of 260/280nm for DNA analysis, the ratio of absorbance at 260 and 280nm gives a measurement of purity for the sample. A ratio in the range of 1.8-2.0 is a satisfactory level. To measure the concentration of a sample of RNA, a similar protocol is utilised, exact the absorbance is measured between 263/230nm and a ratio between 2.0-2.2 is considered acceptable.

2.1.4. Primer design

All designed primers were purchased online from Sigma-Aldrich (Haverhill, UK). Specific primer pairs were designed for annealing to either genomic DNA or cDNA and for use in PCR amplification, Sanger sequencing, side directed mutagenesis or cloning/ligation. Predominately the online software Primer3 (v.0.4.0) was used to design primers for specific sequence and Ensembl to check location and primer regions for SNPs. The synthesised oligonucleotides varied in length from usually 18-26bp, depending on positioning, GC content of annealing sequence and regional SNPs. Gradient PCR reactions were used to optimise the annealing temperature for each set of primers, gradients would be in the region of 55-65°C and through band analysis the greatest optimisation would applied to future PCRs. Designed primers for the entirety of the *ABCA12* transcript (cDNA), *ABCA12* genomic and others associated primers for screening variants and allelic size variants can be found in **Table A1.1, A1.2, A1.3 and A1.5** respectively.

2.1.5. DNA amplification by polymerase chain reaction (PCR)

To begin with a master mix was a produced for each set of PCR reactions, this would then be pipetted out into equal parts with the individual addition of primers and finally DNA added to the appropriate 200 µl (thin walled) PCR tubes (Thermo Scientific). BioTaq (Bioline) and AmpliTaq Gold (Life Technologies) were the two main Taq polymerase systems that were used. The BioTaq master mix contained: 10.4 µl of ddH_2O, 2 µl of 10X buffer, 0.6 µl of $MgCl_2$ (50 mM), 0.4 µl of dNTP, 0.2 µl of each forward and reverse primers (100 µm), and 0.2 µl of Taq polymerase and once in

individual tubes with 14 µl of master mix, 1 µl of DNA. AmpliTaq Gold was used more frequently and optimised for many different PCR reactions with different primers. The standard was a master mix of 7.8 µl of ddH_2O, 1.5 µl of AmpliTaq Gold buffer II, 1.2 µl of $MgCl_2$ (25 mM), 0.3 µl of dNTP, 1 µl of betaine, 1 µl of 10 µm forward and reverses primers; 0.2 µl of TaqGold polymerase and finally the appropriate addition 1µl of DNA after 14 µl were individually pipetted out. For the negative control, to check for contamination of any of the master mix components, 1 µl of ddH_2O was added to a tube with 14 µl of complete reaction. The control and reaction tubes were spun by a bench centrifuge to reduce air bubbles and solution disruption and placed on a thermo cycler. Prior to this point all mixing, solutions and reagents were kept on ice whilst pipetting.

All of the reaction tubes were placed into a DNA engine Tetrad 2 Peltier thermocycler (MJ Research) and the following programme was used to amplify the specific regions of DNA: 95 °C for 10 minutes to initiate the hot start Taq, followed by 37 cycles of: 95 °C for 30 seconds for denaturation of the DNA, producing single stranded DNA, X °C for 30 seconds for the annealing stage, allowing primers to bind to the DNA – the annealing step would be optimised for every set of primers. An extension step of 1 minute per 1Kb of amplicon at 72 °C was then carried out to extend complementary strands, after the 37 cycles was complete, the penultimate, an extension step of 72 °C for 10 minutes was carried out before samples were cooled to 4 °C.

2.1.6. Agarose gel electrophoresis

PCR products and any other DNA fragments were run on agarose gels to separate fragments by weight. A 1% w/v agarose gel can be prepared by heating 1gram of agarose in Tris-Borate-EDTA buffer (TBE) until dissolved in a microwave, ~2 minutes. The agarose-TBE solution was then cooled and then 0.5 µg/ml ethidium bromide was added and mixed until uniform. Whilst still liquid the solution was poured into a casting tray and combs were inserted to create wells. After 10 minutes the solution formed a gel that could be loaded with the PCR products that were mixed with orange G in a 2:1 ratio and the 1Kb Plus DNA ladder 10% v/v (Invitrogen). Samples were electrophoresed at 75-120 volts and as the ethidium bromide interchelates with the DNA was visible and photographed by a transillumination (MultiImage Light Cabinet, Alpha Innotech Corporation and a Sony P-D890).

2.1.7. Gel purification

DNA fragments were separated on electrophoresis gels before excision and purification for further sequencing or cloning. Agarose gels were synthesised following the protocol outlined in **2.1.6.** with the exception of Tris-Acetic acid-EDTA buffer (TAE) preferred over TBE as excised fragments retain a higher concentration of DNA. DNA fragments were excised under UV light by use of a sterile scalpel and fragment containing cuboid segments of gel were retained in 1.5 microcentrifuge tubes. Purification was achieved through the application of the QIAquick Gel Extraction Kit, (Quiagen, UK) following the manufacturer's instructions. Purified DNA was analysed on an agarose gel, by mixing the eluted DNA product 5:1 with loading dye, homogenising by pipetting up and down, before loading on to the gel.

2.1.8. Sanger sequencing

The preferred Sanger sequencing reaction was the BigDye Terminator v3.1 Cycle Sequencing Kit (Applied Biosystems). The protocol was optimised to produce the following components and conditions: PCR product (1-3µl, depending on band brightness) was incubated with 6µl of ExoSAP (GenomeCentre) at 37 °C for 45 minutes followed by 80 °C for 15 minutes and 4 °C for 5 minutes. This degrades any remnants from the PCR reaction that could disrupt the sequencing reaction. Clean fragments were then added to a reaction of 1 µl of Big Dye Terminator Master mix v3.1, 3 µl of better buffer (Microzone), 1 µl of 10 µM of a forward or reverse primer that anneal within the amplified fragment and ddH_2O making a final volume of 11.5 µl. The thermocycler program was 25 cycles at 96 °C for 30 seconds, 58 °C for 15 seconds, 60 °C for 1 minute, finally the products were cooled at 4 °C for 10 minutes.

Precipitation of the ExoSAP products was performed by the addition of; 2.5 µl of 125 mM EDTA and 30 µl of cold absolute ethanol that were incubated on ice for 10 minutes. Pellets were formed by centrifugation of the mixture at 4000 rpm, 4 °C for 20 minutes; they were then washed with 125 µl 70% ethanol and incubated on ice for another 2 minutes, then centrifuged for 5 minutes at 4000 rpm. Precipitated BigDye products were then air dried at RT or on a hot block for 1 minute. They could be then be resuspended in 10 µl HiDi formamide, incubated at 95 °C for 3 minutes and on ice for a further 3 minutes. Products were then centrifuged for 2 minutes to remove any air

bubbles and placed on the ABI Prism 3130xl Genetic Analyser (Applied Biosystems, Life Technologies). Traces were analysed by using the chronograph software Chromas LITE v 2.01 (Technelysium Pty Ltd) and aligned using the Multalin multiple alignment tool (multalin.toulouse.inra.fr/multalin). The analysis of protein sequences and conservation between proteins or species was performed on ClustalW2 multiple sequence alignment tool and with reference to the NCBI protein database respectively (www.ebi.ac.uk/tools/msa/clustalw2) and (http://www.ncbi.nlm.nih.gov/protein).

2.1.9. Reverse-Transcriptase PCR (RT-PCR)

RT-PCR was performed using the Superscript II reverse transcriptase enzyme and kit (Invitrogen). Concentrations of reagents follow the manufacturer's instructions, though are slightly optimised depending on RNA concentration. Per individual sample, making 20 µl of cDNA, the following was pipetted into 200 µl RNase free thin-walled PCR tube: 8 µl of RNase free ddH_2O, 1 µl of oligoDT, 0.5 µl of random primers (as hexamers), 1 µl of dNTP and finally 1.5 µl of RNA (diluted to 110 ng/µl). All the reactions were incubated at 65 ℃ for 5 minutes then removed for the thermo cycler and incubated on ice.

Whilst samples were on ice 4 µl of 5x first strand buffer, 2 µl of 0.1M DTT and 1 µl of RNase OUT (Invitrogen) were added to the reaction. The individual reactions were incubated at 42 °C for 2 minutes before 1 µl (200 units) of superscript II reverse transcriptase (Invitrogen) was added to all apart from any negative controls. Negative controls were prepared with the RNA being used in the synthesis, but with RNase free water instead of the superscript enzyme. Samples were incubated at 42 °C for 50 minutes followed by 70 °C for 15 minutes. PCR of the cDNA using primers complementary to the housekeeping gene HPRT was carried out to check for cDNA quality and genomic DNA contamination in the negative controls.

2.1.10. Real Time PCR (qPCR)

Primer design was carried out as explained in **2.1.4.** with the extra provision of abiding to the GC content range of 55-62%. The annealing temperature (A_T) for primer pairs was calculated by the equation:

$A_T = 69.3 + (0.41 \times GCcontent) – (650 / oligonucleotide\ length)$

The lowest A_T from the pair of primers is used as the A_T for the initial optimisation reactions. Primers used for qPCR are listed in **Table A1.4.** The quantitative real time PCR was performed on a Rotorgene Q thermocycler (Quiagen, UK), by use of conventional methods. For every 20 µl reaction mixture held 2x Rotorgene Multiplex PCR Buffer, 1 µM of forward and reverse primers complimentary to genes under investigation and control, 1 ng of sample cDNA, 500 nM of labelled probe and ddH_2O to complete the mixture. The reaction conditions for qPCR were 10 minutes at 95 °c, followed by 45 cycles of 95 °C for 15 seconds and 60 °C for a further 50 seconds. At every 60 °C stage, data collection was performed by the Rotorgene by means of fluorescence detection in the green and yellow channels, the emission of which was the result of the binding of 6-FAM and HEX labelled probes respectively.

Relative expression of the gene of interest was calculated against the control gene by the delta CT method. Here the expression of the gene of interest is equal to $2^{deltaCT}$, where delta CT is calculated as the difference at which each fluorescence signal rises above background levels. A paired t-test was utilised for the statistical analysis of results. Significance was given at $p<0.05$ (*), highly significant at $p<0.01$ (**) and very high significance at $p<0.001$ (***).

2.2. Molecular biology

2.2.1. TOPO cloning

TOPO TA cloning was used to sub clone PCR products, excised and purified from gels, to isolate possible transcript variants for sequencing. The TOPO TA kit (Invitrogen) was used as per the manufacturer's instruction and utilises the transformation of competent cells described in **2.2.5.** The 6 µl TOPO cloning consists of the following components; 0.5-4 µl (concentration dependent) of PCR product, 1 µl of salt solution, 1 µl of TOPO vector and ddH_2O to make up to 6 µl. The reaction mixtures were mixed gently before incubated at room temperature for 5 minutes. After the transformation of competent cells, clones can be analysed through PCR of TOPO vector M13 forward and reverse primer sequence sites.

2.2.2. Restriction enzyme digest

Restriction enzyme digests were utilised to linearize plasmids, to increase transfection efficiency and to check DNA samples for variants. Restriction digests were performed as per manufacturer's instruction, which for the majority of reactions gave the reaction mixture of: 1 µl of restriction endonuclease, 1 µl of the complementary 10x reaction buffer (New England Biolabs; MA, US), 5 µl of PCR product or 1-2 µg of plasmid DNA and ddH_2O to make a final reaction volume of 10 µl. Reaction vessels were mixed gently and incubated at 37 °C for 1-2 hours followed by an inactivation step of 80 °c for 20 minutes. Restriction digest products were analysed on a 2% agarose gel, as described in **2.1.6.** and plasmids for transfections were aliquoted to reduce freeze-thaw cycle damage on the plasmid DNA.

2.2.3. Transformation of competent cells

The chemical transformation procedure of One Shot TOP10 chemically competent *E. coli* (Invitrogen) was used to amplify plasmid DNA, typically post-cloning, before undergoing mini/maxi preps (Qiagen). Following the manufacturer's instructions; 1-5µl of plasmid DNA was added to a single vial of One Shot *E. coli,* gently mixed and incubated on ice for 30 minutes. The vial containing the plasmid DNA, *E. coli* and reaction mixture was heat shocked for 30 seconds at 42 °C, after which the vial was placed on ice while 250 µl of pre-warmed SOC medium was added. The vial was then incubated at 37 °C for 1 hour at 225 rpm on a shaking incubator, allowing the expression of antibiotic resistance genes. 20-200 µl from the vial was then spread evenly on pre-warmed, labelled LB agar plates made with a specific antibiotic complementary to the One Shot *E. coli* used. Plates were then inverted and incubated at 37 °C overnight before individual colonies were selected in the morning.

2.3. Cell Culture

2.3.1. Cell lines and Conditions

K17 and HI (harlequin ichthyosis patient derived) cell lines were immortalised from the patients using the HPV method and were cultured in EpiLife (Life technologies) with

the HGVS growth supplement provided, the addition 100 µg/ml streptomycin and cultured at 10% CO_2 in a humidified incubator. The NEB1 and HaCaT immortalised human keratinocyte cell lines were used as controls and cultured in DMEM: (Invitrogen/PAA, Gillingham, UK) supplemented with 10% Foetal Calf Serum, 100 µg/ml streptomycin, 1% L-glutamine, 1% RM+ and cultured at 10% CO_2 in a humidified incubator. HEK293T and HeLa immortalised cell lines were also cultured in DMEM (Sigma-Aldrich, UK), supplemented with 10% Foetal Calf Serum, 1% L-glutamine and 100 µg/ml streptomycin and cultured at 5% CO_2 in a humidified incubator. Medium was replenished every 2-3 days or when cells were split upon reaching 80-90% confluency.

Maintenance of the cell culture was performed at high confluency; medium was aspirated, cells washed twice with PBS and dissociation of cells were obtained by incubation with 1x trypsin-EDTA. Serum-containing medium was used to quench the remaining active trypsin. Cells were then transferred to a conical bottomed falcon and centrifuged at 1000 rpm for 5 minutes, producing a trypsin-free pellet. The supernatant was removed, the pellet re-suspended in fresh medium and transferred to an appropriate flask.

2.3.2. Cryopreservation

To cryopreserve cell cultures, maintenance cultures were grown until 80% confluency in given volume and detached from the flask using the trypsin-EDTA method described in **2.3.1.** Cells and trypsin-EDTA mixture was then pelleted by centrifugation, the supernatant was aspirated and the pellet was resuspended in a freezing serum (9:1 of FBS to DMSO). This mixture was then deposited into cryovials that were frozen slowly by use of an isopropanol enriched container, which is placed for 24 hours at -80 °C before transfer into vapour-phase nitrogen storage. When starting a new culture from a cryovial, the vial was defrosted quickly, to limit the amount of cell death and mixed with a standard complete culture medium. The mixture was then centrifuged at 1200 rpm for 5 minutes and the pellet was resuspended and reseeded as a maintenance culture.

2.3.3. Fugene and PEI Transfections

Aforementioned cell lines were seeded on 12-well plates at a seeding density of $5x10^4$ for Fugene transfections and $6x10^5$ for PEI transfections due to the grater toxicity of PEI. Cells were seeded on coverslips for further experimentation using immunofluorescence. 24 hours after seeding transfection experiments were carried out using polystyrene tubes as to not reduce activity of transfection reagents, a possibility with polypropylene tubes. For the Fugene transfection from (Roche, UK), 50 µl (per well of transfection) of PBS was pipetted into two tubes. 500 ng of DNA was placed in the first and 1.5 µl of Fugene was added to the second. Both were incubated for 5 minutes then DNA and Fugene were combined and mixed by agitating the tube. Once mixed the reaction tubes were incubate at room temperature (RT) for a minimum of 15 minutes before their contents were pipetted drop-wise onto the appropriate cells. Transfection mixture and medium was left on the cells for 24 hours and changed after 24 hours, the cells were used for experimentation after a further 24 hours.

PEI transfections were performed on the same time scale and optimisations were carried out on the range of cell lines. A 3:1 ratio of PEI to total DNA, DNA was diluted to 0.5 µg in high glucose medium and mixed. PEI (1 mg/µl) stock was diluted to 1.5 µl in 100 µl of high glucose medium and mixed. Diluted PEI was added to the DNA, vortexed briefly and incubated for 20 minutes whilst cells were prepared for the transfection. PEI/DNA solution was added drop-wise and cells were incubated for 4-6 hours at 37 °C. Transfection medium was removed at this point due to the toxicity of PEI and fresh medium was added to the cells.

2.3.4. Transient siRNA-mediated ABCA12 knock down

ABCA12 knockdown was performed using siRNA complementary for the two prominent transcripts of ABCA12 from Dharmacon (Thermo Scientific, UK) and the Dharmafect1 reagent (Fisher Thermo Scientific, UK). All work was carried out in RNase free and sterile conditions. All siRNA was re-suspended to a concentration of 20µM in siRNA buffer (Thermo scientific) and the subsequent aliquots were stored at -80 °C. Prior to knockdown experiments the transfection conditions were optimised using siGLO control siRNA from Fisher Thermo Scientific, UK.

Cells were seeded at a density of $2x10^5$ cells per well, in a 6-well plate and incubated in standard medium at 37 °C, 5% CO_2 for 24 hours prior to transfection. In individual polystyrene tubes, 10 µl of siRNA (100 nM final concentration) and 6 µl of Dharmafect1 were mixed in an antibiotic and serum free medium and incubated for 5 minutes at RT in polystyrene transfection tubes. The siRNA-containing medium was added to the Dharmafect1, gently mixed-together and incubated for 20 minutes at RT. 1.6 ml of standard (with FCS) antibiotic free medium was then added to the siRNA-Dharmafect1 solution, mixed by inverting several times, and pipetted on to the cells at a final volume of 2 ml/well. The siRNA transfection was incubated for 24 hours at 37 °C before the medium was changed to standard medium containing antibiotics, to reduce the toxic effect of Dharmafect1 has on the cells. Controls were produced using a siRNA non-targeting pool from Fisher Thermo Scientific, (UK). The transfected cells were cultured for a further 2-5 days before harvested for protein or RNA.

2.3.5. Calcium Shift in monolayer

Cell lines were treated in accordance with **2.3.1.** though were cultured in Epilife (Sigma-Aldrich) 0.06 mM Ca^{2+} for at least two passages, to around 60% confluency at 37 ˚C in a humidifier incubator set to 5% CO_2. At this point, 0 hour, medium was changed on both of the duplicates, one was replenished with 0.06 mM Ca^{2+} medium and the other was calcium shifted with the 1.2 mM Ca^{2+} medium. Lysates or RNA was taken every 24 hours from both sets for comparison. This was performed in multiple cell lines in the presence or absence of types of ligands.

2.3.6. Agonist Application in monolayer

Originally cell lines cultured in low and high calcium (**2.3.5.**), through optimisations cell cultures were calcium shifted for 24 hours prior to the application of agonist activators. Cell lines were seeded between $2x10^4$ and $3.5x10^4$ in a 24-well plate depending on growth of cell line. Cells were treated at 70% confluency with either the PPAR-β/δ agonist activator GW0742 suspended in 0.5% DMSO to give a final concentration of 8 µM in culture or the LXR-β agonist activator TO901317 suspended in 0.5% DMSO to give a final concentration of 10 µM in culture (GlaxoSmithKline).

Each time course set has control keratinocytes treated with only the vehicle, DMSO, at 0.5%.

TO901317 is a synonym of N-(2,2,2-tri-fluoroethyl)-N-[4-(2,2,2-tri-fluoro-1-hydroxy-1-trifluoromethyl-ethyl)-phenyl]benzenesulfonamide, a small molecule nonsteroidal LXRβ agonist originally found in an investigation of intestinal cholesterol absorption and liver bile synthesis (Repa et al. 2000). GW0742 is a synonym of 4-[2-(3-Fluoro-4-trifluoromethyl-phenyl)-4-methyl-thiazol-5-ylmethylsulfanyl]-2-methyl-phenoxy}-acetic acid, developed by GlaxoSmithKline for their small molecule portfolio, which contains this lipophilic carboxylic acid (Sznaidman et al. 2003).

2.3.7. Testing for Mycoplasma

Every different cell culture used was tested for mycoplasma using a combination of MycoAlert Assay Control Set and the MycoAlert Mycoplasma Detection Kits (Cambrex) following the manufacturer's instructions. 1.5 ml of medium that had been on cells cultured for 72 hours was centrifuged at 1500 rpm for 5 minutes to create a clear supernatant. 100 µl of the supernatant was then transferred to a well of a 96-well plate, in the same well 100 µl of MycoAlert reagent was added and both were allowed to incubate for 5 minutes at room temperature. The 96-well plate was then read using the luminescence program of a Bio-Tek, Synergy HT Multi-Detection Microplate Reader. After which, 100 µl of the MycoAlert substrate was added to the well and allowed to incubate for a further 10 minutes. This was then also read on the luminescence program and from this data a ratio of more than 1 between the first and second readings was symptomatic of an infected cell culture.

2.3.8. Immortalisation of patient derived HI keratinocyte cell line

The skin biopsy was taken from the patient and processed immediately. After dissection, dispase was used to separation the dermis from epidermis, following which trypsin was used for epidermal dissociation. The stable primary line of isolated keratinocytes were then transfected with a papillomavirus HPV16-derived E6-E7 containing plasmid shown to disrupt senescence (Hawley-Nelson et al. 1989).

2.4. Antibody dilutions

Protein	Antibody	Western Blot	ICC	IHC
ABCA12	AbCam Rb poly ab98976	1/1000 PBS-T	1/200	1/200
ABCA1	AbCam Rb mono ab7360	1/1000 5% Milk PBS-T	1/250	1/250
ABCA1	AbCam Mo mono ab18180	1/1000 PBS-T	1/400	1/400
Vinculin	AbCam Rb poly ab18058	1/1220 5% Milk PBS-T	-	-
Tubulin	AbCam Rb poly ab15568	-	1/750	-
LXRβ	AbCam Mo mono ab76983	1/1000 PBS-T	-	-
Involucrin	AbCam Mo mono 5Y5	1/1000 PBS-T	1/200	1/300
K14	Mo mono LL001	1/750 (PBS-T)	1/300	1/400
K10	AbCam Mo mono ab9026	1/700 5% Milk PBS-T	1/250	1/400
GAPDH	AbCam Rb poly ab37168	1/1000 5% Milk PBS-T	1/200	1/300
TGM1	AbCam Rb poly ab27000	1/800 PBS-T	1/350	1/300
Loricrin	Covance Rb poly PRB145P	1/1000 PBS-T	1/250	1/300

Table 2.1. Table of primary antibodies and their optimised dilutions for Western blotting, immunocytochemistry (ICC) and immunohistochemistry (IHC).

2.5. Immunostaining

2.5.1. Embedding and Sectioning of frozen tissue

Skin biopsies and mouse tissues were embedded from a flash frozen sample into OCT embedding medium (Thermo Scientific, UK) in custom-made tinfoil cages that were designed in accordance of size and shape of tissue and to allow for presentation of the epidermal cross section at the cutting edge. Sections were cut with a thickness of 0.5 µm on a OTF5000 cryostat (Bight Ltd, UK) and adhered to super frost plus slides (Thermo Fisher Scientific) before they were air dried for 10 minutes and then stored at -80 °C. The remaining sample was given a generous covering with the same OCT embedding medium before refreezing at -80 °C.

2.5.2. Immunocytochemistry

For experiments involving immunocytochemistry, cells were seeded onto coverslips placed at the bottom of 12-well dishes and staining normally proceeds at a point when cells have reached a confluency of 70-80%. Medium was aspirated off cells with consideration of coverslip position in well, and then the cells were washed twice in PBS and fixed using 4% paraformaldehyde (PFA) for 30 minutes at RT. After fixation the coverslips were washed 3x in PBS, then permeabilised with 0.1% Triton X100 for 5 minutes. Blocking was performed using 3% BSA in PBS (blocking buffer) for 30 minutes, all of which was at RT.

The coverslips were inverted and placed upon a 50 µl drop of primary antibody, which was diluted in the blocking buffer at the correct dilution for the antibody and incubated for 1 hour at RT or 4 °C over night. The coverslips were washed in PBS to remove unspecific binding of the primary antibody and then incubated with the correct AlexaFluor secondary antibody for 1 hour at RT. DAPI was used as a nuclear stain at a concentration of 100 ng/ml. Coverslips were then mounted with Immu-mount (Thermo Fisher Scientific) and microscopic analysis was performed on the Leica epi-fluorescence microscope (Leica Microsystems (UK) Ltd).

2.5.3. Immunohistochemistry

Cut skin sections were air-dried on the lab bench for 45 minutes were washed twice in PBS and fixed using 4% PFA for 20 minutes at RT. After fixation the histology sections were washed 3x in PBS, then permeabilised with 0.1% Triton X100 for 5 minutes. Blocking was performed using 3% BSA in PBS (blocking buffer) for 30 minutes, all of which was at RT. Blocked sections were then incubated with 150 µl of primary antibody, that had been diluted in blocking solution, for 1 hour at RT or overnight at 4 °C. Sections were washed 3x in PBS and incubated with the appropriate AlexaFluor secondary antibody for 1 hour at RT. After a further 2 washes with PBS the nuclear stain DAPI (100 ng/ml) was applied to the sections that were subsequently washed once more before mounting with Shandon Immu-Mount mounting medium (Thermo Scientific). Immunohistochemistry was analysed using the same microscope as the immunocytochemistry visualization.

Haematoxylin and eosin (H&E) staining for assessing skin histology was carried out on paraffin slides. Slides were placed in a holder and transferred from glass bucket to glass bucket, which held different solutions. To start with the slides were deparaffinised by two separate xylene immersions for 5 minutes each. Then rehydrated by two separate 100% EtOH immersions, each for the 3 minutes, followed by the same, but with solutions of 95% EtOH. Followed by a single was with 70% EtOH for 3 minutes, a rinse with ddH_2O for 5 minutes before staining with haematoxylin for 6 minutes. The excess haematoxylin was rinsed off with running tap water for 10 minutes and dipped in acid alcohol for 1 second and rinsed well with tap water for a further 5 minutes. Slides were then counterstained in eosin for 15 seconds before they were dehydrated by two rounds of 95% EtOH for 3 minutes, followed by two rounds of 100% EtOH for 3 minutes. Following a further two rounds in Xylene for 5 minutes, slides are allowed to dry at room temperature before mounting.

2.5.4. FACS analysis

FACS analysis was achieved by flow cytometry, using immunostaining of Annexin V/propidium iodide. 80% confluent cells were washed in PBS, detached from the plate using trypsin, pelleted, and re-suspended in 400 µl of Binding Buffer (Becton Dickinson). At room temperature the suspended cells were incubated in 2 µl of Annexin

V-FITC for 15 minutes, then Propidium iodide (5 μg/ml) was added to the cell before they were processed via cell sorting.

2.6. Western Blotting

2.6.1. Preparation of protein lysates from cells

Whole cell protein lysates were produced at the termination of cell culture experiments, which, usually, coincides with a high confluency. The cells were washed twice in ice-cold PBS before lysis and detached/lysed with boiling SDS sample buffer. Cells were lysed with around ~150 μl per well (for a 6-well plate) of 2X Laemmli buffer, which has the components of, 0.1 M Tris-HCL, 20% Glycerol, 4% SDS, 0.001% Bromophenol Blue and 1.44 M Beta-mercaptoethanol, (Laemmli 1970). The wells were scraped and the subsequent cell lysates were transferred to 1.5 ml microcentrifuge tubes and centrifuged at 13,000 rpm for 5 minutes. The supernatants were then transferred into new tubes that had been on ice. Sonication was performed on viscous samples and samples would be either loaded on SDS-PAGE or stored at -80 °C.

2.6.2. Gel Electrophoresis (SDS-PAGE, pre-cast TRIS-Acetate or pre-cast Bis-TRIS)

To produce a separating polyacrylamide gel, of 6-12% depending on protein size and resolution, was prepared and pipetted in between two glass plates and that eventually held 0.75 mm spacers in a gel electrophoresis apparatus (Bio-Rad, Hemel Hempstead, UK). All of the Western blot equipment was cleaned with ddH_2O and then 70% ethanol before the procedure was undertaken. The separating gel solution was overlaid with ~1 ml of isopropanol to remove trapped air, and polymerised at RT taking around 15 minutes. After polymerisation the isopropanol was poured away. For 10 ml of a 8% gel the components were as followed: 2.7 ml of ddH_2O, 2.5 ml of 30% polyacrylamide mix (Protogel), 2.5 ml of Tris (1.5 M, pH8.8), 0.1 ml of SDS (10%), 0.1 ml of Ammonium Persulphate (APS, 10%) and 6 μl of N,N,NTetramethylethylenediamine (TEMED).

Next a 5% stacking gel mixture was prepared and pipetted over the resolving gel, and allowed to polymerise at RT for approximately 25 minutes. The gel was run at 12

mA/gel in running buffer until the separation of correct protein weight was achieved. For 5 ml of a stacking gel the components were as followed: 3.4 ml of ddH_2O, 0.8 ml of 30% polyacrylamide mix (Protogel), 0.63 ml of Tris (1M, pH6.8), 50 µl of SDS (10%), 50 µl of Ammonium Persulphate (APS, 10%) and 5 µl of N,N,NTetramethylethylenediamine (TEMED).

The combs were inserted in the top of the gel whilst the separating gel was still in the liquid phase and to expel excess separating gel. Between 8-18 µl of protein sample per well and 5-12 µl of Rainbow Molecular Weight marker (GE Healthcare) or the HMW ladder HiMark (life technologies) were loaded on the set SDS-polyacrylamide gel. Once the separating gel had set the well combs were removed and the gel was situated in the gasket of the tank. Running buffer of; 1.44% Glycine, 0.1 SDS, 0.03% Tris in ddH_2O was pour in the tank in both compartments, but the fluid was not meeting over the top of the gels. Protein samples would usually be heated to 95°C before running, though as predominately blotting was performed for large hydrophobic proteins samples were allowed to defrost and centrifuged at 13,000 rpm for 5 minutes prior to loading.

2.6.3. Transfer to nitrocellulose membrane

After the proteins were run through the gel to the required position, for antibody detection, transfer was performed, to move the proteins from the gel onto a nitrocellulose membrane. Hybond–C Extra (GE Healthcare) nitrocellulose membrane was used in a wet transfer electrophoretic cell system (Bio-Rad). The sponge pads, membrane, and blotting paper were all immersed in transfer buffer before transfer was undertaken. Transfer buffer is, 1.44% Glycine, 0.3% Tris, 20% methanol in ddH_2O. The completed cassette was placed into the transfer tank and submerged in transfer buffer, the tank was ran it either 300 mA for 1.5 hours or 100 mA overnight.

2.6.4. Protein visualisation by Ponceau Red

The efficiency of loading and transfer was tested through the staining of the membrane with Ponceau Red solution. The membrane was immersed in the stain for 5-10 minutes and lanes of protein are resolved when the stain is removed by washing with ddH_2O.

2.6.5. Blocking

Upon completion of transfer and removal of the testing stain, the nitrocellulose membranes were blocked to prevent non-specific binding of the primary antibody to the membrane. Blocking was achieved through 10% (w/v) milk in TBS-Tween for 1.5 hours or in PBS-Tween. TBS-Tween is, 2.423 g of Trizma HCl, 8.006 g of NaCl and 1 ml of Tween20 in ddH_2O.

2.6.6. Primary antibody incubation

Primary antibodies were diluted with either 5% milk TBS-T, 5% milk PBS-T or PBS-T. After blocking the membrane was cut into specific section depending on what size the test protein and control protein were. These sections were then incubated in their specific primary antibody solutions for 2 hours at RT. Any remnant primary antibody was washed off the membrane by 3x 5 minute washes in TBS-T to help ensure specific bind of the secondary antibody. After the washes membranes were incubated with secondary antibodies relative to whichever primaries were used. Secondary antibody dilutions were made with 5% milk TBS-T containing the appropriate horseradish peroxidase (HRP) conjugated anti-rabbit or anti-mouse immunoglobulins (Dako, Ely, Cambridgeshire, UK). Secondary antibodies were diluted 1/2000 for monoclonal primary antibodies and 1/3000 for polyclonal primary antibodies; the membranes were incubated for 1.5 hours at RT.

2.6.7. Secondary antibody incubation and detection

Following the incubation of secondary antibodies membranes were washed again for the same length of time and number of repeats as the washes following the primary incubation. Visualisation was achieved through incubated of the membranes in ECL or ECL Plus solution (Amersham, GE Healthcare, Buckinghamshire, UK) for 5 minutes on Clingfilm as to not let the membranes dry out. Excess development solution was allowed to run off the membranes were arranged to align the lanes of test protein with the correct control in a cassette. In a dark room photographic film (Amersham, GE Healthcare) was placed on the membranes for enough time to allow development of clear bands and fixed using an automated developer machine.

2.6.8. Stripping membranes for antibody re-probing

To re-probe Western blot membranes they had to be stripped by immersion in a stripping buffer at 55°C for 45 minutes. The stripping buffer was made from 12.5 ml of Tris HCL pH 6.8 (0.5M), 20 ml of 10% SDS, 67.5 ml of ddH_2O and 800 µl of ß-mercaptoethanol. The striped membranes were then washed up to three times in PBS-T or TBS-T, depending on the proteins probed for, and developed to analyse the efficiency of the stripping method. If fit for use the membrane would be blocked again in the appropriate solution before continuing with the western blot method described in **2.6.2.**

2.7. General methods

2.7.1. Chemicals and consumables

Chemicals used in these methods were procured from Sigma-Aldrich (MO, US) and laboratory consumables were from Thermo Fisher Scientific (UK), unless stated differently.

2.7.2. Ethical procedure

The patient samples and photographs obtained and processed in the following chapters were obtained with written consent and handled in accordance with the declaration of Helsinki 1964, the ethical guidelines most prominent in medical research for the use of human or animal samples. Patient information was collated where possible, though due to the nature of patient sample handing in some other countries well documented cases were not always possible.

2.7.3. Next generation sequence data analysis

The human reference genome hg19 was used to align raw pair ends of NGS data in the bioinformatic analysis. The preliminary and in-depth bioinformatic analysis was undertaken by Dr Vincent Plagnol (University College London, UK), which includes the quality calibration options, sequence soft clipping and adapter trimming. The resultant NGS data was filtered depending on the putative aetiology of the inherited disease clinical diagnosed or possible diagnosis. Subsequent calls were then further

checked against the 1000 Genomes Project (*www.1000genomes.org*), the Exome Aggregation Consortium (ExAC; *exac.broadinstitute.org*) and the dbSNP (*www.ncbi.nlm.nih.gov/snp*) databases. Possible variants were then securitised visually using the Integrative Genomics Viewer (IGV, Broad Institute, MA, US).

2.7.4. Statistical analysis

In the analysis of sample-control studies in **chapters 4** and **5** the paired t-test statistical method was utilised in the comparison of two population means where samples are correlated. The paired t-test and subsequent p-value function was calculated on Microsoft Excel. Significance was given at $p<0.05$ (*), highly significant at $p<0.01$ (**) and very high significance at $p<0.001$ (***).

Chapter 3: Mutation Analysis of *ABCA12* in Harlequin Ichthyosis

3.1. Introduction

Mutations in the gene *ABCA12* have been associated with several autosomal recessive congenital ichthyosis (ARCIs): lamellar ichthyosis-2 (LI2), largely associated with missense mutations restricted to the first ATP binding domain (NBD1) and non-bullous congenital ichthyosiform erythroderma (NBCIE), associated with missense mutations throughout the protein (Lefévre et al. 2003; Jobard et al. 2002). Homozygous or compound heterozygous nonsense substitutions and frameshifts are found in most harlequin ichthyosis (HI) cases (Thomas et al. 2006; Scott, Rajpopat, et al. 2013). However, missense mutations correlating to particular domains of the ABCA12 protein also underlie some cases of HI. The type and location of mutation in *ABCA12* offers some indication as to the disease presented by the affected and in turn the severity of disease. This spectrum of disease phenotypes produced by an array of mutations to a single gene suggest there is a genotype to phenotype relationship for *ABCA12* (Thomas et al. 2006).

In 2005 it was demonstrated that HI was inherited in an autosomal recessive pattern and *ABCA12* was found to be the causative gene. *ABCA12* was identified by use of a chip array and microsatellite markers to define the region of homozygosity to 2q35 in which the *ABCA12* maps (Kelsell et al. 2005). Causative ABCA12 mutations were predicted to be loss of function (LOF) including nonsense mutations, frameshift producing deletions or whole exon deletions (Kelsell et al. 2005). In parallel, a Japanese group also reported predicted LOF mutations in ABCA12 with HI (Akiyama et al. 2005).

3.1.1. Genetic screening of *ABCA12* in patients clinically diagnosed with HI

This chapter describes the genetic screening of families with at least one case of clinically diagnosed HI towards the identification of mutations in the gene *ABCA12*. The typical HI phenotype in early life consists of: thick hyperkeratotic plates with intermittent fissures separating the skin; eclabium; ectropion; microcephaly and joint contractures with possible *in utero* autoamputation. The neonatal period is complicated by prematurity, respiratory difficulty and secondary infections (Waring 1932; Buxman et al. 1979; Kelsell et al. 2005). Infrequently neonates do not survive, with mortality depending on the treatment received and the severity of disease (Rajpopat et al. 2011). HI patients that survive this period and make it into childhood have a reduction in

phenotypic severity, as presentation resembles a non-bullous congenital ichthyosiform erythroderma (NBCIE) (Thomas et al. 2006).

Here, *ABCA12* mutation analysis was undertaken for 6 unrelated HI cases. A two phase screening strategy was used: first phase, a combination of PCR and Sanger Sequencing to target known recurrent mutations found in specific ethnic groups. If the first phase is unsuccessful the second phase is initiated. The second phase utilises next generation sequencing, to sequence specific larger sections of the genome. These regions can be selected and amplified by whole exome sequencing or by targeted capture of disease-associated regions. Previously, the Kelsell group has also designed a custom microarray for sequence capture and next generation sequencing of the *ABCA12* gene and other genes known to be causative in ichthyoses (Scott et al. 2013). Exome sequencing is now the preferred method due to cost reductions and ease. All of these methods were used for the identification of variants and when they failed in-depth analysis strategies were devised for patients with complex mutations.

The genetic screening of HI aids in the diagnosis of the disease and can be performed prenatally and also preimplantation genetic diagnosis (PGD) can be used. Mutations in the *ABCA12* gene also aids in understanding the genotype to phenotype relationship and how mutations in the same gene can lead to different cutaneous disorders.

3.1.1. Results

3.1.2. Case 1

Case 1, the affected had died prior to confirmation of the initial diagnosis, which was achieved through photo evidence **(Figure 3.1. C)**. With a DNA or tissue sample unattainable from the deceased affected the genetic analysis was performed on a paternal DNA sample. The clinical notes included the information that this family was consanguineous, which meant a possible causative mutation found in the paternal sample in a heterozygous state was likely to present in the maternal sample (Aggarwal et al. 2014).

The paternal sample was screened for known ethnic specific mutations. The family was of Indian ethnicity, thus six mutations previously found in the gene *ABCA12* of HI patients of Indian/Pakistani ancestry were screened; exon 15 p.W601X, exon 23 p.V1089F, exon 27 p.W1294X, exon 39 p.W1928X, exon 42 c.6378delGC and exon 49 c.7322delC (Thomas et al. 2006; Thomas et al. 2009a; Kelsell et al. 2005; Akiyama et al. 2006; Akiyama et al 2005; Rajpopat et al. 2011). The set of exons, complete with flanking intronic regions were amplified, the amplicons cleaned and underwent bidirectional Sanger sequencing as described in **2.1.8.** by use of a ABI Prism 3130xl Genetic Analyser.

The genetic screen of the paternal sample was negative for the ethnic specific mutations, but upon the analysis of exon 49 a heterozygous 5 bp insertion in exon 49 was found. As shown in **Figure 3.1. (A)** the electropherogram of exon 49 of *ABCA12* for the paternal sample shows a double trace that initiates the thymine at c.7317 and indicates the presence of a heterozygous c.7317_7318insACAAA. The sequence alignment of exon 49 in **Figure 3.1. (B)** of control and paternal sequences illustrates the 5 bp insertion due to the extra 5 nucleotides in the paternal sample and a frameshifted sequence.

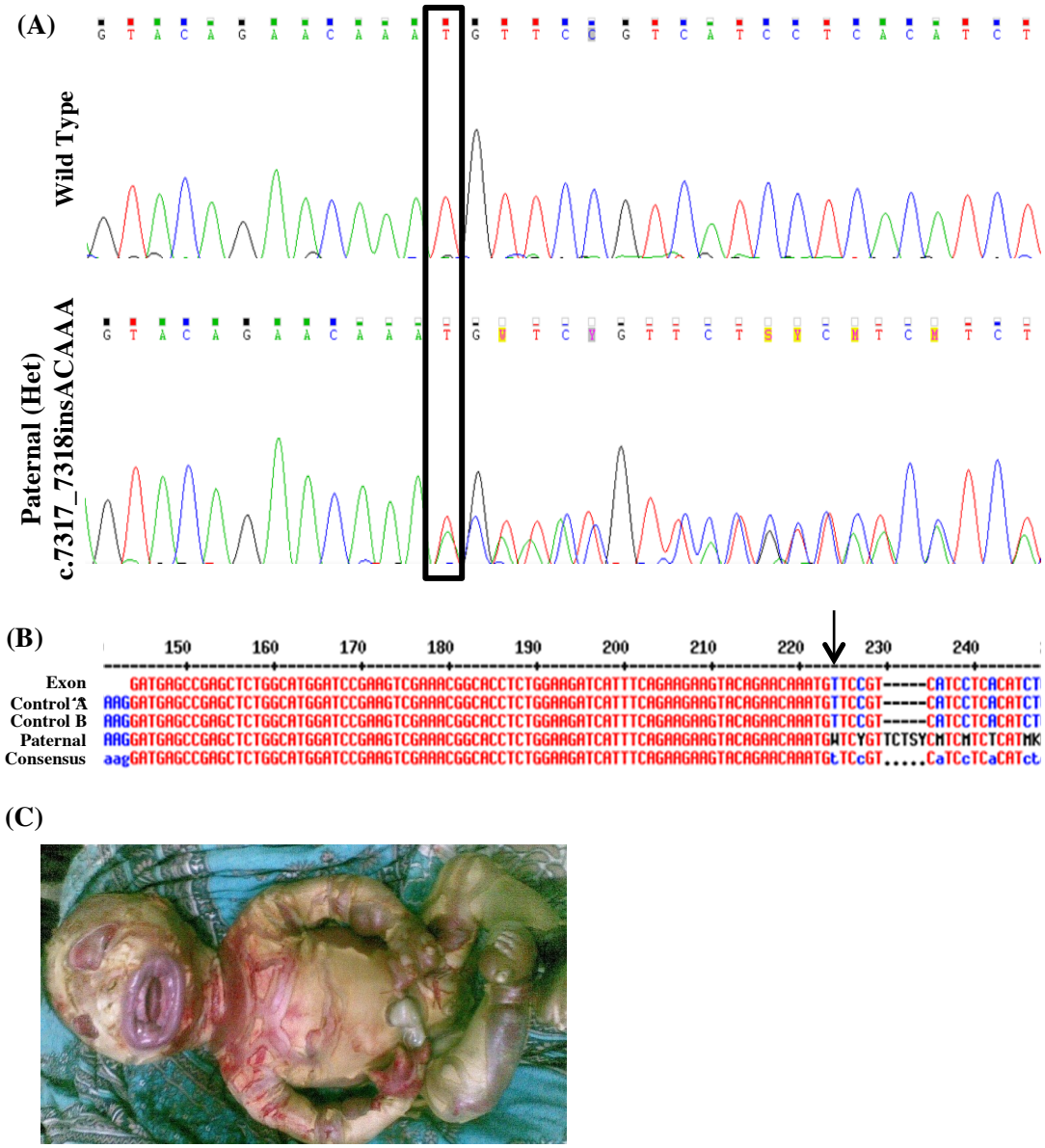

Figure 3.1. Genetic screening of case 1. (A) Electropherograms of exon 49 of *ABCA12*, the double trace that originates from the outlined thymine indicates the presence of a heterozygous c.7317_7318insACAAA in the paternal DNA. **(B)** Sequence alignment of exon 49, comparing two control DNA sequences with the paternal DNA sequence shows an insertion of 5 bp and a frameshifted sequence in the paternal compared with consensus. **(C)** Clinical appearance shows the affected neonate of the paternal sample. Presenting at birth with a typical HI phenotype including, eclabium, ectropion, thick plagues with deep fissures and joint contractures. Photo used in accordance with **2.7.2. Ethical procedure.**

The mutation c.7317_7318insACAAA p.Cys2439fs in exon 49 of *ABCA12* does not produce a premature stop codon before the exon 49 intron 49/50 splice site. The 5 bp insertion does however alter the reading frame, substituting the 9 amino acids CSVILTSHS for the 11 amino acids INVPSSSHLTA at the end of exon 49. *In silico* analysis predicted the formation of a truncated protein or no ABCA12 protein translation due to non-sense mediated decay of the transcript. In the possibility that the mutated ABCA12 protein is translated, with 9 amino acids missing and 11 different amino acids inserted into the second ATP binding cassette domain. There is a very high probability that this considerable change to a conserved domain will have a detrimental effect on the functionality of the protein. This also corroborates with previous genotype-phenotype reports where mutations in the second ATP binding cassette domain of ABCA12 lead to loss-of-function or reduced ABCA12 protein expression causing the severe HI phenotype (Rajpopat et al. 2011; Kelsell et al. 2005; Akiyama et al. 2006).

The discovery of the mutation in *ABCA12* confirmed the retrospective photographic diagnosis and aided in the prenatal diagnosis by molecular testing for the family's then current pregnancy. As the parents were consanguineous, there is a strong likelihood that the maternal sample would also be heterozygous for the mutation c.7317_7318insACAAA p.Cys2439fs in exon 49 of *ABCA12* and the affected child was likely to be homozygous (Aggarwal et al. 2014).

3.1.3. Case 2

DNA from **case 2** was pooled together with other patient DNA samples for custom array targeted capture, which included 24 known disease genes associated with ichthyoses and other epidermal conditions (Scott, Plagnol, et al. 2013). Bioinformatic analysis revealed two likely disease-associated mutations in *ABCA12,* which were subsequently corroborated by PCR and Sanger sequencing of the affected child and parental samples. This analysis was performed in accordance with **2.7.3. Next generation sequence analysis,** where filters were set for variants fitting an autosomal recessive inherited disease. **Case 2** was found to be compound heterozygous for a missense change c.5936C>G, p.A1979G in exon 40 of *ABCA12* and a 1 bp deletion of a thymine resulting in a predicted frameshift and a premature stop codon: c.6858delT,

p.F2286fsX5 of exon 46 of *ABCA12* (Scott, et al. 2013). The missense change c.5936C>G, p.A1979G was found in the paternal sample and the 1 base pair deletion c.6858delT, p.F2286fsX5 was found in the maternal sample (**Figure 3.2.** and **Figure 3.3).**

The effect the deletion had on the transcript was evaluated by the *in silico* transcription analysis tool Expasy translation (http://web.expasy.org/translate/). This deletion causes a frameshift and a subsequent stop codon within 5 bp, which suggests a protein truncated of 7 exons. Proteins like the one translated from this allele are not always produced due to the increased degradation levels of an incomplete transcript by nonsense mediated RNA decay.

The combination of next generation sequencing (NGS) with targeted gene capture when screening multiple implicated genes or a variety of diseases with known aetiologies is a useful asset in the molecular diagnosis of inherited diseases. This was undertaken as the alternative, screening many samples one gene at a time through PCR and Sanger sequencing is time consuming and expensive. The identification of mutations and which genes harbour them aids in the facilitation of prenatal diagnosis and genetic counselling. The analysis of the custom array targeted capture platform utilised in **case 3** was undertaken along side Claire Scott and the follow up sequencing was done independently.

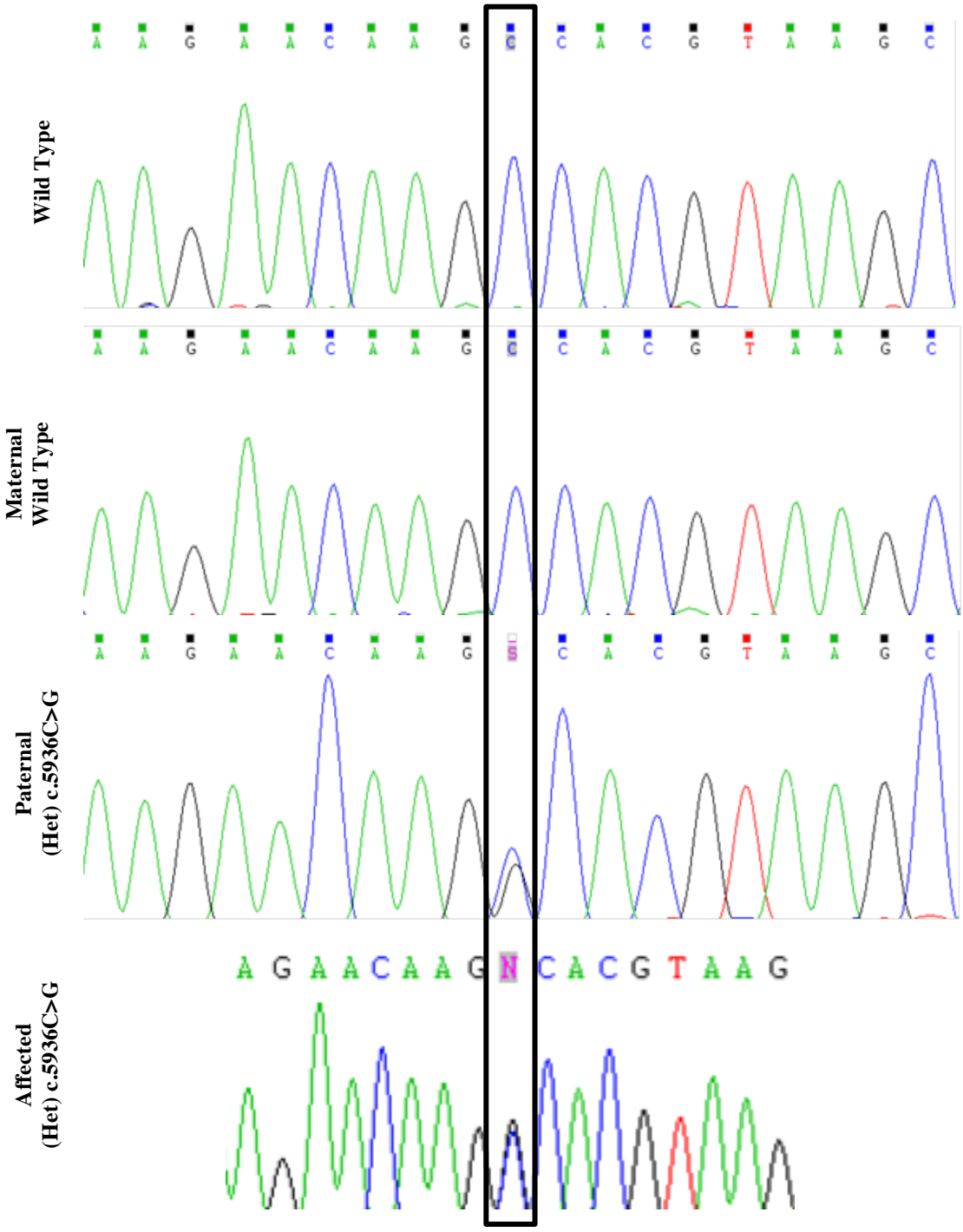

Figure 3.2. Sanger sequencing of the affected and parental samples to evaluate pulled variants in case 2. The missense change c.5936C>G, p.A1979G was found in the paternal sample and the affected, shown in the electropherograms of exon 40 of *ABCA12*. Neither parent carried both heterozygous mutations found in the affected.

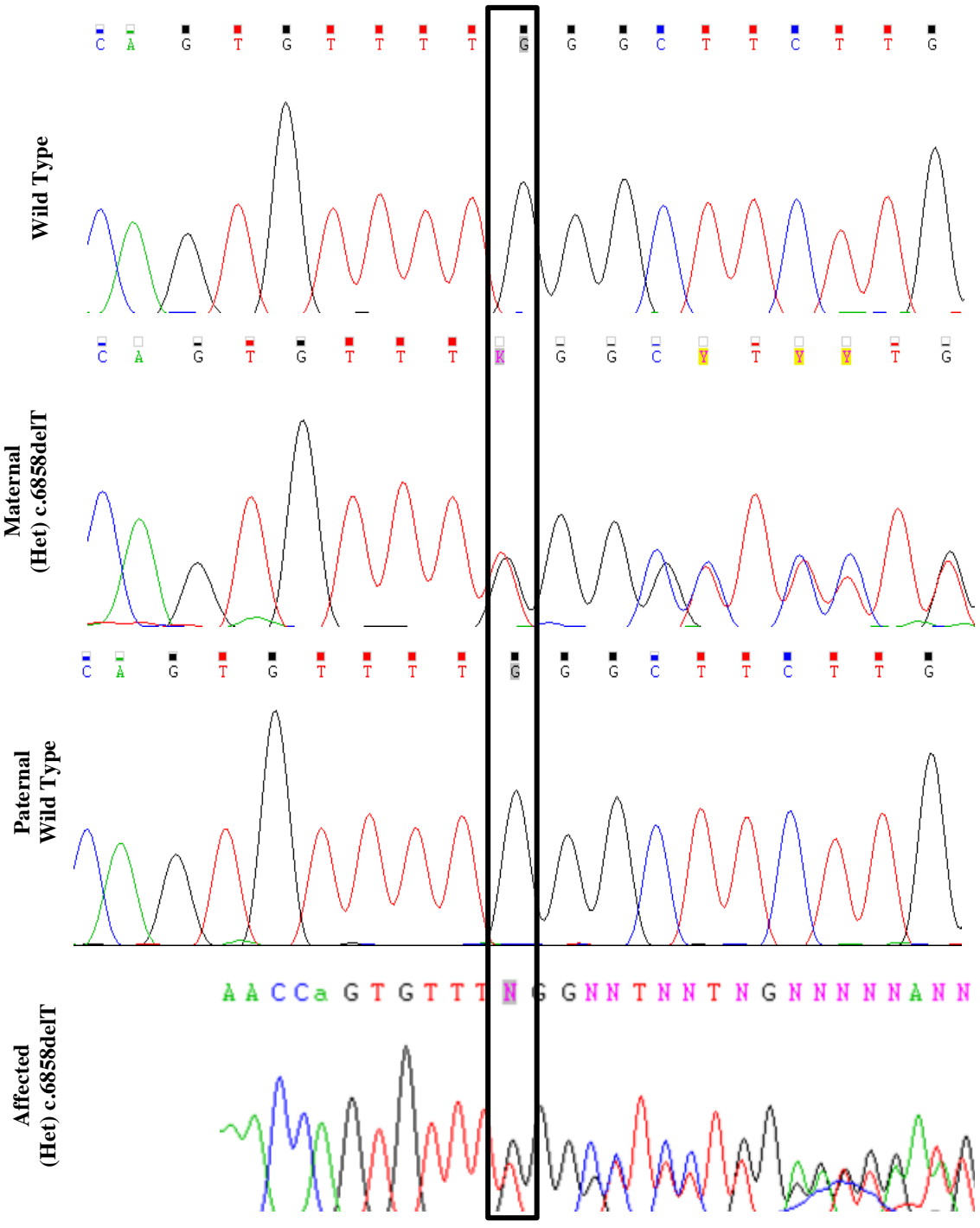

Figure 3.3. Sanger sequencing of the affected and parental samples to evaluate pulled variants in case 2. The 1 base pair deletion c.6858delT, p.F2286fsX5 was found in the maternal sample and the affected, in the electropherograms of exon 46 of *ABCA12*. Neither parent carried both of the heterozygous mutations found in the affected.

3.1.4. Case 3

In **case 3** the affected presented at birth with a severe, though characteristic HI phenotype, shown in **Figure 3.4.** Even with modern neonatal healthcare the affected died 2 months after birth. A limited amount of DNA was retrieved from the affected; however it was enough for exome capture and NGS. Following data alignment the variants presented in **Table 3.1.** were selected as possible causative variants of an ichthyosis and of those, the variants identified in *ABCA12* were isolated as the clinical diagnosis was HI.

From the variants found in the gene *ABCA12,* all but one were common SNPs that caused synonymous changes **(Table 3.1.)**. The variant in exon 17 of *ABCA12* c.T2329A p.S777T had not been reported before and caused a non-synonymous change. However, it did not segregate within the family as both parents carried the variant at a homozygous state. No disease-causing variants were found in *ABCA12* or in any ARCI-associated genes as highlighted in **Table 3.1.**

Figure 3.4. Clinical appearance of the affected in case 3. Shows the affected in the neonatal stage. Presenting at birth with a severe HI phenotype including; thick hyperkeratotic plates, fissures, eclabium, ectropion, and erythematous scales. Photo in accordance with **2.7.2. Ethical procedure.**

Gene	Zygosity	Type	SNP	SIFT	db SNP
ABCA12	HET	synonymous SNV	exon43:c.C6306T:p.Y2102Y	-	RS10498027
ABCA12	HET	synonymous SNV	exon28:c.T4126C:p.L1376L	-	RS34351934
ABCA12	HOM	nonsynonymous SNV	exon17:c.T2329A:p.S777T	0.44	RS7560008
ABCA12	HOM	synonymous SNV	exon8:c.G888A:p.V296V	-	RS17501837
ALOXE3	HET	synonymous SNV	exon16:c.C2124T:p.S708S	-	RS3809881
NIPAL4	HOM	nonsynonymous SNV	exon4:c.A580G:p.R194G	0.54	RS6860507
NIPAL4	HOM	synonymous SNV	exon5:c.T1245C:p.V415V	-	RS4704870
PNPLA1	HET	synonymous SNV	exon3:c.C174T:p.F58F	-	RS2239795
PNPLA1	HET	nonsynonymous SNV	exon6:c.C1010A:p.P337H	-	RS12199580
PNPLA1	HET	nonsynonymous SNV	exon8:c.T1306C:p.S436P	-	RS4713956
SNAP29	HET	synonymous SNV	exon1:c.A18G:p.K6K	-	RS1061064

Table 3.1. Selected variants from the exome data of affected in case 3. Variants found in the analysis of the exome data, shows genes associated with HI and other ARCIs. Variants resolved as either common SNPs with a MAF >0.1 or did not segregate in the family.

As no point mutations or small deletion/insertions were found in the exome of the affected, the next part in the genetic analysis was to check for complex mutations. These can be regulatory and lie outside the coding region, splice site mutations or large exon or multi-exon deletions/insertions that are difficult to detect in heterozygosity. A group of those complex mutations are the large intragenic deletions, which at the *ABCA12* locus have been shown to be causative in HI, such as deletions of exons 8 (Thomas et al. 2006), 12-16, 52-53 (Rajpopat et al. 2011), 23, 28-53 (Kelsell et al. 2005). Full exon deletions in ABC transporters have been associated with other diseases, for example, the deletion of exons 23-29 in the gene *ABCC6* with pseudoxanthoma elasticum and a double deletion of 13 and 17-30 exons in *ABCA1* causing Tangier disease (Miksch et al. 2005; Guo et al. 2002). The first step in screening for complex mutations was to screen areas of known deletions in *ABCA12* in the patient and parental DNA samples. All the screened regions and original mutations are shown in **Table 3.2.**

Mutation		**Exon**
c.529delT	p.Ser177GInfsX26	6
Exon Deletion	-	8
c.2021_2022del2	p.Lys674ArgfsX49	16
c.2025delG	p.Ile676PhefsX13	16
c.3270delT	p.Tyr1090X	23
c.4158_4160del3*	p.Thr1387del	28
c.4262delG	p.Gly1421GlufsX39	29
5012delA	Asn1671IlefsX4	33
c.5125_5128del4	unknown	33
c.6160_6161del2	p.Ala2054AspfsX10	42
c.7322delC	p.Val2442SerfsX28	49

Table 3.2. Previously described deletions within the gene *ABCA12*. Known deletions that have been previously found to be causative in cases of HI. All of which were screened for in the affected and parental samples. * Does not truncate protein.

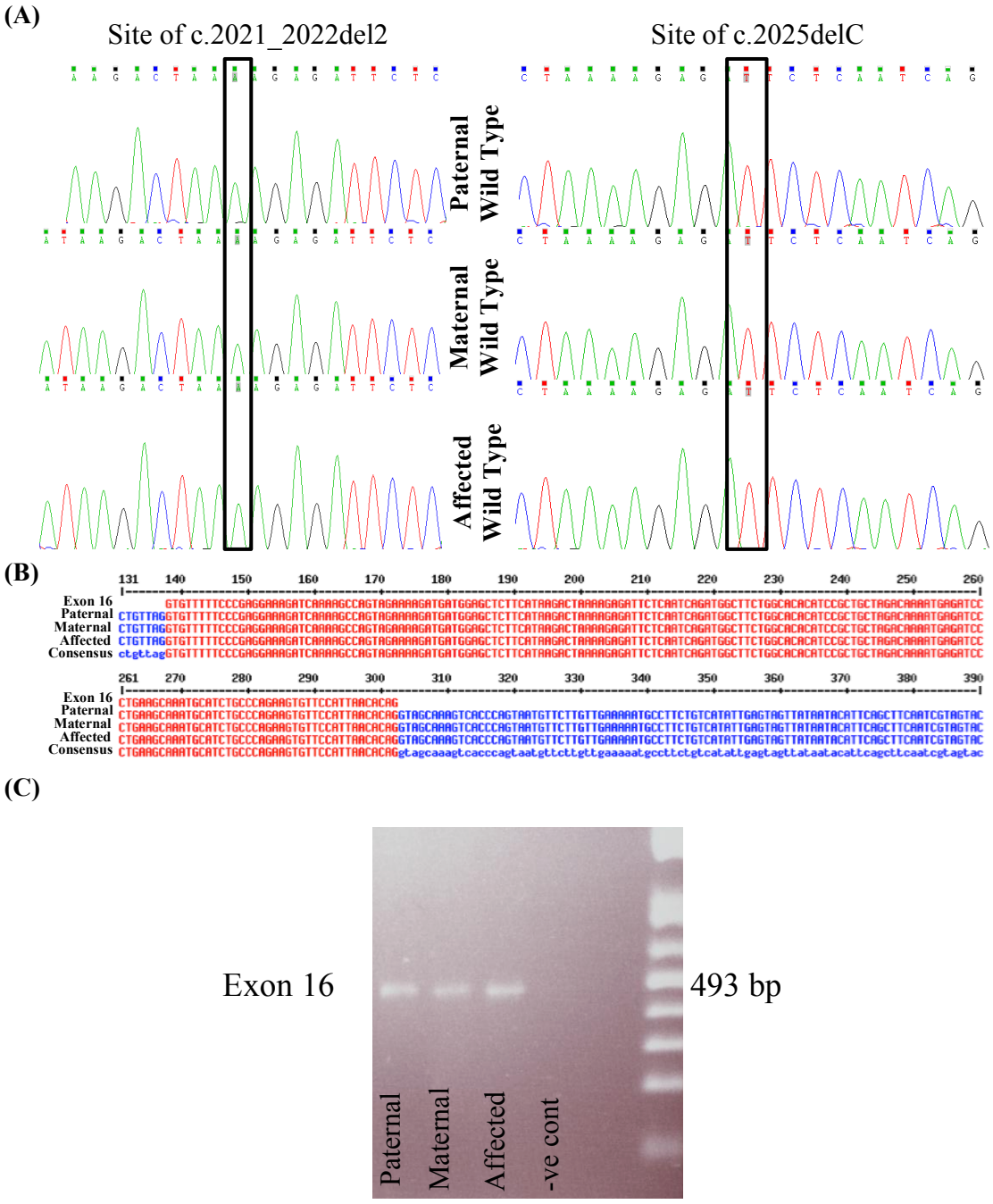

Figure 3.5. An example of the deletion screening analysis undertaken in case 3. (A) Electropherograms of exon 16 of *ABCA12*, outlined position of the two known possible deletions in exon 16, c.2021_2022del2 (p.Lys674ArgfsX49) and c.2025delC (p.Ile676PhefsX13) for all samples. **(B)** Sequence alignment of exon 16**,** comparing paternal, maternal, affected samples with the known sequence for exon 16. **(C)** Photographic capture of an agarose gel, PCR fragments, amplified from all three samples were ran to check for multiple bands.

Figure 3.5 shows an example of the deletion screening analysis undertaken in **case 3** for one of the nine sets of regions screened. Here the PCR fragments that include intronic flanking regions, were run on a high percentage agarose gel to check for multiple bands. Then fragments were sequenced and traces analysed and aligned. None of the deletions were present in any of the samples, as shown in the example for exon 16 in the **Figure 3.5.** After screening for point mutations and insertion/deletions the next screening would be for discrepancies in allelic expression.

Several SNPs at different locations in the gene *ABCA12* were investigated and their inheritance from the paternal genomic sample to the patients was assessed. For example if the paternal sample was homozygous for a specific SNP and the patient sample was WT, then this could suggest a large deletion, removal through splicing or possibly a lack of expression or inheritance of the paternal allele.

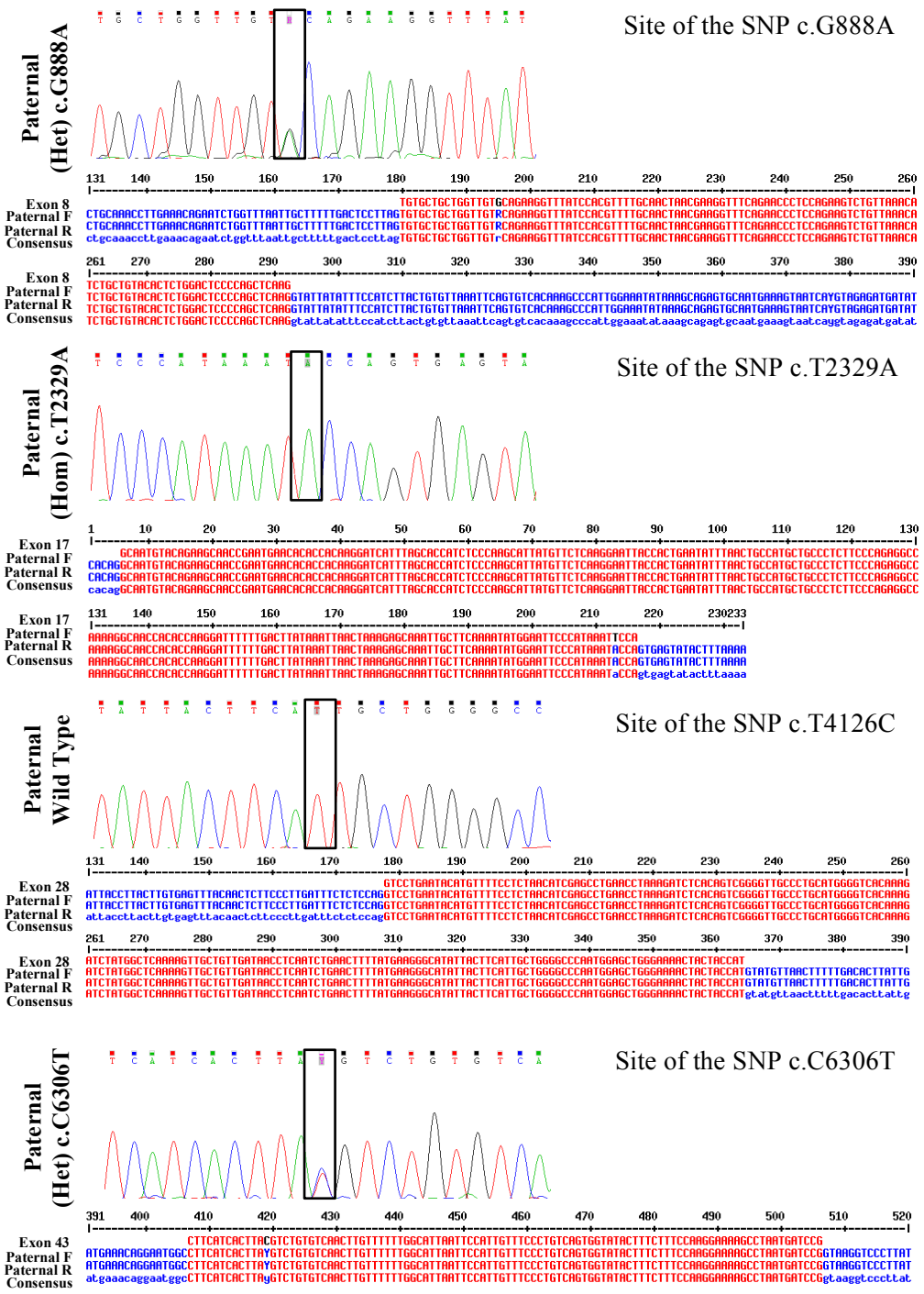

Figure 3.6. Sanger sequencing of the paternal sample to identify allelic discrepancies in case 3. Electropherograms and sequence alignments of 4 exons of *ABCA12* in case 3**.** Paternal sequencing trace is shown to check for all the SNPs in *ABCA12* that were present in the affected, for the identification of allelic expression discrepancies by the presence of paternal variance.

The next part of analysis was to check the inheritance of SNPs from the paternal sample to the patient follows logical patterns of inheritance when taken into account the possible carrier status of the maternal sample. For example, in exon 8 the SNP c.G888A:p.V296V was found in the affected in a homozygous state and heterozygous in the paternal sample. In exon 17 the SNP c.T2329A:p.S777T was present in the affect in a homozygous state and the same in the paternal sample, suggesting it was inherited paternally and maternally. Also in exon 28 the SNP c.T4126C:p.L1376L was found to be heterozygous in the affected, though found not to be present in the paternal sample, suggesting a maternal mode of inheritance, all examples shown in **Figure 3.6.** All SNPs that were homozygous in the patient were either homozygous or heterozygous in the paternal sample, showing no allelic discrepancies. The next part of the analysis was to check the paternal cDNA for transcript discrepancies. Paternal RNA had to be used, as patient material was no longer available.

ABCA12 cDNA was used to check for cDNA transcript discrepancies. Paternal RNA was isolated from hair as described in **2.1.2.** an optimised protocol reduced the necessity for skin biopsies in this case. The total RNA was reverse transcribed to cDNA, which went through PCR and Sanger sequencing to check for SNP heterozygosity retention in the transcription process. PCR, run on an agarose gel, using paternal cDNA extracted from hair, showing there are sufficient amounts of ABCA12 in hair follicles. Amplification of the paternal cDNA with two sets of primers flanking exon 8 and 43 was performed to assess for the retention of two heterozygous SNPs.

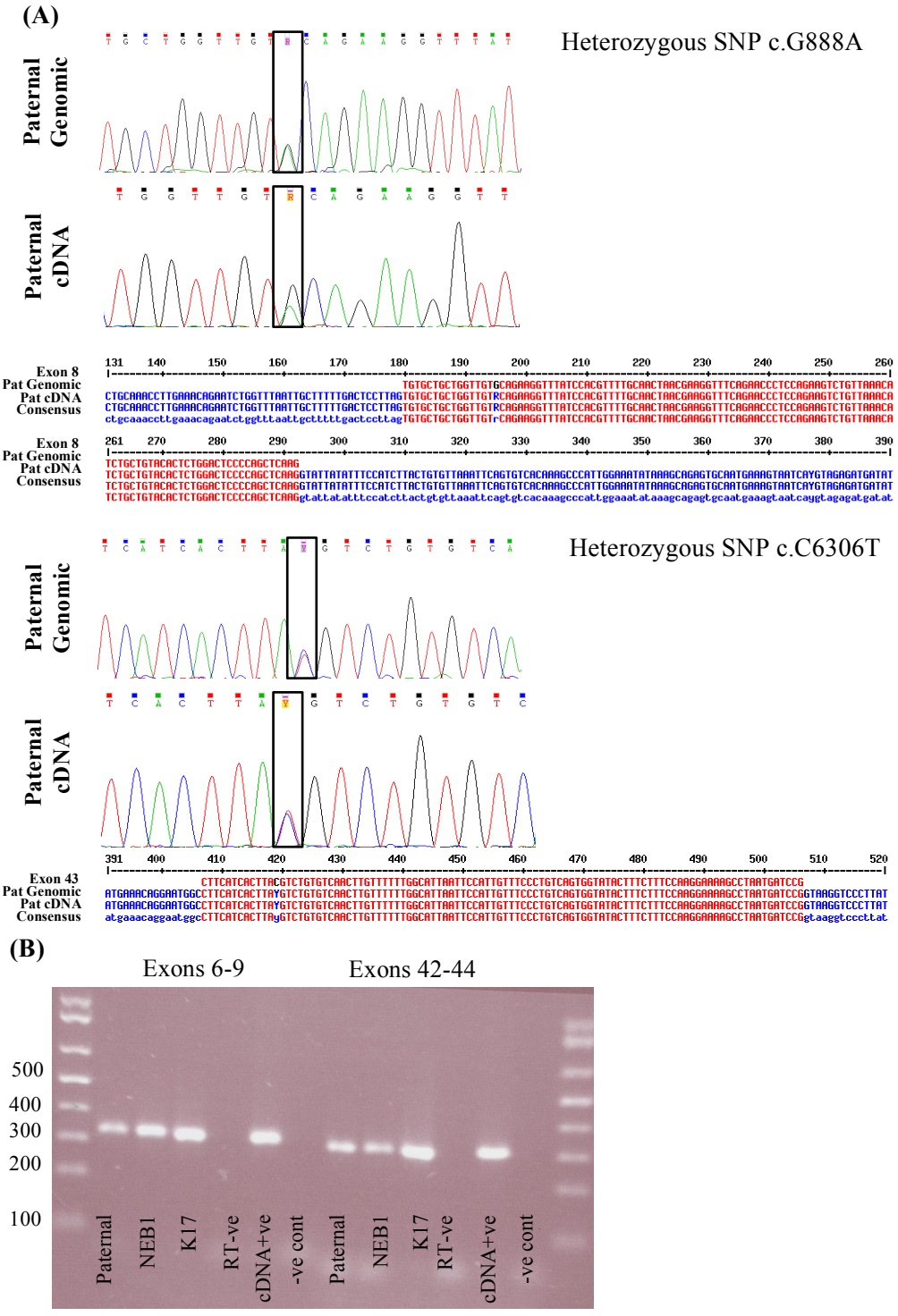

Figure 3.7. Expression discrepancy and aberrant splicing analysis of the paternal sample in case 3. (A) Electropherograms and sequence alignments, of two SNPs in *ABCA12* in genomic and cDNA paternal samples. **(B)** Agarose gel photo capture, amplified *ABCA12* exons of cDNA reverse transcribed from the RNA sample obtained from hair follicles.

Both SNPs in the paternal sample were present in a heterozygote state in the genomic DNA and the cDNA, showing that there is no evidence of lack of expression from one allele or aberrant splicing at these sites (**Figure 3.7.)**. The next step was to continue the analysis of the transcript in the paternal sample. Using the primer pairs from table **A1.1.** the entire *ABCA12* mRNA transcript was amplified and run on an agarose gel to check for small insertions or deletions and then sequenced.

Primer sets were designed to have overlapping sequences and any sequence variants were analysed, an entire *ABCA12* transcript was amplified from paternal cDNA. No multiple banding was seen for the paternal sample and all sizes corresponded to the WT for that amplicon.

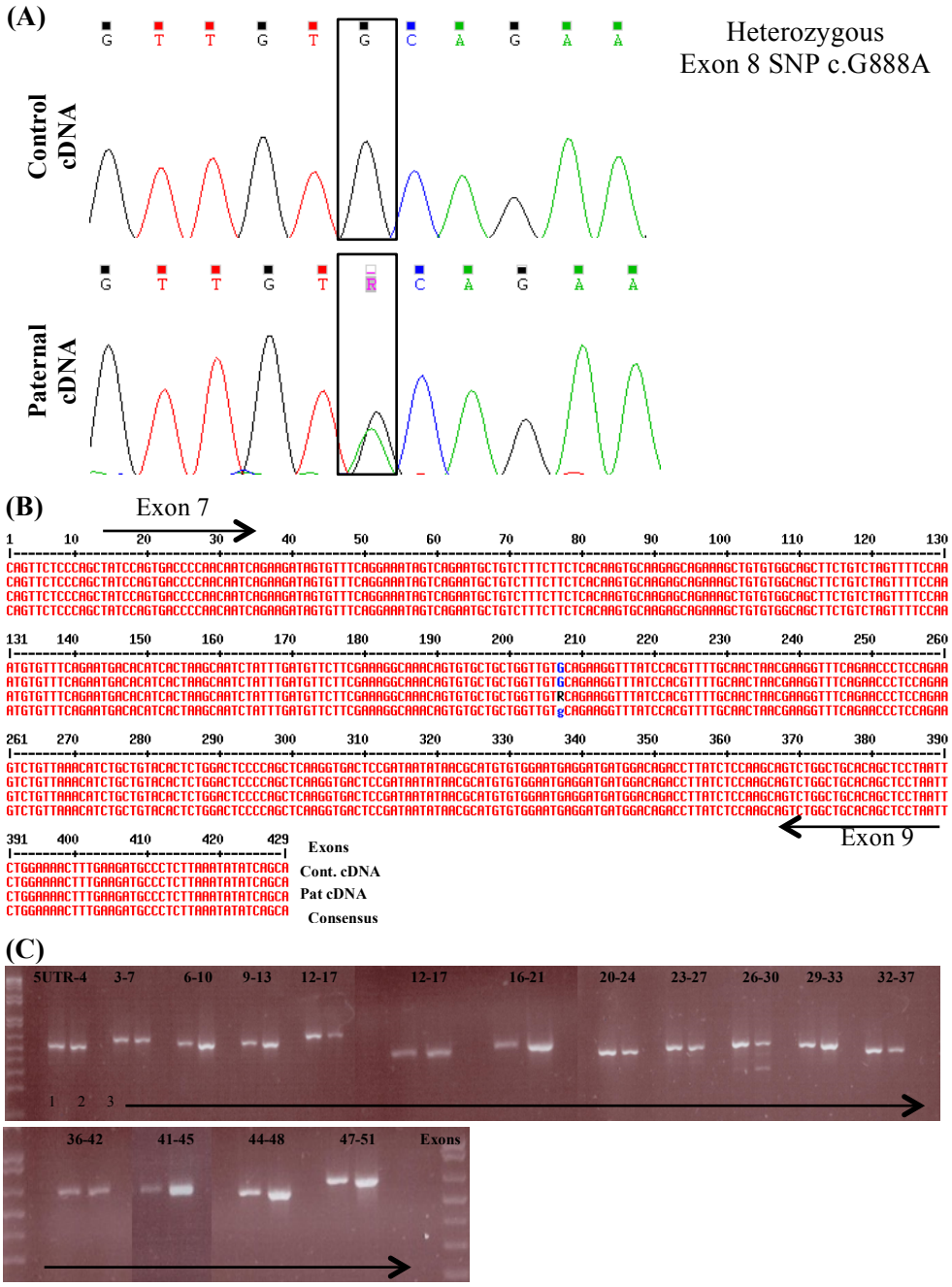

Figure 3.8. PCR and Sanger sequencing in *ABCA12* transcript analysis of case 3. **(A)** Electropherograms of an example of part of the *ABCA12* transcript**,** showing paternal cDNA and control cDNA sequences, highlighting the presence of a SNP in the paternal transcript. **(B)** Sequence alignments, of 1 out of 16 parts of the complete *ABCA12* mRNA transcript from the paternal and control samples. **(C)** Agarose gel photo capture, amplified *ABCA12* exons of cDNA, sample 1 is paternal cDNA, sample 2 is control cDNA and sample 3 is negative control.

Figure 3.8. shows an example of the sequencing analysis of the complete paternal transcript. From the alignment of the paternal, control and reference sequences there were no variants in *ABCA12* apart from the SNPs already analysed and a variation in PCR fragment brightness, though this was not consistently present in either sample. From the analysis of *ABCA12* in the patient and paternal genomic DNA, the exome capture of the patient and the multiple screening of the paternal transcript the data suggest that the causative mutation may well not be located within ABCA12, nor acting on the regulation of the *ABCA12* gene.

From exome data analysis, no other likely disease-associated homozygous or compound heterozygous changes in any genes were identified. However, a heterozygous mutation that was not present in the parents DNA, thus be of *de novo* origin, could be the underlying genetic cause of HI in this case. These variants are shown in **Table 3.3.**

Ref	Alt	Zygosity	Exonic/Spli	Gene	Protein	Mutation	SNP Info	SIFT	NOVEL	QC	Depth: Allele Frequency:
G	A	HET	exonic	SPN	leukosialin precursor	nonsynonymous SNV	SPN:NM_003123:exon2:c.G649A:p.G217R,SPN:NM_001(	0.18	NOVEL	PASS	DP=260;VDB=0.0388;AF1=
A	T	HET	exonic	PRSS36	protease, serine, 36	nonsynonymous SNV	PRSS36:NM_173502:exon13:c.T2093A:p.I698N,	.	NOVEL	PASS	DP=37;VDB=0.0374;AF1=(
C	G	HET	exonic	SDR42E1	short-chain dehydrogenase/reductase family 42E	nonsynonymous SNV	SDR42E1:NM_145168:exon3:c.G551C:p.R184T,	.	NOVEL	PASS	DP=203;VDB=0.0374;AF1=
G	A	HET	splicing	CHMP1A	chromatin modifying protein 1A	splicing	CHMP1A:NM_002768:exon4:c.105+8C>T,NM_001083314.	.	NOVEL	PASS	DP=92;VDB=0.0374;AF1=(
C	T	HET	exonic	CHRNE	acetylcholine receptor subunit epsilon	nonsynonymous SNV	CHRNE:NM_000080:exon10:c.G1042A:p.E348K,	.	NOVEL	PASS	DP=17;VDB=0.0355;AF1=(
C	T	HET	exonic	MFSD6L	major facilitator superfamily domain-containing	nonsynonymous SNV	MFSD6L:NM_152599:exon1:c.G1714A:p.E572K,	.	NOVEL	PASS	DP=103;VDB=0.0172;AF1=
T	C	HET	exonic	ALDH3A2	fatty aldehyde dehydrogenase isoform 2	nonsynonymous SNV	ALDH3A2:NM_001031806:exon7:c.T1090C:p.F364L,ALDI.	.	NOVEL	PASS	DP=83;VDB=0.0374;AF1=(
T	C	HET	splicing	GOSR1	Golgi SNAP receptor complex member 1	splicing	GOSR1:NM_004871:exon5:c.440+6T>C:NM_001007025:.	.	NOVEL	PASS	DP=38;VDB=0.0333;AF1=
-	AACT	HET	splicing	PGAP3	post-GPI attachment to proteins factor 3	splicing	PGAP3:NM_033419:exon3:c.279+4->AGTT	.	NOVEL	PASS	INDEL;DP=60;VDB=0.037
T	G	HET	exonic	PLEKHH3	pleckstrin homology domain-containing family H	nonsynonymous SNV	PLEKHH3:NM_024927:exon13:c.A2305C:p.T769P,	0.26	NOVEL	PASS	DP=30;VDB=0.0308;AF1=(
G	A	HET	exonic	CDK5RAP3	CDK5 regulatory subunit associated protein 3	nonsynonymous SNV	CDK5RAP3:NM_176096:exon3:c.G113A:p.R38H,	.	NOVEL	PASS	DP=58;VDB=0.0399;AF1=(
C	G	HET	exonic	GALK1	galactokinase	nonsynonymous SNV	GALK1:NM_000154:exon1:c.G106C:p.G36R,	.	NOVEL	PASS	DP=16;VDB=0.0401;AF1=(
C	G	Het	exonic	DSC1	desmocollin-1 isoform Dsc1b preproprotein	nonsynonymous SNV	DSC1:NM_004948:exon2:c.G139C:p.V47L,DSC1:NM_024.	.	NOVEL	PASS	DP=65;VDB=0.0253;AF1=
C	T	HET	exonic	LOXHD1	lipoxygenase homology domain-containing protein	nonsynonymous SNV	LOXHD1:NM_144612:exon29:c.G4523A:p.R1508K,LOXH	0.24	NOVEL	PASS	DP=66;VDB=0.0281;AF1=(
C	T	HET	exonic	KDSR	3-ketodihydrosphingosine reductase precursor	nonsynonymous SNV	KDSR:NM_002035:exon9:c.G812A:p.G271E,	.	NOVEL	PASS	DP=83;VDB=0.0333;AF1=
C	T	HET	exonic	DOT1L	histone-lysine N-methyltransferase, H3 lysine-79	nonsynonymous SNV	DOT1L:NM_032482:exon19:c.C1838T:p.T613M,	.	NOVEL	PASS	DP=58;VDB=0.0225;AF1=(
C	T	HET	exonic	UHRF1	E3 ubiquitin-protein ligase UHRF1	nonsynonymous SNV	UHRF1:NM_001048201:exon17:c.C2285T:p.A762V,UHRF	.	NOVEL	PASS	DP=71;VDB=0.0404;AF1=(
T	C	HET	exonic	C3	complement C3 precursor	nonsynonymous SNV	C3:NM_000064:exon19:c.A2387G:p.K796R,	0.17	NOVEL	PASS	DP=83;VDB=0.0374;AF1=(
A	G	HET	exonic	DNAH5	dynein heavy chain 5, axonemal	nonsynonymous SNV	DNAH5:NM_001369:exon52:c.T8804C:p.M2935T,	.	NOVEL	PASS	DP=69;VDB=0.0404;AF1=(
C	G	HET	exonic	DNAH5	dynein heavy chain 5, axonemal	nonsynonymous SNV	DNAH5:NM_001369:exon42:c.G6977C:p.R2326T,	.	NOVEL	PASS	DP=138;VDB=0.0374;AF1=
G	-	HET	splicing	MARCH11	E3 ubiquitin-protein ligase MARCH11	splicing	MARCH11:NM_001102562:exon4:c.694-6C>-	.	NOVEL	PASS	INDEL;DP=68;VDB=0.022
A	G	HET	exonic	EDIL3	EGF-like repeat and discoidin I-like	nonsynonymous SNV	EDIL3:NM_005711:exon10:c.T1139C:p.V380A,	.	NOVEL	PASS	DP=109;VDB=0.0388;AF1=
C	G	HET	exonic	RASA1	ras GTPase-activating protein 1	nonsynonymous SNV	RASA1:NM_002890:exon1:c.C68G:p.P23R,	0.24	NOVEL	PASS	DP=7;VDB=0.0168;AF1=0.
G	A	HET	exonic	FBN2	fibrillin-2 precursor	nonsynonymous SNV	FBN2:NM_001999:exon14:c.C1960T:p.R654C,	.	NOVEL	PASS	DP=216;VDB=0.0333;AF1=
T	C	HET	exonic	PCDHGA9	protocadherin gamma-A9	nonsynonymous SNV	PCDHGA9:NM_018921:exon1:c.T1354C:p.F452L,PCDHC.	.	NOVEL	PASS	DP=99;VDB=0.0374;AF1=
G	C	HET	splicing	DBN1	drebrin 1	splicing	DBN1:NM_004395:exon4:c.255+6C>G,NM_080881:exon4.	.	NOVEL	PASS	DP=248;VDB=0.0374;AF1=
C	G	HET	splicing	TAF8	transcription initiation factor TFIID subunit 8	splicing	TAF8:NM_138572:exon3:c.203-10C>G	.	NOVEL	PASS	DP=88;VDB=0.0374;AF1=(
TAAAT	-	HET	splicing	SERINC1	serine incorporator 1	splicing	SERINC1:	.	NOVEL	PASS	INDEL;DP=21;VDB=0.035
G	A	HET	exonic	HIVEP2	transcription factor HIVEP2	nonsynonymous SNV	HIVEP2:NM_006734:exon5:c.C1756T:p.P586S,	0.35	NOVEL	PASS	DP=151;VDB=0.0404;AF1=
C	A	HET	exonic	TTYH3	protein tweety homolog 3	nonsynonymous SNV	TTYH3:NM_025250:exon9:c.C964A:p.Q322K,	.	NOVEL	PASS	DP=4;VDB=0.0148;AF1=0.
A	C	HET	exonic	STK17A	serine/threonine kinase 17a	nonsynonymous SNV	STK17A:NM_004760:exon4:c.A590C:p.E197A,	0.74	NOVEL	PASS	DP=263;VDB=0.0333;AF1=
T	C	HET	exonic	ERV3-1	endogenous retrovirus group 3, member 1	nonsynonymous SNV	ERV3-1:NM_001007253:exon2:c.A952G:p.T318A,	.	NOVEL	PASS	DP=83;VDB=0.0399;AF1=(
CAA	-	HET	splicing	PION	protein pigeon homolog	splicing	PION:	.	NOVEL	PASS	INDEL;DP=160;VDB=0.04(
G	A	HET	exonic	PVRIG	transmembrane protein PVRIG	nonsynonymous SNV	PVRIG:NM_024070:exon3:c.G182A:p.R61H,	0.43	NOVEL	PASS	DP=19;VDB=0.0399;AF1=(

Table 3.3. Filtered variants from exome data of the affected in case 3. Variants pulled from the exome data set with green denoting the four candidate variants and their respective genes.

Four heterozygous variants could be linked with a possible pathway associated with the HI phenotype. DSC1 desmocollin-1 isoform Dsc1b preproprotein and PCDHGA9 protocadherin gamma-A9; mutations present in both genes could play a role in an ichthyosis-type disease as there is a desmocollin -1 and cadherin reduction in Netherton Syndrome. KSDR 3-ketodihydrosphingosine reductase precursor; although this has previously been linked with lymphoma, the enzyme is involved with sphingolipid biosynthesis. Sphingolipids are the third main component of the permeability barrier with ceramides and cholesterol. GOSR1 Golgi SNAP receptor complex member 1 is involved in general protein trafficking from the endoplasmic reticulum (ER) to Golgi in mammalian cells and is a component of the Golgi SNAP receptor (SNARE) complex. Deleterious mutations could possibly hinder LG development. Primers from table **A1.3.** were used to amplify the exons of interest in these genes and Sanger sequencing was utilised to sequence the fragments. However each variant was also present and heterozygous in either maternal or paternal DNA.

GOSR1 Splice Site variant: Exon 5 :c.440+6T>C

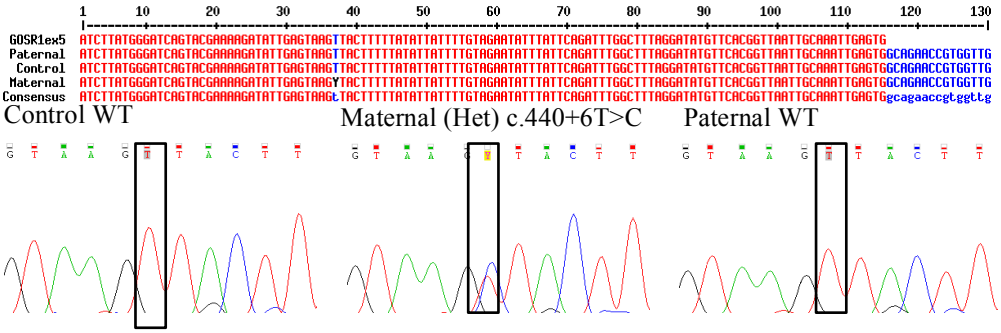

DSC1 Exonic variant: Exon 2 :c.G139C:p.V47L

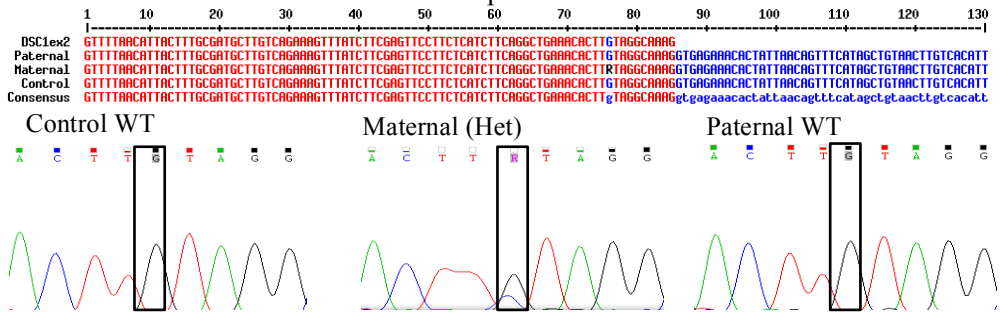

KDSR, Exonic variant: Exon 9 :c.G812A:p.G271E

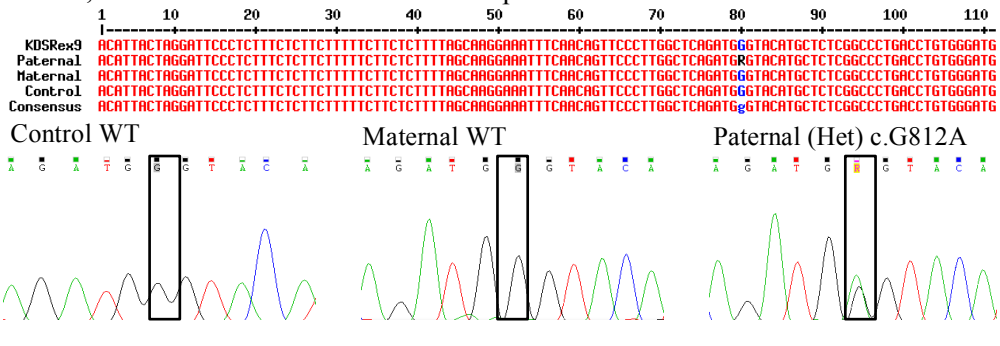

PCDHGA9, Exonic variant: Exon 1 :c.T1354C:p.F452L

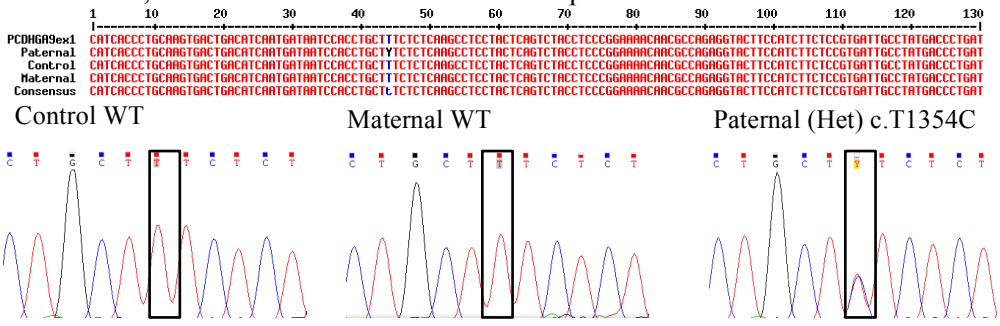

Figure 3.9. Sanger sequencing of candidate variants in case 3. Electropherograms and sequence alignments of the 4 variants, which were selected from the exome data set of the affected and analysed in parental samples.

As one of the parents was heterozygous for the each of the four variants, they are not *de novo* in origin. It is highly unlikely that the HI phenotype of the affected was then caused by these variants. The next step in the analysis of **case 3** is to sequence with whole genome capture both parental samples and filter for any variants in both coding and non-coding genetic regions. This method would also identify copy number changes.

3.1.5. Case 4

The DNA from case 4 was sequenced using the targeted sequence capture array approach described previously **(3.1.3.)** (Scott, Plagnol, et al. 2013). After filtering the data for rare mutations in *ABCA12* a small homozygous deletion was identified 17 bp upstream of the start of exon 40, c.6286-17delTGT. The variant was not automatically flagged as a splice site mutation due to the distance away from the recognition site, but domains of the spliceosome need to bind further upstream for lariat production. Thus *in silico* splice site prediction was used to analyse the product of such a variant.

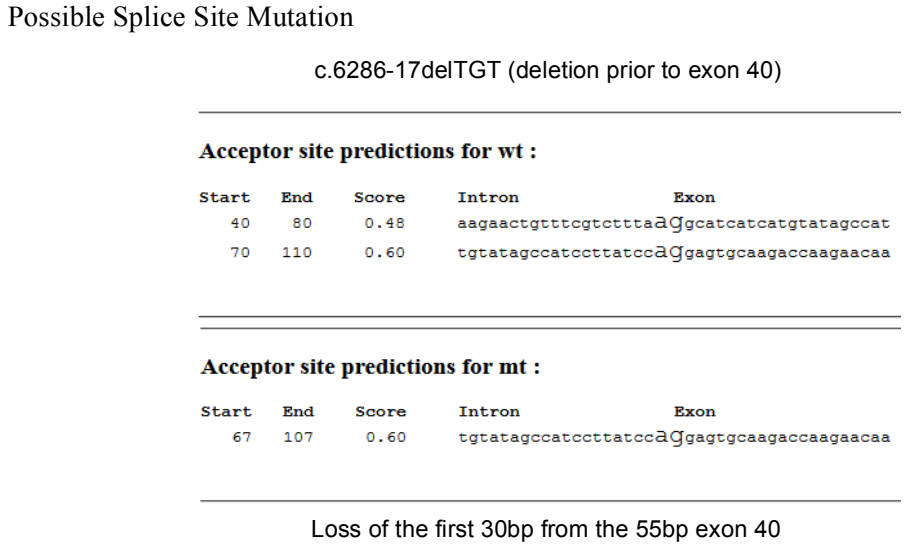

Figure 3.10. Splice site analysis of case 4 of the variant c.6286-17delTGT, when the deletion of TGT was removed from the intronic sequence the acceptor site changed from the WT recognition site that obtained a score 0.48 to the alternative, which received a score of 0.60. www.fruitfly.org/seq_tools/splice.

The alternative acceptor site is predicted to have a high affinity for the spliceosome, it is located 30 bp within exon 40, which itself is only 55 bp long. To complete this case subsequent affected and parental DNA samples would be needed for the validation of variant (c.6286-17delTGT) and cDNA analysis should be performed to confirm the predicted effect on splicing.

3.1.6. Case 5

Parental DNA was analysed, as there was no DNA from the HI affected available. The two phase screening strategy was used: the clinical notes described the affected as middle-eastern, thus the six recurrent mutations listed in **Table 3.4.** were screened for. As none of the recurrent mutations were found the remaining 47 exons of *ABCA12* were amplified by PCR then sequenced through the Big Dye and subsequent Sanger sequencing method in the laboratory.

Ethnicity	Mutation	Exon	Present
Iranian	450insC	5	No
Israeli	Q354del	9	No
Arab(other)	Splice site	26(intronic)	No
Turkish	Y1650X	32	No
Egyptian	R1880X	37	No
Iranian	Splice site	42(intronic)	No

Table 3.4. An example of the first screening in case 5. Showing the first 6 exons to be screened for known ethnic specific recurrent *ABCA12* mutations.

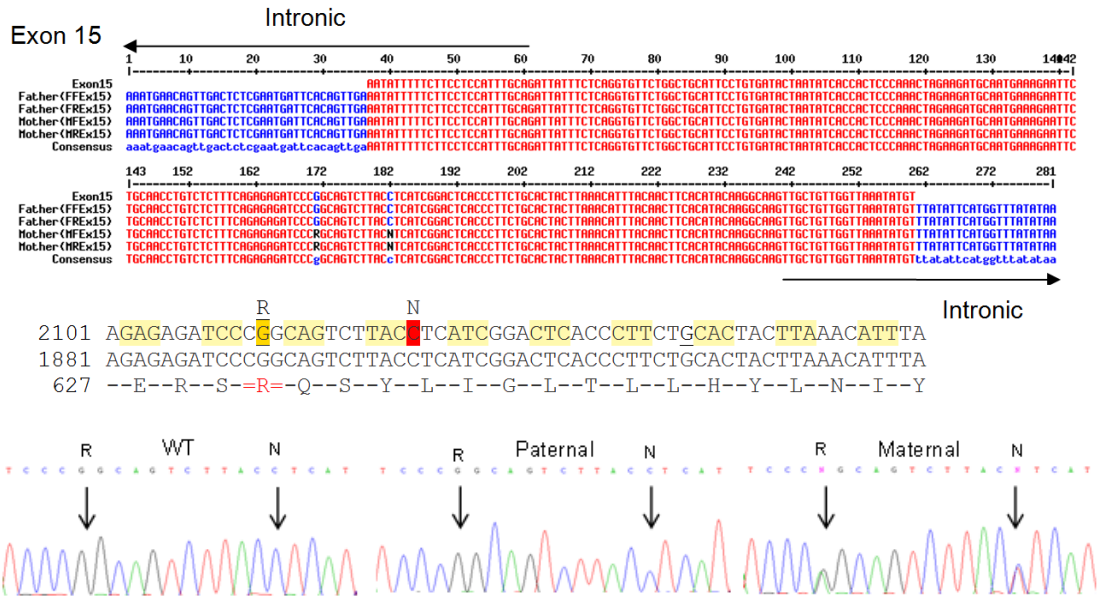

Figure 3.11. Screening of case 5 using Sanger sequencing. Electropherograms and MultAlin sequence alignment of *ABCA12* exon 15, from the sequencing of parental DNA. Arrows indicate the position of the two variants found in the maternal sample. MultAlin (multalin.toulouse.inra.fr/multalin/) SNP data from (www.ensembl.org/).

In **case 5**, no mutation was found in the paternal sample, suggesting a possible deletion or regulatory mutation. The mother was heterozygous for a missense mutation in the second membrane-spanning domain of the ABCA12 protein. The variant labelled R is recorded as a SNP rs76979001, which produces the change c.1892G>A p.R631Q, at a MAF of 0.01, a SIFT of 0.16 (tolerated) and a PolyPhen of 0.118 (benign).

There was no database information available for p.L634F, the greatest indicator as to the nature of this variant was the information available on the preceding amino acid. This residue is associated with two variants, the first p.Y633C, has no ‘rs’ number, though is listed on the COSM database, where it is cited as deleterious (SIFT of 0) and probably damaging (PolyPhen of 0.99). The second is p.Y633X, which is a known disease causing mutation in HI (Rajpopat et al. 2011). Both of which suggest this location on the first transmembrane domain of ABCA12 would yield a dysfunctional protein if mutated. In the fifth transmembrane domain the variant p.V1089F is an example that a missense mutation within these rich hydrophobic amino acid domains can be deleterious (Rajpopat et al. 2011).

This mutation (p.L634F) was the only variant found in the maternal DNA sample, which could possibly contribute to a compound heterozygote disruption of *ABCA12*. In efforts to complete this case a further paternal sample would be ideal to screen the ABCA12 transcript for complex mutations.

3.1.7. Case 6

In **case 6** a provisional clinical diagnosis of HI and blood sampling was performed on the affected and both parents to screen for mutations in *ABCA12* by exome sequencing. Exome sequencing using the DNA from Case 6 was performed using a combination of SureSelect system for target enrichment (Agilent Technologies) and sequencing on a HiSeq system (Illumina) (Blaydon et al. 2013; Brooke et al. 2014). Analysis following **2.7.3.** revealed no likely disease-causing *ABCA12* variants. However, a likely disease causing change in the *ALOX12B* gene was identified: homozygosity for a missense mutation, c.1630T>C (p.Cys544Arg) in exon 12 of *ALOX12B*. Subsequent Sanger sequencing confirmed this finding in the affected and found both parents heterozygous for the mutation, which is in accordance with autosomal recessive inheritance **(Figure 3.13.A)**. The mutation (p.Cys544Arg) localises to the catalytic helix 21 domain, in a region of ALOX12B previously shown to carry mutations that remove the enzymatic activity of ALOX12B **(Figure 3.13.B)** (Eckl et al. 2005). Previously, *ALOX12B* mutations have been associated with NBCIE.

The clinical progression was being assessed whilst these genetic studies were being performed. During the first year of life, the infant showed a steady yet marked improvement and almost complete resolution of skin features. The affected weighed 8800 g (25 p), had a height of 69 cm (< 3 p) and OFC of 45.5 cm (10-25 p) at the age of 13 months. Her neuromotor development was normal and the infant showed only subtle erythema affecting the distal lower limbs associated with overlying fine white scales **(Figures 3.12.A&B)**.

Figure 3.12. Clinical and histopathological appearance of the affected female at the neonatal stage. **(A)** Showing ectropion, joint contractures, large thick yellow plagues with an uneven distribution and bisecting erythematous fissures. **(B)** Appearance of lower extremities at 13 months of age, showing fine white scaling over the entire body. **(C)** Haematoxylin and eosin staining shows a thickened stratum corneum in the affected compared to that of the control. **(D)** Immunostaining for ALOX12B shows a reduction of epidermal staining in the skin of the affected in comparison with control. Photos in accordance with **2.7.2.**

A punch skin biopsy from the affected was obtained from a site on the forearm for histopathological work-up. Haematoxylin and eosin staining showed an epidermis with enlarged stratified layers and a thickened, compressed stratum corneum (hyperkeratosis) in contrast to the normal basket-weave corneum layers in a control skin **(Figure. 3.12.C)**. Immunohistochemical staining revealed that ALOX12B protein expression was reduced in the epidermis of the affected in comparison to control skin, where it appears to be expressed in the stratum granulosum **(Figure. 3.12.D)**. These features were consistent with a disease causing mutation in the *ALOX12B* gene (Eckl et al. 2005).

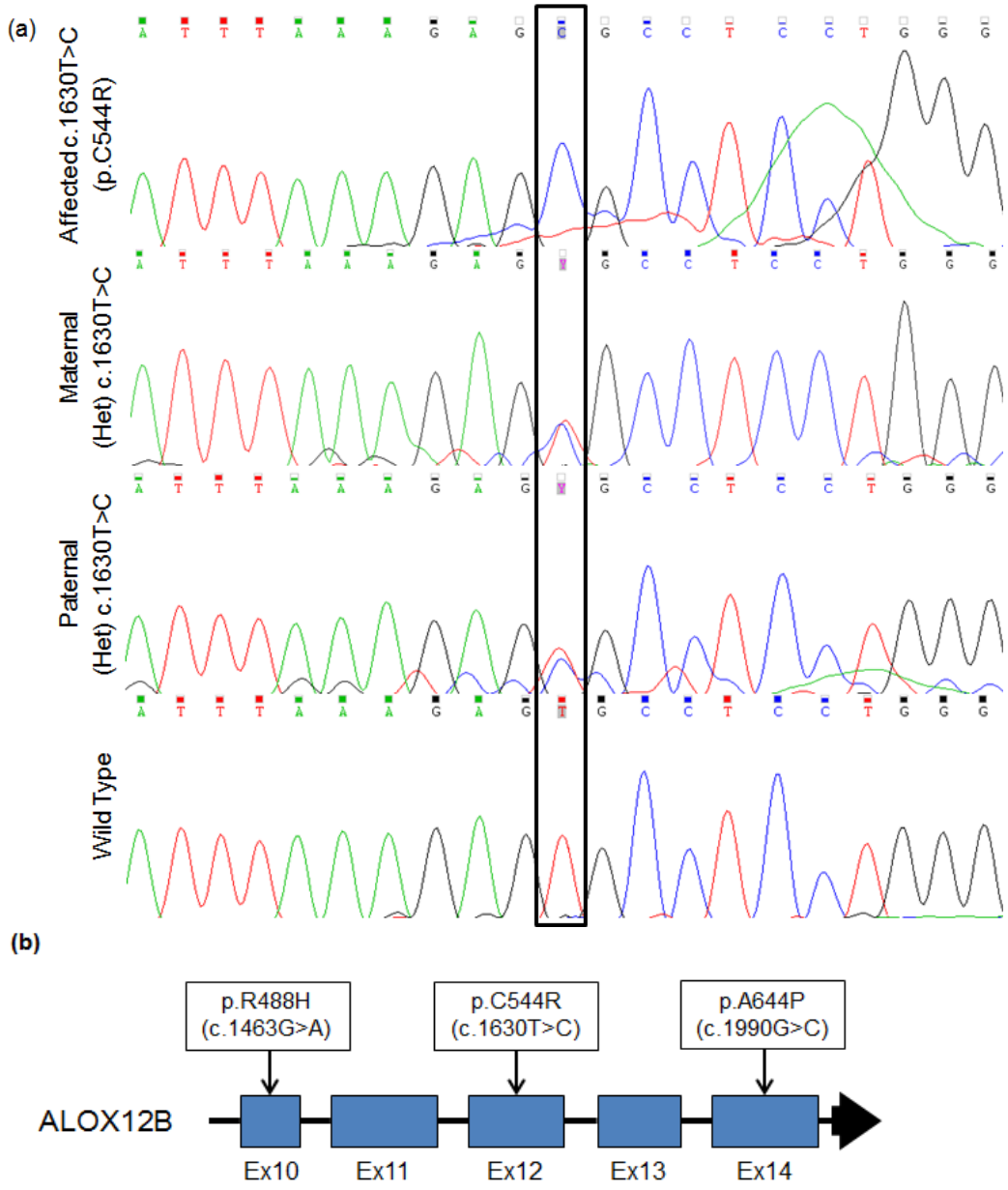

Figure 3.13. Genetic screening of case 6. (A) Electropherograms show the effected was homozygous for the mutation c.1630T>C in *ALOX12B*, which was found to be in the heterozygote state in both parents. **(B)** Partial *ALOX12B* gene schematic depicting the localisation of mutations in neighbouring exons that were previously shown to remove the enzymatic activity of 12RLOX (Eckl et al. 2005).

NGS and Sanger sequencing corroborate that the affected is homozygous for the missense mutation Cys544Arg in exon 12 of the *ALOX12B* gene. *ALOX12B* codes for arachidonate 12-lipoxygenase (12RLOX), an enzyme that produces 12-Hydroxyeicosatetraenoic acid, an eicosanoid, which is a type of signalling molecule, that plays a role in keratinocytes and Langerhans' cell interaction. Many LOX products hold pivotal roles in keratinocyte terminal differentiation and are crucial in barrier formation (Krieg et al. 2001).

Recessive mutations in *ALOX12B* can cause NBCIE (Eckl et al. 2005). The cysteine to arginine substitution (Cys544Arg) within the catalytic helix 21 domain could reduce the enzymatic ability of the lipoxygenase domain it is situated in, as cysteine amino acids are often involved in the formation of disulphide bridges, a critical protein structure (Eckl et al. 2009).

Cases can present with similar phenotypes to HI directly after birth, though skin development into early childhood is considerably different. The two siblings of the affected had died from secondary infections and septicaemia due to an irregular skin barrier formation after presenting with a similar phenotype as the affected at the neonatal/infantile stage. The mutation in the gene *ALOX12B* caused the affected to present with a HI-like phenotype at birth, that both phenotypically and histologically resolved to NBCIE over the first 13 months (Bland et al. 2015).

Case	Sample	Ethnic background	History of consanguinity	Clinical diagnosis	Mutation	Citation
1	DNA	Indian	Yes	HI	c.7317_7318insACAAA p.Cys2439fs	Aggarwal et al. 2014
2	DNA from blood	British caucasian	No	HI	c.5936C>G c.6858delT	Scott et al. 2013
3	DNA from blood, RNA from hair follicle	British caucasian	No	HI	Possible complex or regulatory	-
4	DNA from blood	Pakistani	Yes	HI	c.6286-17delTGT Further analysis needed	-
5	DNA from blood	Indian	Yes	HI	Further analysis needed	-
6	DNA	Turkish	No	NBCIE	c.1630T>C p.C544R	Bland et al. 2015

Table 3.5. Summary of cases in chapter 3.

3.2. Discussion

3.2.1. Genetic screening of *ABCA12* in HI cases

This chapter aimed to identify new *ABCA12* mutations, utilise and develop new strategies when complex mutations were screened for. In this chapter mutations in *ABCA12* were associated with HI for four out of the five cases that were diagnosed as HI. The other (**case 6**) was verified with a clinical diagnosis of NBCIE after an original diagnosis of HI. As expected with a recessive disease biallelic *ABCA12* mutations account for around 98% of HI cases, with the remaining 2% identified with only one mutant allele, suggesting HI is a homogenous disease (Rajpopat et al. 2011). The majority of disease-causing mutations associated with HI are homozygous and are frequently attributed to parental consanguinity.

Exome capture by definition sequences ~5% of the genome and captures the vast majority of the protein coding genes. A great advantage of this study is the sequencing of the entire genome will bring about the discovery of causative mutations in non-coding regions such as mutations involved in regulation, stability of message and splicing.

Genomics England is the governing body in control of the 100,000 genomes project, which has been set up to sequence, in its entirety, the genomes of 100,000 people within the population of England. Around 80% of rare diseases are inherited these include diseases like HI. Those suspected of having an inherited disease without a full molecular diagnosis are possible candidates for the 100,000 genomes project. They would be sequenced along side near family members, where possible parents to aid with the segregation of disease-causing variants.

15,000 patients with rare diseases will have their genome analysed through the 100,000 genomes project, with the overall theme to gain a molecular and clinical ‘big picture’ of many inherited diseases. The immediate benefits are a molecular diagnosis to enable the correct treatment of the affected as well as the option of participation in relative clinical trials where possible. The analysis of this large data set will also lead to the discovery of new pathways of disease and strengthening ones that already exist. As no molecular

diagnosis was concluded on for **case 3** the affected would have been an ideal candidate for this project.

A possible area of interest, which was not covered by the exome sequencing of the affected was the locus of the 3.7-kilobase large non-coding RNA (lncRNA) terminal differentiation-induced ncRNA (TINCR). The lncRNAs are multi-exonic RNA that are regulated by transcription factors and perform regularity roles from stem cell pluripotency to proliferation and differentiation (Guttman et al. 2009). TINCR regulates epidermal terminal differentiation through a posttranscriptional stabilisation, enabling a high concentration of epidermal differentiation gene mRNA (Kretz et al. 2013). Genes including *ABCA12, ALOX12B, ALOXE3, LOR,* and *FLG*. TINCR induces expression of ABCA12 in human keratinocytes via the TLR3-dependent pathway, which increases lipid and LG concentration of epidermis (Borkowski et al. 2013). As a TINCR-deficient epidermis has been shown to be lacking terminal differentiation ultrastructure like LG and reduced ABCA12 expression, it is viable that this locus would be of interest when furthering the investigation of **case 3**.

3.2.2. The genotype-phenotype correlation of *ABCA12* and HI

Homozygous missense mutations have been found to be causative for disease in other members of the ABC transporter subfamily A. In Stargardt disease, missense mutations within conserved domains of ABCA4 account for 80% of case aetiology and in Tangier disease, 60% of causative mutations are missense and found within the conserved domains of ABCA1 (Lewis et al. 1999; Huang et al. 2001).

Missense mutations in ABC1 domain of ABCA12 are predominately linked with causing LI2 in a sub group of the African population and infrequently linked with NBCIE (Lefévre et al. 2003; Sakai et al. 2009). No missense mutations of the ABC1 domain have been found to be causative in HI, only whole exome deletions or deletions resulting in a frameshift in this region develop into HI (Akiyama 2005; Thomas et al. 2006), though in the minority, missense mutations in other domains of the ABCA12 protein are causative in HI. A single missense mutation in NBD1, conserved residues within the ABC1, domain of ABCA12 has been found to causative in HI; however, this *de novo* mutation was paired with a deletion in exon 28 in a compound heterozygote

state (Akiyama et al. 2006). As the missense mutation was found on a single allele and the other allele had a deletion in a conserved residue of NBD1, this still upholds that there are no missense mutations within ABC1 domain at a homozygous state causative for HI.

Homozygous missense mutations in the ABC2 domain of ABCA12 have been found to be causative in HI (Kelsell et al. 2005). ABC transporter domains 1 and 2 have 36% homology and within these domains the NBD1 and 2 share 87.5% homology. All of which suggest both NBDs act in very similar ways to bind nucleotides, where as the ABC domains though form the cassettes that orientate ATP towards the NBDs, they may have slightly different roles in the function of ABCA12. The genotype-phenotype relationship in *ABCA12* is such that type and location of mutation is not only an indicator of phenotype severity, but actually indicate which disease is present. The predominately missense mutation-associated NBCIE and LI2 are much milder phenotypically then HI, where the majority of causative mutations are homozygous deletions or truncations.

The genotype-phenotype relationship may also play a distinct role in the probability of mortality. From previous clinical genetic screenings by the Kelsell group it was noted in 2010 that although HI was still infrequently lethal when causation was linked with compound heterozygous mutations in *ABCA12,* the rate of mortality was reduced in these individuals. This was corroborated with a review of 45 cases of HI in which mortality, though still generally infrequent in HI, it was more common with homozygous mutations (Rajpopat et al. 2011); should probably be viewed as a greater benefit from treatment or survival advantage. Another possibility that may also skew the correlation is that the affected may harbour another mutation for a coexisting recessive disease, which would play a role in reducing the survival rate. More plausible is the relationship of the location and type of mutation in the protein and how it affects the severity of the HI disease phenotype (Rajpopat et al. 2011).

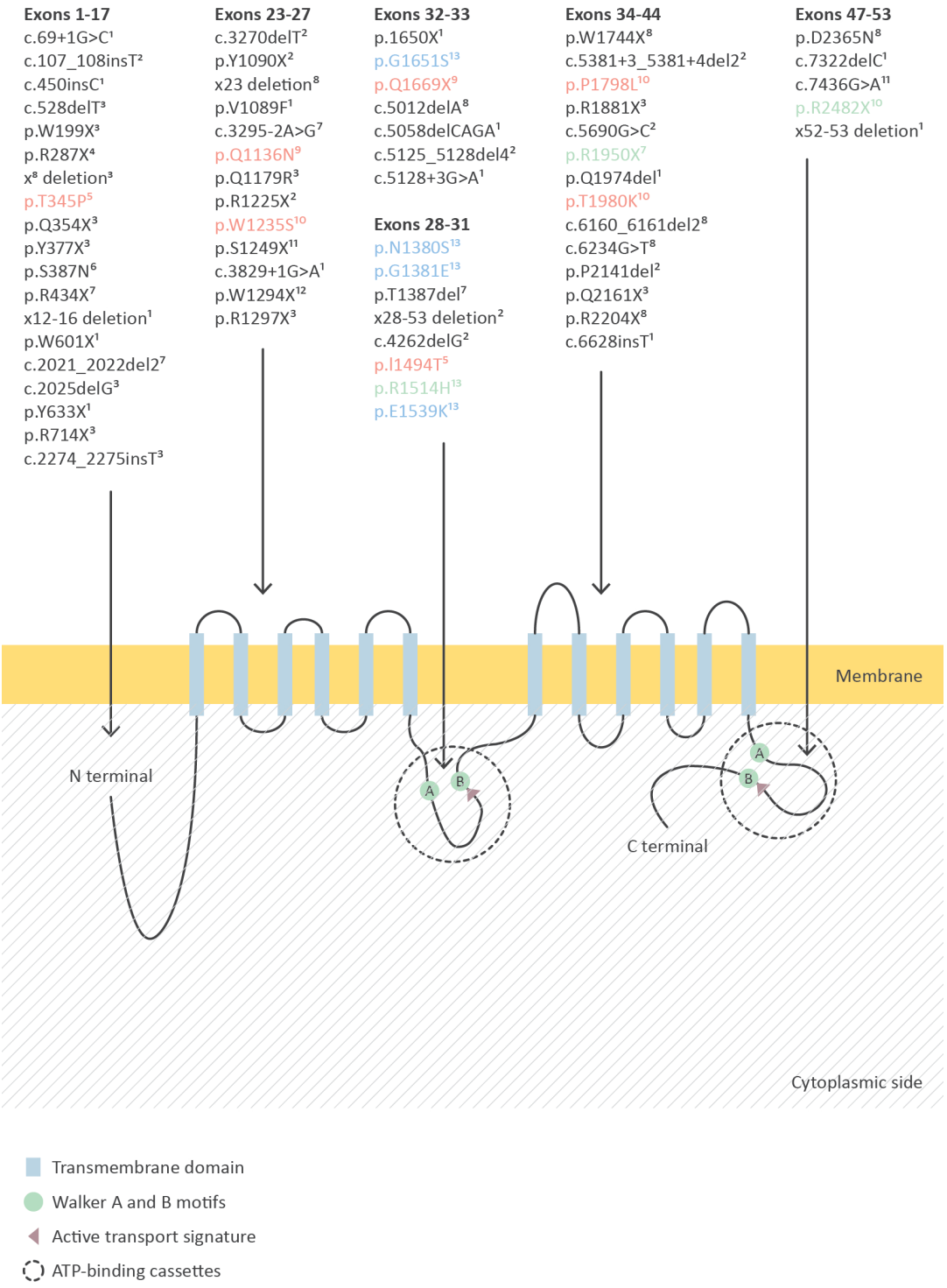

Figure 3.14. A schematic representation of the ABCA12 protein, denoting the location of known mutations and specific domains. Mutations have been grouped depending on the domain they localise to and coloured in accordance with the severity of disease they've been found to be causative in. LI2, CIE and HI causing mutations are coloured blue, orange and grey respectively with green resembling mutations that result in differing phenotypes. 1(Rajpopat et al. 2011), 2(Thomas et al. 2006), 3(Thomas et al. 2009a), 4(Castiglia et al. 2009), 5(Natsuga et al. 2007), 6(Akiyama et al. 2006), 7(Akiyama 2005), 8(Kelsell et al. 2005), 9(Yanagi et al. 2008b), 10(Sakai et al. 2009), 11(Akiyama et al. 2007), 12(Rajpar et al. 2006), 13(Lefévre et al. 2003).

3.3. Summary

In this chapter, multiple molecular genetic techniques were used to ascertain and evaluate possible causative mutations for HI in the gene *ABCA12*. The mutations detected ranged from simple to complex and when a molecular diagnosis could not be defined an outline of future work was proposed. The majority of patients screened were clinically diagnosed with HI presenting with many of the characteristic phenotypes of the disease. The shift of ARCI clinical features as seen in the NBCIE case caused by a mutation in the *ALOX12B* underlies the importance of understanding skin development in early infancy for molecularly or histopathologically confirmed diagnosis and prompt treatment.

Not only does the identification of mutations give molecular diagnostics a greater reservoir to help identify possible causative mutations in future cases. It also aids in the understanding of the functional mechanisms of the ABCA12 protein as described in **chapter 4,** where a patient derived HI cell line was isolated and characterised for further use in the analysis of *ABCA12* and its role in the epidermis.

Chapter 4: Characterisation of a Patient Derived Harlequin Ichthyosis Cell Line

4.1. Introduction

The ABCA12 protein is a member of the ABCA subfamily of ABC transport proteins; it actively transports lipids against a concentration gradient into LG transport vesicles (Sakai et al. 2007). ABCA12 ablation in HI results in absent LG or a reduction in their lipid cargos (Mitsutake et al. 2010). The contents of functional LGs are a myriad of lipids, which when extruded into the extracellular lipid lamellae membrane of the lipid envelope (Uchida & Holleran 2008). When this process is interrupted in HI a disrupted permeability barrier is formed leading to increased TEWL and the possibility of secondary infections. This epidermal defect (due to loss of ABCA12) leads to increased retention of squames through the dysregulated transportation of proteases and premature terminal differentiation (Thomas et al. 2009b).

The precursors of the ceramides ABCA12 transports are present in the basal layers of the epidermis and have been shown to up-regulate the transcription of the gene *ABCA12* through the PPARβ/δ pathway (Jiang et al. 2009). Another nuclear hormone receptor, LXRβ, has been shown to up-regulate the transcription of ABCA1, which transports cholesterol in the epidermis, another constituent of the permeability barrier. This chapter aims to investigate this pathway and its role in epidermal differentiation and how it is modulated in HI, by utilizing a HI patient derived cell line and calcium shift.

4.2. Results

4.2.1. Genetic analysis of patient of patient derived HI cell line

The affected individual was clinically diagnosed with HI at birth and is currently 26 years of age. A DNA sample was sent for whole exome capture and next generation sequencing. Analysis revealed that the HI individual was a compound heterozygote for a nonsense mutation and a putative splice site mutation in *ABCA12*. The nonsense mutation is p.Glu2264X, producing a termination of the protein from exon 45 of *ABCA12*. The severity of this truncation indicates that this allele does not produce a functional protein and the transcripts produced will have an increased rate of degradation by nonsense-mediated RNA decay.

The other heterozygous mutation is a change to the putative acceptor site (AG) preceding exon 35 of ABCA12, c.5382-2a/g. To analyse this variant further and for other investigative studies into HI disease mechanisms, a skin biopsy was performed after informed consent (adult) and ethical approval from East London and City Health Authority Research Ethics Committee and following **2.7.2.** The punch biopsy was halved, with one half flash frozen for IHC to check for markers of premature terminal differentiation, ABCA12 and ABCA1. Immunostaining of ABCA12 in the epidermis of the affect was drastically reduced compared to that of controls, as shown in **Figure 4.6.** The second half was used in the isolation and propagation of the HI patient derived keratinocyte cell line, with dispase and trypsin used for dermis separation and epidermal dissociation respectively. The keratinocytes were immortalised as described in **2.3.8.** This was performed by Dr Andrew South, University of Dundee.

The RNA transcribed to cDNA for the splice site analysis was isolated from the immortalised HI keratinocytes. To analyse this splice site in detail, primers were designed to amplify the region in cDNA and the amplicons were run on a high percentage agarose gel to differentiate between multiple bands produced by the spliceosome recognising different exon 35 acceptor sites in the allele with this mutation. An *in silico* splice site prediction model was utilised to predict the positions of alternative acceptor sites and give an idea of transcript composition with regard to exon 35 and intron 34/35.

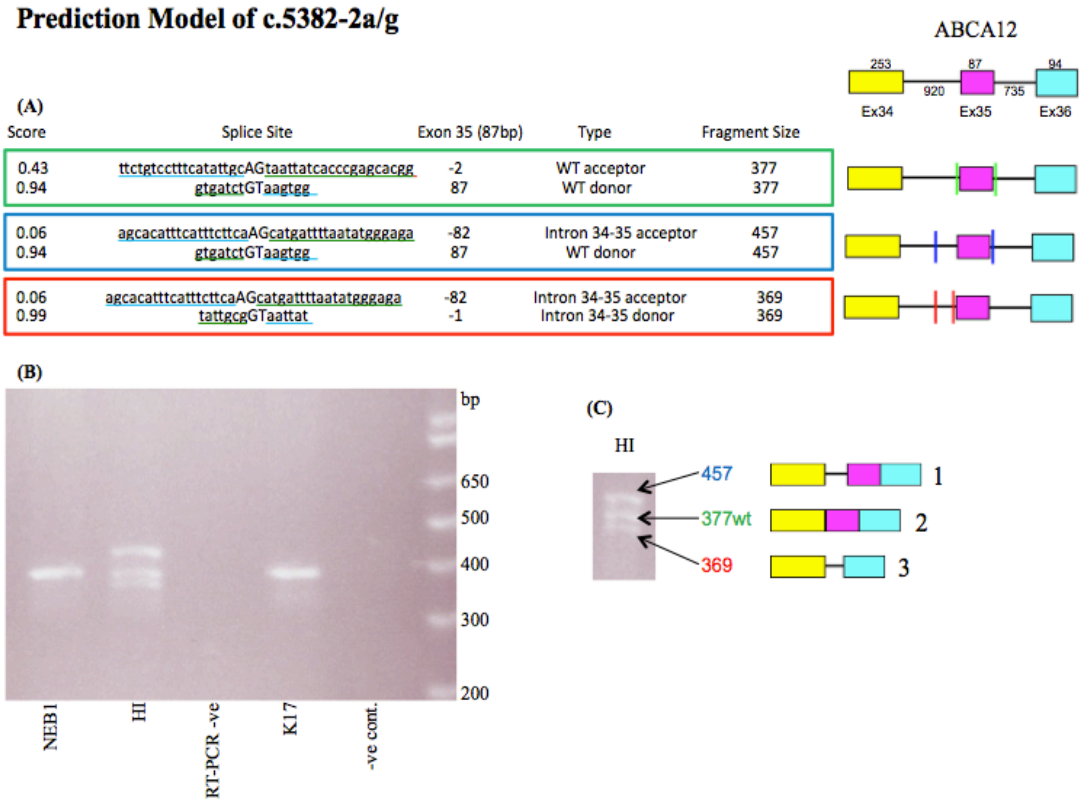

Figure 4.1. ***In silico*** **splice-site prediction and agarose gel electrophoresis of 377bp cDNA fragment. (A)** *In silico* splice site prediction modelling of the WT and HI cell line holding c.5382-2a/g. The WT fragment is highlighted in green and predicts the correct size of fragment amplified, red and blue are possible predicted fragments when the c.5382-2a/g mutation is taken into consideration. **(B)** Gel electrophoresis shows a triple band produced from the PCR of cDNA reverse transcribed from RNA extracted from the HI cell line. Both NEB1 and K17 controls produce an amplicon at 377 bp. **(C)** The set of fragments produced by the amplification of the splice site and their possible prediction models.

Figure 4.1. shows that the splice site mutation in the HI cell line does produce alternative transcripts to those on the Ensembl database, from the electrophoresis gel of PCR amplicons of the splice site region there are 3 distinct fragments are visible. The *in silico* splice site prediction model used www.fruitfly.org/seq_tools/splice for acceptor/donor sites analysed in this method can obtain a maximum score of 1 for level of affinity with the spliceosome. Primers for this section of transcript amplification can be found in **A1.1.**

The middle fragment or the 2nd splice variant is at the same size as the WT fragment produced here from the amplification of cDNA synthesised from RNA extracted from NEB1 and K17 cell lines. The 1st and 3rd splice variants are larger and smaller fragments, respectively, as predicted by the *in silico* prediction, but to conclude on what had been retained and lost in the splicing process the bands were extracted from the gel, cleaned and sequenced.

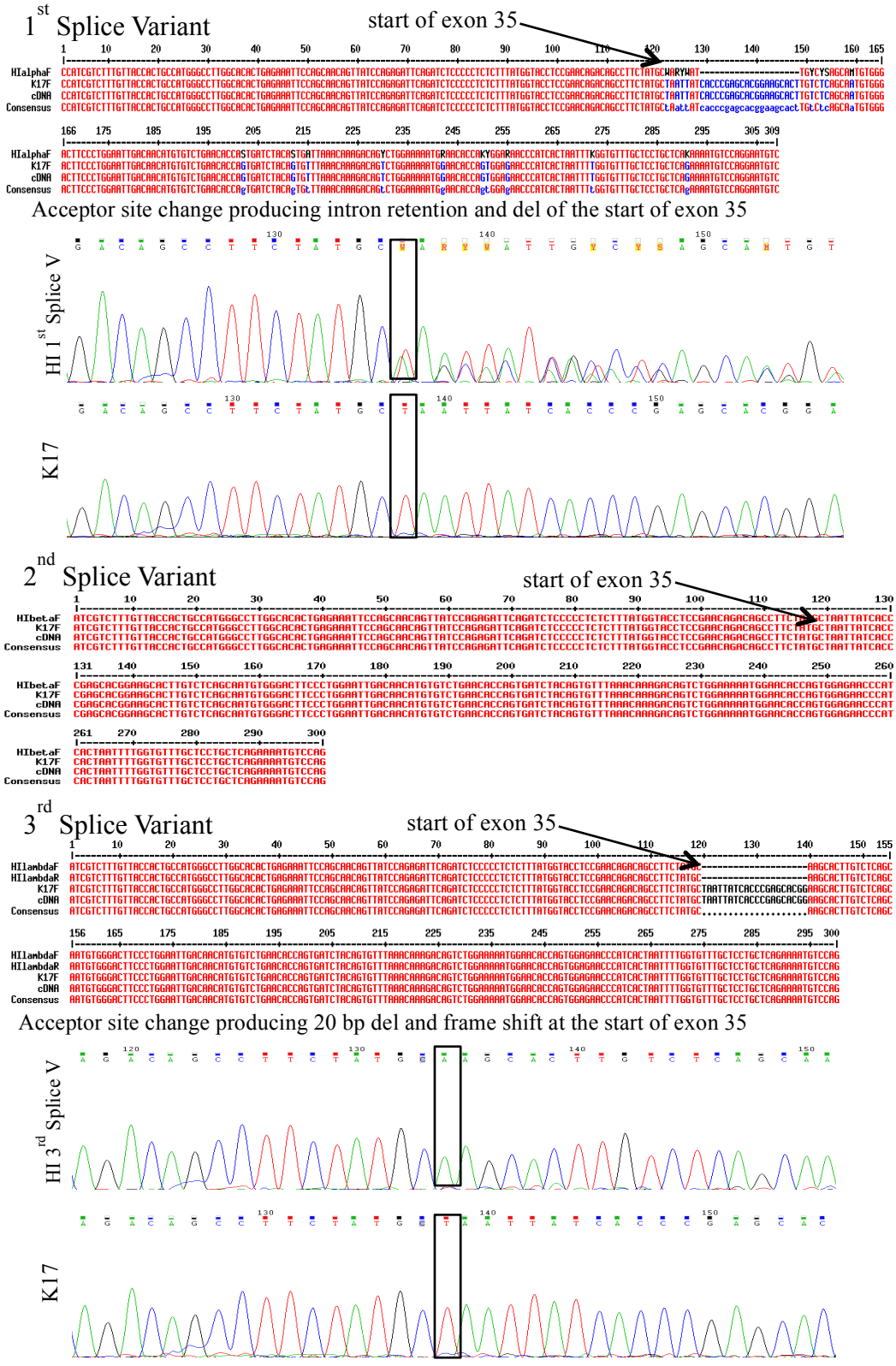

Figure 4.2. Electropherograms of the Sanger sequencing of the 3 splice variants. Produced by PCR of cDNA from the HI and K17 cell lines, the amplified region straddled the possible exon 35 acceptor sites, shown in **Figure 4.3**.

As indicated at the top of **Figure 4.2.** and from **Figure 4.1.** the 2nd splice variant is of WT length and sequence for the HI cell line. This splice variant is probably a product of the alternative allele, as the exon 45 nonsense mutation would not affect the amplification of exon 35 and it's splicing. The 3rd splice variant aligns with the control sequence with a 20 bp deletion (TAATTATCACCCGAGCACGG) from the start of exon 35 producing a frameshift in the transcript. The 1st and largest splice variant is itself a composite of several transcripts that like the 3rd splice variant have a ~20 bp deletions from the start of exon 35, but also contain a retention of varying lengths of intron 34/35. These possible indels are due to the spliceosome selecting a multiple of low affinity alternative acceptor sites that subsequently changes which donor site can be utilised.

Though the *in silico* splice site prediction did predict two alternative splice variants, it did not predict the utilisation of the donor site 20 bp into exon 35. Neither did it account for the range of acceptor sites within intron 34/35 that the spliceosome could recognise and thus produce many different lengths of intron retention. To further investigate if the splice site mutation c.5382-2a/g does lead to the transcription of any translatable mRNA in the HI cell line, the different transcripts within the largest fragment (1st splice variant) would have to be separated and sequenced.

To do this, TA cloning was undertaken on the extracted amplified cDNA from the largest fragment, 1st splice variant. With the use of a topoisomerase I enzyme to unwind and reform supercoiled DNA and a TOPO vector to bind the individual PCR products, this permitted the individual cloning and then sequencing of all possible amplified transcripts, as shown in **Figure 4.3.**

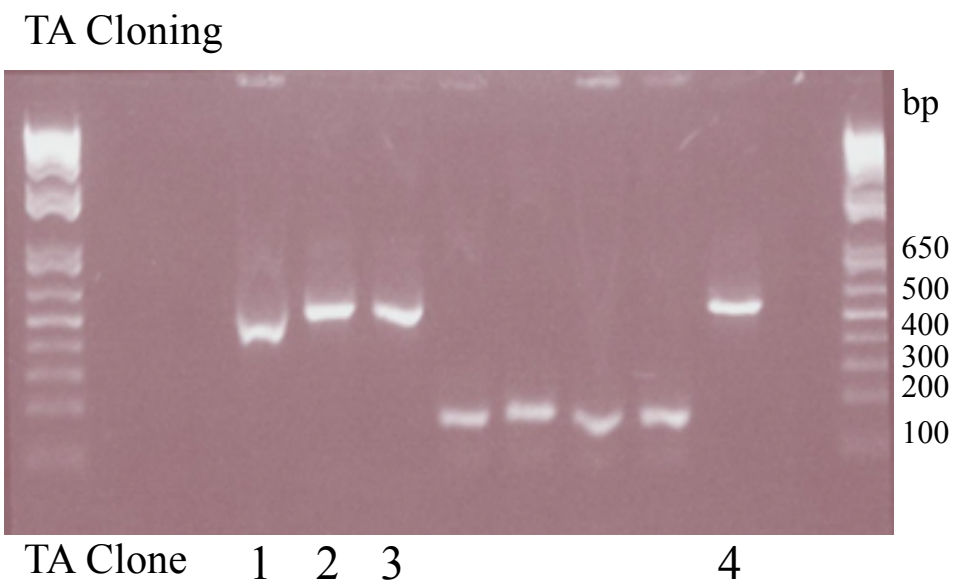

Figure 4.3. TA cloning of aberrant splicing. Electrophoresis gel of HI cell line amplicons, TA cloning and subsequent PCR of exon 35, including exon 34 and 36 to ensure all alternative transcripts are captured. Single colonies were used from separate plates; plates were spread from individual TA cloning reactions, except for colonies 2 and 4, which were taken from the same plate. The four smaller fragments are produced from the amplification of the M13 forward sequence to the reverse of the TOPO vector, when ligation of a PCR fragment does not occur. The four successful TA clones were then sequenced by Sanger sequencing.

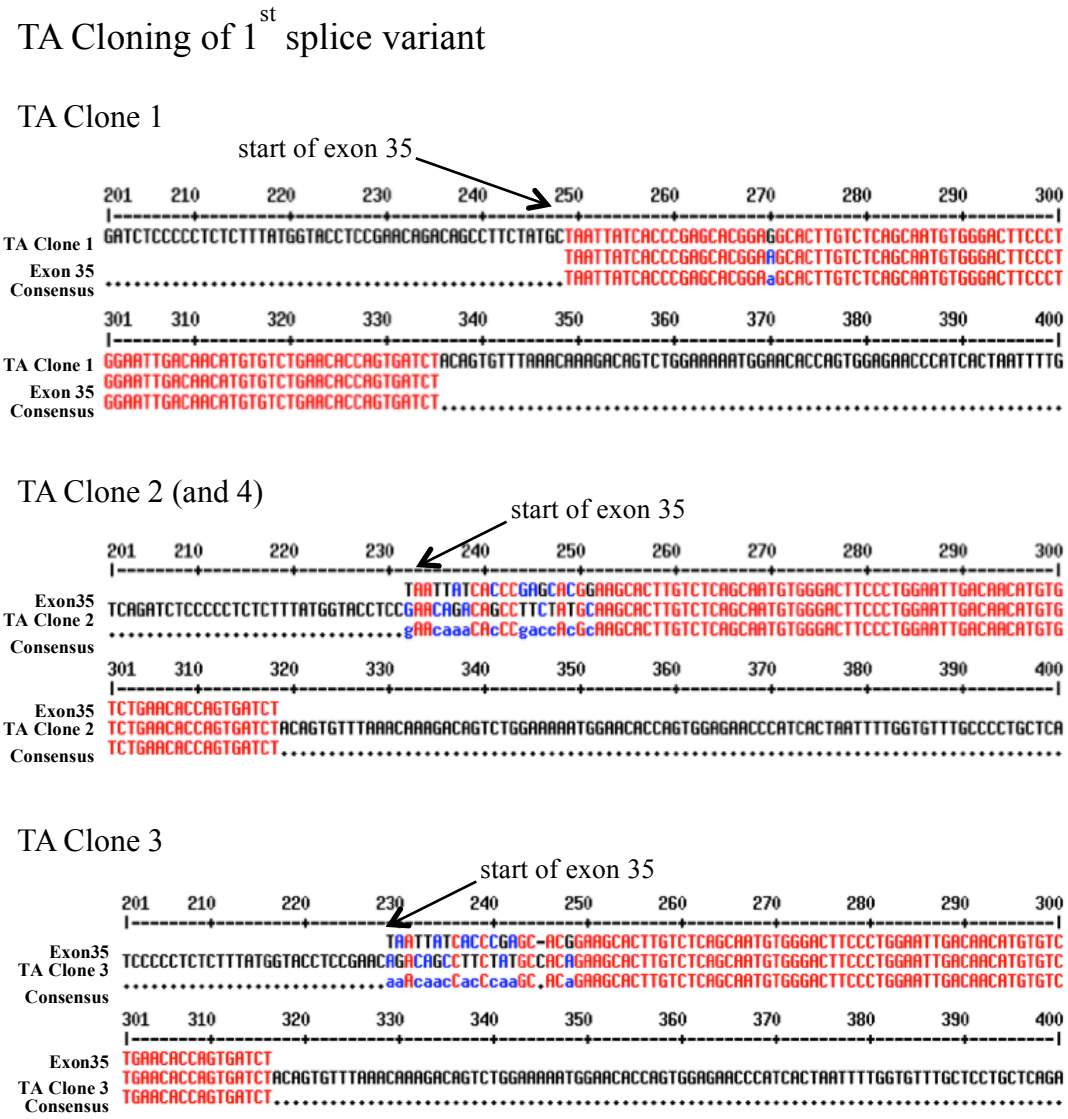

Figure 4.4. The MultAlin sequence alignment of the four TA cloning products. Showing the region covered by the amplicons of the TA cloning, aligned with exon 35 of the *ABCA12* gene. This disseminates the different transcripts within the 1st and largest splice variant and gives an indication as to the variety of splicing acceptor sites utilised.

Figure 4.4. shows the TA clone 1 is same length as 2nd splice variant (WT) with a point mutation; this fragment was extracted with the largest band on the original gel separation of splice variants. The point mutation could have occurred from the low proof reading fidelity of the DNA polymerase utilised in TA cloning.

TA clones 2 and 4 have an acceptor site 20 bp within exon 35 and also hold the longest intronic retention. TA clones 2 and 4 are homologous, as expected when taking colonies for the same TA cloning plate, with the remainder of exon 35 frameshifted and the retained intron coding for a stop codon in 7 bp. TA clone 3 has an acceptor site 15 bp into exon 35, though a shorter intronic retention than TA clones 2 and 4 producing a slightly shorter fragment. This transcript has 42 bp of retained intron of which the last 15 bp replaces the first 15 bp of exon 35, stays in frame and does not code for a stop codon, though will produce a protein with 14 additional amino acids to that found in the K17 cell line and on the Ensembl database.

After freeze thawing and multiple passages, the HI cell line was re-checked for the presence of the causative mutations at the genomic level, to ascertain if they had been retained, as loss can occur during culturing or the immortalisation process.

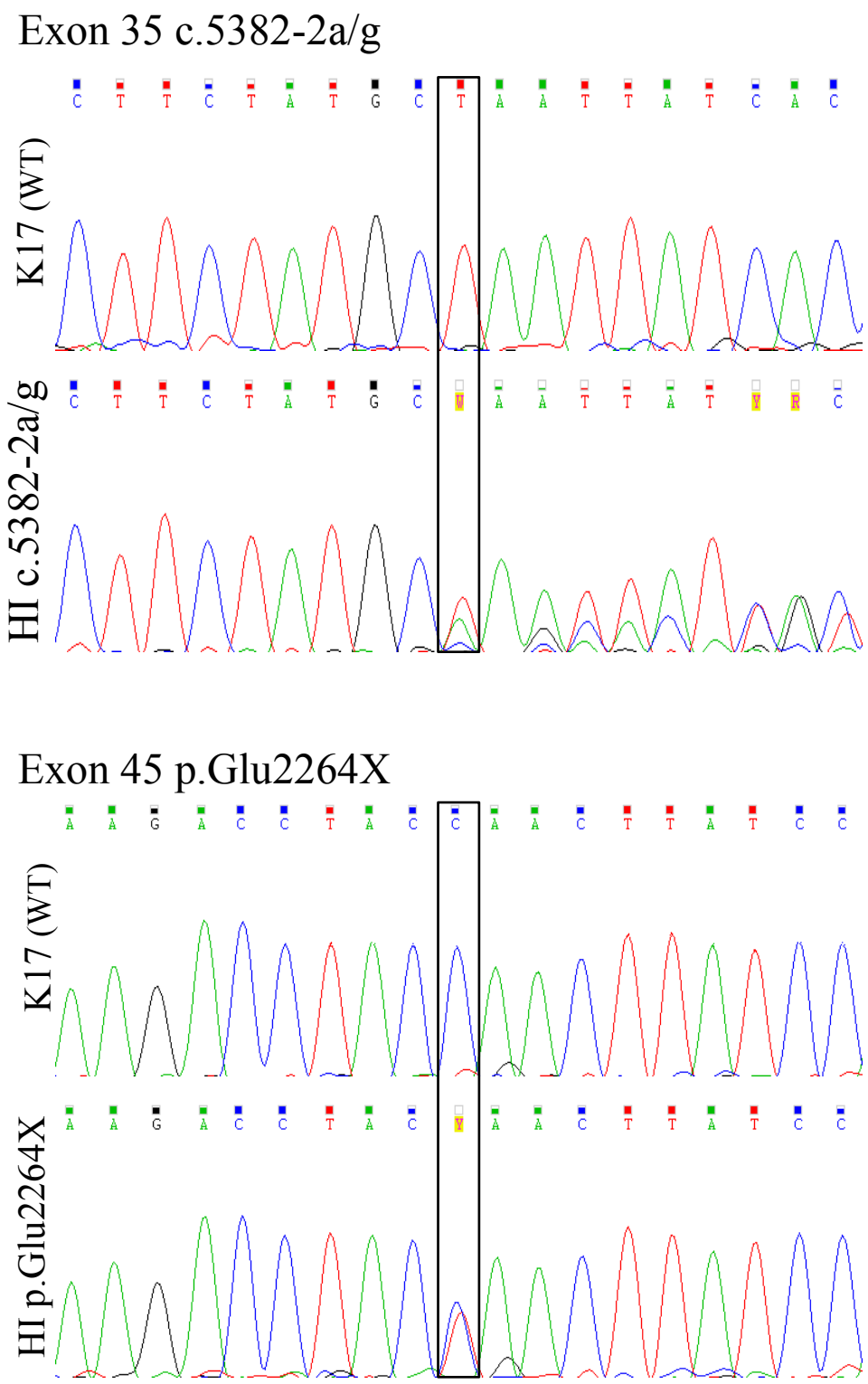

Figure 4.5. Electropherograms of Sanger sequencing for mutation analysis. From the PCR of exons 35 and 45 of *ABCA12* from the genomic DNA of the K17 and HI cell lines. To screen for the found compound heterozygous mutations to check that the HI cell line has retained them. Frozen stocks were cultured through 15 passages to check for mutation retention.

4.2.2. Immunohistochemistry of ABCA12 and ABCA1 in the HI skin

The skin biopsy was processed for histopathological work-up and frozen section were cut to immunostain for the expression and epidermal localisation of ABCA12 and ABCA1 proteins. The negative controls of the immunohistochemistry are in **Figure A1.1.**

The general structure of the HI skin biopsy showed enlarged stratified layers of the epidermis and a thick stratum corneum of retained squames, in contrast to control (normal) skin (NS), which has a thinner, basket weave like stratum corneum **(Figure 4.6)**. The immunohistochemical staining revealed that ABCA12 protein expression was significantly reduced if not absent in the epidermis of the affected in comparison to NS, where ABCA12 protein expression localised to the upper stratum granulosum and stratum corneum. ABCA1 protein expression was also reduced in the epidermis of the HI skin where it localised to the stratum granulosum and corneum, in comparison to the NS where expression also localised to the basal layer as well as the upper stratum granulosum and corneum. The features described were all consistent with a disease causing mutation in the gene *ABCA12* **(Figure. 4.6)**.

A consideration to make is that IHC of the HI epidermis will give a slight skewed appearance of protein expression when compared to NS due to the enlarged stratified layers.

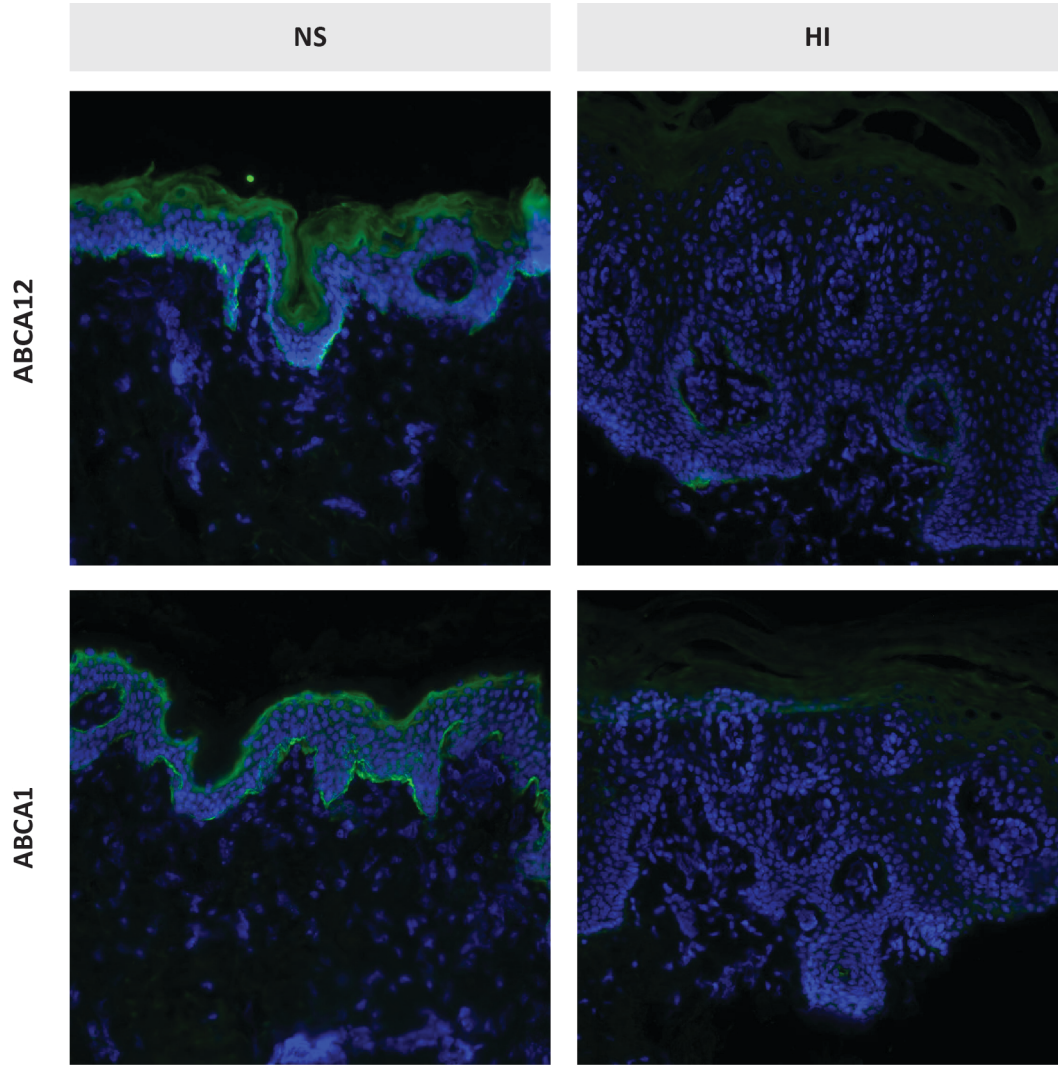

Figure 4.6. Immunohistochemistry of HI patient skin and normal skin. Immunostaining against ABCA12 (upper panel) and ABCA1 (lower panel), showing a dramatic reduction in epidermal ABCA12 expression and to a lesser extent ABCA1 expression in the HI skin compared to NS. IHC ABCA12 and ABCA1 antibodies (green), nuclei stained with DAPI (blue), captured at x20 magnification.

4.2.3. Analysis of transient siRNA mediated *ABCA12* knockdown

The compound heterozygous *ABCA12* mutation indicated that transcription of *ABCA12* would be significantly reduced, which was supported by the near absence of ABCA12 protein in the IHC. The IHC also showed a reduction in ABCA1 in the epidermis of the affected and to investigate if this was due to the ablated ABCA12, through the possible modulation of LXRβ, an *ABCA12* siRNA knockdown (KD) was performed.

K17 keratinocytes were seeded in low calcium media, then 24 hours later were calcium shifted to up-regulate ABCA12, as previous experiments found ABCA12 protein expression to be insufficient for immunoblotting detection at low calcium. This is consistent with the localisation of ABCA12 protein in the upper layers of the epidermis. After 24 hours of high calcium the keratinocytes were KD by transfection with 100 nM (final concentration) of either *ABCA12* siRNA SMARTpool, complementary for the two prominent transcripts of *ABCA12* or non-targeting pool siRNA (NTP) (Dharmacon).

RNA isolates were taken at 24-hour intervals and qPCR of the RT-PCR cDNA was analysed on a Rotorgene Q thermocycler, shown in **Figure 4.7(A)**. A 70-90 % knock down of *ABCA12* was recorded for day 2 and 4 compared to the NTP. By day 6, which was day 8 of calcium shift the keratinocytes were in the final stage of terminal differentiation, outlined in **Figure 4.9.** This *ABCA12* KD was achieved through much optimisation and though the experiment was duplicated, it could not be triplicated.

From the qPCR *ABCA12* KD data, day 4 was chosen to harvest protein lysate for immunoblotting, shown in **Figure 4.7(B).** The two major ABCA12 isoforms were present at similar quantities in the lysate of the calcium shifted K17 cell line, at 293 and 257 kDa. Both of these isoforms achieved an approximately 75 % KD when transfected with the *ABCA12* siRNA. ABCA1 and LXRβ protein expression were also reduced in the K17 cells transfected with *ABCA12* siRNA suggesting a possible down-regulation by the reduction of ABCA12. A reproducible robust KD of ABCA12 for multiple days could not be achieved, possibly due to the calcium shift and the up-regulation of the ABCA12.

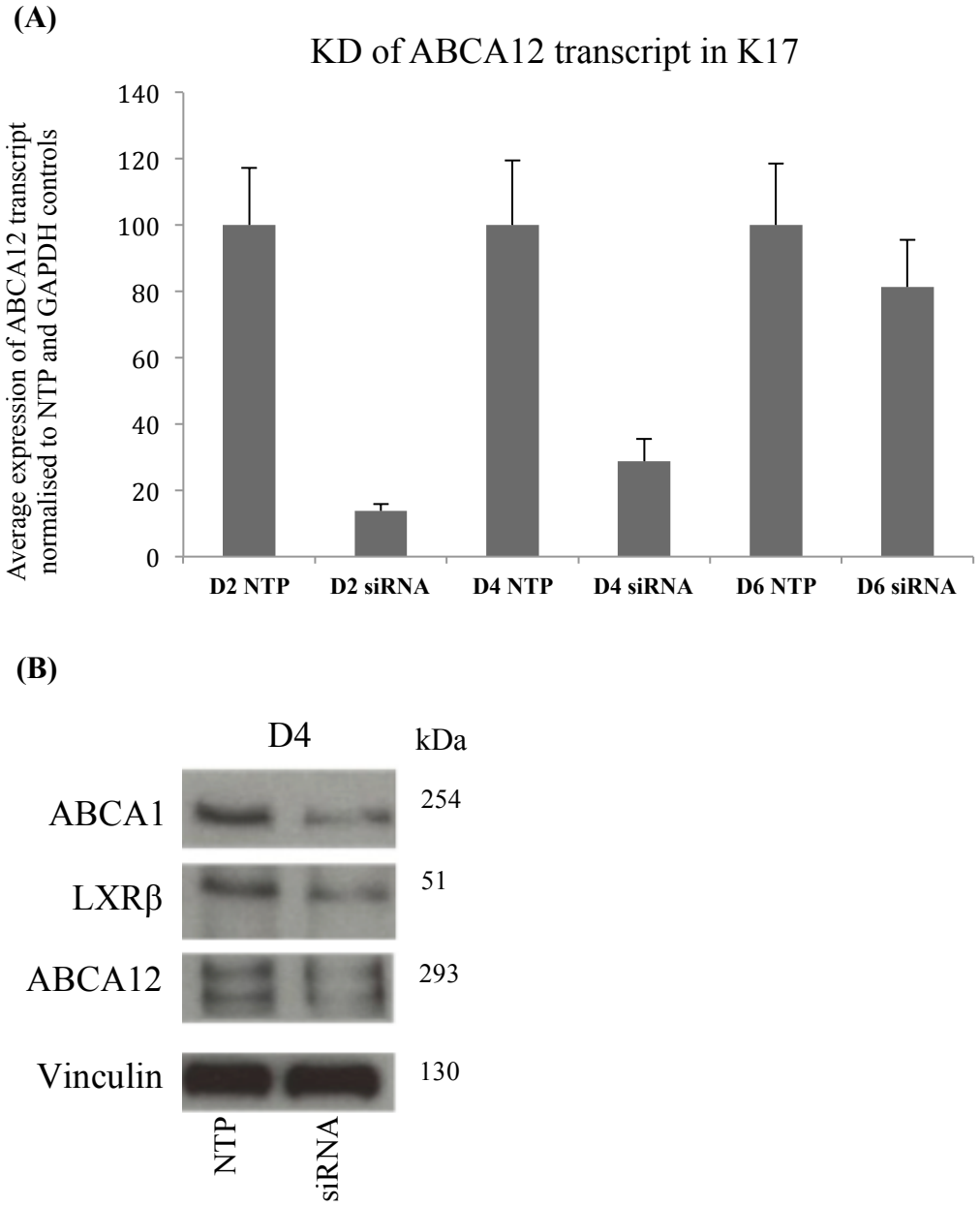

Figure 4.7. Analysis of *ABCA12* knock down in culture. (A) qPCR analysis of total *ABCA12* mRNA levels during ABCA12 KD after calcium shift, in the K17 cell line. The data is expressed as a percentage of the relative NTP control (100%) and is the average of experimental repeats. **(B)** Immunoblotting analysis of *ABCA12* siRNA KD**,** reduction of ABCA12 at the protein level on D4 of KD after calcium shift in the K17 cell line lysate. The immunoblotting of cell lysates for ABCA1 and LXRβ also showed a reduction in the expression of these proteins in comparison to their non-targeting pool (NTP) and vinculin loading controls. Immunoblotting quantification performed on *ImageJ64* software.

4.2.4. Functional analysis of cell line under calcium shift

Transcript analysis was performed to assess the difference in the level of *ABCA12* mRNA between the HI cell line and the K17 cell lines and how this was attenuated after 24 hours of calcium shift. As suggested from the genetic analysis of the HI cell line there is a significantly reduced amount of the *ABCA12* transcript in the HI cell line compared to that of control. In the HI cell line the *ABCA12* transcript was up-regulated under calcium shift relative to low calcium culture, though to a level still significantly lower than the K17 cell line, shown in **Figure 4.8(A)**.

The presence of the *ABCA12* transcript in the HI cell line **Figure 4.8(A),** could be from vestigial transcription from either allele. The mutation p.Glu2264X causes a truncation from exon 45 and the qPCR primers were complementary to sequence within exons 40/41 (forward primer) and 43 (reverse primer). The present *ABCA12* transcript could have been transcribed from this allele and may have not been completely removed through degradation by nonsense-mediated RNA decay. A vestigial amount of the ABCA12 protein is present in immunoblotting of HI cell line lysate, which is possibly due to the epitope of the ABCA12 antibody (abcam ab98976) corresponding to aa's 1979-2028 present before the p.Glu2264X mutation.

The alternate allele, which holds the splice site mutation c.5382-2a/g could possibly be transcribed to produce this vestigial amount of *ABCA12* transcript. Its splice variant TA clone 3 from splice variant 1 has 42 bp of retained intron of which the last 15 bp replaces the first 15 bp of exon 35, though it does stay in frame and does not code for a stop codon, as shown in **(Figure 4.4.).** If transcribed, this transcript may not translate a functional ABCA12 protein, however the transcript itself may be present.

Figure 4.8(B & C) shows the ABCA12 transcript up-regulated through calcium influx in both K17 and HI cell lines, compared to low calcium controls. The significant relative increase is at the 48-hour time point in the K17 cell line. In the HI cell line the relative increase in the ABCA12 transcript occurs earlier at 24 hours and is still elevated at 48 hours. Many markers of terminal differentiation are expressed at relative high levels after calcium shift, though ~4 days (96 hours) after calcium shift all transcription and translation is reduced by half prior to the completion of terminal differentiation (Hennings et al. 1980).

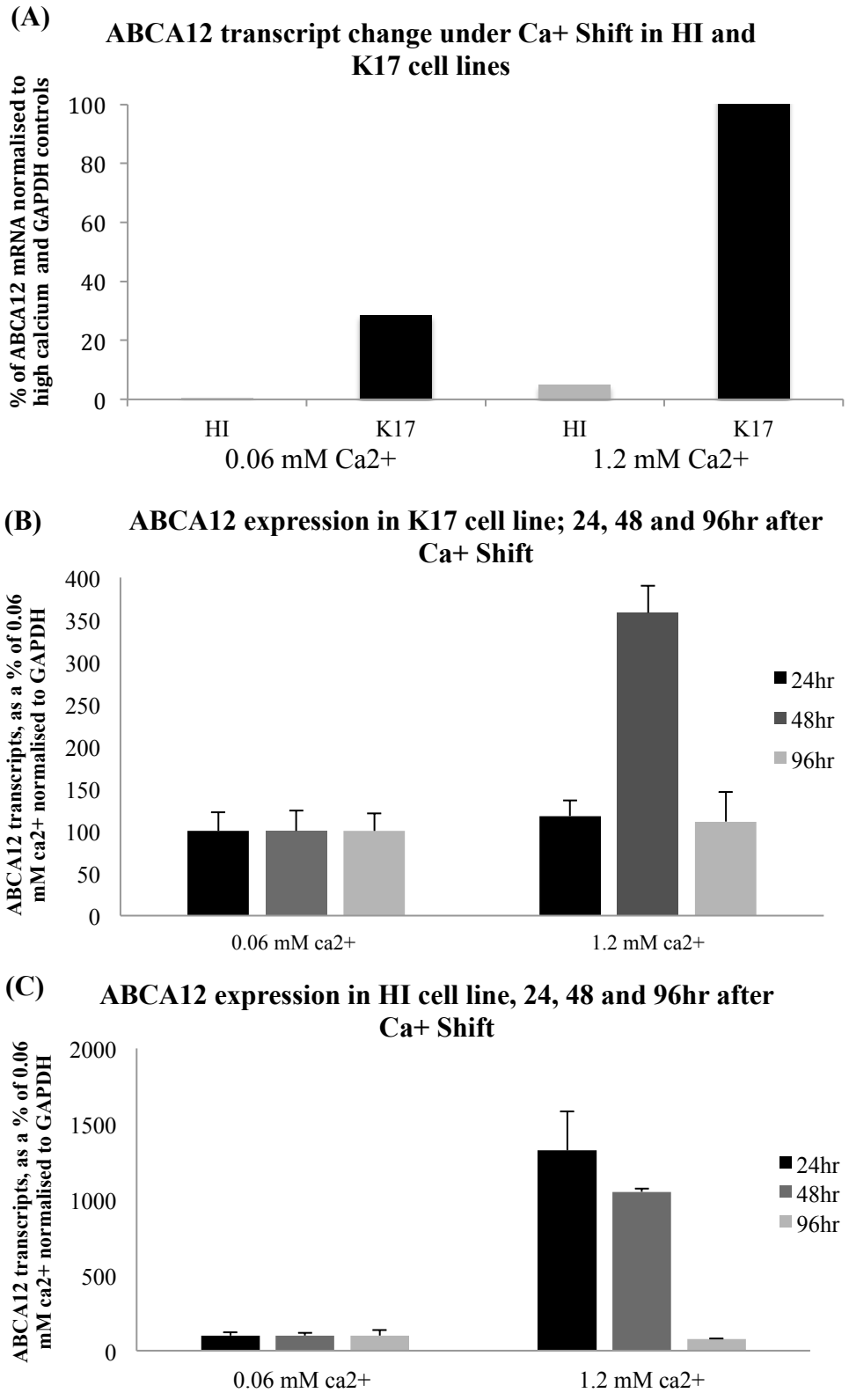

Figure 4.8. qPCR data showing an increase of *ABCA12* mRNA expression in culture under calcium shift. From 0.06 mM ca^{2+} (low Ca) to 1.2 mM ca^{2+} (high Ca) **(A)** Cell were either calcium shifted or low Ca^{2+} media was replenished and RNA was isolated after 24 hours from HI and K17 cell lines. Data was normalised to high Ca^{2+} K17 control at 100% **(B)** Calcium shift in K17 cell line **(C)** Calcium shift in HI cell line **(B & C)** Average of triplicates, data was normalised to individual time point low Ca^{2+} controls at 100%.

4.2.5. FACS analysis of cell death and apoptosis during calcium shift

To analyse terminal differentiation in the HI and control cell lines under calcium shift, the number of dead or apoptotic cells were counted using FACS. Premature terminal differentiation is a well-characterised phenotype of the HI epidermis, with keratinocytes expressing markers of terminal differentiation in earlier layers of the enlarged stratified epidermis. The keratinocytes of the HI epidermis that differentiate prematurely, enter programmed cell death earlier and are retained as squames in the enlarged stratum corneum.

To assess if the HI cell line would mimic these cellular phenotypes in monolayer, HI and K17 cell lines were calcium shifted for 8 days, as observations indicated this was suitable to induce complete terminal differentiation in these cell lines. FACS in control versus HI cell line keratinocytes, are shown as two parameter scatter plots in **Figure 4.9(A)** with cells labelled with AnnexinV/DAPI for the sorting of apoptotic and alive cells respectively. The method described in **2.5.4.** From the scatter plot the migration from a live population subgroup in the K17 data to a subgroup moving towards apoptosis and enucleated 'dead' in HI data is visible.

In **Figure 4.9(B),** the analysis of the FACS data for the average percentage of alive cells at day 8 of calcium shift. 34.4 % of the total K17 population assessed were alive in comparison to 13.03 % for the HI cell line (P value of 0.092 ns). In **Figure 4.9(C),** cells counted for apoptosis resulted in a more similar population size between the K17 (11.07 %) and HI (8.57 %). No significant result was obtained; there is a probable relationship between calcium-induced differentiation and an increase cell mortality in the HI cell line, though other time points and control cell lines would be needed to verify this. FACS analysis at an earlier time point of calcium shift could possibly define an apoptotic population.

FACS analysis of HI cell line under Ca^{2+} Shift

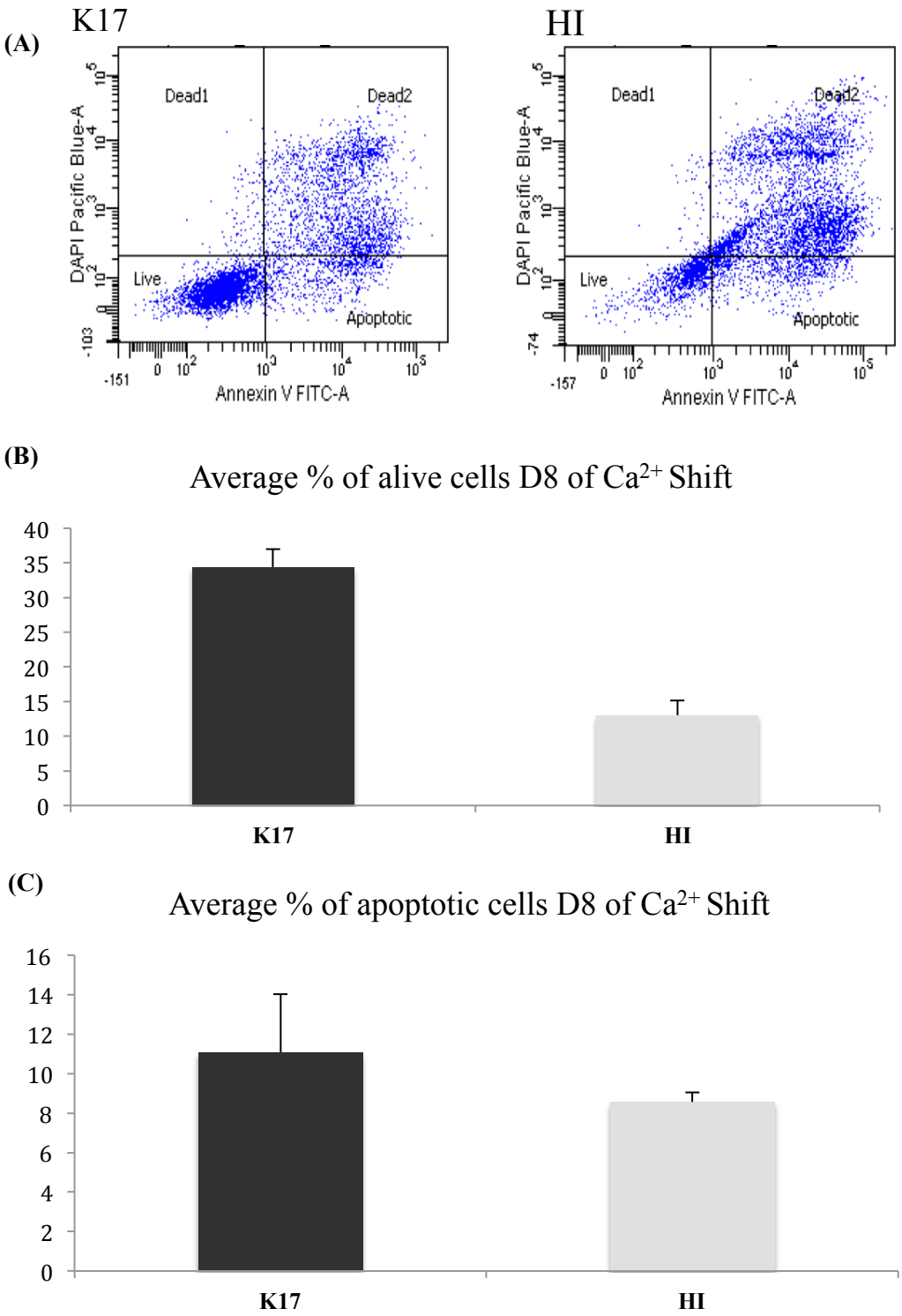

Figure 4.9. FACS analysis of cell death and apoptosis (A) Scatter plot of cells labelled with AnnexinV/DAPI and analysed by flow cytometry. **(B)** Analysis of average % alive cell population in K17 and HI cell lines at D8 of calcium shift. **(C) Analysis of average % apoptotic cell population** in K17 and HI cell lines at D8 of calcium shift. **(B & C)** averages of triplicates.

4.3. Discussion

A patient derived immortalised cell line capable of reproducing the disease phenotype *in vitro* is a valuable tool in the study of any cutaneous disease. The mortal primary cell line is the most accurate representation of a disease *in vitro,* though they are limited by senescence-enforced limited life spans, which can alter between passages and are more complex to maintain. A supply of fresh biopsy samples is difficult to obtain and comes with logistical and ethical concerns.

Mouse models of disease are another valuable tool in the analysis of HI, as they closely reproduce the HI human phenotype. Four HI mouse studies have been published to date, all of which found that *ABCA12* deficiency in mice is embryonic lethal (Zuo et al. 2008; Smyth et al. 2008; Yanagi et al. 2008b; Yanagi et al. 2010). The most recent paper grafted *ABCA12*$^{(-/-)}$ mouse skin on to healthy mice and found an improvement in HI skin differentiation (Yanagi et al. 2010). Hitherto this study, mouse models had been unsuccessful in questioning how HI skin has gradual self-improvement post-infancy. By studying the development of HI skin on mice embryos the earlier publications did lead to the verification of: the reduction of extracellular omega-hydroxy long chain ceramides and the increase of their intracellular glycosylated precursor in HI (Zuo et al. 2008); the reduction of lipid efflux and the accumulation of neutral lipids in HI mouse skin (Smyth et al. 2008); the loss of processed ceramides in the stratum corneum and the reduction of the co-localisation between these ceramides and their transporter ABCA12 (Yanagi et al. 2008b).

An immortalised patient derived HI cell line gives the opportunity to study these and other HI cellular phenotypes in a human *in vitro* model, needing less expenditure than a mouse model. The genetic analysis of the patient derived HI cell line **4.2.1.** defined the causative mutations as a truncation-producing nonsense mutation p.Glu2264X and a putative splice site change of c.5382-2a/g. TA cloning of this allele showed how multiple low affinity acceptor sites can produce several different incorrect transcripts, which would possibly be degraded by nonsense-mediated RNA decay. The transcript of TA clone 1 may possibly be translated, however with the addition of 14 amino acids and the deletion of 2 from the WT ABCA12 protein.

This mutant ABCA12 protein would possibly be a target for endoplasmic reticulum-associated protein degradation (ERAD), due to misfolding of the tertiary structure. In the ER proteins undergo post-translational modifications that aid in conformational changes. Incorrect peptides cause aberrant protein maturation and misfolded proteins are degraded by proteases in the ER before they enter the Golgi. The ABC transporter, cystic fibrosis conductance regulator (CFTR) undergoes this degradation. The ΔF508 mutation in CFTR makes the protein a target for ERAD and due to this degradation CFTR is not present at the plasma membrane of epithelial cells, the core pathomechanism of cystic fibrosis (Cheng 1990).

The HI cell line is an important tool in furthering the understanding of HI cellular phenotype and for the possible use in devising therapeutic strategies. Having a full genetic characterisation and studies into the cell line's *in vitro* behaviour especially in terminal differentiation, furthered in **chapter 5,** allows for the utilisation of the cell line. Not only does HI cell line suggest genotype to phenotype correlation, it has also been shown to differentiate and stratify in organotypic cultures produced in the Kelsell group. However considerations should be taken into when using any immortalised keratinocyte cell line. Culture seeding densities and duplication rates should be carefully monitored as high confluency can initiate differentiation through cell-cell contact and bias differentiation studies (Poumay & Pittelkow 1995). Phenotypically, in monolayer or organotypic culture all of the physical and biological constraints of the epidermal environment are not present, which should be taken into account when making deductions from data.

Keratinocyte apoptosis during calcium shift has previously been reported as a pivotal mechanism involved the dysregulation of differentiation in the HI epidermis. In accordance with the FACS data in **4.2.5.** the protein kinase B (AKT) has been shown to down regulate apoptosis when *ABCA12* is ablated (Yanagi et al. 2011).

ABCA12 packages glycoslyceramide and sphingomyelin from the cytoplasm and Golgi apparatus into the developing LGs of keratinocytes in the upper stratum spinosum and lower stratum granulosum (Sakai et al. 2007; Akiyama 2013). When *ABCA12* is ablated an accumulation of these lipids occurs in keratinocytes of the lower stratum granulosum and a reduction in LGs (Mitsutake et al. 2010). In functional LGs they are accompanied

by other lipids, which when extruded have a range of properties that help manufacture the extracellular lamellar membrane structures of the lipid envelope (Uchida & Holleran 2008). Ceramides of the lower epidermis have been shown to up-regulate the transcription of the gene *ABCA12* through the PPARβ/δ pathway. Showing that ceramide precursors of ABCA12 allocrites induce the expression of the protein that will transport their lipid derivatives (Jiang et al. 2009).

Immunohistochemistry of ABCA12 and ABCA1 in HI skin **(4.2.2.)** and the siRNA mediated *ABCA12* knockdown **(4.2.3.)** show a reduction in the ABCA1 protein when ABCA12 is significantly reduced (HI biopsy) or partially reduced (ABCA12 KD). An aberrant ABCA12 leads to a reduction in ceramide and sphingomyelin transportation and in turn glucosylceramide production causing disruption to LG and lipid bilayer/permeability barrier formation (Mitsutake et al. 2010). It is postulated that this reduces the amount of intracellular cholesterol as it is sequestered by these cellular ultrastructures or the permeability barrier (Hanley et al. 2000; Jiang et al. 2006). This low intracellular cholesterol and processed ceramide concentration leads to a reduction in formation of oxysterols and fatty acids respectively in keratinocytes (Yanagi et al. 2008a), which in turn causes reduced binding of oxysterols to LXRβ and lesser so, fatty acids to PPARβ/δ leading to a reduction in *ABCA1* transcription (Jiang et al. 2006). As the ABCA1 protein is known to transport cholesterol in the epidermis and is down regulated under *ABCA12* ablation there is an opportunity to re-establish this pathway through the activation of LXRβ.

Cholesterol transportation by the ABCA1 protein does not involve the LG, but is integral to obtain the correct lipid envelope composition and in doing so permeability barrier plasticity (Feingold & Jiang 2011). The addition of cholesterol to the myriad of ceramides in the lipid envelope assists in the formation of gel phase lamellar structures that are predicted to have a greater pliability than those made from repeating phospholipids alone (Takahashi et al. 1996). Also without this transportation of cholesterol the intracellular build-up could limit the forward reaction of steroid sulfatase, resulting in an accumulation of cholesterol sulfate (Elias et al. 1984; Zettersten et al. 1998). Cholesterol sulfate stimulates involucrin expression through the differentiation activator protein AP-1 and inhibits serine proteases involved in desquamation (Feingold & Jiang 2011).

A ligand-bound activated LXR/PPAR nuclear hormone receptor will up-regulate the expression of ABCA12, ABCA1 and AP-1 (among other proteins). AP-1 is a transcription enhancer regulating proteins involved in terminal differentiation in keratinocytes (Kömüves & Hanley 2000). The expression of the AP-1 protein is also induced by the calcium activated EGFR by the phosphorylation of ErbB, which helps to drive differentiation in keratinocytes. Proteins involved in late epidermal differentiation such as TGM1, loricrin, SPRR and involucrin all hold AP-1 binding sites in their promoter regions (Hanley et al. 2000; Schmuth et al. 2004).

A different proposed mechanism for the regulation of *ABCA1* by *ABCA12*, which may occur in macrophages, shows the physical binding of ABCA12, ABCA1 and LXRβ proteins. In this system when ABCA12 is ablated, LXRβ is unable to disassociate itself from ABCA1 even when attenuated by receptor-ligand binding, due to heterodimer formation. This reduces the up-regulation by LXRβ (Fu et al. 2013).

ABCA12 is involved in the formation and regulation of a differentiated epidermis whether it is directly or by the lipids it transports. The down-regulation of *ABCA1* through NHRs when *ABCA12* is ablated may also contribute to the HI phenotype by a reduction of cholesterol transported to the permeability barrier or by the build up of cholesterol slufate. Modulation of the AP-1 promoter by either calcium shift or NHR is a key regulatory pathway in epidermal differentiation, a process, which is dysregulated in HI skin. In HI the reduction of ceramide transportation into LG, which supply the constituents of the permeability barrier is the core pathomechanism of the disease. The premature terminal differentiation of the epidermis and the retention of squames in the enlarged stratum corneum due to a deficiency in protease transportation in HI are either a direct cause of the malformed permeability barrier, or a dysregulated/compensatory pathway from the aberrant ABCA12 or both.

4.4. Summary

In this chapter the patient derived HI cell line was characterised by a range of molecular genetic and *in vitro* techniques. Analysis of the complex splice site mutation assessed the use of low affinity acceptor sites by the spliceosome. The *in vitro* studies gave an indication to the cellular pathways disrupted by this compound heterozygote mutation and to what extent the HI cellular phenotype was reproduced in monolayer.

Chapter 5 will further the analysis of the pathway disrupted in the HI patient derived cell line. Calcium shift will be used to assess how the premature terminal differentiation phenotype manifests in HI cell line by the evaluation of markers of epidermal terminal differentiation. This will be done in combination with the application of NHR agonists as a potential strategy to recover a down-regulated *ABCA1* and the possible modulated differentiation.

Chapter 5: A Possible therapeutic strategy for Harlequin Ichthyosis utilising Nuclear Hormone Receptor Agonists

5.1. Introduction

The formation and regeneration of the epidermis complete with a functional permeability barrier and cornified enveloped is a multifaceted process, which involves the regulation of a magnitude of proteins. This extremely complex regulatory pathway is initiated by the calcium gradient, which triggers differentiation of keratinocytes by the phosphorylation of the ErbB receptors, which leads to the up-regulation of AP-1 and a full range of successive transcriptional activation (Hanley et al. 2000; Saeki et al. 2012). AP-1 also contains a hormone response element located close to its promoter region, which nuclear hormone receptors can bind to and induce transcription (Edwards et al. 2002). PPARs and LXRs are nuclear hormone receptors, which are involved in the promotion of differentiation in keratinocytes. When activated by specific ligands PPAR and LXR promote the transcription of a range of proteins including AP-1, ABCA12 and ABCA1, leading to an increase in lipid synthesis and LG formation (Feingold 2007). The transcription enhancer protein AP-1, which can be induced through calcium shift or by nuclear hormone receptor agonists in keratinocytes, promotes the transcription of epidermal differentiation proteins including involucrin, SPRR, TGM1 and loricrin, which all contain AP-1 binding sites (Hanley et al. 2000; Schmuth et al. 2004; Kömüves & Hanley 2000).

The loss of *ABCA12* in HI skin appears to affect the process of keratinocyte differentiation. Proteins expressed specifically during normal terminal keratinocyte differentiation are dysregulated in HI **(Figure 5.1.)** (Thomas et al. 2009b). They are expressed early in HI epidermis and localise to the stratum spinosum and stratum basale, characteristic of a premature terminal differentiation phenotype (Thomas et al. 2009a).

ABCA1 is the membrane transport protein responsible for cholesterol efflux in keratinocytes (Huang et al. 2001). Cholesterol is a fundamental constituent of the cell membrane and is also present in the extracellular compartments of the upper layers of the epidermis where it is involved in the formation of the lipid envelope lamellae which make up the permeability barrier that limits TEWL (Schurer & Elias 1991). Loss of *ABCA12* expression has been shown to down regulate the ABCA1 protein, shown in **4.2.2.** and **4.2.3.** and other publications (Schmitz & Langmann 2005; Fu et al. 2013).

The activation of LXRs and PPARs through the binding of oxysterols and fatty acids induces a significant increase in transcript and protein levels of ABCA1. LXRβ has been shown to induce the greatest regulatory affect in human foreskin keratinocytes and in murine epidermis (Jiang et al. 2006). Coinciding with this investigation on the effect of LXR and PPAR agonists on keratinocytes, it was shown through IHC that PPARβ/δ activation stimulates general epidermal differentiation in mice and lipid accumulation in keratinocytes (Schmuth, Haqq, et al. 2004). Also cholesterol efflux was shown to be increased through the application of the LXRβ agonist TO901317 in ABCA12 knock-out mouse skin-derived fibroblasts, which had a significant decrease of the *ABCA1* transcription compared to WT (Smyth et al. 2008).

This chapter aims to explore the premature terminal differentiation phenotype in the immortalised HI keratinocytes. Then, the application of LXRβ and PPARβ/δ agonists was explored to assess their impact on the protein expression of ABCA1 in HI keratinocytes.

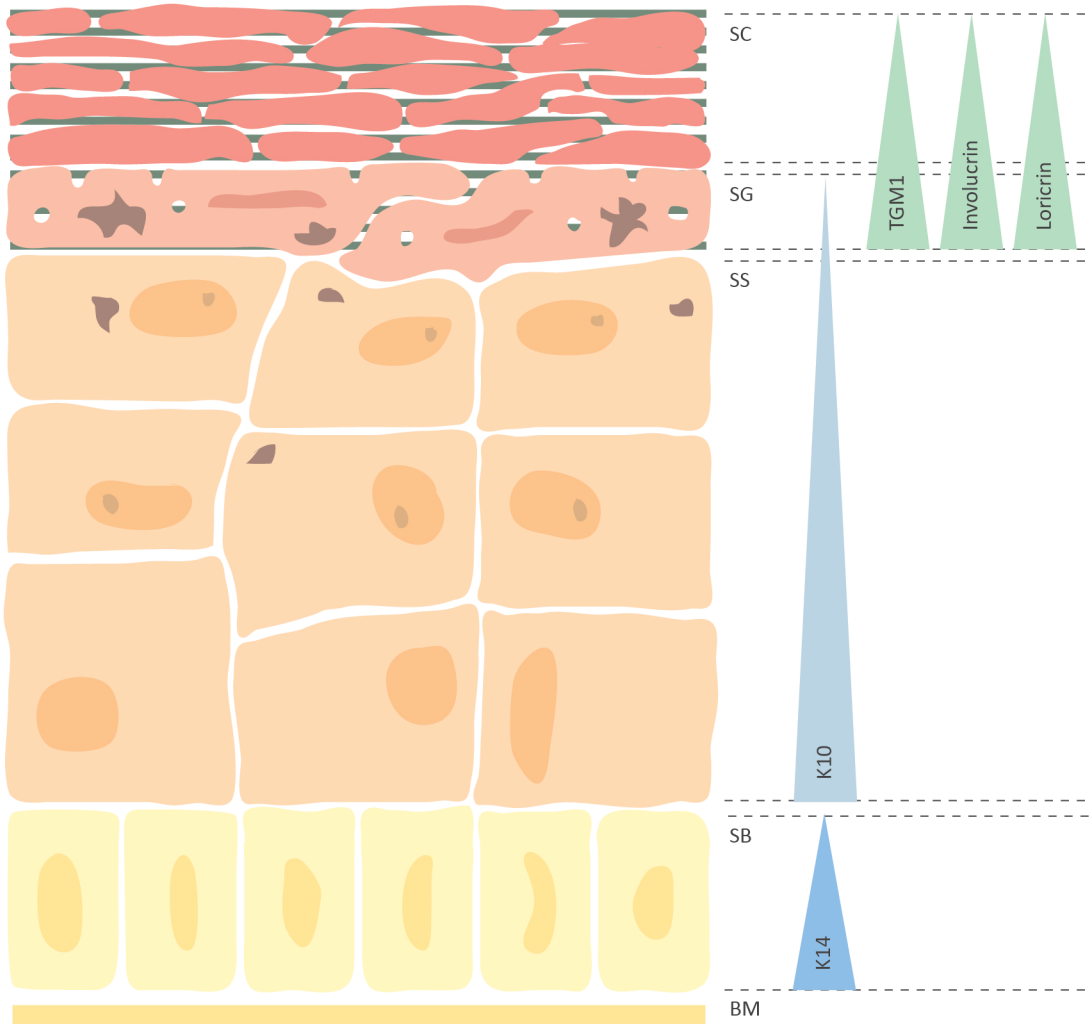

Figure 5.1. Schematic diagram of the epidermis and localisation of markers of epidermal differentiation. Differentiation modifies keratinocyte morphology, cellular content and function producing the permeability barrier and cornfield envelope. The change in protein content is highlighted on the right by arrows indicating the expression of: K14, a keratin marker of proliferation in the epidermis, K10, a keratin present in the supra basal layers of the epidermis, expressed at the initiation of differentiation and the terminal differentiation markers, TGM1, involucrin and loricrin present in the cornified envelope. BM, basement membrane; SB, stratum basale; SS, stratum spinosum; SG, stratum granulosum; SC, stratum corneum.

5.2. Results

5.2.1. Immunohistochemistry of terminal differentiation markers in the HI skin

IHC of normal and HI patient (from which the HI cell line was derived) skin biopsies with antibodies targeting markers of late epidermal differentiation revealed an abnormal expression profile of the terminal differentiation markers TGM1, involucrin and keratin 2e (K2E) in the epidermis of the HI skin **(Figure 5.2.)**. The uppermost panel shows the expression of the cornified envelope cross-linking protein TGM1. Coinciding with its function, TGM1 predominately localised to the stratum corneum in the epidermis of the normal skin. However in the epidermis of the HI skin TGM1 localised to the lower stratum granulosum and was continuously expressed from this layer onwards with a possibly membranous localisation. Involucrin was expressed in the stratum granulosum and stratum corneum in the epidermis of the normal skin, in contrast to the epidermis of the HI skin where it was present in all suprabasal layers. K2E is a marker of the upper stratum spinosum and stratum granulosum keratinocytes of the fully developed epidermis (Smith et al. 1999). K2E showed an expression consistent to this in the epidermis of the normal skin, but was present in all suprabasal layers in the HI epidermis, although at a possibly lower level of expression. The negative controls of the immunohistochemistry are in **Figure A1.1**.

This analysis of the HI patient skin confirms the previously reported early expression of these late differentiation markers in HI skin (Thomas et al. 2009a). This may be due to early gene activation or a physical response due to the incorrect development of the epidermis. The premature expression of this range of differentiation markers is unique to HI, although other ichthyoses do present with a myriad of differentiation defects. For example, epidermolytic ichthyosis has an irregular staining pattern for K10 in suprabasal layers of the epidermis, which combined with defective profilaggrin processing generates corneocytes prematurely and hyperkeratosis (Ishida-Yamamoto et al. 1994). Both X-linked ichthyosis and NBCIE (**chapter 3**) display a disruption to epidermal formation and desquamation, which produce a dramatically thickened stratum corneum, but do not alter the expression of terminal differentiation markers (Zettersten et al. 1998; Epp et al. 2007).

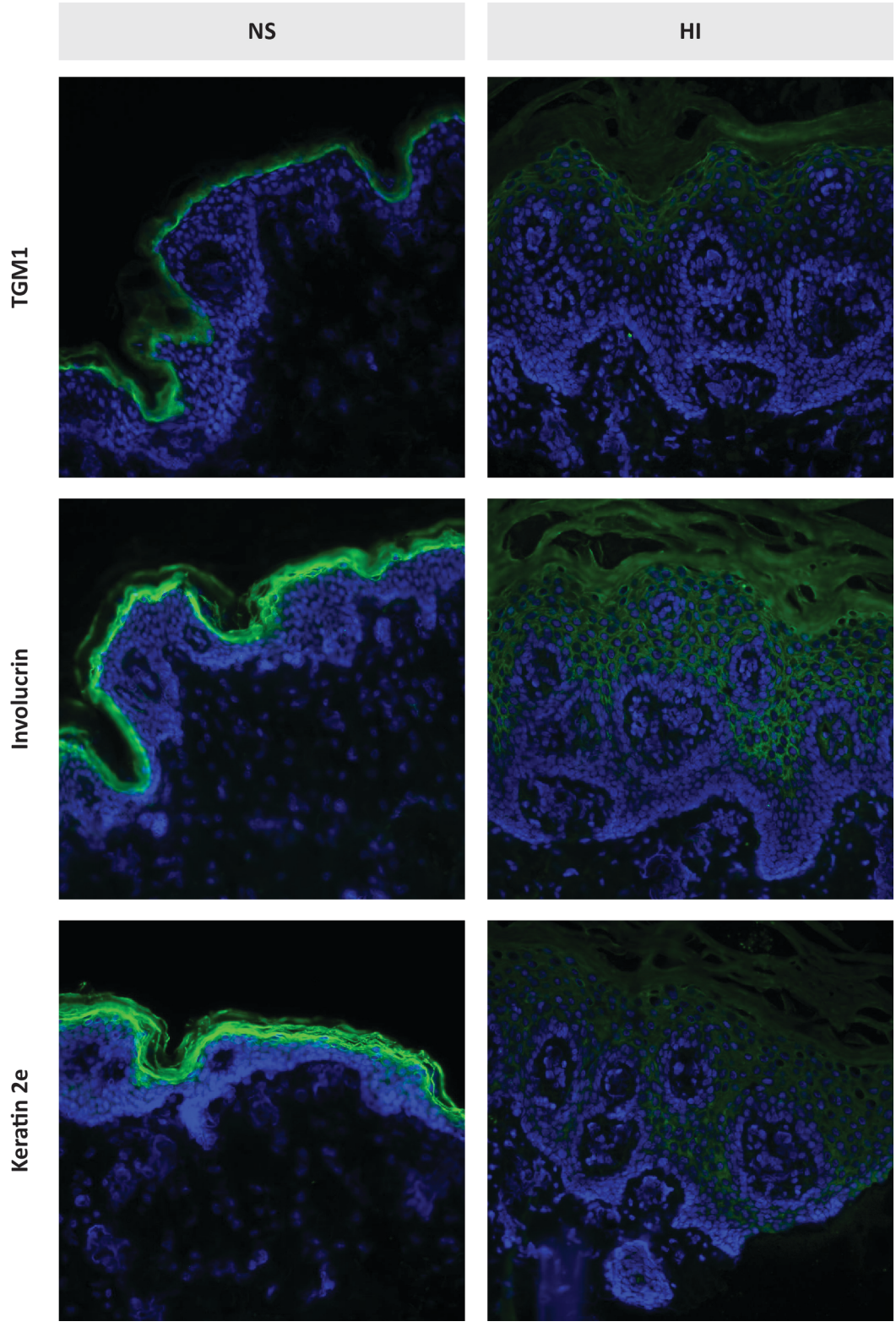

Figure 5.2. Immunohistochemistry of HI patient and normal skin. Immunostaining against TGM1 (upper panel), involucrin (middle panel) and K2e (lower panel). Showing a dispersed expression with a premature localisation for these terminal differentiation markers in the enlarged stratification of the HI skin compared to NS. Immunostaining (green), nuclei stained with DAPI (blue), captured at x20 magnification.

5.2.2. Activation of PPARβ/δ and LXRβ increases ABCA1 mRNA and protein expression in the HI cell line

In **chapter 4**, reduced ABCA1 protein expression was observed by IHC in HI skin compared to control **(4.2.2.)** and also after *ABCA12* siRNA knockdown in control keratinocytes by Western blotting **(4.2.3.)**. To assess the efficacy of the PPAR and LXR activation in the renewal of ABCA1 protein expression in the HI cell line, small molecule agonists complementary to the PPARβ/δ and LXRβ nuclear hormone receptors were used. These subtypes were chosen as PPARβ/δ is expressed in the epidermis at a greater concentration than either of the α and γ PPAR isoforms (Westergaard et al. 2003). The LXR subtypes α and β are expressed equally in the epidermis, although as with PPARβ/δ, LXRβ appears to have the greatest regulatory effect in the epidermis (Chen et al. 2011).

The PPARβ/δ agonist (lipophilic acetic acid GW0742) and the LXRβ agonist (benzensulfonamide TO901317) were optimised to have a final concentration of 8 and 10 μM respectively. Similarly, these were the optimal concentrations used in a previous study to up-regulate cholesterol sulfotransferase in keratinocytes (Jiang et al. 2005). The immortalised HI keratinocytes were incubated with high or low calcium media for 24 hours before both cultures were incubated with either the vehicle control, 8 μM of the PPARβ/δ agonist or 10 μM the LXRβ agonist for a further 48 hours. At the 48 hour time point, total RNA was isolated and qPCR of the RT-PCR cDNA was analysed on a Rotorgene Q thermocycler, shown in **Figure 5.3(A)**. Data is expressed as fold increase of DMSO at 1 fold expression, PPARβ/δ agonist at low calcium increased *ABCA1* mRNA fold expression to 3.3 and 2.4 in high calcium. The LXRβ agonist increased the *ABCA1* mRNA fold expression to 5.7 and 5.0 in low and high calcium respectively. All three *ABCA1* transcripts are up-regulated at similar levels by the LXRβ agonist in keratinocytes (Jiang et al. 2006).

The application of the PPARβ/δ and LXRβ agonists on the HI cell line was performed in keeping with the conditions of the calcium shift experiment **(2.3.5.** and **2.3.6.)**. After 24 hours of calcium shift, the HI keratinocytes were incubated with either the vehicle control, 8 μM of the PPARβ/δ agonist or 10 μM the LXRβ agonist for 72 hours with whole cell lysates taken every 24 hours. The representative Western blot and subsequent densitometry to determine the protein expression of ABCA1 are shown in **Figure**

5.3(B). The densitometry values are mean averages of repeats (n=4) and statistical significance was deduced through t-test against vehicle control after loading control normalisation. * $P < 0.05$ ** $P < 0.01$ *** $P < 0.001$

These results suggest that the level of *ABCA1* transcript is not modulated by calcium shift, which corroborates with the IHC of normal skin **(4.2.2.)** that shows ABCA1 protein present in the basal layers of the epidermis and with a previous study (Jiang et al. 2006). They show that activation of PPARβ/δ and LXRβ up-regulates mRNA and protein levels of ABCA1 in the patient derived HI cell line. After 48 hours of exposure to the agonists, LXRβ produces a greater up-regulation of both ABCA1 mRNA and protein compared to that of PPARβ/δ activation. The activation of PPARβ/δ showed a significant (**) increase compared to the vehicle control in ABCA1 protein consistently for each of the 3 days following the application of the GW0742 agonist. The activation of LXRβ showed a significant increase in ABCA1 protein over the vehicle control for the 3 days; D1*, D2*** and D3**, which was greater than PPARβ/δ activations on days 2 and 3.

In **Figure 5.3(A & B)** DMSO is the vehicle control that GW0742 (PPARβ/δ) and TO901317 (LXRβ) were suspended in at a concentration of 0.5 %. Multiple stocks of HI and K17 cells were used to for these experiments and their repeats. Supplementary data for the immunoblotting for ABCA1 after the NHR activation with agonist application shows an up-regulation in the levels of ABCA1 in a range of immortalised keratinocyte cell lines in **A1.2.**

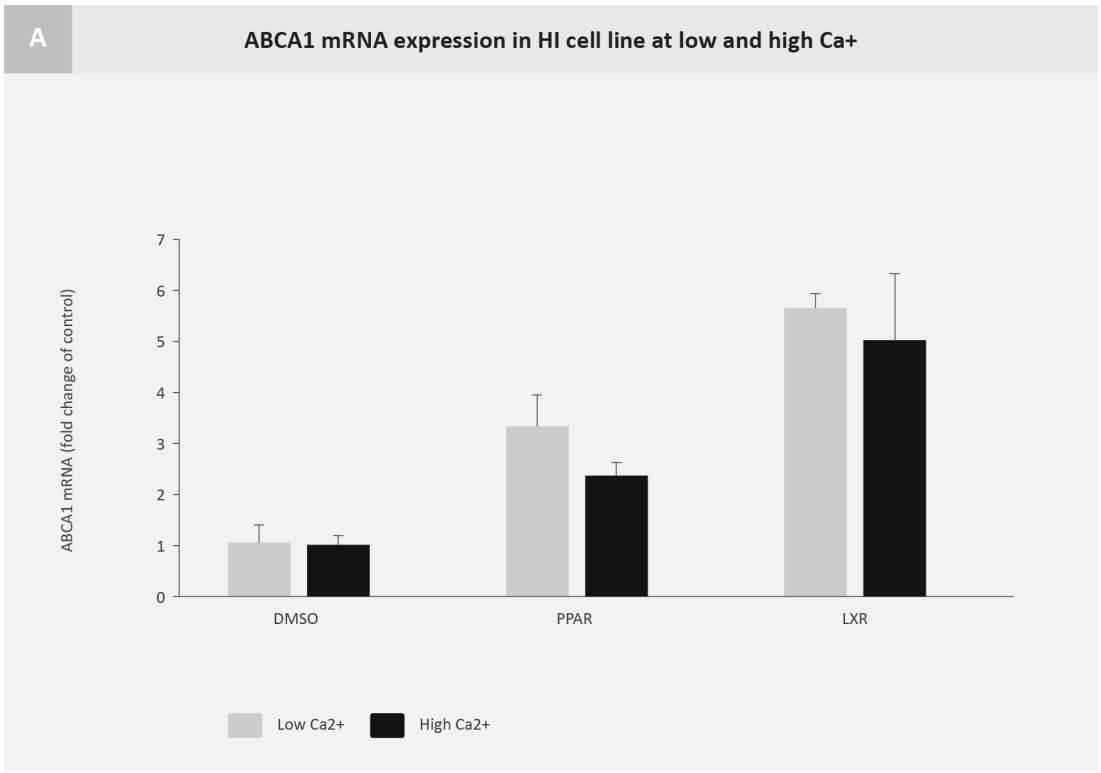

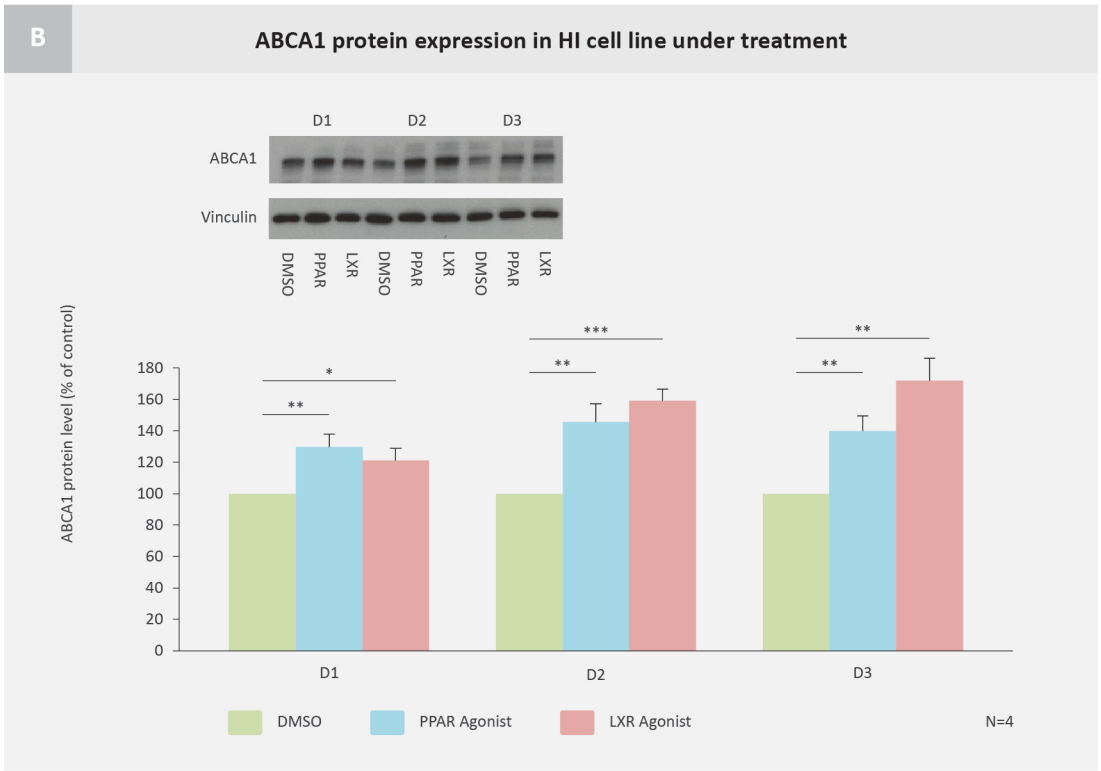

Figure 5.3. PPAR and LXR activation increases ABCA1 mRNA and protein expression. (A) Increase of ABCA1 mRNA expression, HI cell line keratinocytes under went calcium shift, from 0.06 mM ca^{2+} (low Ca) to 1.2 mM ca^{2+} (high Ca) then incubated with either vehicle control (DMSO), PPARβ/δ agonist (PPAR) or LXRβ agonist (LXR) for a further 48 hours. GAPDH was used as an internal control and qPCR data was normalised to the DMSO control for respective calcium concentrations and plotted as an average fold expression of the repeats. **(B)** Immunoblotting analysis of ABCA1 under

treatment, HI cells were calcium shifted for 24 hours, then incubated with either vehicle control (DMSO), PPARβ/δ agonist (PPAR agonist) or LXRβ agonist (LXR) agonist for 1-3 days. Western blot was performed on whole cell lysate and densitometry values are shown as a mean ± SD percentage of 4 repeats. Data was normalised to DMSO controls at 100% for individual time points and to their respective vinculin loading control.

5.2.3. The modulation of terminal differentiation markers under calcium shift and the application of agonists

Markers of differentiation in the epidermis are expressed at discreet points along the path of a keratinocyte differentiation, as highlighted in **Figure 5.1.** The premature expression of markers of late differentiation in the HI epidermis indicates a disruption to this differentiation in the initial stages of the process, which occur in the lower epidermis under an increase to the calcium concentration.

To continue the investigation of premature terminal differentiation from the IHC of **Figure 5.2.** markers of differentiation were to be assessed under calcium shift in the HI and control cell lines to evaluate if this HI characteristic is present in monolayer. A modulation in HI cell line differentiation marker protein levels would suggest the premature terminal differentiation phenotype is not a direct consequence of a physical malformation in the epidermis, for example a malformed permeability barrier. To assess this the terminal differentiation markers, involucrin, TGM1 and loricrin would be analysed alongside the suprabasal differentiation marker K10 and the marker of epidermal proliferation K14. The application of the PPARβ/δ and LXRβ agonists on the HI cell line would then investigate the activation of these regulatory pathways on the disrupted protein levels of differentiation markers.

Involucrin

Involucrin is a well-documented marker of late differentiation in the epidermis, where it is present in the stratum granulosum and stratum corneum. In HI skin, involucrin localises prematurely to the suprabasal layers. Involucrin mRNA has been shown to be up-regulated through AP-1 by both calcium shift and LXRβ activation in control

keratinocytes (Hanley et al. 2000). When activated in unison these factors have an accumulative on the level of involucrin mRNA.

The HI and K17 keratinocytes were seeded for 24 for hours in low calcium conditions before calcium shifted for 5 days with 24 hours separating time points, as described in **2.3.5.** The low calcium control for each time point was used to distinguish between the modulation of differentiation markers by calcium shift and other *in vitro* factors. Whole cell lysates were taken at each time point for high and low calcium variables for both cell lines. The representative involucrin Western blots and densitometry to determine protein expression are shown in **Figure 5.4(A)**. The densitometry values are mean averages of repeats (n=3) and a t-test was used to establish statistical significance against relative low calcium controls following loading control normalisation. * $P < 0.05$ ** $P < 0.01$ *** $P < 0.001$

Figure 5.4(A) shows an accumulation of the involucrin protein in the K17 cell line over the 5 days of calcium shift in the high calcium culture compared to that of the low calcium. The HI cell line has an overall greater up-regulation of involucrin than the K17 cell line under calcium shift for each of the 5 days. Days 1-3 (D1*, D2** and D3*) show a significant up-regulation of involucrin from the calcium shift of HI keratinocytes compared to the calcium shift of K17 keratinocytes. Thus, involucrin expression was up regulated earlier and to a greater concentration under calcium shift in the HI cell line in comparison to the K17 cell lines, in keeping with a premature terminal differentiation phenotype.

The application of the PPARβ/δ and LXRβ agonists on the HI cell line was performed as described previously (**5.2.2.),** immunoblotting and densitometry was performed on an average of 3 repeats for involucrin, as shown in **Figure 5.4(B)**. In DMSO controls the level of involucrin protein increases over the 3 days when normalised to their respective loading control. These are equivalent to days 2, 3 and 4 of the calcium shift in the HI cell line and show the same pattern of involucrin protein expression up-regulation. This indicates that the DMSO is not having an obvious detrimental affect on the keratinocytes. A significant (D2*) down-regulation of involucrin protein expression was shown for both PPARβ/δ and LXRβ agonists 48 hours after their application. Only the LXRβ agonist showed a significant (D3*) down-regulation after 72 hours, although the

general trend for both agonists was a down-regulation of involucrin protein expression in the HI cell line for the 3 time points. This suggests that agonist application in the HI call line is reducing the level of the prematurely expressed involucrin.

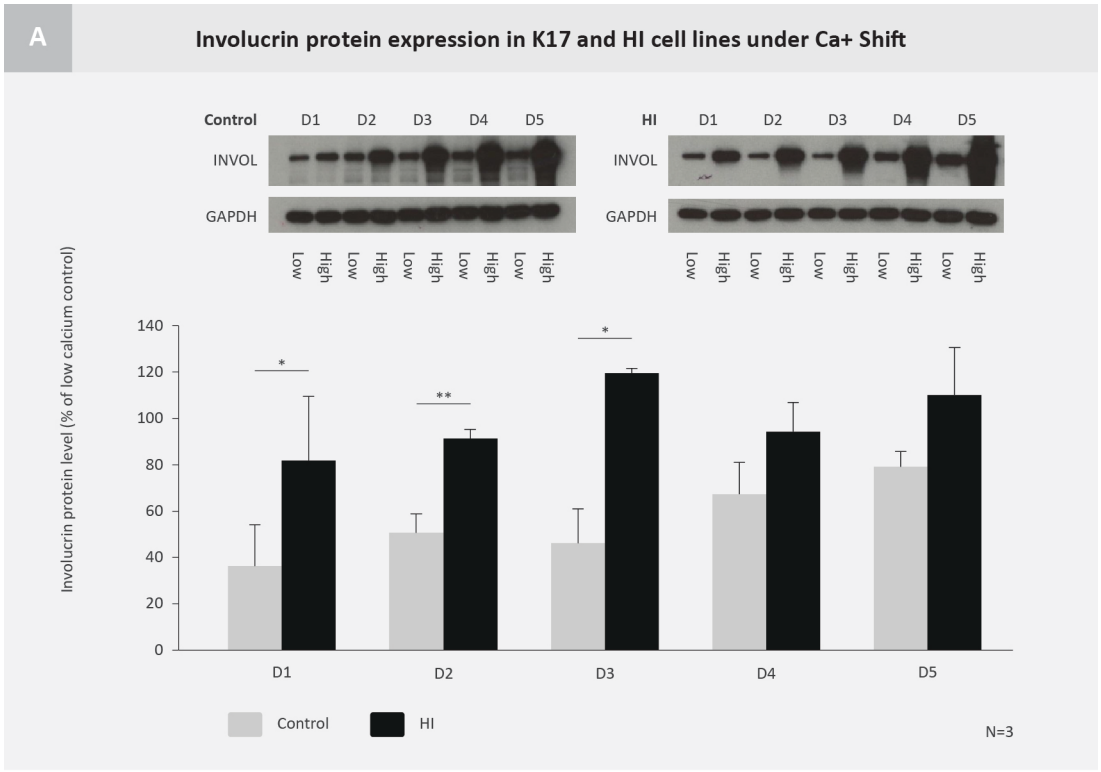

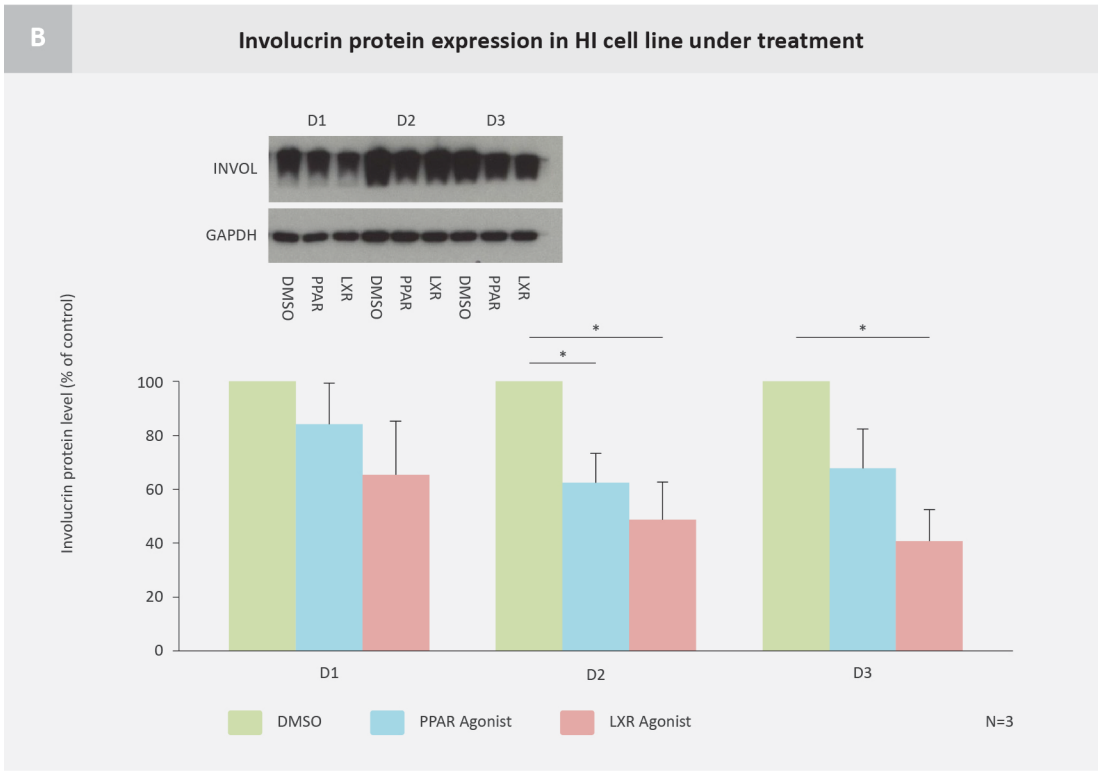

Figure 5.4. Western blot analysis of the modulation of involucrin protein expression under calcium shift and treatment. (A) Immunoblotting of involucrin under calcium shift, HI and K17 cell line keratinocytes were either calcium shifted or low Ca^{2+} media was replenished, 0.06 mM ca2+ (low Ca) to 1.2 mM ca2+ (high Ca). Whole cell lysates were taken every 24 hours for 5 days after calcium shift. Densitometry of involucrin western blot was normalised by the internal GAPDH loading control and to the individual time point low Ca control and plotted as a mean ± SD percentage expression of the 3

experimental repeats. **(B)** Immunoblotting analysis of involucrin under treatment, HI cells were calcium shifted for 24 hours, then incubated with either vehicle control (DMSO), PPARβ/δ agonist (PPAR agonist) or LXRβ agonist (LXR) agonist for 1-3 days. Western blot was performed on whole cell lysate and densitometry values are shown as a mean ± SD percentage of 3 repeats. Data was normalised to DMSO controls at 100% for individual time points and to their respective GAPDH loading control.

TGM1

TGM1 is a marker of late epidermal differentiation and an enzyme that cross links the structural proteins of the cornified envelope in the stratum corneum (Hennings et al. 1981). In the HI epidermis TGM1 localises prematurely to the lower stratum granulosum. TGM1 has been shown to be up regulated in control keratinocytes, which have undergone calcium shift and been treated with PPARα and LXRβ agonists (Hanley et al. 1998; Hanley et al. 2000). The conditions and analysis of TGM1 protein expression under calcium shift and the application of PPARβ/δ and LXRβ agonists were performed as described for the analysis of involucrin.

The analysis of TGM1 in the comparative calcium shift of the HI and K17 cell lines is shown in **Figure 5.5(A)**. Compared to their low calcium controls, the HI cell line produced a greater up-regulation of TGM1 than that of the K17 cell line, for 3 days following the calcium shift. After statistical analysis of repeats TGM1 protein expression at D1* and D3* was shown to be significantly greater in the HI cell line, which is possibly an *in vitro* consequence of the premature terminal differentiation phenotype. The application of either PPARβ/δ or LXRβ agonists yielded no significant modulation of TGM1 protein expression over the 4 days following treatment of the HI cell line keratinocytes, as shown in **Figure 5.5(B)**. * $P < 0.05$

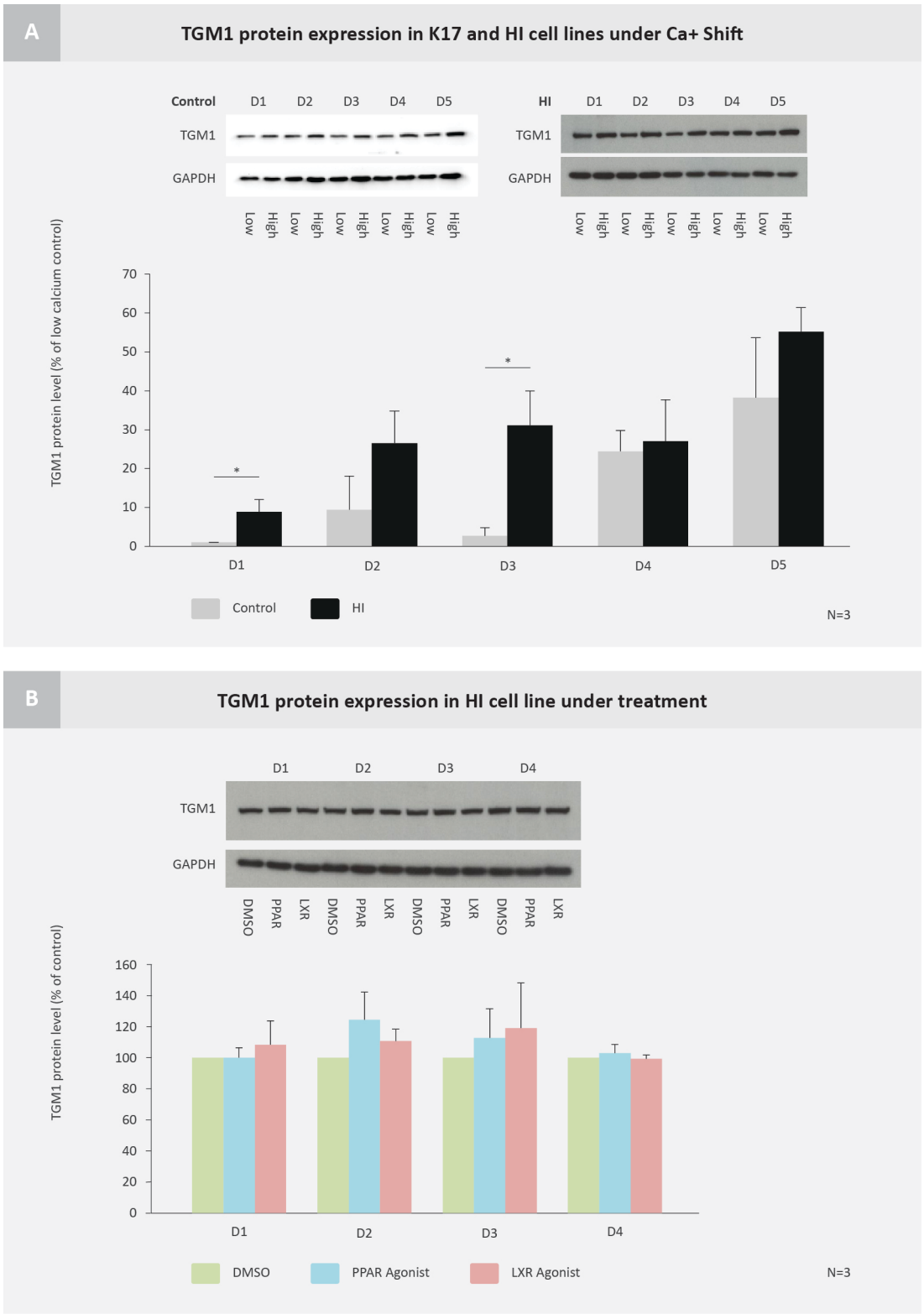

Figure 5.5. Western blot analysis of the modulation of TGM1 protein expression under calcium shift and treatment. (A) Immunoblotting of TGM1 under calcium shift, HI and K17 cell line keratinocytes were either calcium shifted or low Ca^{2+} media was replenished, 0.06 mM ca2+ (low Ca) to 1.2 mM ca2+ (high Ca). Whole cell lysates were taken every 24 hours for 5 days after calcium shift. Densitometry of TGM1 western blot was normalised by the internal GAPDH loading control and to the individual time point low Ca control and plotted as a mean ± SD percentage expression of the 3

experimental repeats. **(B)** Immunoblotting analysis of TGM1 under treatment**,** HI cells were calcium shifted for 24 hours, then incubated with either vehicle control (DMSO), PPARβ/δ agonist (PPAR agonist) or LXRβ agonist (LXR) agonist for 1-4 days. Western blot was performed on whole cell lysate and densitometry values are shown as a mean ± SD percentage of 3 repeats. Data was normalised to DMSO controls at 100% for individual time points and to their respective GAPDH loading control.

Loricrin

Loricrin is a component of the cornified envelope in the stratum corneum and is expressed in differentiated keratinocytes. Select PPARγ agonists, when applied to control keratinocytes under calcium shift have been shown to up regulate both the mRNA and protein levels of loricrin (Yan et al. 2015). In a ABCA12 KO HI mouse model the level of the loricrin protein in the epidermis had no significant modulation in comparison to WT mice at the same developmental stage (Smyth et al. 2008). The analysis of loricrin protein expression under calcium shift and the application of PPARβ/δ and LXRβ agonists were performed as described for the analysis of involucrin.

In **Figure 5.6(A & B)** the immunoblotting of loricrin exhibits a double band, only the smaller of the two bands, which was present in both cell lines, was used for the densitometry quantification. A cDNA was reverse transcribed from RNA isolated from the HI and K17 cell lines to evaluate the genetic origins of this double band, **Figure 5.7**. Under calcium shift both HI and K17 keratinocytes showed a similar up-regulation of loricrin protein levels relative to low calcium controls. This up-regulation of loricrin was plotted as HI against K17 and showed only minor discrepancies in loricrin protein levels between the two cell lines for each time point, as shown in **Figure 5.6(A)**. Loricrin protein expression exhibited no significant modulation for the 4 days following the application of either PPARβ/δ or LXRβ agonists on HI cell line keratinocytes, as shown in **Figure 5.6(B)**.

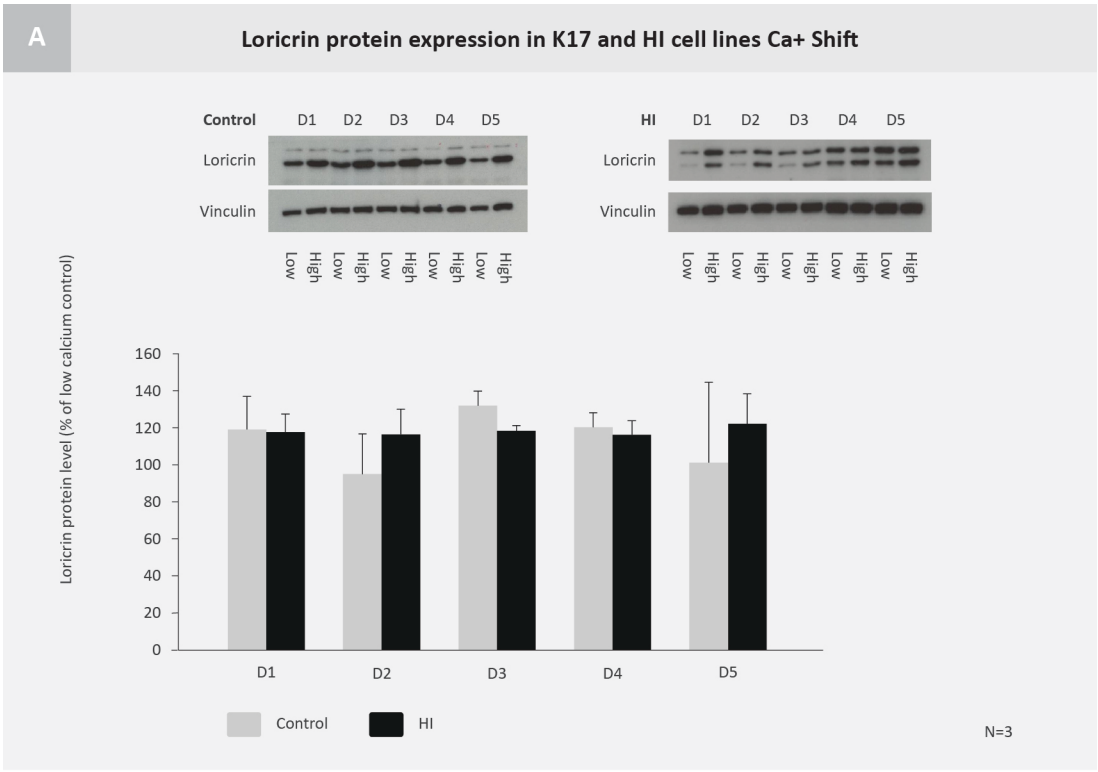

Figure 5.6. Western blot analysis of the modulation of loricrin protein expression under calcium shift and treatment. (A) Immunoblotting of loricrin under calcium shift, HI and K17 cell line keratinocytes were either calcium shifted or low Ca^{2+} media was replenished, 0.06 mM ca2+ (low Ca) to 1.2 mM ca2+ (high Ca). Whole cell lysates were taken every 24 hours for 5 days after calcium shift. Densitometry of loricrin western blot was normalised by the internal vinculin loading control and to the individual time point low Ca control and plotted as a mean ± SD percentage expression of the 3

experimental repeats. **(B)** Immunoblotting analysis of loricrin under treatment, HI cells were calcium shifted for 24 hours, then incubated with either vehicle control (DMSO), PPARβ/δ agonist (PPAR agonist) or LXRβ agonist (LXR) agonist for 1-4 days. Western blot was performed on whole cell lysate and densitometry values are shown as mean ± SD percentage of 3 repeats. Data was normalised to DMSO controls at 100% for individual time points and to their respective vinculin loading control.

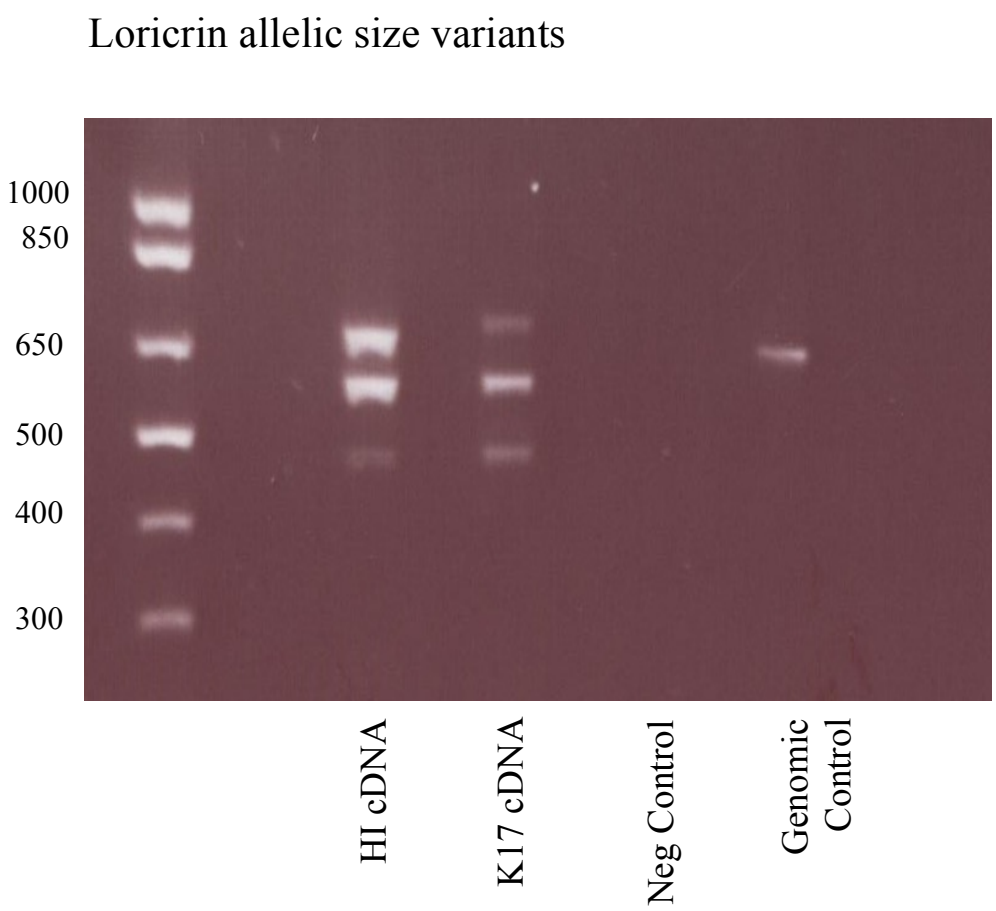

Figure 5.7. Electrophoresis gel of loricrin size variants analysis in HI and K17 cell lines. PCR of 583 bp section of exon 2 of the loricrin gene. Amplification of the highly repetitive glycine loop domains, producing 3 distinct bands from the PCR of cDNA of both cell lines. Table **A1.5.** Primers used for screening loricrin variants.

The amplification of the 583 bp of exon 2 (1196 bp), as shown in **Figure 5.7.** produces three distinct fragments in the HI and K17 cell lines and a single band in the genomic control. The middle fragment was produced by the amplification of an allele containing a sequence of WT length for this part of exon 2. The smallest fragment is possibly due to the amplification of an allele with deletions within this highly repetitive region. Exon 2 is the only coding exon in the *loricrin* gene and is known to contain polymorphic deletions within the glycine rich loop domains (Yoneda et al. 1992). The glycine loops are known to be flexible structures within the loricrin protein, which aids to the plasticity of the cornified envelope, as loricrin makes up 50% of the protein content in the cornified envelope (Hohl et al. 1991).

K10

K10 is part of the type 1 cytokeratin family and forms heterodimer intermediate filaments with K1 in the suprabasal keratinocytes of the epidermis. In a HI KO mouse model, K10 was up regulated in basal layer keratinocytes compared to control mice (Smyth et al. 2008). The analysis of the protein expression of K10 under calcium shift and during the application of PPARβ/δ and LXRβ agonists was performed as described in the analysis of involucrin.

The first two days following calcium shift indicated a significant up-regulation (D1** and D2**) in the HI cell line of the protein expression of K10 in comparison to the K17 cell line, after normalisation with low calcium controls, shown in **Figure 5.8(A)**. Showing a premature expression of a marker of suprabasal keratinocyte differentiation marker in the HI cell line. It should be noted that variations in the number and size of the glycine loop repeats present in the V2 subdomain can lead to broad size polymorphism of *K10* (Korge et al. 1992). As with loricrin this can lead to double banding in the immunoblotting of the K10 protein as seen in the K17 cell line, though this may also be caused by heterodimer formation of keratins.

24 hours after treatment a significant (D1* and D1**) down-regulation of K10 protein expression was shown for PPARβ/δ and LXRβ agonists respectively in the HI cell line. The down-regulation continued for until 48 hours post treatment, though only the

PPARβ/δ agonist was a significant change at D2*, as shown in **Figure 5.8(B)**. This suggest, in corroboration with the involucrin results that the application of these specific nuclear hormone receptor agonists down-regulates the K10 protein level, which is prematurely expressed under calcium shift in the HI cell line. * $P < 0.05$ ** $P < 0.01$

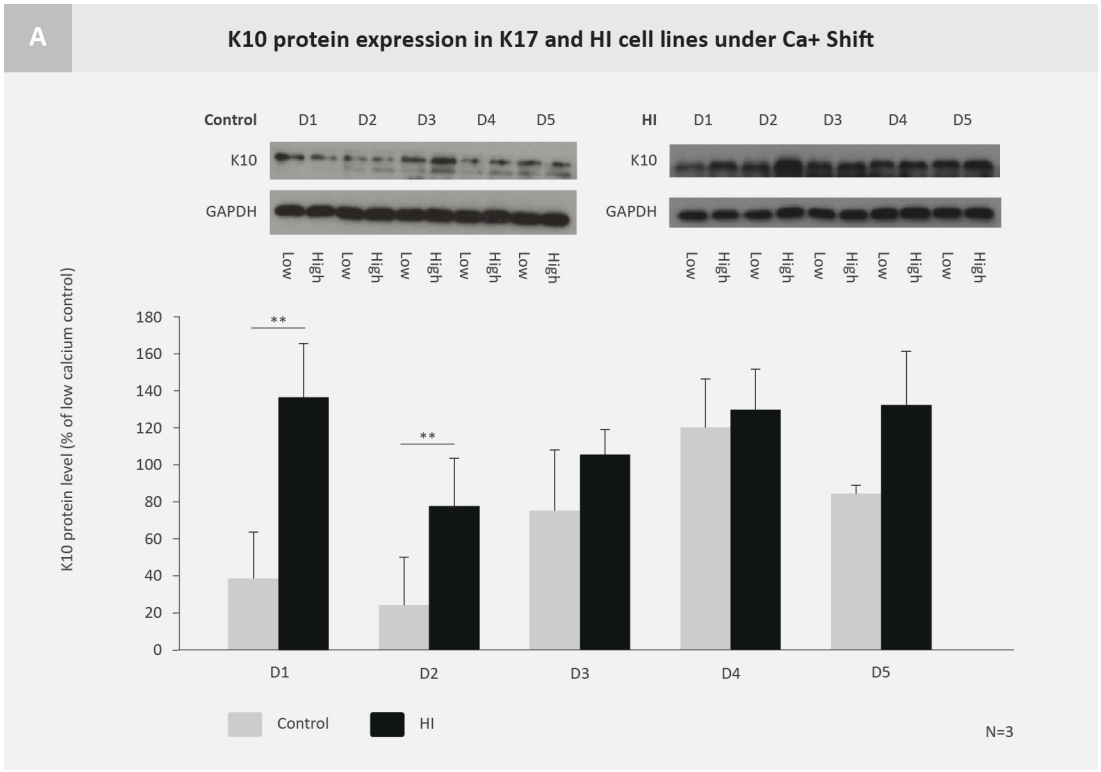

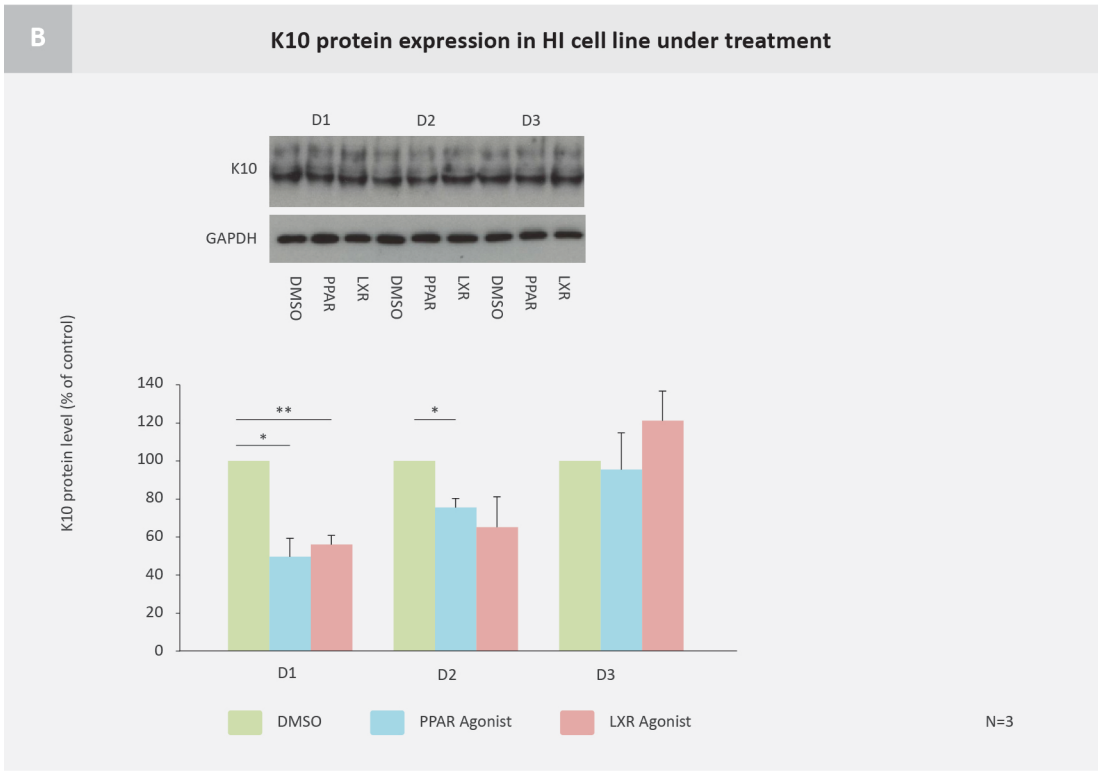

Figure 5.8. Western blot analysis of the modulation of K10 protein expression under calcium shift and treatment. (A) Immunoblotting of K10 under calcium shift, HI and K17 cell line keratinocytes were either calcium shifted or low Ca^{2+} media was replenished, 0.06 mM ca2+ (low Ca) to 1.2 mM ca2+ (high Ca). Whole cell lysates were taken every 24 hours for 5 days after calcium shift. Densitometry of K10 western blot was normalised by the internal GAPDH loading control and to the individual time point low Ca control and plotted as a mean ± SD percentage expression of the 3 experimental repeats. **(B)**

Immunoblotting analysis of K10 under treatment, HI cells were calcium shifted for 24 hours, then incubated with either vehicle control (DMSO), PPARβ/δ agonist (PPAR agonist) or LXRβ agonist (LXR) agonist for 1-3 days. Western blot was performed on whole cell lysate and densitometry values are shown as a mean ± SD percentage of 3 repeats. Data was normalised to DMSO controls at 100% for individual time points and to their respective GAPDH loading control.

K14

K14 is one of the main structural proteins expressed by the proliferating keratinocytes of the stratum basal. K14 expression is not modulated in control keratinocytes under either PPAR or LXR agonists. The analysis of K14 in HI and K17 keratinocytes under calcium shift and the application of PPARβ/δ and LXRβ agonists on the HI cell line were undertaken as described for the analysis of involucrin.

Both the HI and K17 cell lines showed no modulation of K14 under calcium shift. They did however show an increase in K14 protein expression in the low calcium controls over the 5 days, in keeping with the role of K14 in proliferation of undifferentiated keratinocytes. In comparison between the two cells there was no significant of K14 expression, as shown in **Figure 5.9(A)**. Shown in **Figure 5.9(B),** K14 protein expression exhibited no significant modulation for the 3 days following the application of either PPARβ/δ or LXRβ agonists on HI cell line keratinocytes.

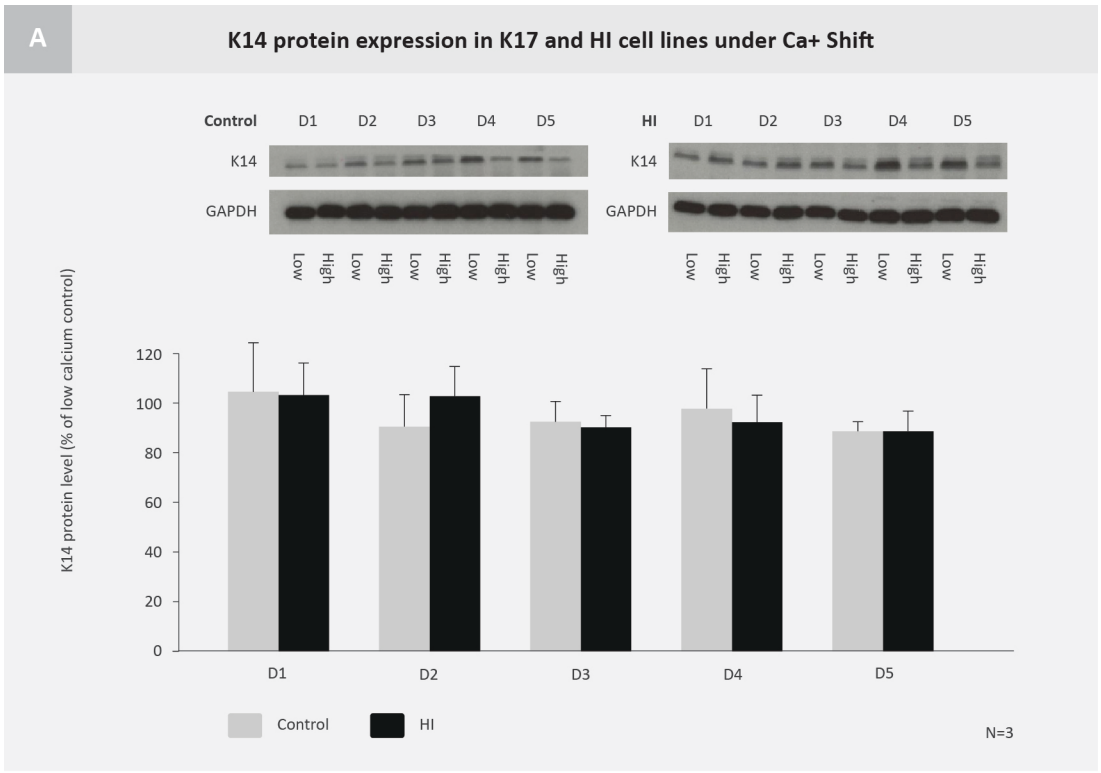

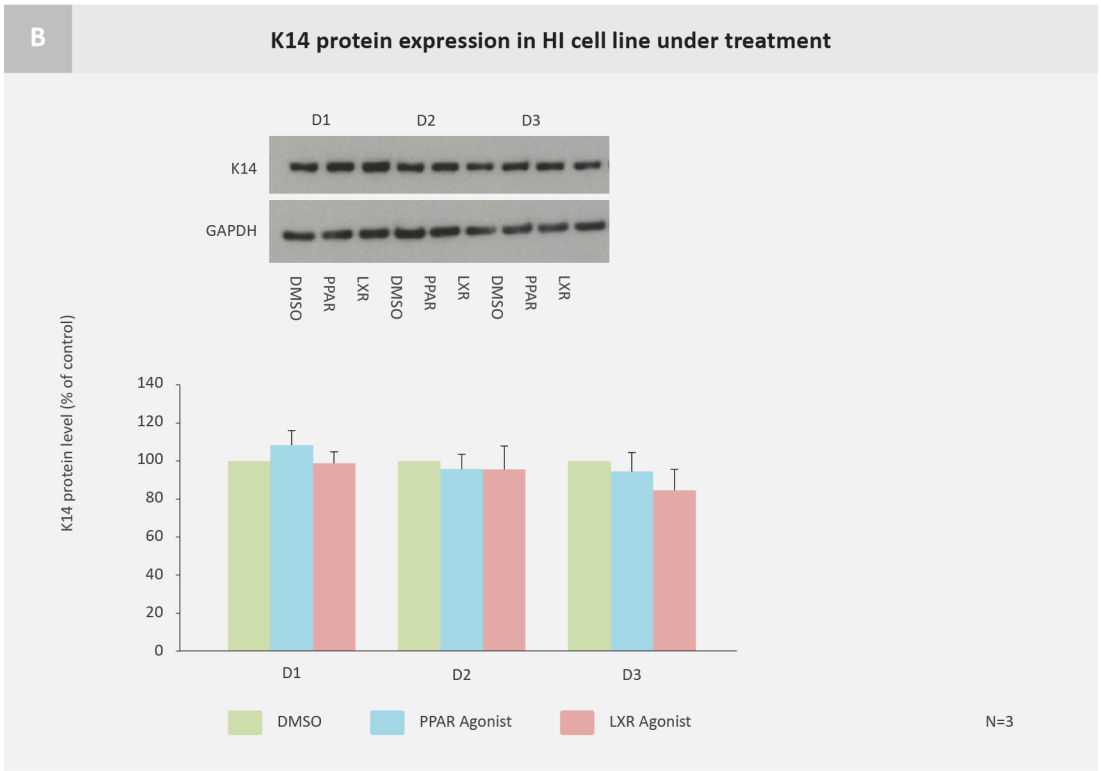

Figure 5.9. Western blot analysis of the modulation of K14 protein expression under calcium shift and treatment. (A) Immunoblotting of K14 under calcium shift, HI and K17 cell line keratinocytes were either calcium shifted or low Ca^{2+} media was replenished, 0.06 mM ca2+ (low Ca) to 1.2 mM ca2+ (high Ca). Whole cell lysates were taken every 24 hours for 5 days after calcium shift. Densitometry of K14 western blot was normalised by the internal GAPDH loading control and to the individual time point low Ca control and plotted as a mean ± SD percentage expression of the 3 experimental repeats. **(B)**

Immunoblotting analysis of K14 under treatment**,** HI cells were calcium shifted for 24 hours, then incubated with either vehicle control (DMSO), PPARβ/δ agonist (PPAR agonist) or LXRβ agonist (LXR) agonist for 1-3 days. Western blot was performed on whole cell lysate and densitometry values are shown as a mean ± SD percentage of 3 repeats. Data was normalised to DMSO controls at 100% for individual time points and to their respective GAPDH loading control.

5.3. Discussion

The up-regulation of AP-1 by the binding of specific agonists to nuclear hormone receptors has been shown to increase the mRNA and proteins levels of many of the markers of epidermal terminal differentiation. This up-regulation of multiple genes occurs at high calcium conditions either *in vivo* within the upper layers of the epidermis or *in vitro* when media calcium concentrations are changed from low to high calcium. The calcium gradient in the epidermis induces the activity of protein kinase C, which through the AP-1 transcriptional complex increases the expression of involucrin, TGM1 and K10 among others proteins of epidermal differentiation (Denning et al. 1995; Rossi et al. 1998). Calcium shift and the activation of nuclear hormone receptors can up regulate the transcription of AP-1 independently or simultaneously, when coinciding with one another, an accumulative affect has been observed (Hanley et al. 1998; Hanley et al. 2000).

The calcium shift investigation of HI and K17 cell lines describes an *in vitro* model of premature terminal differentiation from the expression of differentiation markers and the positive control, shown in **5.2.3.** Both HI and K17 cell lines showed an up-regulation of involucrin, TGM1 and K10 for the 5 days of calcium shift and comparatively the HI cell line produced a significant up-regulation. There was no comparative modulation for loricrin as both cell lines showed an equal up-regulation of loricrin under calcium shift, which corroborates with the non-modulated loricrin expression of HI KO murine epidermis (Smyth et al. 2008). A combination of up-regulation and earlier expression is present in the HI cell line as the first 3 days is when the differentiation markers profile expression has the most apparent and significant difference between the HI and K17 cell lines.

This suggests, in confirmation with the IHC of HI skin (**5.2.1.**) that an aberrant ABCA12 leads to an early or premature activation of these late differentiation markers. This product of the dysregulation in the HI epidermis is possibly a consequence of atypical promotion of transcriptional regulators in keratinocytes.

The calcium shift of the HI patient derived cell line produces a premature and exaggerated response in the markers epidermal differentiation. From studies on the activation of nuclear hormone receptors and calcium shifting in control keratinocytes the activation of the PPARβ/δ and LXRβ nuclear hormone receptors in combination with high calcium should produce a putative accumulation of AP-1 induction and thus up-regulation of markers with AP-1 binding domains. However the application of the agonists GW0742 (PPARβ/δ) and TO901317 (LXRβ) on the HI cell line significantly reduced the protein expression of involucrin and K10. There was no modulation of TGM1 over the time course following the application of agonists, though it was up regulated by calcium shift. Loricrin showed no modulation through either calcium shift or agonist application, though there was discrepancies between isoform expression levels.

The electrophoresis gel of loricrin size variants indicates the presence of polymorphisms within the glycine loop structures of the loricrin proteins in both cell lines, shown in **Figure 5.7.** (Hohl et al. 1991). Due to the high percentage homology of the smaller two fragments amplified from different alleles there is a predisposition for heteroduplex formation during amplification (Yoneda et al. 1992). Heteroduplexes take more time to migrate through the matrix of an electrophoresis gel due to the uncomplimentary base pairs forming a kink in the backbone of the DNA molecule. This heteroduplex formation is the possible mechanism for the largest fragment present in both cell lines. To assess this possible heteroduplex formation, cloning the largest fragment should produce clones containing only the two smaller fragments if a heteroduplex is present.

ABCA1 expression was up-regulated through the LXRβ agonist TO901317 in human foreskin keratinocytes and through topical application, mouse epidermis (Jiang et al. 2006). This agonist was also shown to up regulate cholesterol transportation in

fibroblasts derived from a HI mouse model, which exhibited a decrease in *ABCA1* transcription compared to WT mice (Smyth et al. 2008). In the HI cell line the activation of PPARβ/δ or LXRβ induced an increase of *ABCA1* mRNA in low or high calcium and a significant increase in the level of the ABCA1 protein over 72 hours. This suggests that PPARβ/δ and more so LXRβ activation could be used to re-establish ABCA1 expression in HI keratinocytes.

The ABCA12 protein packages glycoslyceramide from the cytoplasm and Golgi apparatus into the developing LGs of keratinocytes in the lower stratum granulosum and when ABCA12 is ablated these ceramides accumulate in the cytoplasm (Sakai et al. 2007; Akiyama 2013). Ceramides like oxysterols have a regulatory, alongside their structural, function in keratinocytes (Galadari et al. 1998). Ceramides activate PPARβ/δ in the epidermis, which has been shown to stimulate differentiation (Schmuth, Haqq, et al. 2004).

The efflux of cholesterol in keratinocytes is maintained by *ABCA1*, an increase in free cholesterol was shown in fibroblasts derived from ABCA12 aberrant mice (Smyth et al. 2008). The concentration of free cholesterol reduces between the stratum basale and the stratum granulosum and is then re-established in the stratum corneum in the epidermis of normal skin (Lampe et al. 1983). A metabolic pathway that reduces the concentration of free cholesterol in the lower layers of the epidermis is the formation of cholesterol sulfate. This reaction is catalysed in the epidermis by cholesterol sulfotransferase type 2B isoform 1b (SULT2B1b) and the product, cholesterol sulfate, is a key regulator of differentiation as well as desquamation and lipid envelope formation (Hanley et al. 2001).

The ablation of ABCA12 and down-regulation of ABCA1 leads to an accumulation of free cholesterol and ceramides in the cytosol of HI keratinocytes. The cholesterol derivative, cholesterol sulfate, induces AP-1 independently of nuclear hormone receptors and increases the expression of epidermal differentiation proteins, which hold AP-1 regulatory sites (Hanley et al. 2001). This dysregulated activation would coincide with the initiation of calcium-induced differentiation, which cumulatively may produce the premature terminal differentiation phenotype in the HI epidermis and the early up-regulation of these proteins in the HI cell line under calcium shift. The formation of

cholesterol from cholesterol sulfate in the epidermis is catalyzed by the enzyme steroid sulfatase. Steroid sulfatase is aberrant in patients with X-linked ichthyosis, which have a build up of cholesterol sulfate in the suprabasal layers of the epidermis (Williams & Elias 1981). In X-linked ichthyosis the dysregulation of cholesterol sulfate causes a disruption to epidermal formation, desquamation and the permeability barrier, showing the importance of cholesterol sulfate regulation in the epidermis (Zettersten et al. 1998). Upon treatment of the HI cell line with the PPARβ/δ and LXRβ agonists, up-regulate ABCA1 and re-establish cholesterol efflux, reducing the amount of free cholesterol for cholesterol sulfate synthesis. From the results obtained in this chapter, AP-1 induction from the accumulation of calcium shift and cholesterol sulfate is greater than that of calcium shift and PPARβ/δ and LXRβ activation, which occurs under the application of agonists to differentiating HI keratinocytes. This would account for the significant increase in ABCA1 and the significant decrease of involucrin and K10 protein levels exhibited during premature terminal differentiation by the application of PPARβ/δ and LXRβ agonists.

5.4. Summary

This chapter shows how the patient derived HI cell line under, calcium shift, shows similar behaviour to the HI skin, shown by IHC and previous investigations into the premature terminal differentiation phenotype of the HI epidermis. The application of PPARβ/δ and LXRβ agonists on the HI cell line exhibited an up-regulation on the transcript and protein levels of the possibly reduced ABCA1. This application also reduced specific markers of differentiation, which were activated prematurely in the HI cell line under calcium shift.

Chapter 6: Final Discussion and Future Work

6.1. Background

The ABC transporter, ABCA12, transports ceramides into LGs in keratinocytes under calcium efflux in the upper layers of the epidermis. The extent to which this mechanism enables the correction function of the epidermis is apparent in HI epidermis where no functional ABCA12 is present. However, the HI epidermis not only presents with a defective transportation of ceramides but rather a range of functional impairments including premature terminal differentiation and deregulation of desquamation due to the impaired transportation of proteases and TEWL.

This thesis focused firstly on expanding the genetic role of ABCA12 in HI through the molecular diagnostics of HI patients and the genetic characterisation of the patient derived HI cell line. Secondly on the functional role of ABCA12 in HI through the analysis of the functional representation of the HI cell line and the application of nuclear hormone receptor agonists.

6.2. Mutation analysis of ABCA12 and the genotype – phenotype relationship

Utilising a range of molecular techniques, causative mutations were located in the gene *ABCA12* for four out of the five cases clinically diagnosed as HI at birth. The other clinical diagnosis was reassessed to be NBCIE, a less severe ARCI after a homozygous mutation in the gene *ALOX12B* was identified (Bland et al. 2014).

HI is the most severe disorder in the family of ARCI, which also contains NBCIE and LI. Mutations in *ABCA12* have found to be causative for each of these distinct diseases, which indicate a complex genotype to phenotype relationship. An example of this complexity is that missense mutations within one specific domain of ABCA12, the ABC1 domain, are associated with NBCIE and LI (Lefévre et al. 2003; Sakai et al. 2009). However, HI-associated *ABCA12* mutations are often deletions and truncations of ABCA12 (Akiyama 2005; Thomas et al. 2006). The *ABCA12* genotype to phenotype relationship not only dictates which ARCI is present, but also has a possible role in the survival rate of HI, with homozygous mutations in *ABCA12* correlating with a higher chance of mortality (Rajpopat et al. 2011).

Mutations in other ABCA genes lead to inherited disorders and show a mutation location bias to conserved ABC domains. In Stargardt disease, which is a macular degeneration of the retina mutations in the ABC transporter domains of ABCA4 represent 80% of the causative mutations molecularly diagnosed. The missense mutations of a conserved domain are also found to be causative in the majority of Tangier disease cases, which is a deficiency of HDL due to an aberrant ABCA1 (Lewis et al. 1999; Huang et al. 2001).

Another skin disease that has a spectrum of genotype-phenotypes is dystrophic epidermolysis bullosa (DEB). A well established aetiology between DEB and the gene *COL7A1* has been established for both recessive (RDEB) and dominant (DDEB) modes of inheritance (Bruckner-Tuderman 2010; Dang & Murrell 2008). The most severe DEB phenotype is produced by recessive nonsense mutations resulting in a truncated transcript and a loss of the collagen VII protein, which presents as extreme scarring and large blistering of the feet and hands or of areas with bony protrusions. Premature stop codons and missenses mutations in the gene *COL7A1* present as a milder RDEB, whereas DDEB is the least severe form of DEB in which the blistering phenotype lessens with age (Chung & Uitto 2010; Bruckner-Tuderman 2010).

In summary, mutations in *ABCA12* have been found to be causative in three distinct diseases within ARCI group: HI, NBCIE and LI2. After the early months/years of skin development, there is a reduction in the severity of the presentation of HI, which develops to resemble NBCIE, showing the importance of understanding skin development and molecular diagnosis in the clinical management of HI.

6.3. Treatment of HI

HI is the most severe type of ARCI and with modern neonatal care it is infrequently fatal. With no well-established treatment, management of HI currently has more of a supportive role; however, it was observed that the prescription of an oral retinoid drug possibly increases the survival rate (Rajpopat et al. 2011). Genetic counselling and preventative preimplantation of known carriers are two preventative measures currently possible due to the identification of causative mutations in *ABCA12*.

Modern management of the HI patient at the neonatal stage is undertaken with the use of temperature and humidity controlled incubators, antibiotics, pain control, fluids, electrolytes and topical emollient oil (Sharpe & Hyman 2014). After the neonatal period and into childhood, the HI skin develops and changes to resemble a severe NBCIE. At this stage patients can present with further complications including; a loss of thermoregulation, alopecia, contractures, diminished stature and scarring (Dyer et al. 2013). With a greater number of HI patients surviving past infancy further later life repercussions may become apparent as clinical data is accrued, e.g; patients with the skin disease RDEB have a high probability of developing squamous cell carcinoma (SCC) in later life, due to skin malformations associated with the disease (Reed et al. 1974). Around 90% of patients diagnosed with severe RDEB are likely to present SCC in middle age, with SCC formation in areas which were previously blistered or scared (Fine et al. 2009; Mallipeddi 2002).

Topical and oral retinoids are currently used in the clinical treatment of HI and other ichthyoses. The application of retinoids on the skin induces a range of immune response and differentiation proteins in keratinocytes, though the ubiquitous expression of the RXR nuclear hormone receptor throughout the skin and that RXR can form active dimers with RAR, PPAR and LXR accumulates in an unspecific response when activated (Gericke et al. 2013). For example, retinoic acid induces epidermal proteins, which are not usually expressed at the same point of differentiation and do not contribute in the formation of the permeability barrier (Mihály et al. 2012).

Isotretinoin (13-cis-retinoic acid) is an oral retinoid treatment most commonly prescribed for the treatment of severe acne. Recently, isotretinoin was prescribed on day 7 of life for a HI patient in combination with the defined management and was reported to help reduce scales, fissures and improve the ectropion and eclabium after 3 and half months (Sharpe & Hyman 2014). Isotretinoin alongside other oral retinoids, acitretin and etretinate were administered from the first week of life to many of the HI patients analysed in a study of 45 patients. This study showed a higher survival rate for HI patients treated with the oral retinoids of 83% than those treated without of 24%. As previously discussed mutation type may affect the probability of survival, as highlighted in this study where all the patients that did not survive were homozygous for mutations

in *ABCA12*. Less than half of those that did survive regardless of treatment had homozygous *ABCA12* mutations (Rajpopat et al. 2011). One of these cases did however develop cataracts, a known side effect of retinoid treatment in adults (Brecher & Orlow 2003).

Part of this thesis looked to develop possible alternative therapeutic strategies to retinoids and in particular the use of the nuclear hormone receptors PPARβ/δ and LXRβ to induce ABCA1 expression. To accomplish this a keratinocyte cell line was derived from a HI patient who had a compound heterozygote mutation in the gene *ABCA12*. The nonsense p.Glu2264X and c.5382-2a/g, a complex splice site mutation of the putative acceptor site, which lead to the use of multiple low affinity acceptor sites. Functional analysis of the HI cell line and IHC of the patient biopsy revealed a characteristic HI epidermal phenotype and a reduction in the protein expression of the cholesterol transporter ABCA1. ABCA1 cholesterol transportation in the epidermis functions to add cholesterol to the range of ceramides in the lipid envelope, which has been shown to aid in permeability barrier plasticity (Takahashi et al. 1996; Feingold & Jiang 2011).

The patient derived HI cell line was shown to initiate a premature terminal differentiation under calcium shift by the significant increase of the expression levels of K10, involucrin and TGM1 proteins compared to controls. The addition of PPARβ/δ and LXRβ agonists on the HI cell line increased the transcript and protein levels of the reduced ABCA1. The application of these agonists on the HI cell line reduced the expression of the proteins expressed prematurely under calcium shift. In the HI cell line the PPARβ/δ and LXRβ agonists up regulate ABCA1 and possibly increase cholesterol transportation, reducing cholesterol sulfate synthesis. Thus, topical application of the nuclear hormone agonists may offer a therapeutic option for HI.

Gene and protein replacement therapy are alternative possible therapeutic strategies for treating HI, which are currently in development for the treatment of other inherited skin disorders. In the treatment of Netherton syndrome the first attempt at gene therapy was undertaken using a recombinant adeno-associated retrovirus vector, which was cloned with the WT sequence of *SPINK5*. Transfection of Netherton syndrome-derived patient keratinocytes with the recombinant viral particles lead to a 75% recovery of SPINK5 mRNA expression and translated into a functional LEKTI protein (Roedl et al. 2011).

This strategy was furthered by the use of a *SPINK5* lentiviral vector, with an involucrin promoter sequence transfected organotypic culture and *in vivo* mouse-human skin graft models. Results corroborated with the earlier study as LEKTI expression was restored; furthermore, epidermal formation was improved in both models and due to the secretory nature of LEKTI corrective satellite populations formed (Di et al. 2011). A phase one clinical trail has been proposed utilising this system and vector, which aims to graft *SPINK5*-corrected keratinocyte stem cells on patients with a Netherton syndrome molecular diagnosis (Di et al. 2013).

A similar strategy was employed in the initial studies into the treatment of epidermolysis bullosa (EB); an *ex vivo* system of expanding corrected keratinocytes into sheets for skin grafting by use of a WT retroviral vector and epidermal stem cells. These skin grafts were applied to patients with EB and developed an adherent epidermis, which after the first year follow up showed a significant reduction of blisters, inflammation and infections (Mavilio et al. 2006). Corrective gene transfer as a therapeutic strategy however, does have disadvantages such as the random integration of the exogenous gene into the patient's genome, a process known to induce carcinogenesis due to atypical oncogene promotion. In HI, corrective gene transfer of *ABCA12* has reportedly been achieved in HI keratinocytes *in vitro* where it recovered glucosylceramide cellular distribution (Akiyama 2005).

A possible therapeutic strategy, which has not yet been explored in the treatment of HI, is protein replacement therapy. In theory, recombinant WT ABCA12 protein could be injected or topically applied to the skin, without the drawbacks of gene therapy to re-establish glucosylceramide transportation. The intradermal application of recombinant collagen VII was investigation as a treatment to RDEB. The addition of collagen VII to collagen VII KO mice reduced mortality, eased blistering and increased the number of dermal epidermal junction anchoring fibrils (Remington et al. 2009). In patients with RDEB autologous fibroblasts were injected to the intradermal region at sites of blistering to increase the transcript level of *COL7A1*. The translated protein was mutated, however, the number of vestigial anchoring fibrils increased, which help to reduce blistering and aid wound healing (Wong et al. 2008).

In the treatment of Netherton syndrome, small particle inhibitors are being investigated to perform the inhibition of the serine protease inhibitors KLK5 and KLK7 when LEKTI is aberrant. 1,2,4-Triazole derivatives were found to inhibit KLK5 and KLK7 and did not produce a cytotoxic response in keratinocytes. These inhibitors may re-establish desquamation through the cessation of the deregulated proteolytic cascades in Netherton syndrome and relieve symptoms of the disease (Tan et al. 2013).

Three apparent complications to the utilisation of ABCA12 protein therapy in HI is the administration of the treatment through the HI epidermis, especially the hyperkeratotic plates. Also, as ABCA12 is known to function within keratinocytes the large transporter must be modified to enter the cell and then to access the Golgi apparatus where LG are formed and ABCA12 is known to function at the correct stage of differentiation. A summary of the possible therapeutic strategies for HI is shown in **Figure 6.1.**

6.4. Future Work

Organotypic cultures would ensure that the *in vivo* epidermis was more closely represented in an *in vitro* culture and would further the investigations that were undertaken in monolayer. This work would give a truer representation of the nuances of complex cellular behaviours, such as cell migration, differentiation and proliferation (Oh et al. 2013). In this study the HI patient derived cell line would be used to simulate the HI epidermis and enable the analysis of the premature terminal differentiation phenotype and further the understanding of the application on nuclear hormone receptor agonists in HI as a potential future therapeutic strategy. IHC and Nile red lipid staining could be used to evaluate these organotypic cultures and the changes in their composition under the application of agonists. This could also yield results on the recovery of ABCA1 expression, barrier perturbation, the possible increased level of cholesterol sulfate and if there is any modulation in the markers of terminal differentiation, which are premature in HI.

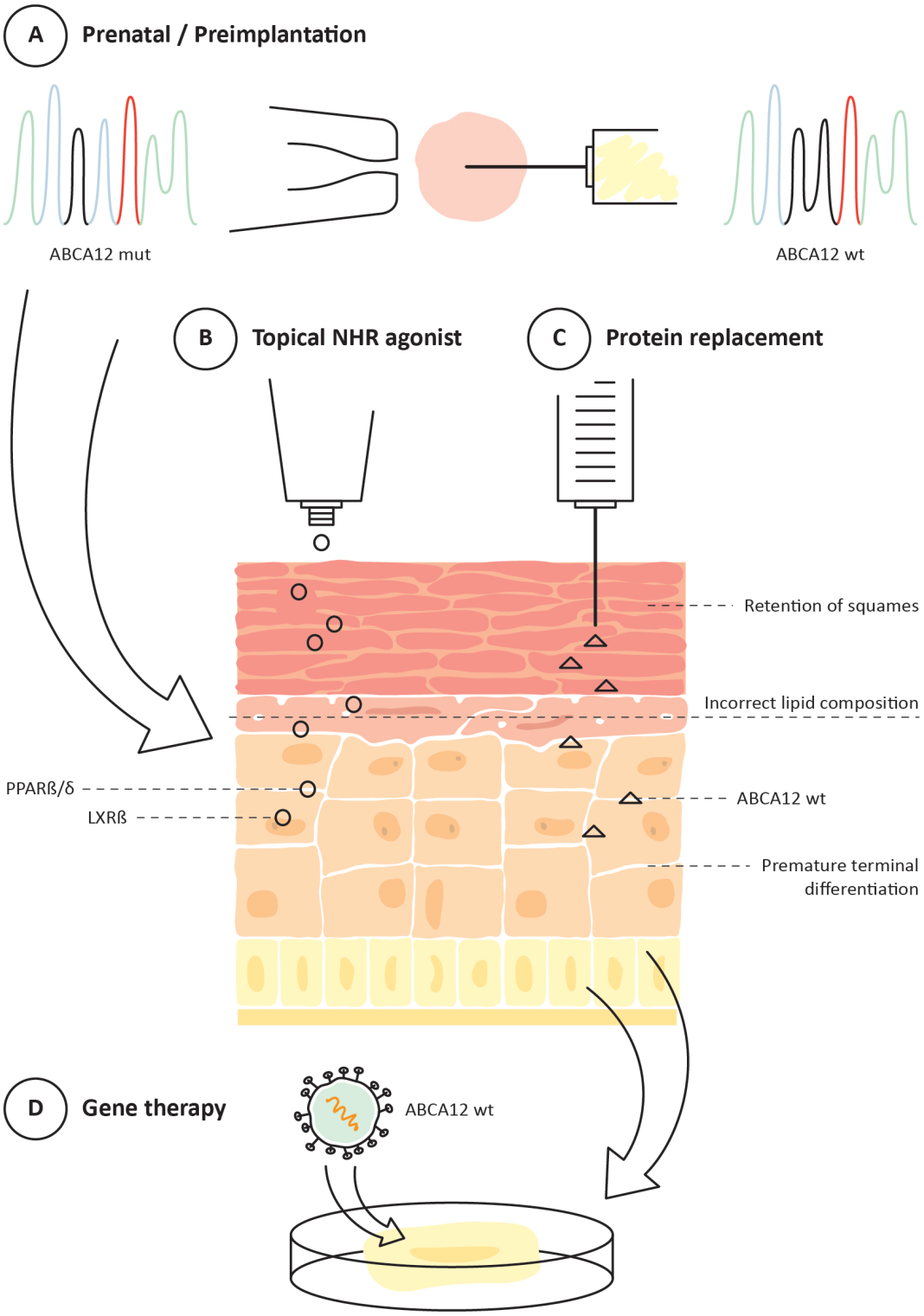

Figure 6.1. Possible therapeutic strategies for HI. (A) Prenatal testing gives the opportunity for an early diagnosis and even preimplantation in special cases to ensure a functional ABCA12. **(B)** The topical application of NHR agonists, specifically PPARβ/δ and LXRβ activation. **(C)** The addition of a recombinant functional ABCA12 protein a specific epidermal layer. **(D)** Gene therapy and the possibility of *ABCA12* gene correction by retroviral vector transfection of epidermal stem cells.

Chapter 7: Bibliography

Akiyama, M. et al., 2007. Compound Heterozygous *ABCA12* Mutations Including a Novel Nonsense Mutation Underlie Harlequin Ichthyosis. *Dermatology*, 215(2), pp.155–159. Available at: http://www.karger.com/DOI/10.1159/000104269.

Akiyama, M. et al., 2006. Compound heterozygous mutations including a de novo missense mutation in ABCA12 led to a case of harlequin ichthyosis with moderate clinical severity. *The Journal of investigative dermatology*, 126(7), pp.1518–23. Available at: http://www.ncbi.nlm.nih.gov/pubmed/16675967 [Accessed April 21, 2013].

Akiyama, M. et al., 1996. Cornified cell envelope proteins and keratins are normally distributed in harlequin ichthyosis. *Journal of cutaneous pathology*, 23(6), pp.571–575.

Akiyama, M., 2006. Harlequin ichthyosis and other autosomal recessive congenital ichthyoses: the underlying genetic defects and pathomechanisms. *Journal of dermatological science*, 42(2), pp.83–9. Available at: http://www.ncbi.nlm.nih.gov/pubmed/16481150 [Accessed January 3, 2014].

Akiyama, M., 2005. Mutations in lipid transporter ABCA12 in harlequin ichthyosis and functional recovery by corrective gene transfer. *Journal of Clinical …*, 115(7). Available at: http://www.jci.org/cgi/content/abstract/115/7/1777 [Accessed January 3, 2014].

Akiyama, M., 2013. The roles of ABCA12 in epidermal lipid barrier formation and keratinocyte differentiation. *Biochimica et biophysica acta*, pp.8–13. Available at: http://www.ncbi.nlm.nih.gov/pubmed/23954554 [Accessed September 17, 2013].

Akiyama, M., 2011. Updated molecular genetics and pathogenesis of ichyoses. *Journal of medical science*, 73, pp.79–90.

Baker, H. & Kligman, A., 1967. Technique for estimating turnover time of human stratum corneum. *Archives of Dermatology*, 95(4), pp.408–411.

Barresi, C. et al., 2011. Increased sensitivity of histidinemic mice to UVB radiation suggests a crucial role of endogenous urocanic acid in photoprotection. *The Journal of investigative dermatology*, 131(1), pp.188–94. Available at: http://www.ncbi.nlm.nih.gov/pubmed/20686493 [Accessed November 12, 2014].

Bikle, D.D., 2010. Vitamin D and the skin. *Journal of bone and mineral metabolism*, 28(2), pp.117–130.

Bland, P.J. et al., 2014. A severe collodion phenotype in newborn period associated with a homozygous missense mutation in ALOX12B. *British Journal of Dermatology*, p.n/a–n/a. Available at: http://dx.doi.org/10.1111/bjd.13627.

Blank, I.H., 1952. Factors which influence the water content of the stratum corneum. *The Journal of investigative dermatology*, 18(6), pp.433–40. Available at: http://www.ncbi.nlm.nih.gov/pubmed/13096868.

Blaydon, D.C. et al., 2013. Mutations in AQP5, encoding a water-channel protein, cause autosomal-dominant diffuse nonepidermolytic palmoplantar keratoderma. *American journal of human genetics*, 93(2), pp.330–5. Available at: http://www.pubmedcentral.nih.gov/articlerender.fcgi?artid=3738836&tool=pmcentrez&rendertype=abstract [Accessed September 25, 2014].

Blaydon, D.C. et al., 2011. Mutations in CSTA, encoding Cystatin A, underlie exfoliative ichthyosis and reveal a role for this protease inhibitor in cell-cell adhesion. *American journal of human genetics*, 89(4), pp.564–71. Available at: http://www.pubmedcentral.nih.gov/articlerender.fcgi?artid=3188842&tool=pmcentrez&rendertype=abstract [Accessed January 12, 2014].

Borgoño, C. a. et al., 2007. A potential role for multiple tissue kallikrein serine proteases in epidermal desquamation. *Journal of Biological Chemistry*, 282(6), pp.3640–3652.

Borkowski, A.W. et al., 2013. Activation of TLR3 in keratinocytes increases expression of genes involved in formation of the epidermis, lipid accumulation, and epidermal organelles. *The Journal of investigative dermatology*, 133(8), pp.2031–40. Available at: http://www.pubmedcentral.nih.gov/articlerender.fcgi?artid=3686920&tool=pmcentrez&rendertype=abstract.

Bouwstra, J. a. et al., 2003. *Structure of the skin barrier and its modulation by vesicular formulations*,

Brecher, A.R. & Orlow, S.J., 2003. Oral retinoid therapy for dermatologic conditions in children and adolescents. *Journal of the American Academy of Dermatology*, 49(2), pp.171–182. Available at: http://linkinghub.elsevier.com/retrieve/pii/S0190962203015640?showall=true.

Brooke, M. a et al., 2014. Cryptogenic multifocal ulcerating stenosing enteritis associated with homozygous deletion mutations in cytosolic phospholipase A2-α. *Gut*, 63(1), pp.96–104. Available at: http://www.ncbi.nlm.nih.gov/pubmed/23268370 [Accessed October 3, 2014].

Brooks-Wilson, A. et al., 1999. Mutations in ABC1 in Tangier disease and familial high-density lipoprotein deficiency. *Nature genetics*, 22(4), pp.336–345.

Broome, a.-M., Ryan, D. & Eckert, R.L., 2003. S100 Protein Subcellular Localization During Epidermal Differentiation and Psoriasis. *Journal of Histochemistry & Cytochemistry*, 51(5), pp.675–685. Available at: http://jhc.sagepub.com/lookup/doi/10.1177/002215540305100513 [Accessed November 18, 2014].

Bruckner-Tuderman, L., 2010. Dystrophic epidermolysis bullosa: pathogenesis and clinical features. *Dermatologic clinics*, 28(1), pp.107–114.

Buxman, M.M. et al., 1979. Harlequin ichthyosis with epidermal lipid abnormality. *Archives of dermatology*, 115(2), pp.189–193.

Calléja, C. et al., 2006. Genetic and pharmacological evidence that a retinoic acid cannot be the RXR-activating ligand in mouse epidermis keratinocytes. *Genes & development*, 20(11), pp.1525–38. Available at: http://www.pubmedcentral.nih.gov/articlerender.fcgi?artid=1475764&tool=pmcentrez&rendertype=abstract [Accessed January 12, 2014].

Candi, E., Schmidt, R. & Melino, G., 2005. The cornified envelope: a model of cell death in the skin. *Nature reviews. Molecular cell biology*, 6(4), pp.328–40. Available at: http://www.ncbi.nlm.nih.gov/pubmed/15803139 [Accessed March 8, 2013].

Castiglia, D. et al., 2009. Trisomic rescue causing reduction to homozygosity for a novel ABCA12 mutation in harlequin ichthyosis. *Clinical Genetics*, 76(4), pp.392–397. Available at: http://dx.doi.org/10.1111/j.1399-0004.2009.01198.x.

Caubet, C. et al., 2004. Degradation of corneodesmosome proteins by two serine proteases of the kallikrein family, SCTE/KLK5/hK5 and SCCE/KLK7/hK7. *Journal of Investigative Dermatology*, 122, pp.1235–1244.

Chen, W. et al., 2011. Enzymatic Reduction of Oxysterols Impairs LXR Signaling in Cultured Cells and the Livers of Mice Wenling. *Cell metabolism*, 5(1), pp.73–79.

Cheng, S.H., 1990. Defective intracellular transport and processing of CFTR is the molecular basis of most cystic fibrosis. *Cell*, 63, pp.827–834.

Cheng, T. et al., 2006. Cystatin M/E is a high affinity inhibitor of cathepsin V and cathepsin L by a reactive site that is distinct from the legumain-binding site: A novel clue for the role of cystatin M/E in epidermal cornification. *Journal of Biological Chemistry*, 281(23), pp.15893–15899.

Chu, D., 2008. *Fitzpatrick's Dermatology in General Medicine* D. Leffel, ed., McGraw Hill's publishing companis.

Chu, D.H., 2005. Development and Structure of Skin. In *Fitzpatrick Dermatology*. pp. 57–92.

Chung, H. & Uitto, J., 2010. Type VII Collagen: The Anchoring Fibril Protein at Fault in Dystrophic Epidermolysis Bullosa. *Dermatology*, 28(1), pp.93–105.

Clerc, S.G. & Thompson, T.E., 1995. Permeability of Dimyristoyl Phosphatidylcholine / Dipalmitoyl Phosphatidylcholine Bilayer Membranes with Coexisting Gel and Liquid-Crystalline Phases CH3-. *Biophysical Journal*, 68(June), pp.2333–2341.

Cline, P.R. & Rice, R.H., 1983. Modulation of involucrin and envelope competence in human keratinocytes by hydrocortisone, retinyl acetate, and growth arrest. *Cancer Research*, 43(JULY), pp.3203–3207.

Dale, B. et al., 1990. Heterogeneity in harlequin ichthyosis, an inborn error of epidermal keratinization: variable morphology and structural protein expression and a defect in lamellar granules. *Journal of Investigative Dermatology*, 94, pp.6–18.

Dang, N. & Murrell, D.F., 2008. Mutation analysis and characterization of COL7A1 mutations in dystrophic epidermolysis bullosa. *Experimental Dermatology*, 17(7), pp.533–568.

Dean, M., Hamon, Y. & Chimini, G., 2001. The human ATP-binding cassette (ABC) transporter superfamily. *Journal of lipid research*, 42, pp.1007–1017.

Denning, M.F. et al., 1995. Specific protein kinase C isozymes mediate the induction of keratinocyte differentiation markers by calcium. *Cell growth & differentiation : the molecular biology journal of the American Association for Cancer Research*, 6(2), pp.149–157.

Deraison, C. et al., 2007. LEKTI Fragments Specifically Inhibit KLK5, KLK7, and KLK14 and Control Desquamation through a pH-dependent Interaction. *Molecular biology of the cell*, 18(September), pp.3607–3619.

Descargues, P. et al., 2006. Corneodesmosomal cadherins are preferential targets of stratum corneum trypsin- and chymotrypsin-like hyperactivity in Netherton syndrome. *The Journal of investigative dermatology*, 126, pp.1622–1632.

Di, W.-L. et al., 2011. Ex-vivo gene therapy restores LEKTI activity and corrects the architecture of Netherton syndrome-derived skin grafts. *Molecular therapy : the journal of the American Society of Gene Therapy*, 19(2), pp.408–416. Available at: http://dx.doi.org/10.1038/mt.2010.201.

Di, W.-L. et al., 2013. Phase I study protocol for ex vivo lentiviral gene therapy for the inherited skin disease, Netherton syndrome. *Human gene therapy. Clinical development*, 24(4), pp.182–190.

Dobbie, J.W. et al., 1995. Lamellar body secretion: ultrastructural analysis of an unexplored function of synoviocytes. *British journal of rheumatology*, 34, pp.13–23.

Dotto, G.P., 1999. Signal transduction pathways controlling the switch between keratinocyte growth and differentiation. *Critical reviews in oral biology and medicine : an official publication of the American Association of Oral Biologists*, 10(4), pp.442–457.

Dyer, J.A., Spraker, M. & Williams, M., 2013. Care of the newborn with ichthyosis. *Dermatologic therapy*, 26(1), pp.1–15.

Eckert, L. & Rorket, E.A., 1989. Molecular Biology of Keratinocyte Differentiation. *Environmental Health Perspectives*, 80, pp.109–116.

Eckert, R.L. & Green, H., 1986. Structure and Evolution of the Human lnvolucrin Gene. *Cell*, 46, pp.583–589.

Eckl, K.-M. et al., 2009. Molecular analysis of 250 patients with autosomal recessive congenital ichthyosis: evidence for mutation hotspots in ALOXE3 and allelic heterogeneity in ALOX12B. *The Journal of investigative dermatology*, 129(6),

pp.1421–8. Available at: http://www.ncbi.nlm.nih.gov/pubmed/19131948 [Accessed September 13, 2014].

Eckl, K.-M. et al., 2005. Mutation spectrum and functional analysis of epidermis-type lipoxygenases in patients with autosomal recessive congenital ichthyosis. *Human mutation*, 26(4), pp.351–61. Available at: http://www.ncbi.nlm.nih.gov/pubmed/16116617 [Accessed January 29, 2014].

Edwards, I.J. et al., 2002. Improved glucose control decreases the interaction of plasma low-density lipoproteins with arterial proteoglycans. *Metabolism: clinical and experimental*, 51(10), pp.1223–1229. Available at: http://linkinghub.elsevier.com/retrieve/pii/S0026049502000707?showall=true.

Edwards, P. a, Kast, H.R. & Anisfeld, A.M., 2002. BAREing it all: the adoption of LXR and FXR and their roles in lipid homeostasis. *Journal of lipid research*, 43(1), pp.2–12. Available at: http://www.ncbi.nlm.nih.gov/pubmed/11792716.

Edwards, P. a, Kennedy, M. a & Mak, P. a, 2002. LXRs; oxysterol-activated nuclear receptors that regulate genes controlling lipid homeostasis. *Vascular pharmacology*, 38(4), pp.249–56. Available at: http://www.ncbi.nlm.nih.gov/pubmed/12449021.

Egberts, F. et al., 2004. Cathepsin D is involved in the regulation of transglutaminase 1 and epidermal differentiation. *Journal of cell science*, 117(Pt 11), pp.2295–307. Available at: http://www.ncbi.nlm.nih.gov/pubmed/15126630 [Accessed May 21, 2014].

Elias, P.M., 1983. Epidermal Lipids , Barrier Function , and Desquamation. *Journal of Investigative Dermatology*, 80(6), pp.44–49.

Elias, P.M. & Feingold, K.R., 2005. *Skin Barrier* P. M. Elias & K. R. Feingold, eds., CRC Press.

Envelope, K.C. et al., 1992. Biophysical Characterization of Involucrin Reveals a Molecule Ideally Suited to Function as an Intermolecular Cross-bridge of the. *The Journal of biological chemistry*, 267(17), pp.12233–12238.

Epp, N. et al., 2007. 12R-lipoxygenase deficiency disrupts epidermal barrier function. *The Journal of cell biology*, 177(1), pp.173–82. Available at: http://www.pubmedcentral.nih.gov/articlerender.fcgi?artid=2064121&tool=pmcentrez&rendertype=abstract [Accessed December 1, 2014].

Fartasch, M., 2004. The epidermal lamellar body: a fascinating secretory organelle. *The Journal of investigative dermatology*, 122(5), pp.XI–XII. Available at: http://www.ncbi.nlm.nih.gov/pubmed/15140249 [Accessed January 2, 2014].

Feingold, K. & Jiang, Y., 2011. lipids coordinately regulate the formation of the protein and lipid domains of the stratum corneum: Role of fatty acids, oxysterols, cholesterol sulfate, and ceramides as. *Dermato-endocrinology*, (June), pp.113–118.

Available at: http://www.landesbioscience.com/journals/29/article/14996/ [Accessed January 8, 2014].

Feingold, K.R., 2007. Thematic review series: skin lipids. The role of epidermal lipids in cutaneous permeability barrier homeostasis. *Journal of lipid research*, 48(12), pp.2531–46. Available at: http://www.ncbi.nlm.nih.gov/pubmed/17872588 [Accessed October 13, 2014].

Fine, J.D. et al., 2009. Epidermolysis bullosa and the risk of life-threatening cancers: The National EB Registry experience, 1986-2006. *Journal of the American Academy of Dermatology*, 60(2), pp.203–211. Available at: http://dx.doi.org/10.1016/j.jaad.2008.09.035.

Fischer, J., 2009. Autosomal recessive congenital ichthyosis. *The Journal of investigative dermatology*, 129(6), pp.1319–1321. Available at: http://dx.doi.org/10.1038/jid.2009.57.

Fluhr, J.W. et al., 2001. Generation of Free Fatty Acids from Phospholipids Regulates Stratum Corneum Acidi®cation and Integrity. *The Journal of investigative dermatology*, (i), pp.44–51.

Fortugno, P. et al., 2011. Proteolytic Activation Cascade of the Netherton Syndrome–Defective Protein, LEKTI, in the Epidermis: Implications for Skin Homeostasis. *Journal of Investigative Dermatology*, 131, pp.2223–2232.

Francisco, C.S., Francisco, S. & Hospital, M., 2004. PATHOPHYSIOLOGIC BASIS FOR GROWTH FAILURE IN CHILDREN WITH. *j.jpeds*, 10.1016(145), pp.82–92.

Freinkel, R.K. & Woodley, D.T., 2001. *The Biology of the Skin*, Parthenon Publishing.

Fu, D.J. et al., 2014. Keratin 9 is required for the structural integrity and terminal differentiation of the palmoplantar epidermis. *The Journal of investigative dermatology*, 134(3), pp.754–63. Available at: http://www.pubmedcentral.nih.gov/articlerender.fcgi?artid=3923277&tool=pmcentrez&rendertype=abstract [Accessed November 6, 2014].

Fu, Y. et al., 2013. ABCA12 regulates ABCA1-dependent cholesterol efflux from macrophages and the development of atherosclerosis. *Cell metabolism*, 18(2), pp.225–38. Available at: http://www.ncbi.nlm.nih.gov/pubmed/23931754 [Accessed December 3, 2013].

Fuchs, E., 1998. A Structural Scaffolding of Intermediate Filaments in Health and Disease. *Science*, 279(5350), pp.514–519. Available at: http://www.sciencemag.org/cgi/doi/10.1126/science.279.5350.514 [Accessed September 16, 2014].

Galadari, S. et al., 1998. Purification and characterization of ceramide-activated protein phosphatases. *Biochemistry*, 37(32), pp.11232–8. Available at: http://www.ncbi.nlm.nih.gov/pubmed/9698369.

Gericke, J. et al., 2013. Regulation of retinoid-mediated signaling involved in skin homeostasis by RAR and RXR agonists/antagonists in mouse skin. *PloS one*, 8(4), p.e62643. Available at: http://www.pubmedcentral.nih.gov/articlerender.fcgi?artid=3634743&tool=pmcentrez&rendertype=abstract [Accessed January 12, 2014].

Gilfix, B.M. & Green, H., 1984. Bioassay of retinoids using cultured human conjunctival keratinocytes. *Journal of cellular physiology*, 119(2), pp.172–174.

Gray, G.M. et al., 1982. Lipid composition of the superficial stratum corneum cells of pig epidermis. *British Journal of Dermatology*, 106(1), pp.59–63. Available at: http://dx.doi.org/10.1111/j.1365-2133.1982.tb00902.x.

Grubauer, G., Feingold, K.R., et al., 1989. Lipid content and lipid type as determinants of the epidermal permeability barrier. *Journal of lipid research*, 30(1), pp.89–96. Available at: http://www.ncbi.nlm.nih.gov/pubmed/2918253.

Grubauer, G., Elias, P.M. & Feingold, K.R., 1989. Transepidermal water loss: the signal for recovery of barrier structure and function. *Journal of lipid research*, 30(3), pp.323–33. Available at: http://www.ncbi.nlm.nih.gov/pubmed/2723540.

Guo, Z. et al., 2002. Double deletions and missense mutations in the first nucleotide-binding fold of the ATP-binding cassette transporter A1 (ABCA1) gene in Japanese patients with tangier disease. *Journal of Human Genetics*, 47(6), pp.325–329.

Guttman, M. et al., 2009. Chromatin signature reveals over a thousand highly conserved large non-coding RNAs in mammals. *Nature*, 458(7235), pp.223–227.

Hachem, J.-P. et al., 2006. Serine protease signaling of epidermal permeability barrier homeostasis. *The Journal of investigative dermatology*, 126(9), pp.2074–86. Available at: http://www.ncbi.nlm.nih.gov/pubmed/16691196 [Accessed January 2, 2014].

Haftek, M. et al., 1996. A longitudinal study of a harlequin infant presenting clinically as non-bullous congenital ichthyosiform erythroderma. *British Journal of Dermatology*, 135(3), pp.448–53.

Haller, T. et al., 1998. Dynamics of surfactant release in alveolar type II cells. *Proceedings of the National Academy of Sciences of the United States of America*, 95(February), pp.1579–1584.

Hanley, K. et al., 2001. Cholesterol sulfate stimulates involucrin transcription in keratinocytes by increasing Fra-1, Fra-2, and Jun D. *Journal of lipid research*, 42(3), pp.390–398.

Hanley, K. et al., 1998. Keratinocyte differentiation is stimulated by activators of the nuclear hormone receptor PPARalpha. *The Journal of investigative dermatology*, 110(4), pp.368–375.

Hanley, K. et al., 2000. Oxysterols induce differentiation in human keratinocytes and increase Ap-1-dependent involucrin transcription. *The Journal of investigative dermatology*, 114(3), pp.545–53. Available at: http://www.ncbi.nlm.nih.gov/pubmed/10692116.

Hawley-Nelson, P. et al., 1989. HPV16 E6 and E7 proteins cooperate to immortalize human foreskin keratinocytes. *The EMBO journal*, 8(12), pp.3905–3910.

Heathfield et al., 2013. Stargardt disease: towards developing a model to predict phenotype. *Eur J Hum Genet*, 21(10), pp.1173–6.

Hennings, H. et al., 1980. Growth and differentiation of mouse epidermal cells in culture: effects of extracellular calcium. *Current problems in dermatology*, 10(January), pp.3–25.

Hennings, H., Steinert, P. & Buxman, M.M., 1981. Calcium induction of transglutaminase and the formation of epsilon(gamma-glutamyl) lysine cross-links in cultured mouse epidermal cells. *Biochemical and biophysical research communications*, 102(2), pp.739–745.

Hohl, D. et al., 1991. Characterization of Human Loricrin. *The Journal of biological chemistry*, 266(10), pp.6626–6636.

Hohl, D., 1990. Cornified cell envelope. *Dermatologica*, 180, pp.201–211.

Holleran, W.M., Takagi, Y. & Uchida, Y., 2006. Epidermal sphingolipids: Metabolism, function, and roles in skin disorders. *FEBS Letters*, 580, pp.5456–5466.

Hsu, W.Y. et al., 1989. [Harlequin fetus--a case report]. *Zhonghua yi xue za zhi = Chinese medical journal; Free China ed*, 43(1), pp.63–66.

Huang, W. et al., 2001. Novel mutations in ABCA1 gene in Japanese patients with Tangier disease and familial high density lipoprotein deficiency with coronary heart disease. *Biochimica et Biophysica Acta - Molecular Basis of Disease*, 1537(1), pp.71–78.

Huber, M. et al., 1995. Mutations of keratinocyte transglutaminase in lamellar ichthyosis. *Science (New York, N.Y.)*, 267(5197), pp.525–8. Available at: http://www.ncbi.nlm.nih.gov/pubmed/9544844.

Hyde, S.C. et al., 1990. Structural model of ATP-binding proteins associated with cystic fibrosis, multidrug resistance and bacterial transport. *Nature*, 346(6282), pp.362–365.

Igarashi, S. et al., 2004. Cathepsin D, but not cathepsin E, degrades desmosomes during epidermal desquamation. *The British journal of dermatology*, 151(2), pp.355–361.

Ishida-Yamamoto, A. et al., 2004. Epidermal lamellar granules transport different cargoes as distinct aggregates. *The Journal of investigative dermatology*, 122(5), pp.1137–44. Available at: http://www.ncbi.nlm.nih.gov/pubmed/15140216.

Ishida-Yamamoto, A. et al., 1994. Filaggrin expression in epidermolytic ichthyosis (epidermolytic hyperkeratosis). *The British journal of dermatology*, 131(6), pp.767–779.

Jiang, S. et al., 2010. Differential expression of stem cell markers in human follicular bulge and interfollicular epidermal compartments. *Histochemistry and cell biology*, 133(4), pp.455–65. Available at: http://www.ncbi.nlm.nih.gov/pubmed/20229054 [Accessed January 2, 2014].

Jiang, Y.J. et al., 2009. Ceramide stimulates ABCA12 expression via peroxisome proliferator-activated receptor {delta} in human keratinocytes. *The Journal of biological chemistry*, 284(28), pp.18942–52. Available at: http://www.pubmedcentral.nih.gov/articlerender.fcgi?artid=2707228&tool=pmcentrez&rendertype=abstract [Accessed August 20, 2013].

Jiang, Y.J. et al., 2005. LXR and PPAR activators stimulate cholesterol sulfotransferase type 2 isoform 1b in human keratinocytes. *Journal of lipid research*, 46(12), pp.2657–2666.

Jiang, Y.J. et al., 2008. PPAR and LXR activators regulate ABCA12 expression in human keratinocytes. *The Journal of investigative dermatology*, 128(1), pp.104–9. Available at: http://www.ncbi.nlm.nih.gov/pubmed/17611579 [Accessed March 26, 2013].

Jiang, Y.J. et al., 2006. Regulation of ABCA1 expression in human keratinocytes and murine epidermis. *Journal of lipid research*, 47(10), pp.2248–58. Available at: http://www.ncbi.nlm.nih.gov/pubmed/16825673 [Accessed December 12, 2013].

Jobard, F. et al., 2002. (ALOX12B) are mutated in non-bullous congenital ichthyosiform erythroderma (NCIE) linked to chromosome 17p13 . 1. *Human Molecular Genetics*, 11(1), pp.107–114.

Kalinin, A., Marekov, L. & Steinert, P.M., 2001. Assembly of the epidermal cornified cell envelope. *Journal of cell science*, 114, pp.3069–3070.

Kelsell, D.P. et al., 2005. Mutations in ABCA12 underlie the severe congenital skin disease harlequin ichthyosis. *American journal of human genetics*, 76(5), pp.794–803. Available at: http://www.pubmedcentral.nih.gov/articlerender.fcgi?artid=1199369&tool=pmcentrez&rendertype=abstract.

Kitiratschky, V.B.D. et al., 2008. ABCA4 gene analysis in patients with autosomal recessive cone and cone rod dystrophies. *European journal of human genetics : EJHG*, 16(7), pp.812–9. Available at: http://www.pubmedcentral.nih.gov/articlerender.fcgi?artid=2579899&tool=pmcentrez&rendertype=abstract [Accessed January 16, 2014].

Knight, H.M. et al., 2009. A cytogenetic abnormality and rare coding variants identify ABCA13 as a candidate gene in schizophrenia, bipolar disorder, and depression. *American journal of human genetics*, 85(6), pp.833–46. Available at:

http://www.pubmedcentral.nih.gov/articlerender.fcgi?artid=2790560&tool=pmcentrez&rendertype=abstract [Accessed March 11, 2013].

Kömüves, L. & Hanley, K., 2000. Stimulation of PPARα promotes epidermal keratinocyte differentiation in vivo. *Journal of investigative ...*, pp.353–360. Available at: http://www.nature.com/jid/journal/v115/n3/abs/5600806a.html [Accessed January 12, 2014].

Korge, B.P. et al., 1992. Extensive size polymorphism of the human keratin 10 chain resides in the C-terminal V2 subdomain due to variable numbers and sizes of glycine loops. *Proceedings of the National Academy of Sciences of the United States of America*, 89(3), pp.910–914.

Krebsová, a et al., 2001. Identification, by homozygosity mapping, of a novel locus for autosomal recessive congenital ichthyosis on chromosome 17p, and evidence for further genetic heterogeneity. *American journal of human genetics*, 69(1), pp.216–22. Available at: http://www.pubmedcentral.nih.gov/articlerender.fcgi?artid=1226037&tool=pmcentrez&rendertype=abstract.

Kretz, M. et al., 2013. Control of somatic tissue differentiation by the long non-coding RNA TINCR. *Nature*, 493(7431), pp.231–5. Available at: http://www.pubmedcentral.nih.gov/articlerender.fcgi?artid=3674581&tool=pmcentrez&rendertype=abstract [Accessed July 11, 2014].

Krieg, P., Marks, F. & Fürstenberger, G., 2001. A gene cluster encoding human epidermis-type lipoxygenases at chromosome 17p13.1: cloning, physical mapping, and expression. *Genomics*, 73(3), pp.323–30. Available at: http://www.ncbi.nlm.nih.gov/pubmed/11350124 [Accessed September 16, 2014].

Lampe, M. a, Williams, M.L. & Elias, P.M., 1983. Human epidermal lipids: characterization and modulations during differentiation. *Journal of lipid research*, 24(2), pp.131–140.

Lechler, T. & Fuchs, E., 2005. Asymmetric cell divisions promote stratification and differentiation of mammalian skin. *Nature*, 437(7056), pp.275–80. Available at: http://www.pubmedcentral.nih.gov/articlerender.fcgi?artid=1399371&tool=pmcentrez&rendertype=abstract [Accessed December 17, 2013].

Lefévre, C. et al., 2003. Mutations in the transporter ABCA12 are associated with lamellar ichthyosis type 2. *Human molecular genetics*, 12(18), pp.2369–78. Available at: http://www.ncbi.nlm.nih.gov/pubmed/12915478 [Accessed April 16, 2013].

Lewis, R. a et al., 1999. Genotype/Phenotype analysis of a photoreceptor-specific ATP-binding cassette transporter gene, ABCR, in Stargardt disease. *American journal of human genetics*, 64(2), pp.422–434.

Lorand, L. & Graham, R.M., 2003. Transglutaminases: crosslinking enzymes with pleiotropic functions. *Nature reviews. Molecular cell biology*, 4(2), pp.140–56.

Available at: http://www.ncbi.nlm.nih.gov/pubmed/12563291 [Accessed November 2, 2014].

De Luca, L.M., 1977. The direct involvement of vitamin A in glycosyl transfer reactions of mammalian membranes. *Vitamins and hormones*, 35, pp.1–57.

Mallipeddi, R., 2002. Epidermolysis bullosa and cancer. *Clinical and Experimental Dermatology*, 27(8), pp.616–623.

Man, M.-Q. et al., 2006. Basis for improved permeability barrier homeostasis induced by PPAR and LXR activators: liposensors stimulate lipid synthesis, lamellar body secretion, and post-secretory lipid processing. *The Journal of investigative dermatology*, 126(2), pp.386–92. Available at: http://www.ncbi.nlm.nih.gov/pubmed/16374473 [Accessed January 2, 2014].

Manabe, M. et al., 1991. Interaction of filaggrin with keratin filaments during advanced stages of normal human epidermal differentiation and in Ichthyosis vulgaris. *Differentiation*, 48(1), pp.43–50. Available at: http://www.sciencedirect.com/science/article/pii/S030146811160279X.

Mao-Qiang, M. et al., 2004. Peroxisome-proliferator-activated receptor (PPAR)-gamma activation stimulates keratinocyte differentiation. *The Journal of investigative dermatology*, 123(2), pp.305–12. Available at: http://www.ncbi.nlm.nih.gov/pubmed/15245430.

Mao-Qiang, M., Elias, P.M. & Feingold, K.R., 1993. Fatty acids are required for epidermal permeability barrier function. *The Journal of clinical investigation*, 92(2), pp.791–8. Available at: http://www.pubmedcentral.nih.gov/articlerender.fcgi?artid=294916&tool=pmcentrez&rendertype=abstract.

Mavilio, F. et al., 2006. Correction of junctional epidermolysis bullosa by transplantation of genetically modified epidermal stem cells. *Nature medicine*, 12(12), pp.1397–1402.

Meyer-Hoffert, U., Wu, Z. & Schröder, J.-M., 2009. Identification of lympho-epithelial Kazal-type inhibitor 2 in human skin as a kallikrein-related peptidase 5-specific protease inhibitor. *PloS one*, 4(2), p.e4372.

Mihály, J. et al., 2012. Reduced Retinoid Signaling in the Skin after Systemic Retinoid-X Receptor Ligand Treatment in Mice with Potential Relevance for Skin Disorders. *Dermatology*, 225(4), pp.304–311. Available at: http://www.karger.com/doi/10.1159/000345496 [Accessed June 25, 2013].

Miksch, S. et al., 2005. Molecular genetics of pseudoxanthoma elasticum: type and frequency of mutations in ABCC6. *Human Mutation*, 26(3), pp.235–248. Available at: http://dx.doi.org/10.1002/humu.20206.

Mildner, M. et al., 2010. Knockdown of filaggrin impairs diffusion barrier function and increases UV sensitivity in a human skin model. *The Journal of investigative*

dermatology, 130(9), pp.2286–94. Available at: http://www.ncbi.nlm.nih.gov/pubmed/20445547 [Accessed November 12, 2014].

Milner, M.E. et al., 1992. Abnormal lamellar granules in harlequin ichthyosis. *The Journal of investigative dermatology*, 99(6), pp.824–829.

Mitsutake, S. et al., 2010. ABCA12 dysfunction causes a disorder in glucosylceramide accumulation during keratinocyte differentiation. *Journal of dermatological science*, 60(2), pp.128–129.

Moran, J.L. et al., 2007. A mouse mutation in the 12R-lipoxygenase, Alox12b, disrupts formation of the epidermal permeability barrier. *The Journal of investigative dermatology*, 127(8), pp.1893–7. Available at: http://www.ncbi.nlm.nih.gov/pubmed/17429434 [Accessed September 13, 2014].

Natsuga, K. et al., 2007. Novel ABCA12 mutations identified in two cases of non-bullous congenital ichthyosiform erythroderma associated with multiple skin malignant neoplasia. *The Journal of investigative dermatology*, 127(11), pp.2669–2673.

Nemes, Z. et al., 1999. A novel function for transglutaminase 1 : Attachment of long-chain -hydroxyceramides to involucrin by ester bond formation. *Proc. Natl. Acad. Sci. USA*, 96(July), pp.8402–8407.

Norlén, L., 2001a. Skin barrier formation: the membrane folding model. *The Journal of investigative dermatology*, 117(4), pp.823–9. Available at: http://www.ncbi.nlm.nih.gov/pubmed/11676818.

Norlén, L., 2001b. Skin barrier structure and function: the single gel phase model. *The Journal of investigative dermatology*, 117(4), pp.830–6. Available at: http://www.ncbi.nlm.nih.gov/pubmed/11676819.

Numaga-Tomita, T. & Putney, J.W., 2013. Role of STIM1- and Orai1-mediated Ca2+ entry in Ca2+-induced epidermal keratinocyte differentiation. *Journal of cell science*, 126, pp.605–12. Available at: http://www.pubmedcentral.nih.gov/articlerender.fcgi?artid=3613182&tool=pmcentrez&rendertype=abstract.

Oh, J.W. et al., 2013. Organotypic skin culture. *The Journal of investigative dermatology*, 133(11), p.e14. Available at: http://dx.doi.org/10.1038/jid.2013.387.

Oji, V. & Traupe, H., 2006. Ichthyoses: Differential diagnosis and molecular genetics. *Eur J Dermatol*, 16(4), pp.349–359.

Paramio, J.M. et al., 1999. Modulation of Cell Proliferation by Modulation of Cell Proliferation by Cytokeratins K10 and K16. *Molecular and cellular biology*, 19(4).

Pendaries, V. et al., 2014. Knockdown of filaggrin in a three-dimensional reconstructed human epidermis impairs keratinocyte differentiation. *The Journal of investigative*

dermatology, 134(12), pp.2938–46. Available at: http://www.ncbi.nlm.nih.gov/pubmed/24940654 [Accessed November 12, 2014].

Peter M. Elias, Mary L. Williams, M.E.M., Jeannette A. Bonifas, Barbara E. Brown, S. & Grayson, and Ervin H. Epstein, J., 1984. Stratum Corneum Lipids in Disorders of Cornification. *JCI The Jornal of Clinical Investigation*, pp.1414–1421. Available at: http://europepmc.org/articles/370941?pdf=render.

Pillai, S. et al., 1993. Localization and quantitation of calcium pools and calcium binding sites in cultured human keratinocytes. *Journal of cellular physiology*, 154(1), pp.101–112.

Ponec, M., 1994. *The Keratinocyte Handbook* I. M. Leigh, E. Lane, & F. M. Watt, eds., Cambridge Univ. Press, Cambridge, U.K.: Cambridge Univ. Press, Cambridge, U.K.

Poulson, N.D. & Lechler, T., 2010. Robust control of mitotic spindle orientation in the developing epidermis. *The Journal of cell biology*, 191(5), pp.915–22. Available at: http://www.pubmedcentral.nih.gov/articlerender.fcgi?artid=2995176&tool=pmcentrez&rendertype=abstract [Accessed November 6, 2014].

Poumay, Y. & Pittelkow, M.R., 1995. Cell density and culture factors regulate keratinocyte commitment to differentiation and expression of suprabasal K1/K10 keratins. *The Journal of investigative dermatology*, 104(2), pp.271–276.

Presland, R.B. et al., 1997. Evidence for specific proteolytic cleavage of the N-terminal domain of human profilaggrin during epidermal differentiation. *The Journal of investigative dermatology*, 108(2), pp.170–178.

Rajpar, S.F. et al., 2006. A novel ABCA12 mutation underlying a case of Harlequin ichthyosis. *British Journal of Dermatology*, 155(1), pp.204–206. Available at: http://dx.doi.org/10.1111/j.1365-2133.2006.07291.x.

Rajpopat, S. et al., 2011. Harlequin ichthyosis: a review of clinical and molecular findings in 45 cases. *Archives of dermatology*, 147(6), pp.681–6. Available at: http://www.ncbi.nlm.nih.gov/pubmed/21339420 [Accessed April 10, 2013].

Rassner, U. et al., 1999. Coordinate assembly of lipids and enzyme proteins into epidermal lamellar bodies. *Tissue & cell*, 31(5), pp.489–498.

Reed, W.B. et al., 1974. Epidermolysis bullosa dystrophica with epidermal neoplasms. *Archives of dermatology*, 110(6), pp.894–902.

Remington, J. et al., 2009. Injection of recombinant human type VII collagen corrects the disease phenotype in a murine model of dystrophic epidermolysis bullosa. *Molecular therapy : the journal of the American Society of Gene Therapy*, 17(1), pp.26–33.

Repa, J.J. et al., 2000. Regulation of absorption and ABC1-mediated efflux of cholesterol by RXR heterodimers. *Science (New York, N.Y.)*, 289(5484), pp.1524–1529.

Resing, K. a et al., 1989. Identification of proteolytic cleavage sites in the conversion of profilaggrin to filaggrin in mammalian epidermis. *The Journal of biological chemistry*, 264(3), pp.1837–45. Available at: http://www.ncbi.nlm.nih.gov/pubmed/2912987.

Roedl, D. et al., 2011. rAAV2-mediated restoration of LEKTI in LEKTI-deficient cells from Netherton patients. *Journal of dermatological science*, 61(3), pp.194–198.

Rossi, a et al., 1998. Effect of AP1 transcription factors on the regulation of transcription in normal human epidermal keratinocytes. *The Journal of investigative dermatology*, 110(1), pp.34–40.

Ruse, M. et al., 2001. S100A7, S100A10, and S100A11 Are Transglutaminase Substrates †. *Biochemistry*, 40(10), pp.3167–3173. Available at: http://pubs.acs.org/doi/abs/10.1021/bi0019747.

Saeki, Y. et al., 2012. An ErbB receptor-mediated AP-1 regulatory network is modulated by STAT3 and c-MYC during calcium-dependent keratinocyte differentiation. *Experimental Dermatology*, 21, pp.293–298.

Sakai, K. et al., 2009. ABCA12 is a major causative gene for non-bullous congenital ichthyosiform erythroderma. *The Journal of investigative dermatology*, 129(9), pp.2306–2309.

Sakai, K. et al., 2007. Localization of ABCA12 from Golgi apparatus to lamellar granules in human upper epidermal keratinocytes. *Experimental dermatology*, 16(11), pp.920–6. Available at: http://www.ncbi.nlm.nih.gov/pubmed/17927575 [Accessed January 2, 2014].

Sandler, B. & Hashimoto, K., 1998. Collodion baby and lamellar ichthyosis. *Journal of cutaneous pathology*, 25(2), pp.116–21. Available at: http://www.ncbi.nlm.nih.gov/pubmed/23871423.

Schmitz, G. & Langmann, T., 2005. Transcriptional regulatory networks in lipid metabolism control ABCA1 expression. *Biochimica et biophysica acta*, 1735(1), pp.1–19.

Schmitz, G. & Müller, G., 1991. Structure and function of lamellar bodies, lipid-protein complexes involved in storage and secretion of cellular lipids. *Journal of lipid research*, 32(10), pp.1539–70. Available at: http://www.ncbi.nlm.nih.gov/pubmed/1797938.

Schmuth, M., Haqq, C.M., et al., 2004. Peroxisome proliferator-activated receptor (PPAR)-beta/delta stimulates differentiation and lipid accumulation in keratinocytes. *The Journal of investigative dermatology*, 122(4), pp.971–83. Available at: http://www.ncbi.nlm.nih.gov/pubmed/15102088.

Schmuth, M., Elias, P.M., et al., 2004. The effect of LXR activators on AP-1 proteins in keratinocytes. *The Journal of investigative dermatology*, 123(1), pp.41–8. Available at: http://www.ncbi.nlm.nih.gov/pubmed/15191540.

Schultz, J., Tu, H. & Luk, A., 2000. Role of LXRs in control of lipogenesis. *Genes & ...*, pp.2831–2838. Available at: http://genesdev.cshlp.org/content/14/22/2831.short [Accessed January 8, 2014].

Schurer, N.Y. & Elias, P.M., 1991. The biochemistry and function of stratum corneum lipids. *Advances in lipid research*, 24, pp.27–56.

Scott, C. a, Plagnol, V., et al., 2013. Targeted sequence capture and high-throughput sequencing in the molecular diagnosis of ichthyosis and other skin diseases. *The Journal of investigative dermatology*, 133(2), pp.573–6. Available at: http://www.ncbi.nlm.nih.gov/pubmed/22992804 [Accessed August 15, 2013].

Scott, C. a, Rajpopat, S. & Di, W.-L., 2013. Harlequin ichthyosis: ABCA12 mutations underlie defective lipid transport, reduced protease regulation and skin-barrier dysfunction. *Cell and tissue research*, 351(2), pp.281–8. Available at: http://www.ncbi.nlm.nih.gov/pubmed/22864982 [Accessed April 16, 2013].

Sharpe, K. & Hyman, S.E., 2014. A case of harlequin ichthyosis treated with isotretinoin. *Dermatology Online Journal*, 20(2), pp.4–8.

Shulenin, S. et al., 2004. ABCA3 gene mutations in newborns with fatal surfactant deficiency. *The New England journal of medicine*, 350, pp.1296–1303.

Simpson, C.L., Patel, D.M. & Green, K.J., 2011. Deconstructing the skin: cytoarchitectural determinants of epidermal morphogenesis. *Nature reviews. Molecular cell biology*, 12(9), pp.565–80. Available at: http://www.pubmedcentral.nih.gov/articlerender.fcgi?artid=3280198&tool=pmcentrez&rendertype=abstract [Accessed March 7, 2013].

Slatter, T.L. et al., 2008. Novel rare mutations and promoter haplotypes in ABCA1 contribute to low-HDL-C levels. *Clinical Genetics*, 73(2), pp.179–184. Available at: http://dx.doi.org/10.1111/j.1399-0004.2007.00940.x.

Smith, L.T., Underwood, R.A. & McLean, W.H., 1999. Ontogeny and regional variability of keratin 2e (K2e) in developing human fetal skin: a unique spatial and temporal pattern of keratin expression in development. *The British journal of dermatology*, 140(4), pp.582–591.

Smyth, I. et al., 2008. A mouse model of harlequin ichthyosis delineates a key role for Abca12 in lipid homeostasis. *PLoS genetics*, 4(9), p.e1000192. Available at: http://www.pubmedcentral.nih.gov/articlerender.fcgi?artid=2529452&tool=pmcentrez&rendertype=abstract [Accessed April 28, 2013].

Steinert, P.M., 1998. Biochemical Evidence That Small Proline-rich Proteins and Trichohyalin Function in Epithelia by Modulation of the Biomechanical Properties of Their Cornified Cell Envelopes. *Journal of Biological Chemistry*, 273(19),

pp.11758–11769. Available at: http://www.jbc.org/cgi/doi/10.1074/jbc.273.19.11758 [Accessed December 2, 2014].

Steinert, P.M. et al., 1998. Small Proline-Rich Proteins Are Cross-Bridging Proteins in the Cornified Cell Envelopes of Stratified Squamous Epithelia. *Journal of Structural Biology*, 122(1–2), pp.76–85. Available at: http://www.sciencedirect.com/science/article/pii/S1047847798939570.

Stremmel, W. et al., 2012. Mucosal protection by phosphatidylcholine. *Digestive diseases (Basel, Switzerland)*, 30 Suppl 3, pp.85–91.

Swartzendruber, D.C. et al., 1987. Evidence that the corneocyte has a chemically bound lipid envelope. *The Journal of investigative dermatology*, 88(6), pp.709–713.

Swensson, O. et al., 1998. Specialized keratin expression pattern in human ridged skin as an adaptation to high physical stress. *British Journal of Dermatology*, 139(5), pp.767–775. Available at: http://doi.wiley.com/10.1046/j.1365-2133.1998.02499.x.

Sznaidman, M.L. et al., 2003. Novel selective small molecule agonists for peroxisome proliferator-activated receptor delta (PPARdelta)--synthesis and biological activity. *Bioorganic & medicinal chemistry letters*, 13(9), pp.1517–1521.

Takahashi, H., Sinoda, K. & Hatta, I., 1996. Effects of cholesterol on the lamellar and the inverted hexagonal phases of dielaidoylphosphatidylethanolamine. *Biochimica et Biophysica Acta (BBA) - General Subjects*, 1289(2), pp.209–216. Available at: http://www.sciencedirect.com/science/article/pii/0304416595001700.

Takeichi, T. et al., 2013. Novel ABCA12 splice site deletion mutation and ABCA12 mRNA analysis of pulled hair samples in harlequin ichthyosis. *Journal of dermatological science*, 69(3), pp.259–61. Available at: http://www.ncbi.nlm.nih.gov/pubmed/23200509 [Accessed April 16, 2013].

Tan, X. et al., 2013. 1,2,4-Triazole derivatives as transient inactivators of kallikreins involved in skin diseases. *Bioorganic & medicinal chemistry letters*, 23(16), pp.4547–4551.

Thomas, A.C. et al., 2006. ABCA12 is the major harlequin ichthyosis gene. *The Journal of investigative dermatology*, 126(11), pp.2408–13. Available at: http://www.ncbi.nlm.nih.gov/pubmed/16902423 [Accessed January 3, 2014].

Thomas, A.C. et al., 2009a. Premature terminal differentiation and a reduction in specific proteases associated with loss of ABCA12 in Harlequin ichthyosis. *The American journal of pathology*, 174(3), pp.970–8. Available at: http://www.pubmedcentral.nih.gov/articlerender.fcgi?artid=2665756&tool=pmcentrez&rendertype=abstract [Accessed January 14, 2014].

Thomas, A.C. et al., 2009b. Premature terminal differentiation and a reduction in specific proteases associated with loss of ABCA12 in Harlequin ichthyosis. *The*

American journal of pathology, 174(3), pp.970–8. Available at: http://www.pubmedcentral.nih.gov/articlerender.fcgi?artid=2665756&tool=pmcentrez&rendertype=abstract [Accessed January 3, 2014].

Tlacuilo-Parra, J.A., Guevara-Gutiérrez, E. & Salazar-Páramo, M., 2004. Acquired ichthyosis associated with systemic lupus erythematosus. *Lupus* , 13 (4), pp.270–273. Available at: http://lup.sagepub.com/content/13/4/270.abstract.

Trost, a et al., 2010. Aberrant heterodimerization of keratin 16 with keratin 6A in HaCaT keratinocytes results in diminished cellular migration. *Mechanisms of ageing and development*, 131(5), pp.346–53. Available at: http://www.ncbi.nlm.nih.gov/pubmed/20403371 [Accessed November 6, 2014].

Uchida, Y. & Holleran, W.M., 2008. Omega-O-acylceramide, a lipid essential for mammalian survival. *Journal of dermatological science*, 51(2), pp.77–87. Available at: http://www.ncbi.nlm.nih.gov/pubmed/18329855 [Accessed March 17, 2013].

Vasiliou, V., Vasiliou, K. & Nebert, D.W., 2009. Human ATP-binding cassette (ABC) transporter family. *Human genomics*, 3(3), pp.281–290.

De Veer, S.J. et al., 2014. Proteases: common culprits in human skin disorders. *Trends in molecular medicine*, 20(3), pp.166–78. Available at: http://www.ncbi.nlm.nih.gov/pubmed/24380647 [Accessed December 17, 2014].

Venereol, A.D. et al., 2000. Desquamation in the Stratum Corneum. *Acta Derm Venereol*, pp.15–16.

Vielhaber, G. et al., 2001. Localization of ceramide and glucosylceramide in human epidermis by immunogold electron microscopy. *The Journal of investigative dermatology*, 117(5), pp.1126–36. Available at: http://www.ncbi.nlm.nih.gov/pubmed/11710923.

Walker, J.E. et al., 1982. Distantly related sequences in the alpha- and beta-subunits of ATP synthase, myosin, kinases and other ATP-requiring enzymes and a common nucleotide binding fold. *The EMBO journal*, 1(8), pp.945–951.

Wallace, L., Roberts-Thompson, L. & Reichelt, J., 2012. Deletion of K1/K10 does not impair epidermal stratification but affects desmosomal structure and nuclear integrity. *Journal of cell science*, 125(Pt 7), pp.1750–8. Available at: http://www.ncbi.nlm.nih.gov/pubmed/22375063 [Accessed November 6, 2014].

Waring, J.I., 1932. Early Mention of a Harlequin Fetus in America. *Journal of Diseases of Children*, 43(2).

Warner, R.R., Stone, K.J. & Boissy, Y.L., 2003. Hydration disrupts human stratum corneum ultrastructure. *The Journal of investigative dermatology*, 120(2), pp.275–84. Available at: http://www.ncbi.nlm.nih.gov/pubmed/12542533.

Westergaard, M. et al., 2003. Expression and localization of peroxisome proliferator-activated receptors and nuclear factor kappaB in normal and lesional psoriatic skin. *The Journal of investigative dermatology*, 121(5), pp.1104–17. Available at: http://www.ncbi.nlm.nih.gov/pubmed/14708613.

Williams, M. & Elias, P., 1985. Heterogeneity in autosomal recessive ichthyosis: Clinical and biochemical differentiation of lamellar ichthyosis and nonbullous congenital ichthyosiform erythroderma. *Archives of Dermatology*, 121(4), pp.477–488. Available at: +.

Williams, M.L. & Elias, P.M., 1981. Stratum corneum lipids in disorders of cornification. Increased cholesterol sulfate content of stratum corneum in recessive X-linked ichthyosis. *Journal of Clinical Investigation*, 68(6), pp.1404–1410.

Wong, T. et al., 2008. Potential of fibroblast cell therapy for recessive dystrophic epidermolysis bullosa. *The Journal of investigative dermatology*, 128(9), pp.2179–2189.

Yamano, G. et al., 2001. ABCA3 is a lamellar body membrane protein in human lung alveolar type II cells. *FEBS letters*, 508, pp.221–225.

Yan, Y. et al., 2015. Various peroxisome proliferator-activated receptor (PPAR)-gamma agonists differently induce differentiation of cultured human keratinocytes. *Experimental dermatology*, 24(1), pp.62–65.

Yanagi, T. et al., 2011. AKT has an anti-apoptotic role in ABCA12-deficient keratinocytes. *The Journal of investigative dermatology*, 131(9), pp.1942–5. Available at: http://www.ncbi.nlm.nih.gov/pubmed/21633372 [Accessed October 13, 2014].

Yanagi, T. et al., 2008a. Harlequin ichthyosis model mouse reveals alveolar collapse and severe fetal skin barrier defects. *Human molecular genetics*, 17(19), pp.3075–83. Available at: http://www.ncbi.nlm.nih.gov/pubmed/18632686 [Accessed January 3, 2014].

Yanagi, T. et al., 2008b. Harlequin ichthyosis model mouse reveals alveolar collapse and severe fetal skin barrier defects. *Human molecular genetics*, 17(19), pp.3075–83. Available at: http://www.ncbi.nlm.nih.gov/pubmed/18632686 [Accessed October 13, 2014].

Yanagi, T. et al., 2010. Self-improvement of keratinocyte differentiation defects during skin maturation in ABCA12-deficient harlequin ichthyosis model mice. *The American journal of pathology*, 177(1), pp.106–18. Available at: http://www.pubmedcentral.nih.gov/articlerender.fcgi?artid=2893655&tool=pmcentrez&rendertype=abstract [Accessed January 14, 2014].

Yoneda, K. et al., 1992. The human loricrin gene. *The Journal of biological chemistry*, 267(25), pp.18060–6. Available at: http://www.ncbi.nlm.nih.gov/pubmed/1355480.

Yoneda, K. & Steinert, P.M., 1993. Overexpression of human loricrin in transgenic mice produces a normal phenotype. *Proc. Natl. Acad. Sci. USA*, 90(November), pp.10754–10758.

Young, A.R., 1997. Chromophores in human skin. *Physics in Medicine and Biology*, 42(5), pp.789–802. Available at: http://stacks.iop.org/0031-9155/42/i=5/a=004?key=crossref.cb06ddbbae5e3f3da09af47fb92b633e.

Zeeuwen, P.L.J.M. et al., 2007. Colocalization of cystatin M/E and cathepsin V in lamellar granules and corneodesmosomes suggests a functional role in epidermal differentiation. *The Journal of investigative dermatology*, 127, pp.120–128.

Zeeuwen, P.L.J.M. et al., 2010. The cystatin M/E-cathepsin L balance is essential for tissue homeostasis in epidermis, hair follicles, and cornea. *The FASEB journal : official publication of the Federation of American Societies for Experimental Biology*, 24, pp.3744–3755.

Zettersten, E. et al., 1998. Recessive x-linked ichthyosis: role of cholesterol-sulfate accumulation in the barrier abnormality. *The Journal of investigative dermatology*, 111(5), pp.784–790.

Zheng, Y. et al., 2011. Lipoxygenases mediate the effect of essential fatty acid in skin barrier formation: a proposed role in releasing omega-hydroxyceramide for construction of the corneocyte lipid envelope. *The Journal of biological chemistry*, 286(27), pp.24046–56. Available at: http://www.pubmedcentral.nih.gov/articlerender.fcgi?artid=3129186&tool=pmcentrez&rendertype=abstract [Accessed December 1, 2014].

Zuo, Y. et al., 2008. ABCA12 maintains the epidermal lipid permeability barrier by facilitating formation of ceramide linoleic esters. *The Journal of biological chemistry*, 283(52), pp.36624–35. Available at: http://www.pubmedcentral.nih.gov/articlerender.fcgi?artid=2605993&tool=pmcentrez&rendertype=abstract [Accessed December 3, 2013].

Chapter 8: Appendices

8.1. Appendix 1

Primer sequences used in genotyping studies, all the oligonucleotides shown are arranged 5'-3'.

Forward primer	Reverse primer	Exons	Product (bp)
CAGCCCTCAAGGAAGCTATG	CTTGGGTGCTCTGGAATGAT	5'UTR-4	514
TCTTTCCATTCCTGCAGACC	AGACAGAAGCTGCCACACAG	3-7	602
TGCCTTTCTAACATGACCCTTT	GTGAACCTCTGGCCAAACTG	6-10	547
GCAGATTTCTGCATTTTCTCCT	GTGAACCTCTGGCCAAACTG	*5'UTR-10	305
TGTGGAATGAGGATGATGGA	TTCATTTGCAGTGCCTGTTC	9-13	562
TGACTGGAGATCCAAGCAAA	CCTTGTGGTGTGTTCATTCG	12-17	654
CTGCCCAGAAGTGTTCCATT	GCTGATCGATGATGTCAATGTT	16-21	637
TTGAAACAGATAGATGAACTCGAT	TAAGCCAGGCAAAGAAATGG	20-24	685
GACCTCCGGCTTCATGAGTA	CCAAATCGCTCCTTCCAATA	23-27	620
TGCTTGGTATGTCAGGAATGTC	CTTCCTCTTCATGCCTCCTG	26-30	658
GCACCTTCTCCTATATGGTTCC	TTGTGACTCTTTGGTCAAGTTCA	29-33	697
ACCGTGGAGGAGGTCTTTCT	TCGTTGCCCAGTGAGGTTA	32-37	678
TGTTTGCTCCTGCTCAGAAA	AAACGCTACAGGCACCAAGT	36-42	610
ATTGGCGTGACATGCTACTG	TCTCCCTTACATGTGAAGAATTAAA	41-45	616
TCTCAGGGCACCATGTTTTT	TGAAGGGCATCAGGTGAAGT	44-48	565
CTGGGTCACGTTGATTCTCA	GCTGCATGAACTTTGTGAGG	47-51	550

CACTGGCCTTGATAGGGAAA	CAAAATGAAGCCATTGGTCA	48-3'UTR	635

Table A1.1. ABCA12 cDNA primers. Primers designed to negate SNPs and produce amplicons with overlapping flanking regions to ensure full coverage of transcript and a continuous sequence. Exons *5'UTR-10 checks for presence of the secondary *ABCA12* transcript.

Exon	Forward primer	Reverse primer	Size (bp)
1	CAGCCCTCAAGGAAGCTATG	TTGGGGGCATGTTAAGACTC	389
2	CAGTTGGTCAAATATTCAGCTTG	CTTTCTGACTAACTTGAAAATCTAGGG	392
3	CATAACACCCTCCAAGACTGC	CTAAGCTTGCATGGCTTCCT	425
4	CATTGGTGTGTGGTTAGGTGA	CCATACTCAGGCAACCATGA	407
5	GGAATTTGCCACTTTTCCAG	GGTGCTCCAAACATCTTGCT	362
6	CACATTCATGCATTCGCTCT	CCAGTCAGCATTTCCCAGTC	465
7	TGGAGTTACAGGGAAAAGATCC	TCCATAACCTTGATGACCACAG	594
8	TTTGTTGAGATTTTGTGCATGA	TCCCTTTCTCCACACTTTGATT	459
9	CAAATATTTCCAACAAAAGAGCA	TGCAAGCTCAGAACTGAAAAAG	487
10	CCGGCCAACTGCATAGTATT	CAAATCACCAGACTGAAACTGA	395
11	CTGGTTTCCTAAATGACCTTGC	GTCGTAAGTAGGGCCATTATAAATCT	349
12/13	CCAAATGCCAACTAACCACATA	GAGTTTGGTTGGGAACTTCAAA	696
14	AGACATCTGCCCCTGAGAAG	TGAGGCCTCCAGGTTTATCA	395
15	GTTTGATTCTTGAGGACCTTTTG	TAAATGGATCTCATCCCTCATAGT	410
16	TCTTAGGTAAACGCCCAGGAAT	TGGCAAAAAGTGTTGCTAGGTA	493
17	AAAAGGAATTATGGAAACTGTAAGGA	TCTTGACATGTGGTAAGTGCTG	483
18	CTGTCAATTTGCCATGTGGA	GCACATATCCAGGGCAGAAG	386
19	GCTGTCATTTGAAACTTTTGACC	CCCTGTCTCAGACCTTCTCTCT	439
20	CCAACCCCCAATCTTCTCTT	CCAGGGTCTCATTTTTCTTTG	404
21	CGACCCATTTTCTTTGGTGT	TGGTTGCCTACATGAAAGGTT	502
22	TCTGAGGTTGACACCTCCAAT	TGGTGAATGTTGTTCCTTTCA	594
23	TGGGGTAATACCGATTATTTTCA	TCAGCTGCTTTTGTGATTTG	412
24	GGCATATTTCACATAGCAAGCA	GGCATATTTCACATAGCAAGCA	584
25	GCATGGTTGGTAAGGGACTG	CTGTGACACACAGCACAGTTG	288
26	CAACAGCATTCAGCTATGCAAG	GAAGTCAACCATAAAAAGCATGTATCTG	326

27	TGGAAACTGAGACCACCTTTT	GAGTCCAAAGACGCATGTGTAG	443
28	GAACCCTGGTTCTCCACTCTTA	CTTCCTCCATCTGGGAAATGTA	517
29	GTTTGCCCTTGACTGAGAAGA	CTGGCCGGTAAGGATAATGA	519
30	TGAATCCTCAAGAGTTTATTGTACC	CTCAAACTCCCAGGCTCAAG	495
31	CTGGCCCTGAATTTTTCTTG	CCAGGATTTCGATGCTCACT	492
32	GCTCATCACCTCACCCTCTG	CTGTCTAGCTGGGGCAACAT	504
33	CCCAGCTAGACAGCACGTATC	GGAGGCTTAAATTTCCTTAGTGTT	461
34	CAATGGAAGGTCCAAGGCTA	CTCATGGCCTTCATTCAGGT	506
35	CACGGCAAGACTCTGTCTCA	CAGCTTTCTTCCAGGCAAAT	326
36	TGAAAAATCAGTAAATTGTTCTGTGA	TGAGCTGCCCAGATCCATA	370
37	TCTTGGTGTAGGTGAGATGACTTC	AAGGCTGTTTAAATAAAACTGAGAA	441
38	CAGAAACAAAAAGTTGAGCTCCT	CAGAATTGGAACCACTGTGC	330
39	GAGAACAGTGCATAATCTTCCAA	CTGCCACCTGTGAAGAAACA	349
40	AAAAAGGTCCCCCAAATAAAAT	CCAGCCCTTCTAGATTGACATT	302
41	CCTTATTTGTGTCACAGCCAAC	CACTGGATGAAGATAAGCCTGA	462
42	GAATGTTAGAAGCAATGGGAACA	CATGTCAAATGAAACCCCAAG	387
43	TGCCTCAGCCTCCTAAAGTG	GATGAGGCCCAAAAAGAATTT	409
44	CAAATTCAGCCTATATGGGAAA	GCCAAACATTTCCATATTACCAA	510
45	GTGACATGAAAACCCATCAAAA	CCAGGCTGGTCTCAAACTCT	458
46	CCAGGGAGAAGAGGGAGAGA	CATTTCCACCCACCTTAATAGC	335
47	GTCACTGACCACCATGACCA	CCACTGCCAGAAGGAAAATG	395
48	GCTTTAAGGGTTTTGGCACA	GCTTTGCACAATAGCTAGCACA	326
49	TTGAACTTTTTGACAGCAGCA	CTTTTCCCACCTGTCATCCT	334
50	TAGCCTGGGCAACAGAGTG	GCTTCCAAAGATTAGCTTGTCC	390
51	CCAGTTTGCAACATGTCCTG	GTAGAGACGGGGTTTCACCA	400
52	CTGTAGCATCATTTTCAGTGGA	TGCTAAGTTTTTCAGGTGCAAG	398
53	CGCTTGCACTAGGAGAGAGG	GCAACAACACTCACTGACCTT	406

Table A1.2. ABCA12 genomic primer pairs. Primers designed to capture the entirety of the 53 exons and around 100bp of flanking intronic sequence of *ABCA12*, utilised in the genotyping of *ABCA12.*

Primer	Sequence	Product (bp)
GOSR1ex5F	TGAATTCCATAAAACCAAAGCA	193
GOSR1ex5R	AATCTCAACCACGGTTCTGC	193
DSC1ex2F	GTGATCAAATTTAATTCCTGATATTTT	238
DSC1ex2R	CCGGCCTACTATGTGGTTTT	238
KDSRex9F	CGAGCACACTCCACTGTTTC	209
KDSRex9R	GCAGAGCTTACCTGCTGGAG	209
PCDHGA9ex1F	ACGGTGACTGCAACAGACAG	274
PCDHGA9ex1R	GGATGGTATCCTCTGCCAAG	274

Table A1.3. Genomic primer pairs. Primer sequences for four different candidate genes used in screening variants found in a patient's exome data in **3.1.4.**

Primer	Sequence	Product (bp)
GAPDHF	TGGCCCCTCCGGGAAACTGT	92
GAPDHR	CCTTGCCCACAGCCTTGGCA	92
ABCA1F	TTAAACGCCCTCACCAAAGAC	281
ABCA1R	AAAAGCCGCCATACCTAAACTCAT	281
ABCA12F	GTGGGAGCGTCAAGTACTCC	583
ABCA12R	CCTCCAGAGGAACCACCTC	583

Table A1.4. Primers used for qPCR (Rotorgene) with at least one primer of each primer pair bridging neighbouring exons.

Primer	Sequence	Product (bp)
LORICRIN-2F	GTGGGAGCGTCAAGTACTCC	583
LORICRIN-2R	CTCCAGAGGAACCACCTC	583

Table A1.5. Primer sequences used for the screening of loricrin allelic size variants in 5.2.3.

8.2. Appendix 2

Appendix data from the functional studies of chapters 4 and 5

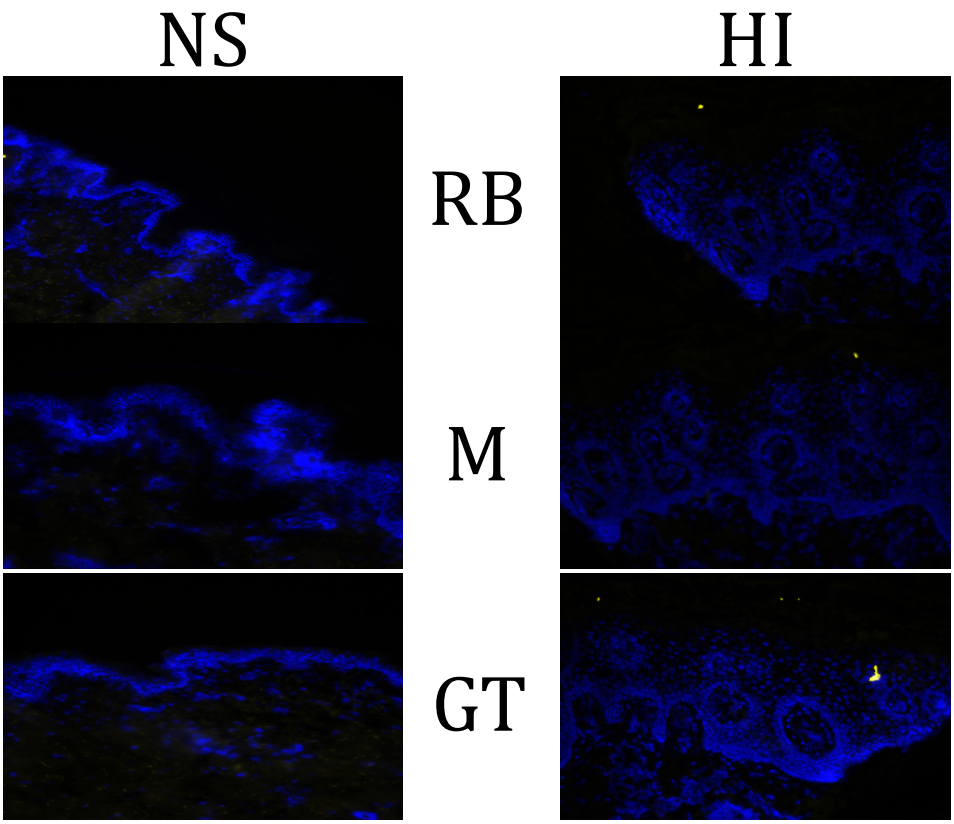

Figure A1.1. Negative controls from the immunohistochemistry of HI and NS. For the terminal differentiation markers and ABCA12 and ABCA1 analysis in the epidermis of HI skin **5.2.1. & 4.2.2.**

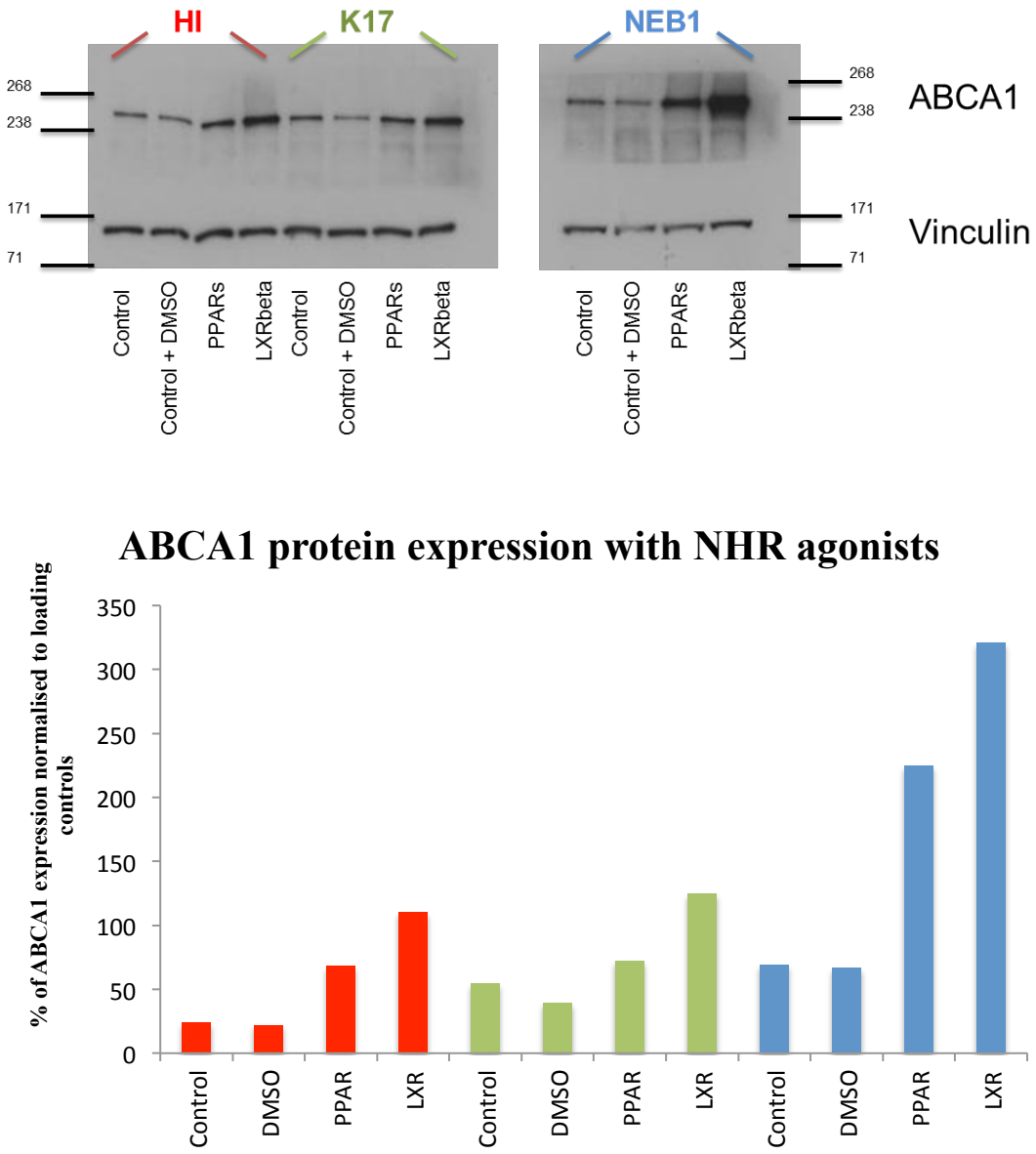

Figure A1.2. A preliminary study of the modulation of the protein expression of ABCA1 in keratinocytes under PPARβ/δ and LXRβ activation. This experiment was preformed using the same protocol and conditions, with the exception of a different ABCA1 antibody, which furthers the accuracy of the results in **5.2.2.**